Springer
Tokyo
Berlin
Heidelberg
New York
Barcelona
Budapest
Hong Kong
London
Milan
Paris
Santa Clara
Singapore

N. Tamaki, K. Ehara (Eds.)

Computer-Assisted Neurosurgery

With 138 Figures, Including 21 in Color

Springer

Norihiko Tamaki, M.D.
Professor and Chairman
Department of Neurosurgery
Kobe University School of Medicine
7-5-1 Kusunoki-cho, Chuo-ku, Kobe 650, Japan

Kazumasa Ehara, M.D.
Associate Professor
Department of Neurosurgery
Kobe University School of Medicine
7-5-1 Kusunoki-cho, Chuo-ku, Kobe 650, Japan

ISBN 978-4-431-65891-7 ISBN 978-4-431-65889-4 (eBook)
DOI 10.1007/978-4-431-65889-4

Library of Congress Cataloging-in-Publication Data

Computer-assisted neurosurgery / N. Tamaki, K. Ehara (Eds.).
p. cm.
Papers presented at the International Symposium on Computer-Assisted Neurosurgery and selected papers presented at the 6th Annual Meeting of Japanese Society of Computers in Neurosurgery, which were held in Kobe, Japan, on January 24-26, 1997.
Includes bibliographical references and index.
ISBN 978-4-431-65891-7
1. Computer-assisted neurosurgery—Congresses. I. Tamaki, Norihiko. II. Ehara, K. (Kazumasa), 1949- . III. International Symposium on Computer-Assisted Neurosurgery (1997 : Kōbēshi, Japan) IV. Japanese Society of Computers in Neurosurgery. Meeting (6th : 1997 : Kōbēshi, Japan)
[DNLM: 1. Neurosurgery—methods—congresses. 2. Image Interpretation, Computer-Assisted—congresses. 3. Image Processing, Computer-Assisted—congresses. 4. Therapy, Computer-Assisted--congresses. WL 368 C7378 1997]
RD593.5.C65 1997
617.4'8059—dc21
DNLM/DLC
for Library of Congress 97-43643

Printed on acid-free paper

Typesetting: Best-set Typesetter Ltd., Hong Kong

SPIN: 10652477

Preface

Computer technology has developed remarkably in the field of neurosurgery during the past 10 to 20 years. Great achievements have been made recently in neuroimaging techniques and computer technology for neuronavigation, from frameless, armless systems to robotic microscopes.

Contained in the present volume are all the papers presented at the International Symposium on Computer-Assisted Neurosurgery and selected papers presented at the 6th Annual Meeting of the Japanese Society of Computers in Neurosurgery, which were held in Kobe, Japan, on January 24–26, 1997.

This volume is a comprehensive description and review of current technical advancements in computer-assisted neurosurgery, with a special focus on advanced intraoperative neuroimaging, various neuronavigation system, robotic microscopes, and strategies for preoperative and intraoperative surgical planning using high-power workstations with three-dimensional software.

We express our thanks to the contributors for their participation and cooperation, and to Springer-Verlag for personal and technical assistance in publishing this work.

We sincerely hope that this volume will contribute to improving neurosurgical technology and outcomes.

The Editors

Contents

Part 3. Advanced Neurosurgical Planning Using Computer-Assisted Systems

Part 4. Intraoperative Imaging and Brain Shift

Part 5. Computer-Assisted Neurosurgery of Difficult Lesions

Part 1
Technical Advances in Computer-Assisted Neurosurgery – Frameless, Armless Systems to Robotic Microscopes

Neuronavigator: Its Current Usage and Its Future

Eiju Watanabe

Summary. Neuronavigator, the first commercialized surgical navigation system, was reported in 1987. It translates the site of operation into CT/MRI coordinates, providing a surgeon with exact three-dimensional orientation during surgery. It serves as a functional guiding system when it is combined with a preoperative functional mapping such as magnetoencephalography (MEG) or functional MRI (fMRI). This usage enhances the safety of brain surgery in the realm of brain function.

Key words. Surgical navigation—Magnetoencephalography (MEG)—Computer—Functional mapping

Background

Ten years have passed since we first published an article about the navigation system [1]. In due course, more than ten navigation systems have been invented using similar ideas [2–5]. This chapter describes the current status of the newly revised navigation system and also discusses what will be added to conventional neurosurgery with the help of the navigation system.

Methods

Basic requirements to establish surgical navigation are as follows: (1) frameless system, (2) automatic feedback of the operating point in reference to the preoperative CT/MRI, and (3) volumetric approach to the lesion. The neuronavigator consists of a personal computer and a multijoint sensing arm [6–9]. The three-dimensional coordinates of the arm tip are always monitored by a computer, automatically translated into CT/MRI coordinates, and finally displayed with a cursor on the CT/MRI images on the computer screen.

Recently we have determined a minimum construction of the navigation system. For routine and relatively small surgeries, the preoperative preparation should be

Department of Neurosurgery, Tokyo Metropolitan Police Hospital, 2-10-41 Fujimi, Chiyoda-ku, Tokyo 102, Japan.

Fig. 1. Minimum construction of the neuronavigator, using parm-top PC with Windows 95

simplified, and the navigation system should be easily portable between clinics. We are using a notebook PC (Fig. 1). The system can be carried in a suitcase to another clinic if necessary, which I sometimes do. The CT/MRI images are transported by a video-capturing system connected to the CT/MRI computer. It captures the video signal, which is transmitted from a CT/MRI computer to a monitor screen, and converts CT/MRI images into bitmap files that are accessible by the PC Windows system. The system allows us direct transport of the images into PC without any LAN networks. Although it is expected to be replaced by the Ethernet, we should still wait for several years until every institute has its own LAN equipment.

Three-Dimensional Digitizer

There are principally four methods to detect three-dimensional (3-D) coordinates during surgery: the mechanical arm [6], magnetic field gradient [2], sonodetector [1], and optical detector. When surgery starts, the tip segment of the arm is replaced with a sterilized one and the arm is covered with a sterilized polyethylene sleeve. The arm system is introduced into the surgical field only when the surgeon needs the navigation.

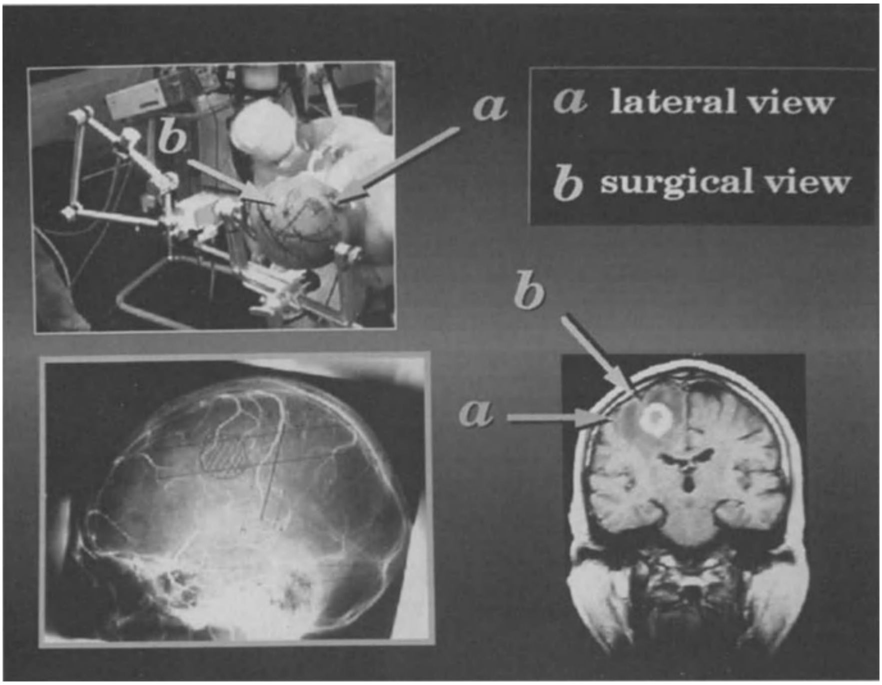

Fig. 2. Designing the craniotomy by the neuronavigator

We use a small trick that we call the "virtual tip." When the pointing tip is shortened by some length, the system still indicates the location of the tip that it assumed before shortening; we call this theoretical point the "virtual tip." As this point has an imaginary existence, it can freely be introduced into the tissue before actual invasion. The virtual tip can also be controlled by software from the Windows screen. If the virtual tip has reached the tumor, it means that the tumor will be found at the known length ahead of the actual tip. This is particularly useful when a surgeon searches for a tumor from the scalp surface. When the virtual tip follows the tumor margin, the actual tip is delineating the proper position and size of the craniotomy.

Figure 2 shows one example. The tumor was located in the high frontal area, a location that is sometimes very difficult to locate on the scalp because of poor anatomical landmarks. Axial CT or MRI images give us an incorrect impression of the tumor location that is too low to approach the tumor. A craniotomy should be made at location "b" in Fig. 2, which is very difficult to obtain from the axial view. The navigator gives us the proper location by simply using the virtual tip method.

Applications

Needless to say, the standard usage of the navigator is tumor detection. Figure 3 shows a representative case with a glioma. The tumor was found on CT at a checkup for epilepsy.

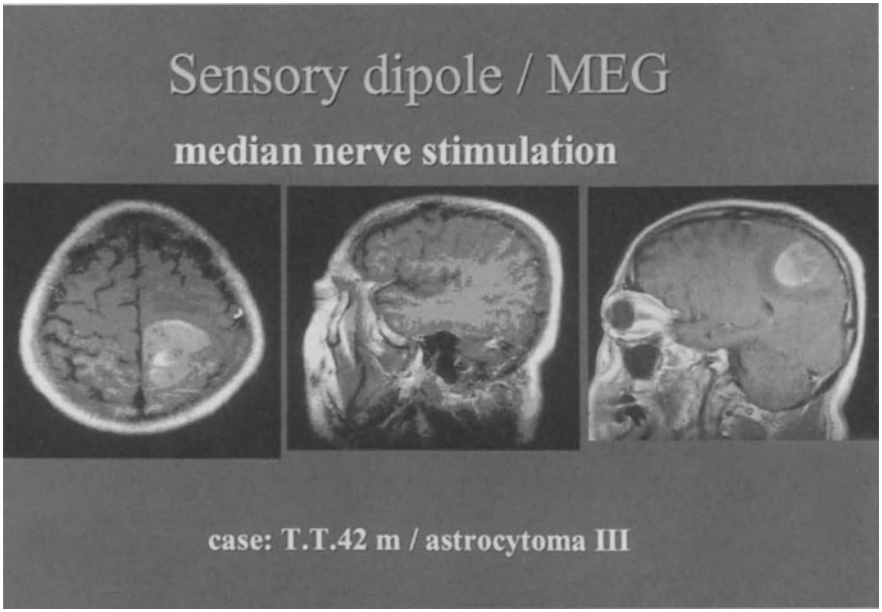

Fig. 3. MRI of case 1. A *dot* indicates a sensory dipole measured by magnetoecephalography (MEG)

A low-density area was found in the frontal lobe of a 10-year-old boy with convulsions. Removal of the lesion was performed under navigator guidance. There was no visual difference between the normal brain and the lesion. With the navigator guidance the lesion was biopsied, revealing a low-grade astrocytoma. The tumor was totally removed.

As for future applications, we are trying to use the navigator to translate information from functional mapping as follows.

Magnetoencephalography Methods

With a 37-channel squid system, a sensory evoked field was obtained that indicated the location of the sensory cortex. The median nerve was stimulated at the patient's wrist, and the evoked magnetic field was averaged for 200 repetitions. The primary somatosensory cortex (Brodmann's area 3b) and then the central sulcus were determined by the sensory dipole. When these location were transferred onto the patient's cortex with the navigator, the central sulcus and the motor cortex were easily recognized.

Case One

This 42-year-old man underwent surgery for a tumor in the right parietal area (Fig. 3). Preoperative magnetoencephalography (MEG) showed the sensory dipole, which was back-traced and projected onto the MRI image (star in Fig. 4). The central sulcus was identified according to the sensory dipole, which revealed that the tumor was located

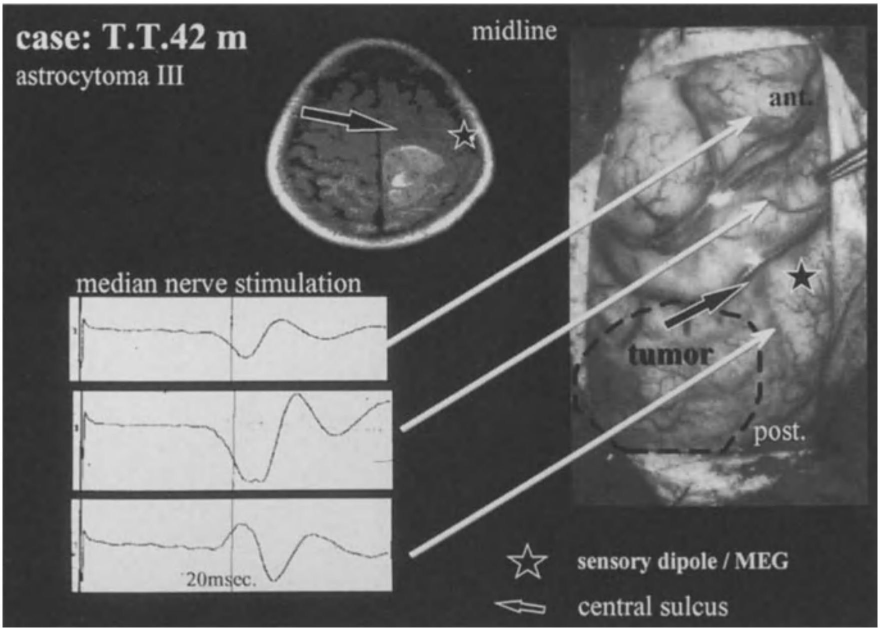

Fig. 4. Intraoperative navigation of case 1. The tumor and central sulcus were defined by the navigator, and these locations were confirmed by cortical somatosensory evoked potentials (SEP). *Star*, sensory dipole

in the primary sensory cortex. Surgery was conducted under neuronavigator guidance to remove the tumor with the intention of preserving the motor strip. The MEG-defined hand area and the MRI-defined tumor boundary were projected onto the cortex after the dura was opened. The cortical somatosensory evoked potential (SEP) after median nerve stimulation was recorded from the cortical surface at several points around the central sulcus. The inversion of N20 and P20 was documented at the sulcus that was identified as the central sulcus by the navigator. The motor strip was easily identified and protected in the operating field. The tumor was successfully removed, inducing no motor paresis.

Case Two

This patient showed monoparesis in his right hand. MRI revealed an enhanced mass lesion. MEG revealed a sensory dipole, indicating that the mass was lying in the motor cortex (Fig. 5). During the operation, it was extremely difficult to detect the tumor with visual inspection or palpation. The tumor was partially excised, preserving the motor cortex just outside the lesion. The patient showed no worsening of preoperative hand paresis. The histological examination showed an oligodendroglioma grade II.

Spinal Surgery

Use of the navigator in operations outside the cranium is also possible. We applied navigator guidance in the anterior approach for cervical spondylosis. In drilling the

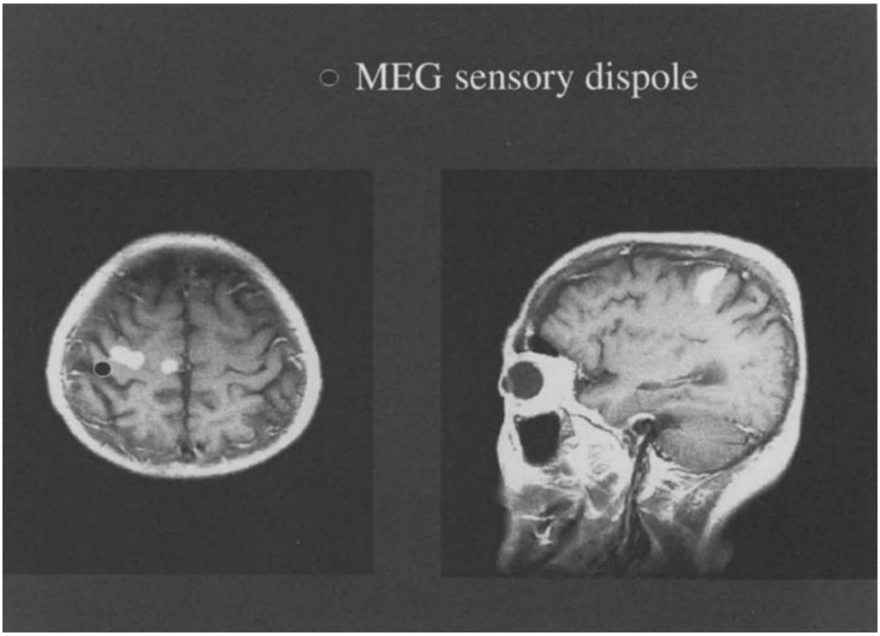

Fig. 5. MRI of case 2. A *dot* indicates a sensory dipole measured by MEG

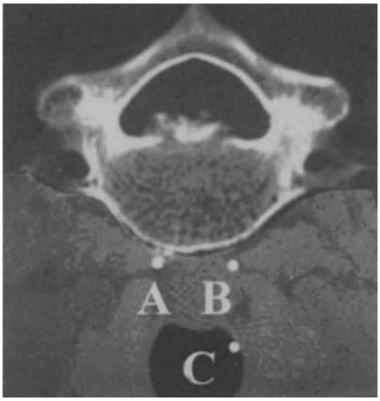

Fig. 6. Application of the navigator in the anterior approach to cervical spondylosis surgery. Points *A*–*C* were drawn on the preoperative CT. A plate with the same triangular configuration was inserted in the surgical field to serve as fiducials for registration

osteophytes after discectomy, we sometimes experience difficulties in determining the lateral limit of the vertebral body. First, three points were drawn on a preoperative CT of cervical spine, two (points A and B in Fig. 6) on the medial edges of the bilateral longus colli muscles and one (point C in Fig. 6) placed within the surgical field (as in Fig. 6). A triangular plate was made of metal so as to hold these three points with the same configuration and size as the three points drawn on the CT image. During the operation, the plate was sterilized and inserted in the surgical field after the exposure of the anterior surface of the cervical spine. The two corners of the triangle were adjusted at the medial margin of the longus colli muscles, corresponding to the plan on the preoperative CT image. The navigator was calibrated by registering these three points on the plate as fiducials. The validity of this method was first examined with three plastic models followed by two clinical cases with cervical spondylosis. The laterality was correctly monitored with errors within 2 mm in clinical trials.

Accuracy

The overall accuracy of the NeuroNavigator is about 2.5 mm [3]. Because we use nasion and tragi as fiducials, the accuracy becomes better when the target lies nearer to the skull base. We must remember that the brain tissue deviates when considerable amounts of cerebrospinal fluid (CSF) or tumor tissue are removed. In a practical sense, however, it is often recognized that just opening the dura mater does not cause significant deviation of the tissue. Insofar as we use the preoperative CT/MRI images in navigation, this problem cannot be avoided. The easiest way to overcome this problem are to obtain orientation at the earlier phase of surgery. A fundamental solution for this problem would be a real-time image-updating technique such as intraoperative CT or MRI.

Conclusion

As for future applications, use of the navigator to translate the information from the functional mapping into the surgical field is promising. As was shown, MEG is one of the effective alternatives to localize the somatosensory cortex of the individual brain. Using this type of guidance, we could easily achieve lower postoperative morbidity in a shorter operation time.

Surgical navigation is not the aim but rather is the major starting point toward comprehensive image-guided surgery. More sophisticated systems such as a robotic surgical microscope, an operating robot, or a navigating surgical theater might be our ideal for the future.

References

1. Watanabe E, Watanabe T, Manaka S, et al (1987) Three-dimensional digitizer (Neuronavigator): new equipment for computerized tomography-guided stereotactic surgery. Surg Neurol 27:543–547
2. Friets EM, Strohbehn W, Hatch JF, Roberts DW (1989) A frameless stereotactic operating microscope for neurosurgery. IEEE Trans Biomed Eng 36:608–617
3. Kato A, Yoshimine T, Hayakawa T, et al (1991) A frameless, armless navigational system for computer-assisted neurosurgery. J Neurosurg 74:845–849
4. Moesges R, Schloendorff G (1988) A new imaging method for intraoperative therapy control in skull base surgery. Neurosurg Rev 11:245–247
5. Reinhardt H, Meyer H, Amrein E (1988) A computer-assisted device for the intraoperative CT-correlated localization of brain tumors. Eur Surg Res 20:51–58
6. Watanabe E, Mayanagi Y, Kosugi Y, et al (1991) Open surgery assisted by the Neuro-Navigator, a stereotactic articulated, sensitive arm. Neurosurgery (Baltim) 28:792–800

7. Watanabe E, Mayanagi Y, Takakura K (1992) Stereotactic guidance of TCD probe using a computer-assisted frame-less stereotactic guiding system (Neuronavigator). Recent Adv Neurosonol: 481–486
8. Watanabe E, Kosugi Y (1993) Intraoperative neuronavigator system in neurosurgery and computer surgery. In: Fujino T (ed) Simulation and computer-aided surgery. Wiley, Chichester, pp 157–162
9. Watanabe E (1993) The neuronavigator: a potentiometer-based localizing arm system. In: Maciunas RJ (ed) Interactive image-guided neurosurgery. American Association of Neurological Surgeons, Park Ridge (IL), pp 135–147

Computer-Assisted and Frameless Stereotaxy in Australia: The Operating Arm System

Malcolm F. Pell

Summary. The trend toward minimally invasive surgery, coupled with the increasing use of computer software and hardware, has led to a greater use of stereotactic procedures as part of mainstream neurosurgery. Computer-assisted and frameless stereotactic systems allow the performance of stereotactic procedures without the need for mechanical linkage to a stereotactic frame. Both mechanical and optical digitizers are used in Australia, the most widely used system being the Operating Arm System (OAS) from Radionics (Burlington, MA, USA). This system has the advantages of simplicity of use, software programs of image fusion, and a functional stereotactic atlas, and can be used for both frameless and framed stereotactic cases. The initial Australian experience with the OAS at St. Vincent's Hospital and Concord Hospital in Sydney and its use in 106 cases is presented.

Key words. Frameless stereotaxy—Intracranial neurosurgery—Image fusion—Mechanical digitizer—Functional atlas

Introduction

With the rapid and dramatic improvement in neuroradiological imaging and current technology assisted by the increasing use of computer hardware and related software, modern stereotatic neurosurgery has become an important part of mainstream neurosurgery and is now available throughout the world. Conventional stereotactic frame systems allow precise spatial information from computerized tomography (CT), magnetic resonance imaging (MRI), and angiography to be used for operative procedures such as biopsy, excision, or aspiration of various intracranial lesions [1–5].

Conventional stereotactic neurosurgery uses an external frame to localize specific targets and permit the accurate guidance of operative instruments within the intracranial space. There has been increasing interest in the field of frameless stereotaxy, which is the process of achieving spatial correspondence or registration in the head

St. Vincent's Hospital, 438 Victoria Street, Darlinghurst, Sydney, NSW 2010, Australia and Concord Repatriation General Hospital, Hospital Road, Concord, Sydney, 2139, Australia.

with a CT or MRI image using three-dimensional digitizers and contemporary graphic computers without mechanical linkage to a frame. Continual advances in computer-based cranial images such as CT, MRI, and positron emission tomography (PET), faster and more affordable computers, the adaptation of digitizers to the operating room, and the desire of neurosurgeons to use such equipment have allowed the concept of minimally invasive surgery to become increasingly important in neurosurgery [6,7].

The first report of a frameless stereotactic system that described spatial registration of the operative field into a computer graphics system without a head frame was that by Roberts and colleagues in 1986 [8]. Roberts used scalp markers identified on a preoperative CT scan and assigned intraoperative coordinates by touching these markers with a sonic pointer, giving the position in relation to the operating microscope (also equipped with sonic emitters). In 1987 Watanabe and colleagues [9] described a mechanical digitizer that correlated the position of the tip of the instrument with its location on the corresponding CT slice in a system called the Neuronavigator [10]. Since these reports there has been worldwide research in the area of frameless localization, including that of Guthrie and his co-workers in developing the Operating Arm System (Radionics, Burlington, MA, USA) [11,12] and the ISG Viewing Wand (Elekta, Stockholm, Sweden) [13–15].

Computer-assisted and frameless stereotaxy allows intraoperative imaging and localization of cranial coordinates. A number of localization techniques are being used or under investigation, including mechanical digitizers [11–13], sonic

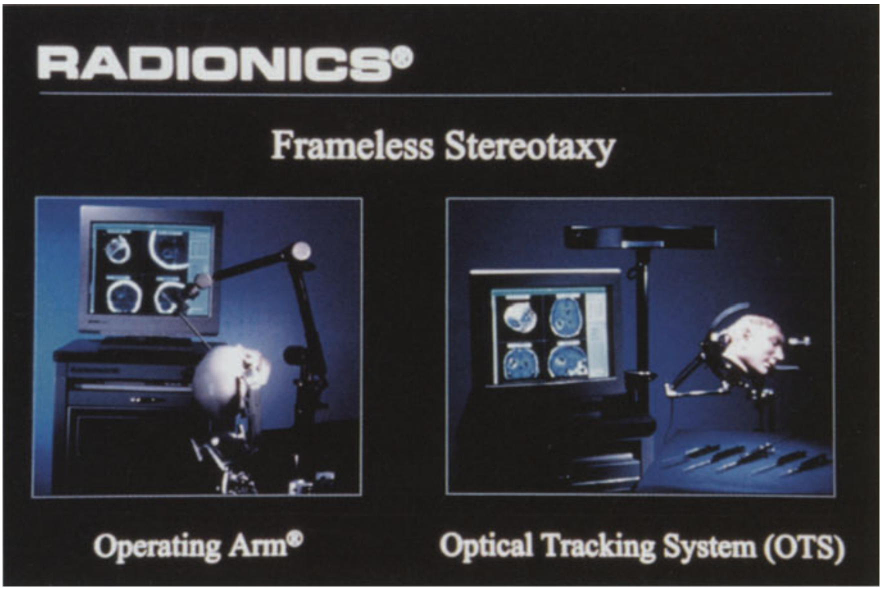

Fig. 1. Frameless stereotactic systems produced by Radionics (Burlington, MA, USA). The Operating System is a mechanical digitizer (*left*); the Optical Tracking System is based on optical digitizers (*right*)

localizers [16–18], optical systems employing light-emitting diodes [19], and electromagnetic fields [20–22]. Sonic localization is determined by several microphones arranged in the vicinity of the operative field. They receive signals from sound emitters mounted on the digitizer, but the smaller sonic probes must be in the line of sight of the microphones. Also, extraneous sound, temperature, and moving air can affect the measurements of the probe position [17,18,23]. Optical localization is similar to sonic localization except that cameras are used to detect pulsed light emitted from diodes on the pointer or operative instruments such as forceps [19]. One such system is the Optical Tracking System (OTS) (Radionics), which is commercially available in Australia. It is not constrained by mechanical linkage (it has a single trailing wire) but does require line-of-sight transmission. Electromagnetic digitizers used for magnetic positron trackers for intraoperative probe localization use a transmitter to produce a magnetic field and a sensor to detect these magnetic fields [20–23].

At present mechanical digitizers are the most widely used form of intraoperative frameless localization. The first Australian installation of a frameless stereotactic system was at St. Vincent's Hospital, Sydney, in March 1994. This was the Operating Arm System (OAS), which includes an ergonomically designed articulated mechanical arm together with computer hardware and graphics software. There are now 11 frameless systems installed at Australian hospitals, of which 7 were obtained from the Radionics Company, either Operating Arm Systems or Optical Tracking Systems (Fig. 1). The remainder of this chapter describes the Operating Arm System.

Materials and Methods

The Operating Arm System (OAS) has several functional components [6]. The operating arm is a six-jointed mechanical digitizer accurate to within 0.5 mm. For clinical data gathering, the arm is mechanically linked to the patient's head in the operating room by the starburst clamp that attaches to the Mayfield headholder. Four case-specific end attachments have been devised for the operating arm: a simple probe, a spring-loaded depth probe, a shunt-passing stylet, and a small cannula through which a probe can be passed toward the point at which the arm is aimed. There is also a May Field-compatible table mount floor stand. A graphics computer with user interface completes the system.

Reference points consist of at least four surgical staples fixed to the scalp. In our institution we routinely apply six staples to the scalp, two each at the frontal area, the temporal area, and the posterior parietal area. This method allows us to choose the most convenient four staples for registration depending on the position of the patient's head and the location of the arm. Surgical skin staples are preferred to commercially available skin localizers because they are less likely to move and are inexpensive. These staples are applied under local anesthetic at the time of CT scanning, which allows scanning to be done at a different time from the actual operation so long as the staples are attached to the skin. It is not uncommon to perform the CT scan as much as 3 days before the operation.

The OAS computer is a graphics workstation that can display the CT data as desired by the surgeon. The computer is mounted on a cart to allow movement in and around the operating room. The OAS computer user interface is designed for maximum convenience for the operating surgeon both before and during the surgery.

The steps in performing a procedure using the OAS are data acquisition, data input, and data review. Data acquisition utilizes the skin staples affixed to the scalp. The patient undergoes a CT scan with slices of 3-mm separation and 3-mm thickness. The scan must include the area of interest containing the tomor and the staples, which are visible on the scout film, to allows for both staple registration and the three-dimensional reconstruction.

Data input refers to the transfer of the image data from the CT scan into the computer workstation. Depending on the type of CT or MRI scanner in use, this can be done by half-inch magnetic tape, optical disk, DAT tape, or direct Ethernet link to the computer. On starting the system, the user is provided with a number of options controlled by a standard "mouse." When a new patient is selected the system reads the data tape and automatically processes the images.

Data review allows the surgeon to use the stored data during the operative procedure. After the image is loaded into the OAS, it is available for use in a variety of ways, all prompted by simple mouse-controlled menus. The surgeon commences by selecting reference markers. Four staples are chosen and their coordinates stored. Registration with the patient is then undertaken. The system then displays each reference mark and requires that the surgeon touch the corresponding point on the patient's head with the operating arm for calibration and registration. For example, if a left frontal staple point is chosen from the computer workstation using the mouse to

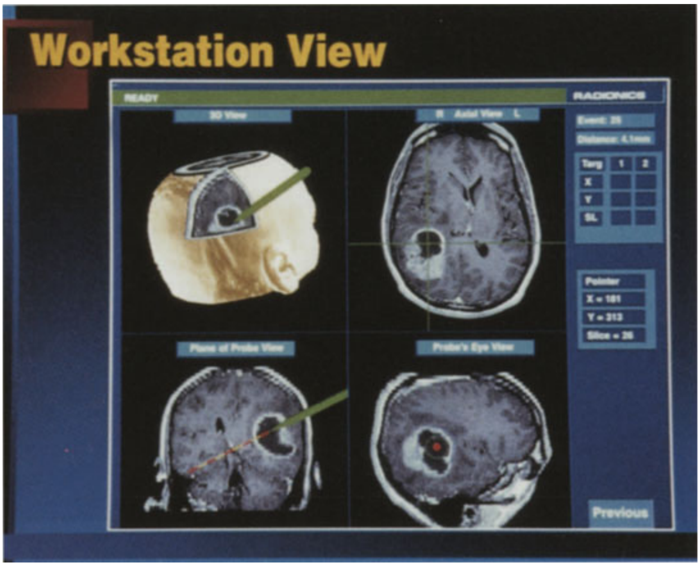

Fig. 2. Workstation views of a right-posterior parietal tumor: three-dimensional image, axial view, and plane of probe view

identify the point on the CT scan, then the left frontal staple on the patient's head is touched with the operating arm for registration and the foot pedal is pressed to record the localization. This is done for four different staple points. To reduce error, staples are placed on the scalp in a vertical position and the upper point of the staple used for registration. If the staple appears on more than one slice of the CT scan on the computer workstation, then the point on the upper slice is chosen as the registration marker. After touching each reference point, the registration point is completed and the operating arm now operates in a spatial context. If the error in registration and calibration is more than 5 mm, the computer does not allow the user to proceed any further without checking the registration process.

After the reference marks are selected and planning and registration are complete, the system displays a three-dimensional rendering of the patient's head and allows the surgeon to rotate the image, usually so the orientation is the same as the surgeon's view of the head on the operating table. The relationship of the arm's probe relative to the patient's imaging is then displayed in a variety of formats (Fig. 2).

The three-dimensional view is helpful for overall orientation. The standard axial and coronal slice at the probe location can be interactively updated. The surgeon's eye view and plane of probe view facilitate the planning of the optimal incision size and trajectory. Switching between different modes of viewing is easily accomplished, without the need of a technician and without leaving the sterile field, by the "Arm as a Mouse" software. If the arm tip is pulled more than 15 cm from the head, the menu on the computer screen will change and the surgeon can choose which format he wishes to view simply by clicking on the foot pedal.

Results

Since the installation of the OAS at St. Vincent's Hospital, Sydney, in March 1994 and of a second system at the Concord Repatriation Hospital in January 1996, 106 cases have been handled using frameless and computer-assisted surgery. Of these 106 cases, there were 42 framed cases using the conventional CRW stereotactic frame (Radionics) and 64 frameless cases using the staples for registration. All cases except 1 utilized the Phillips CT Scanner (Phillips, Best, The Netherlands); 1 MRI stereotactic biopsy used the GE Scanner (G.E., Waukesha, WI, USA). Functional cases for thalamic stimulation were all performed on the GE MRI Scanner, but these are not included in this series. However with the new software update that has the functional stereotactic atlas, future functional cases will utilize the computerized stereotactic system.

The frameless cases were handled with fiducial markers placed either on the day of surgery or as much as 3 days before surgery. (If surgery was to be performed on a Monday, then the staples placement and registration in the CT scan was routinely done on the preceding Friday or Saturday.) All the framed cases were for stereotactic biopsy. Of the frameless cases, 20 were for localization of lesions both immediately preoperatively with the patient on the operating table and intraoperatively once the craniotomy had been turned. There were 32 cases requiring volumetric resection of tumours, mainly gliomas, and 12 cases for stereotactic biopsy of larger mass lesions.

Discussion

Frameless and computer-assisted stereotaxy allows intraoperative imaging and localization of cranial coordinates. At present, mechanical digitizers are the most widely used form of intraoperative frameless localization. The Operating Arm System uses a mechanical arm together with computer hardware and graphics software and is currently the most common frameless stereotactic system in use in Australia. This system has a number of advantages over its commercially available competitors, including simplicity of use and the "Arm as a Mouse" software; it can be used for both framed and frameless stereotactic procedures and for preoperative planning (Fig. 3a) or intraoperative interactive localization (Fig. 3b), and continual software upgrades are available.

Its simplicity of use is one of the major advantages of the OAS. The user-friendly software allows the neurosurgeon to rapidly master the use of the equipment without an extensive knowledge of computer programs. Technical support is not required during the course of the operation. The "Arm as a Mouse" software is easy to use and allows the surgeon to change the menu on the computer screen without the need of an assistant and without a break in sterile technique. If the arm tip is pulled more than 15 cm from the head, the mode of viewing of the computer data can be changed simply by moving the arm up or down.

The OAS can be used for both framed and frameless stereotactic procedures. The OAS can be used in conjunction with the conventional Cosman–Roberts–Wells (CRW) (Radionics) head ring. The computer-assisted OAS does not make the CRW stereotactic frame obsolete and enhances the use of the CRW head ring, particularly for biopsy of high-accuracy cases, such as the brainstem, where the stability of the head ring is essential.

With a normal framed stereotactic case, coordinates are taken from the CT scan console, recorded on the CRW worksheet, and then transferred to the Radionics SCS-1 computer to determine the three-dimensional coordinates of the chosen target. Each step of this process has a potential for error in the transcribing of the values, particularly in relation to positive and negative values. Using the OAS, this process of recording and transcribing the data is avoided. The images from the CT scan are transferred to the computer workstation by magnetic tape, optical disk, or Ethernet cable. The nine fiducial points are then registered by the "mouse" and three-dimensional coordinates are then given to any target chosen. Using the OAS for framed stereotactic cases has the advantages of reducing human recording of coordinates, allowing for interactive target localization in the event that a previously chosen target biopsy has been nondiagnostic and, with the use of the multiplanar formats of the images, choosing trajectories to avoid damage to eloquent areas of the brain (Fig. 4).

The major use of the OAS is for frameless stereotactic procedures where the conventional head ring is not necessary, allowing not only for patient comfort but also a larger approach area. CT or MRI scans can be performed without the time constraints imposed by the frame-based applications, and the CT scans and loading of the image data into the OAS workstation can be done days before surgery so long as the staples used as skin markers remain in place. The frameless system can be used for anatomical localization of small or superficial tumors, both on the surface of the scalp, or the

a

b

Fig. 3a,b. The Operating Arm System (OAS) is used for both preoperative registration (**a**) and intraoperative localization (**b**)

cortical surface intraoperatively, particularly when the tumor lies below this cortex and there is no surface change to indicate its precise location. This is particularly useful for localizing small subcortical metastases (Fig. 5).

The OAS frameless system is also used for volumetric resection of tumors, particularly gliomas, where the brain–tumor interfaces are not well demarcated (Fig. 6). Real-time interactive updates are shown on the computer, and the axial, sagittal, and

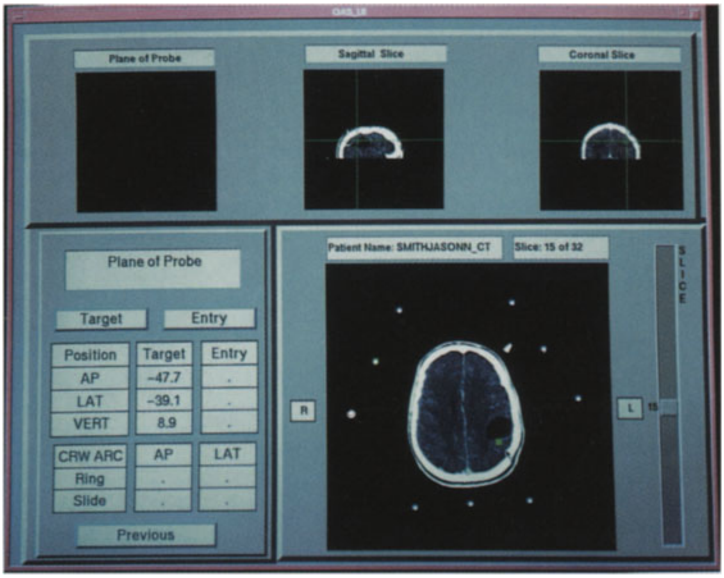

Fig. 4. The OAS used for framed stereotactic cases: coordinates of the target and the axial, sagittal, and coronal views aid in determining the most appropriate trajectory

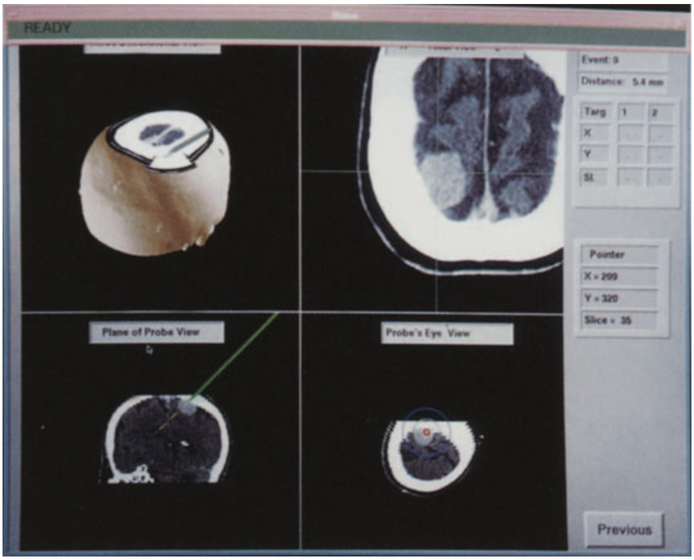

Fig. 5. Use of the OAS in determining the location of a small convexity meningioma in the right-posterior parietal region

coronal planes allow the surgeon to visualize the boundaries of the tumor as shown on the CT scan while tumor resection is under way. Brain shift during the operative procedure can be a potential source of error, but this should be minimal if care is taken with the removal of any cerebrospinal fluid and if tumor margins are outlined using the computer before any debulking procedure. Volumetric resection of a tumor is complete only as far as the information on tumor boundaries provided by the CT or

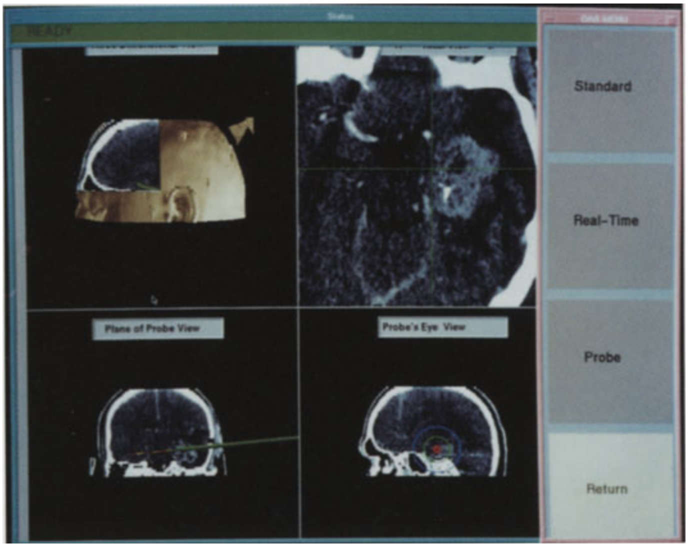

Fig. 6. Use of the OAS in the volumetric resection of a mesial temporal lobe glioma

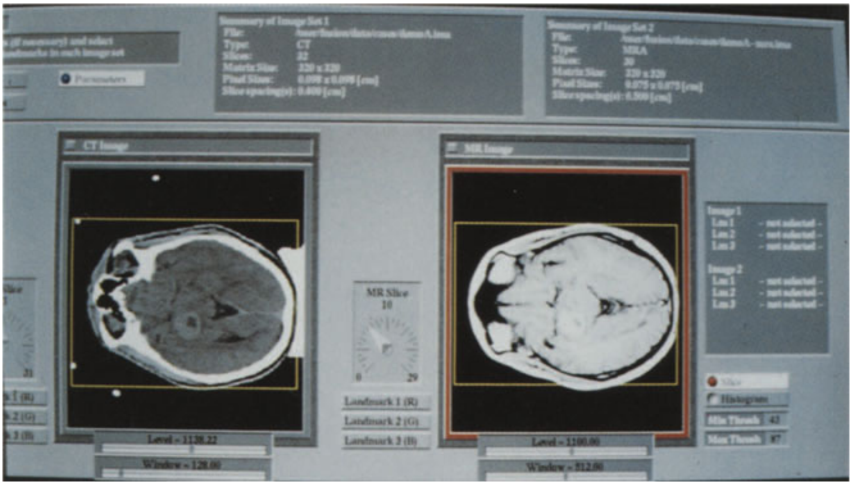

a

Fig. 7a–c. Image fusion of CT and MRI images shows computer workstation planning for fusion (**a**) and slice overlay verification in the axial (**b**) and coronal (**c**) planes

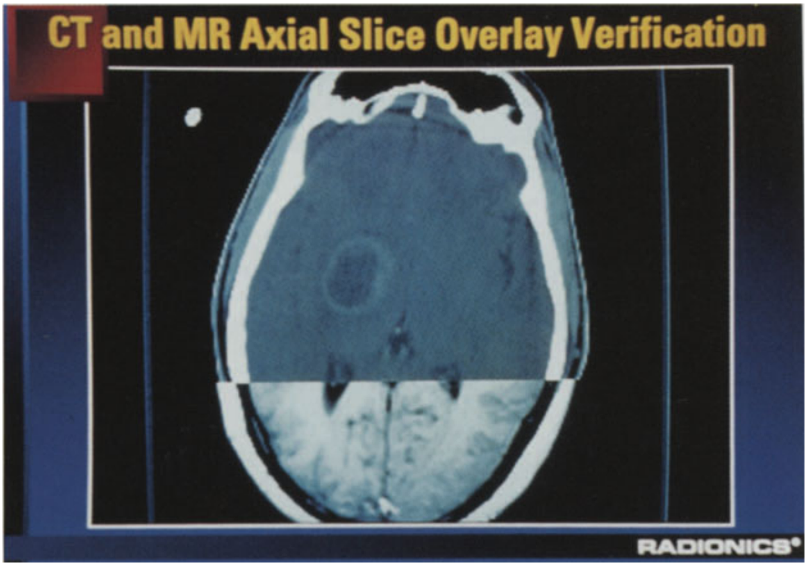

b

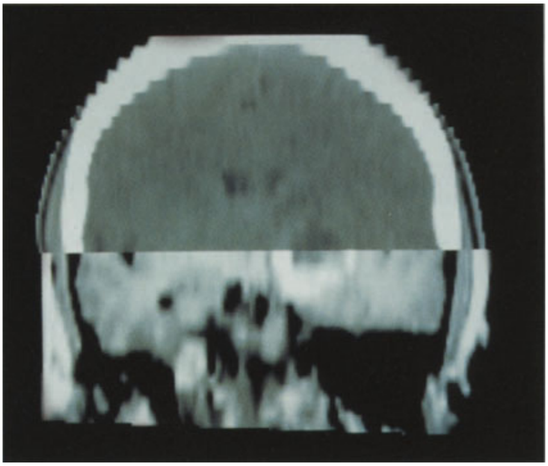

c

Fig. 7a–c. (*Continued*)

MRI data, and this does not allow for microscopic infiltration within regions of edema surrounding the tumor.

As with the frame-based stereotactic systems, there is an inherent error in the OAS and other frameless systems. Guthrie studied both phantom and real patients for error [6,7]. With 40 targets on phantom testing, the average error was 2.8 mm, ranging from 0 to 6 mm. With real patients and 33 target points, the average error was 3.8 mm. The patient must lie still during acquisition of the data on the CT scan. CT couch movement errors are avoided by observing the console data during the CT scan. When using staples as reference points, the staples should be placed as far apart as possible and the same point of the staple used for registration. If a surgeon misses a calibration point, error will be introduced.

The OAS allows for software updates as new programs become available. The most recent software update includes a program for image fusion and a functional stereotactic atlas. The image fusion program merges the CT and MRI images to give greater anatomical detail, particularly for lesions such as gliomas that may not be as obvious on the CT scan as on the MRI scan (Fig. 7). A regular MRI scan is stored on DAT tape and when fed into the stereotactic workstation can be merged with a CT scan taken in stereotactic space in the usual fashion. The fused image is then used for a more accurate resection of the tumour. The functional stereotactic atlas improves the accuracy of calculating targets for functional neurosurgery. When a target is chosen on the CT or MRI scan for radiofrequency lesioning or the insertion of deep brain electrodes for stimulation, the stereotactic atlas can be merged with the CT scan and the corresponding nucleus of the thalamus or area of the globus pallidus identified. There is also a spinal software package, which aids in the placement of pedicle screws for lumbar fusion procedures.

As each new software program becomes available there will be wider applications of computer-assisted and frameless stereotaxy, making it a necessary part of everyday neurosurgical procedures. The OAS is at the forefront of these developments and is recommended for use by neurosurgeons interested in learning to use a frameless stereotactic system.

References

1. Apuzzo MJ, Chandrasoma PT, Cohen D, et al (1987) Computer imaging stereotaxy: experience and perspective related to 500 procedures applied to brain masses. Neurosurgery 20:930–937
2. Bradford R, Thomas DGT, Bydder GM (1987) MRI-directed stereotactic biopsy of cerebral lesions. Acta Neurochir 39:25–27
3. Thomas DGT, Nouby RM (1989) Experience in 300 cases of CT-directed stereotactic surgery for lesion biopsy and aspiration of haematoma. Br J Neurosurg 3:321–326
4. Pell MF, Thomas DGT (1991) The initial experience with the Cosman-Roberts-Wells stereotactic system. Br J Neurosurg 5:123–128
5. Pell MF, Thomas DGT, Krateminos GP (1993) Stereotactic management of intrinsic brain stem lesions. Ann Acad Med Singapore 22:447–451
6. Guthrie BL (1994) Graphic-interactive cranial surgery: the operating arm system. In: Pell MF, Thomas DGT (eds) Handbook of stereotaxy using the CRW apparatus. Williams & Wilkins, Boston, pp 193–211
7. Guthrie BL (1993) Graphic interactive cranial surgery. Clin Neurosurg 41:489–516
8. Roberts DW, Strohbehn JW, Hatch JF, et al (1986) A frameless stereotactic integration of CT imaging and the operating microscope. J Neurosurg 65:545–549
9. Watanabe E, Watanabe T, Manake S, et al (1987) Three-dimensional digitizer (Neuronavigator): new equipment of CT-guided stereotaxy surgery. Surg Neuro 27:543–547
10. Watanabe E, Mayanazi Y, Kosugi Y, et al (1991) Open surgery assisted by the Neuronavigator, a stereotactic articulated sensitive arm. Neurosurgery 28:792–799
11. Guthrie BL, Kaplan R, Kelly PJ (1990) Neurosurgical stereotactic operating arm. Stereotactic Funct Neurosurg 54/55:497
12. Guthrie BL, Adler JR Jr (1992) Computer-assisted preoperative planning, interactive surgery and frameless stereotaxy. Clin Neurosurg 38:112–131

13. Zinreich SJ, Tebo SA, Long DM, et al (1993) Frameless stereotaxic integration of CT imaging data: accuracy and initial applications. Radiology 188:735–742
14. Sandeman DR, Patel N, Chandler C, et al (1994) Advances in image-directed neurosurgery: preliminary experience with the ISG Viewing Wand compared with the Leksell G Frame. Br J Neurosurg 8:529–544
15. Kitchen ND, Lemieux L, Thomas DGT (1993) Accuracy in frame-based and frameless stereotaxy. Stereotactic Funct Neurosurg 61:195–206
16. Barnett GH, Kormos DW, Steiner CP, et al (1993) Intraoperative localisation using an armless, frameless stereotactic wand. J Neurosurg 78:510–514
17. Reinhardt HF, Zweifel HJ (1990) Interactive sonar-operated device for stereotactic and open surgery. Stereotactic Funct Neurosurg 54/55:393–397
18. Reinhardt HF, Horstmann GH, Gratzl O (1993) Sonic stereometry in microsurgical procedures for deep-seated brain tumours and vascular malformations. Neurosurgery 32:51–57
19. Bucholz R (1993) Frameless stereotaxy and intraoperative navigation. Practical course presented at the International Congress of Neurological Surgeons, Vancouver, British Columbia, 1993
20. Kato A, Yoshimine T, Hayakawa T, et al (1991) A frameless, armless navigation system for computer-assisted neurosurgery. Technical note. J Neurosurg 74:845–849
21. Tan KK, Grzeszczuk R, Levin DN, et al (1993) A frameless stereotactic approach to neurosurgical planning based on retrospective patient-image registration. Technical note. J Neurosurg 79:296–303
22. Roberts TS, De Soto LA, Haynor DR (1994) Electromagnetic navigation systems: use with the CRW. In: Pell MF, Thomas DGT (eds) Handbook of stereotaxy using the CRW apparatus. Williams & Wilkins, Boston, pp 213–217
23. Barnett GH, Kormos DW, Steiner CP, et al (1993) Use of a frameless, armless stereotactic wand for brain tumor localisation with two-dimensional and three-dimensional neuroimaging. Neurosurgery 33:674–678

Introduction of the Passive Marker Neuronavigation System VectorVision

Stefan Vilsmeier and Fotios Nisiropoulos

Summary. The VectorVision neuronavigation system from BrainLAB is the most advanced image-guided surgery system currently available. Its unique wireless passive marker technology enables real freehand guidance and easily integrates all kinds of instruments. Intelligent software functions and advanced three-dimensional visualization provide the physicist with all necessary image reconstructions. Microscopy, neuroendoscopy, and ultrasound imaging as well as spinal applications are modular integrated and fully implemented into the software. VectorVision facilitates surgery that is less invasive. The system's more targeted approach allows smaller incisions and craniotomies. Easy and safe intraoperative localization of deep-seated lesions as well as differentiation of normal and lesion tissue are supported. Combined, these features reduce the risk of complications and save time and cost. Easy on-site calibration minimizes downtime and the need for outside service.

Key words. Passive marker technology—Quick patient referencing—Multiple instrument—Ultrasound integration—Neuroendoscopy—Microscopy—Spinal application

Introduction

The ability to noninvasively visualize intracranial structures has been revolutionized by advancements in diagnostic imaging. Although many refinements in visualizing diagnostic data obtained from CT, MR, and other imaging modalities have been developed, there was no dynamic link of a three-dimensional (3-D) image to the surgical procedure. As a result, the surgeon had to transform the diagnostic images into a mental picture to create this link of 2-D data to 3-D patient anatomy as seen during surgery so as to perform the procedures less invasively and with as little trauma as possible.

Previous attempts have been made to develop technologies to transform 2-D images into clinically useful 3-D representations within milliseconds with the highest accuracy. In general, three technological steps were developed:

BrainLAB GmbH, Medical Computersystems, Ammerthalstr. 8, 85551 Heimstetten, Germany.

1. In the beginning, articulated mechanical arms were developed to perform image-guided surgery. This technology is based on potentiometers that are built into the joints and, depending on the inclination and the corresponding resistor value, deliver the 3-D position data of the arms to a workstation. The varying tolerances of the resistors, however, precluded achieving the necessary accuracy. Although the potentiometers were replaced by very expensive rotary encoders, the systems still suffered too many restrictions and did not have the capability of extension of the surgeon's personal skills.
2. Ultrasonic-based systems were, later, a small step toward more flexibility, but their accuracy was insufficient and their use cumbersome, so this technology appeared only briefly in the evolution of surgical instruments.
3. The development of optical tracking systems was another big step forward, representing today's standard technology in image-guided surgery, but also had to go through an intermediate stage. The first generation of these systems was pointing devices equipped with active infrared light-emitting diodes (LEDs) that are tracked by a stereoscopic camera array. Each camera image is separately digitized and converted into a fixed set of 3-D coordinates. A workstation then calculates the actual position of the instrument with respect to a fixed reference in the 3-D space. However, the cables that are attached to the instruments to provide the power supply for the LEDs often disturb the surgeon during a procedure. The angular flexibility and freedom of movement is strongly reduced by the small shape and the limited light-emitting angle of the LEDs, because the cameras of optical tracking systems need an unobstructed view to the tools to track them continuously.

Sterilization further appeared as a considerable problem: the built-in electronics in the tools, which are all proprietary to each manufacturer, cannot be autoclaved but must be gassterilized. Even then, the reliability of the electronic parts is not satisfactory. All these issues represent a step back rather than real progress. It is, however, not the technology of tracking instruments optically that is lacking but the marker technology. Instead of tracking tiny infrared LEDs, BrainLAB developed a neuronavigation system that tracks the reflections of infrared light and not the light source.

Passive Marker Technology

BrainLAB VectorVision is an intraoperative image-guided localization system. It links a freehand probe, tracked by a passive marker sensor system, to virtual computer image space on a patient's preoperative CT or MRI images. The system consists of two infrared cameras that emit infrared flashes. These flashes are reflected by passive marker spheres mounted on the Mayfield headrest and selected surgical instruments. The infrared reflection images of the markers are digitized by the two cameras, each of which "sees" the markers on the Mayfield headrest and instruments from a different angle. The software uses both images to calculate the 3-D position of each marker sphere and therefore the 3-D position of the entire instrument relative to the headrest, which is rigidly fixed to the patient's head.

When designing the software, one of the major challenges was to determine the identity of the various marker images seen by each of the cameras. Which markers seen by one camera correspond to which markers seen by the other camera? In addition, it was necessary to deduce which markers correspond to which tool. This is a specific problem that only occurs in passive marker systems, making the software design much more complicated than that for mechanical or active infrared systems. BrainLAB solved these questions by tracking the sequential instrument positions as they move. Using known distances and other geometrical information available, the software is able to deduce the identity of the markers. As described, this principle requires that the cameras have an unobstructed view of the tool markers at all times that navigation is desired during surgery.

Diagnostic Examination

To provide a link between patient anatomy and the diagnostic image data, it is necessary to establish a fixed reference between these two points. The system needs to know the patient's orientation in 3-D space relative to the cameras. For this purpose BrainLAB developed special low-profile markers—to reduce skin movement—that are adhered to the patient's skin before starting the diagnostic imaging. These markers consist of two parts, an adhesive socket that is attached to the patient's scalp near the area of projected exposure and draping and an 8-mm spherical aluminum marker which is inserted into the sockets for preoperative CT (Figs. 1,2). This design allows us to scan the patient the night before the procedure and also allows the patient to sleep with the attached sockets only. Usually, the sockets are well tolerated and do not fall off while the patient sleeps. For security, a circle can be drawn with a felt-tip marker around the sockets so they can be reattached in the right place if the patient loses them overnight.

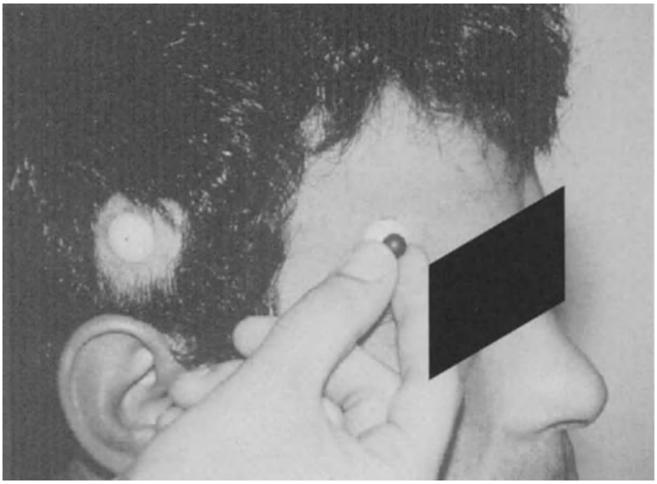

Fig. 1. The spherical CT markers are attached to the patient's scalp near the area of projected surgical exposure and draping. Marker sites are selected on minimally mobile scalp areas

Fig. 2. Diagnostic CT examination of the patient

The marker sites are selected on minimally mobile scalp areas to provide proximity to the planned surgical site so they can be palpated under surgical draping and to provide as much distance as possible between individual sites. Although only three marker sites are essential, the attachment of two more is recommended to provide redundancy; the software can handle up to five markers. After the diagnostic examination the spherical aluminum markers are replaced by indented patient fiducials and inserted into the sockets. The cone in the middle represents the center of gravity of the spherical markers and ensures precise referencing of the patient, because a defined point is used for registration. Further, the physician can locate and register them easily, even after the patient has been draped for surgery, before or at any time during the procedure. Because all VectorVision's components can be used in a sterile environment, the process of registration is truly straightforward.

Lesion Segmentation

While the patient is en route to surgery, the CT images are archived on an optical disk or transferred via network to the VectorVision workstation. After only a few seconds, the CT images are displayed on the computer screen and the doctor rapidly delineates the lesion volume of interest. The software automatically generates a 3-D anatomical volume image, fusing the CT image data acquired that morning with a series of preoperative MR scans. This enables the doctor to view the 3-D image of the complex lesion, and adjacent neural and vascular structures, from all angles. After only 15–20 min, the surgeon has developed a strategic plan for the optimal surgical approach. Meanwhile the patient has been transferred from the holding area into the operating room (OR) (Figs. 3,4).

As VectorVision runs under Windows NT, the most widely available and powerful state-of-the-art operating system on PCs and workstations, the physicist can also plan the procedure on a notebook remote from the workstation and save the plan on a diskette to transfer it later in the OR so that the plan can be explained to the patient, or others, before the operation.

System Calibration

In contrast to the camera arrays of the very first optical tracking systems, BrainLAB uses only two cameras with high-resolution field matrix CCD chips. The cameras are not built into a housing but screwed flexibly to a camera bar; this enables adjusting the cameras individually to each specific OR setup. Instead of keeping the cameras mounted to the camera bar, a stationary ceiling-mounted system is also easily possible. When the angle or the distance between the cameras is changed or readjusted, a quick and easy calibration procedure is then performed by the user.

Calibration is performed by waving a calibration rod with two reflective marker spheres with a defined distance between in front of the cameras (Fig. 5). After a few seconds an acoustic signal indicates that the surgical space has been established as a set of coordinates within the system. An automatic safety limit of <0.30 mm for

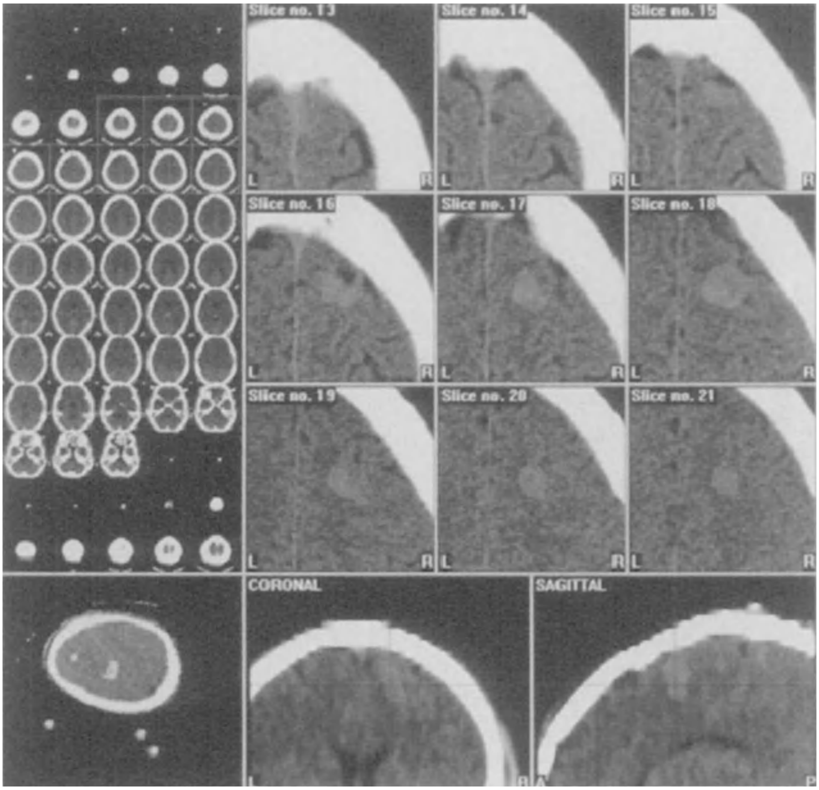

Fig. 3. Multiple displays and reconstructions enable a precise and more targeted preplanning of surgical approach

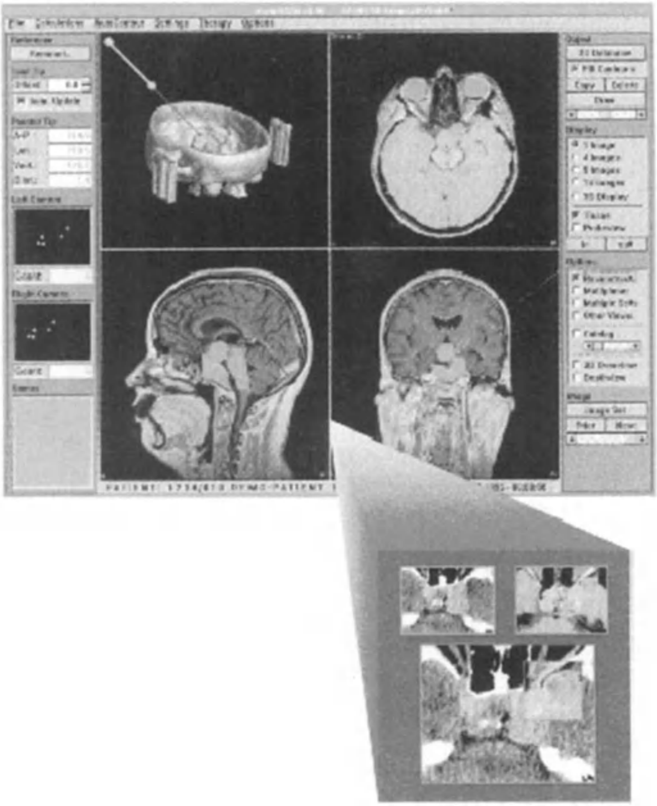

Fig. 4. The image fusion of CT and MRI provides the physicist with more detailed visual information on both soft tissues and bony structures

calibration accuracy ensures precise calibration results. Under normal conditions the cameras need not to be calibrated before every procedure, but sometimes when the system is moved between ORs, the cameras can bounce against doors or walls and the relative position between the cameras becomes misadjusted. Thus, this simple calibration procedure enables the users to recalibrate the system themselves within seconds for quality assurance without needing to return the system to the manufacturer or to accept shortcomings during steady use of the system.

Patient Preparation

The logistic course for a procedure always requires accurate planning and organization to ensure a safe and time-efficient operation without any unnecessary delay or disturbance. The strict observance of sterility is of course one of the main issues here. Thus, the OR staff is trained carefully and has gained experience in handling preparation in the OR as a routine. For that reason, integration of an additional device such

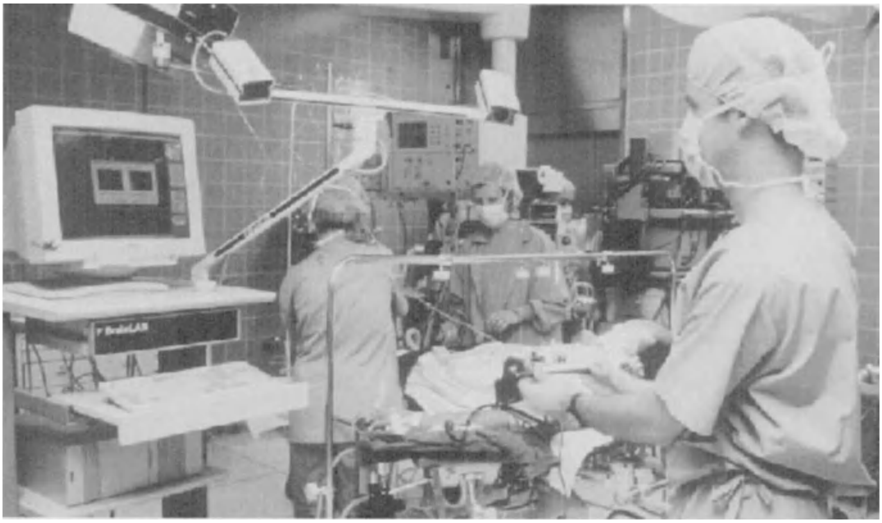

Fig. 5. Calibration of the infrared cameras is easy and quick

as a neuronavigation system must not cause considerable delays in the logistic course. The preoperative preparation course for VectorVision and the referencing of the patient has taken all such issues into account.

As already mentioned, the spherical CT markers are replaced after diagnostic imaging by the indented fiducials for patient referencing simply by a few turns (Fig. 6). After intubation and positioning in the Mayfield (OMI, OH, USA) headholder, the patient is draped with a sterile transparent 10 × 10 drape. Then, the autoclavable reference clamp, equipped with disposable reflective marker spheres, is attached to the headholder to establish the system's coordinate space.

Up to this point no delay or disturbance of preparation has been caused by the use of VectorVision. Also, sterility is not affected at any time (Fig. 7). The registration process of the patient is also done in the sterile environment. All components of VectorVision are autoclavable, as is the reference clamp or the pointer tool, and equipped with disposable marker spheres, and thus sterile.

After then entering the VectorVision mode in the software, the system detects and extracts all patient markers by knowing their density and shape automatically from the image set within a second. Now, the physician just touches the center of the indented fiducials, covered by the transparent plastic drape, with the sterile pointer tool in any order for some seconds until each is confirmed by an acoustic signal. The fiducials have a unique shape, so they can easily be found even under a thick linen drape (Fig. 8a,b). To register the patient, at least any three markers must be identified. If any one of the five attached markers should be unreachable with the tool or has fallen off, the surgeon then retouches an already identified fiducial to proceed. The total referencing process requires only about 2 min and is unmatched by other systems in easy, safe, and time-efficient use. Also, logistic course and sterility are not affected [1].

Fig. 6. Preparation of the patient: the spherical CT markers are replaced by the indented patient fiducials for patient registration

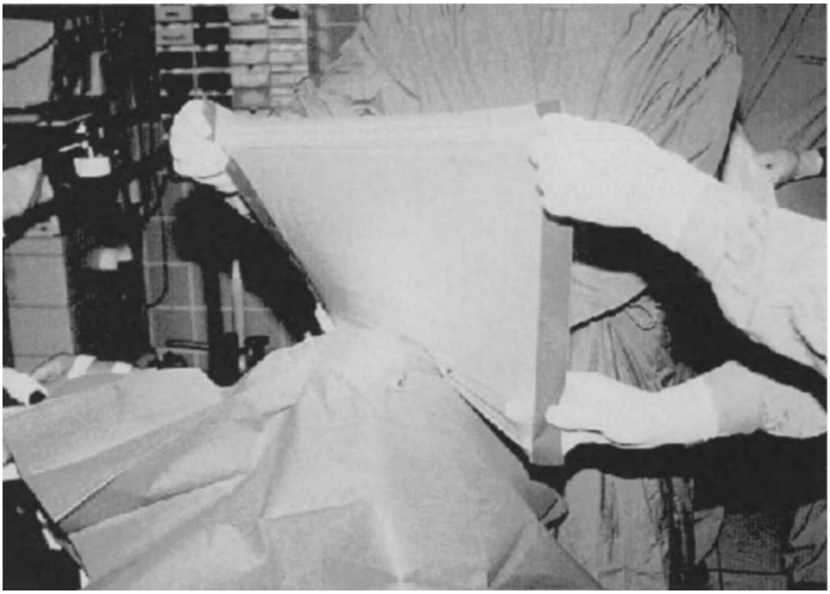

Fig. 7. After sterile prep, a clear transparent total-region adhesive Vi-drape is applied over the operative site and the patient markers. Surrounding areas are draped in the traditional way

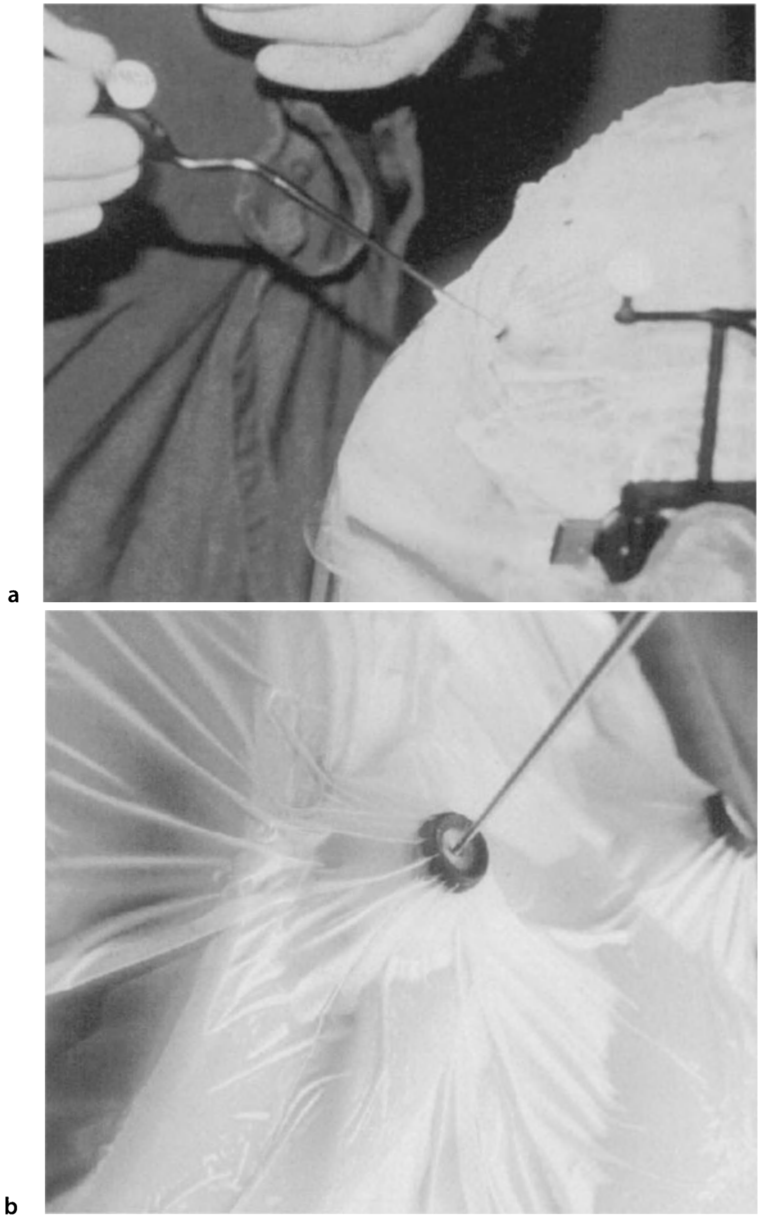

Fig. 8a,b. The tip of the gas- or autoclave-sterilized VectorVision probe is touched to each of the five conical markers on the patient's scalp. Within moments, the BrainLAB software automatically registers this data, calculating each coordinate link with the corresponding marker point from the CT data set. Subsequently, the software continuously tracks the probe's position as it relates to the preoperative diagnostic data

Use of Multiple Instruments and Ultrasound Probes

One of the unique advantages of passive marker technology is that it is easily adaptable to any already existing instrument in the OR. Every physician is accustomed to his or her own armamentarium and likes, for example, the balance or the feeling of the spring of a certain bipolar forceps. The pointer tool alone has no further function other than pointing to a target or planning an incision. So, why not combine all these features and use a suction device or a favorite forceps simultaneously as a pointer? Of course, other systems already provide proprietary instruments that are equipped with LEDs and again are wired and cumbersome to sterilize. But are they as fine as the existing ones?

BrainLAB thus designed different lightweight passive marker arrays that can simply be attached with adjustable brackets to any instrument, enabling its simultaneous use during procedure (Figs. 9,10). After mounting one of the four arrays to the instrument it must only be calibrated in its length. This is done by touching the indented center of the reference tripod on the Mayfield headholder for a few seconds. The software then recognizes automatically the specific array and calibrates the length

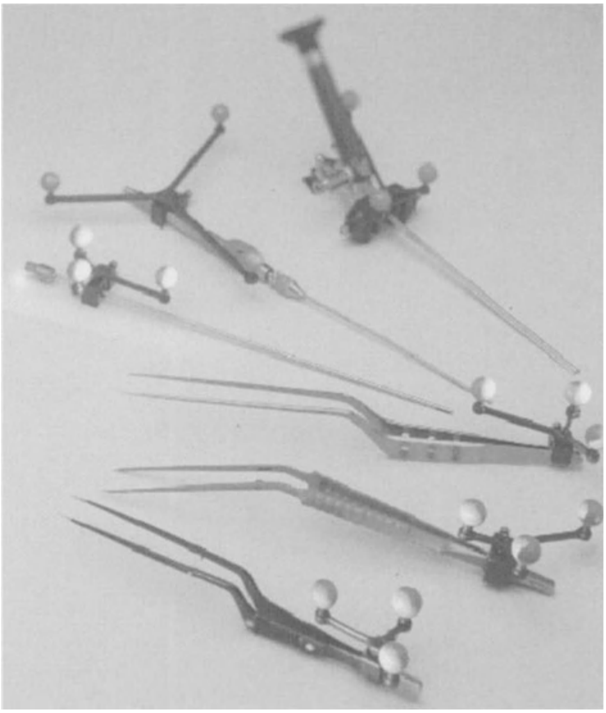

Fig. 9. VectorVision universal adapters allow the surgeon to attach the passive markers to any, and all, preferred instruments

of the instrument (Fig. 11). In this manner, a bipolar forceps is turned into a pointing device and the surgeons do not have to change their tool.

Further, new and efficient operation techniques and applications have been developed; for example, image-guided endoscopy is now possible by just attaching a marker array to the rigid endoscope and calibrating the endoscope's length. The reduced visibility of structures in the immediate vicinity of the endoscopic lens is a well-known phenomenon in neuroendoscopy that bears a considerable risk for unwanted destruction of tissue during procedure. By linking image-guided surgery and endoscopy so that the tip of the endoscope is projected on the corresponding CT scans of the patient, which automatically appear on the computer monitor depending on the movement of the endoscope, ventriculocisternostomy can be performed less traumatically, enabling far more extensive dissection and excision of tissue.

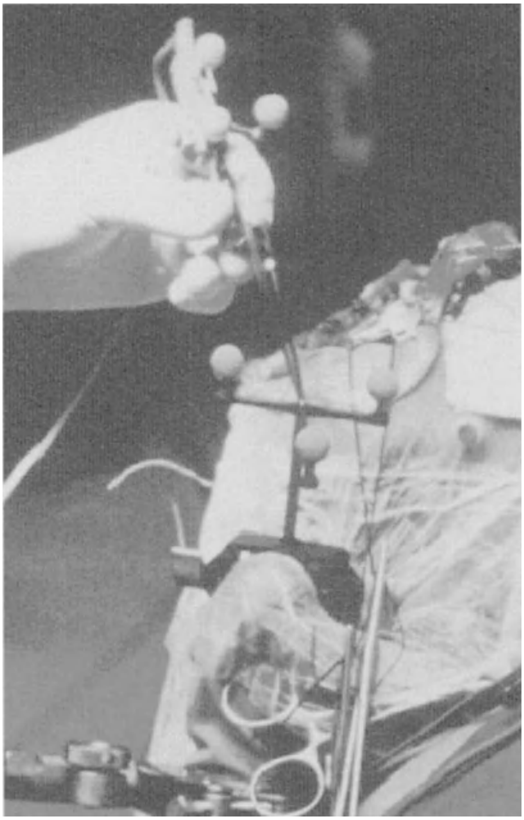

Fig. 10. VectorVision supports the surgeon in achieving lesion access and identification, as well as total lesion resection, without impact on vital structures and with a minimum of collateral damage from the entry corridor or from undue mechanical impact on proximate neural and vascular structures

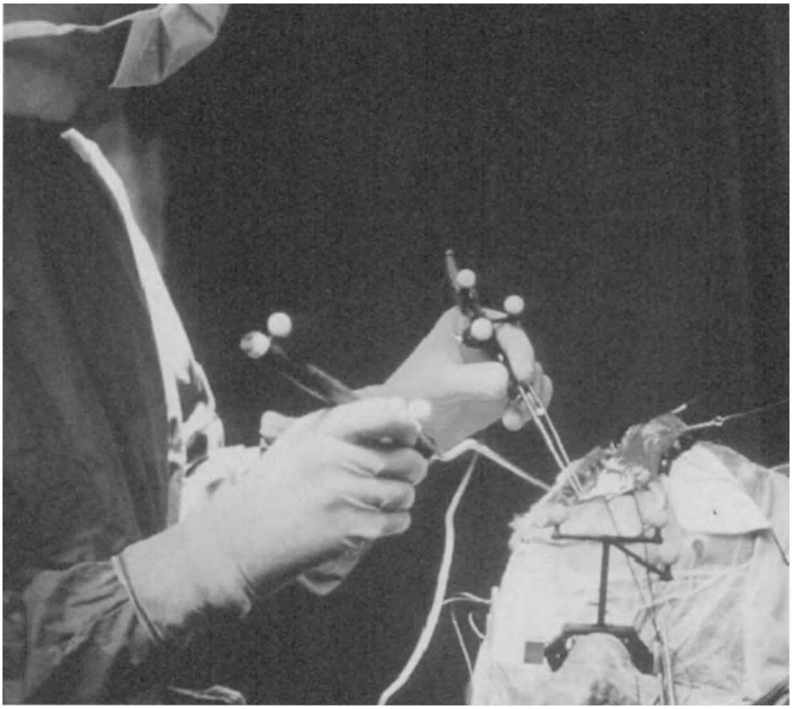

Fig. 11. The surgeon registers the tip of the forceps at the calibration cone of the marker array mounted to the Mayfield (OMI, OH, USA). This supplies the software with the offset of the tip of the forceps relative to the attached reflective markers. Now, the forceps can be tracked simultaneously with the probe.

The integration and implementation of ultrasound images into VectorVision is a further step forward in image-guided surgery to control anatomical changes intraoperatively. Currently the physician must rely on preoperative CT and MR images to reach a planned target or to avoid critical structures in different brain regions. As the procedure continues, however, the more the intraoperative changes differ from preoperative anatomical conditions by brain shift.

VectorVision displays the scan plane of a calibrated ultrasound probe that is equipped with a marker array and also shows the corresponding reconstruction in the CT and MR image sets, including a colored outlined lesion either as a superimposed video image or in an extra display beneath the ultrasound image. In this manner, visualization and quantification of the anatomical shift are easy for the physician. Further stages for acquiring a 3-D ultrasound image by a rotating ultrasound head and by morphing the preoperative diagnostic images to the intraoperative ultrasound images are in preparation and can support the surgeon as a "magic eye."

Because passive markers need no electrical supply, even applications in an open MR become interesting as no signal disturbance is caused by the marker arrays. The implementation of ultrasound is certainly the more comfortable and economical alternative to open MR scanners.

Microscope Tracking

Based on the same principle, not only "common" instruments or ultrasound probes are tracked by VectorVision, but also microscopes with and without built-in robotics are integrated into the system. The pointer tip is hereby represented by the focal point of the microscope so that the microscope is operated like a virtual pointing device. According to the adjusted focus all available reconstructions are reformatted on-line in VectorVision. The 3-D position of the microscope head is determined by a marker frame that contains several redundant marker spheres to provide a maximum tracking angle $>180^\circ$ and to maintain the flexibility and maneuverability of the microscope (Fig. 12).

The VM900 microscope (Möller-Wedel, Wedel, Germany) offers an external bidirectional computer interface that provides X–Y position data of the motorized axes and data of the focal length and zoom factor. These data sets are read out and processed by the BrainLAB workstation. Alternatively, the VectorVision software can send data to the microscope and control the built-in robotics the same way. By having access to these data and parameters, a "smart" Autofocus function was developed by BrainLAB. In contrast to Autofocus of other microscopes, which adjusts the focus mostly only to

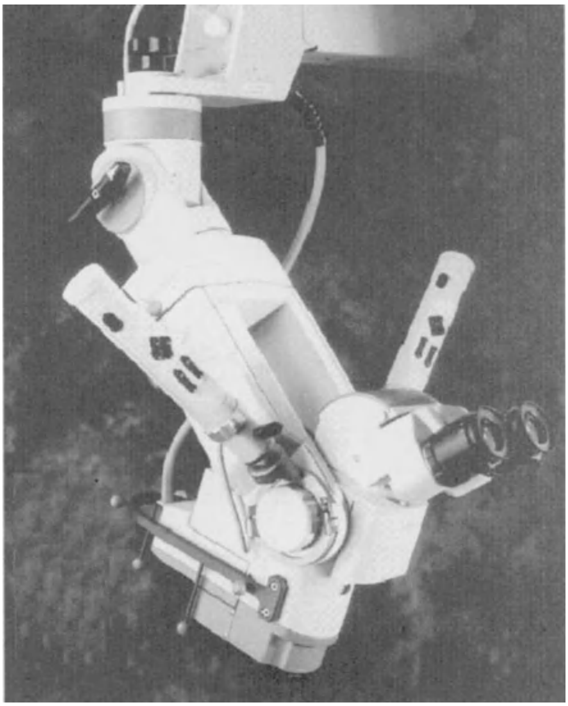

Fig. 12. VectorVision has the capability to incorporate visual information from operating microscopes. The microscope is supplemented with a marker ring, which contains BrainLAB reflective marker spheres to determine its 3-D position

the middle of the field of view, VectorVision adjusts the focus always to the pointer tip, respective to the level of the tip, so that exactly the desired area of interest within the field of view is focused automatically. The corresponding preoperative image slices and reconstructions are again updated to the focus, and a separate window on the computer screen displays the outlined lesion and the superimposed video image taken from the microscope camera in the corresponding area of interest.

The same video overlay of computer-generated images and microscope images is also available in a heads-up-display (HUD), which keeps the surgeon constantly informed without the need to move the eyes between the remote computer screen and the ocular. BrainLAB also supports microscopes that do not offer access to focus parameters or are not equipped with robotics, such as Zeiss or Leica. Therefore, a similar autofocus function but with a fixed focus is implemented and the depth of field utilized. Although the focus remains fixed over a certain range, the reconstruction plane according to the pointer tip is superimposed on the microscope's video image and that way delivers an acceptable match.

Because VectorVision "knows" at any time the 3-D position data of all utilized tools and has access to the motorized *X–Y* axes of the microscope, it can induce it to track an instrument continuously and to focus to the instrument tip. As long the instrument remains within the field of view the microscope will keep still so as not to disturb the surgeon's work. As soon the instrument leaves the field of view, the microscope will follow it and readjust automatically without any need to touch the microscope's steering handles. Issues of balance and maneuverability of a microscope thus become secondary.

Even the adjustment to preplanned trajectories or points for certain approaches is integrated, and the trajectories mirrored into the HUD supply the physician with further safe and helpful guidance to the preplanned target. Also, specific operation techniques as the target-centered pivoting function around a certain point are enabled by VectorVision, for example, an optical access under a craniotomy with automatic re-focusing of the target or point of intersection of different viewing angles.

Spinal Applications

BrainLAB offers also a module for spinal applications, which become more and more interesting in conjunction with image-guided surgery systems. As for cranial procedures, it is necessary to establish a fixed reference of the patient in 3-D space. Because of the torsion of the vertebrae, this is far more difficult and challenging than with the rigid skull bone.

A reference clamp with reflective markers is attached at any level to span the coordinate space for the system. Specially designed flexible feet adjust automatically to the surface of the spinous process and ensure the rigid fixation of the reference markers to the patient. In this way, the patient is again dynamically tracked throughout the procedure. For registering the patient, several anatomical landmarks on bony structures are selected to perform a surface-matching procedure between the preoperative CT images of the vertebrae and their actual local relation under respect of torsion and luxation. This procedure improves the necessary accuracy and reformats the acquired image set to the anatomical conditions.

Different multiplanar reconstruction planes and spine-specific displays provide visual on-line information for placing pedicle screws or the percutaneous treatment of disk herniations. In this way, the surgeon attaches an adaptable marker array on the drill and uses it as a pointer to determine the entry angle and the correct orientation of the screw trajectory. Even the necessary screw length and diameter are adjustable and are displayed to simulate the volume of bone to be penetrated. An additional X-ray image with the C-arc is no longer necessary, and irradiation of the patient is avoided. The integration of ultrasound into the spinal module will also enable in the future the percutaneous treatment of far lateral disk herniations and minimally invasive procedures in the vicinity of L5.

BrainLAB recently introduced a patient fixation system based on a vacuum mouthpiece that completely immobilizes the patient's head. This device with attached markers enables stereotactic accuracy, but in a frameless manner, and serves as an excellent referencing system for anterior cervical approaches. The impression of the teeth delivers reproducible positioning of the patient.

Reference

1. Sipos EP, Tebo SA, Zinreich SJ, Long DM, Brem H (1996) In vivo accuracy testing and clinical experience with the ISG viewing wand. Neurosurgery 39:194–204

EasyGuide Neuro: A New Approach to Image-Guided Surgery

Manfred Baur

Summary. The EasyGuide Neuro system has been designed to support modern microneurosurgery. It allows for precise craniotomy and path planning and is a valuable tool to correlate the information contained within digital medical images (CT or MR images) with the patient's anatomy. EasyGuide Neuro provides information on the three-dimensional situation in the patient, minimizing the risk of damaging vital structures by giving precise local information.

Key words. Computer-assisted surgery planning—Precise localization—Real-time accuracy—Tracking—Ease of use

Introduction

Advanced experiments using image guidance systems in medicine were being performed as early as the late 1980s. Watanabe et al. [1] belong to the first generation of neurosurgeons using image guidance based on an electromechanical arm. In the same period, Adams et al. [2] reported a research project at the Aachen University of Technology (Aachen, Germany) on an optical navigator for brain surgery.

Recent advances in digital medical imaging technology in combination with improvements in terms of very fast processing power and system speed in general computer technology have allowed the development of fast and economically affordable three-dimensional (3-D) image calculation units. As a result the technology needed for reliable navigation systems became readily available, and image-guided surgery (IGS) is gaining widespread acceptance.

Equipment

The EasyGuide Neuro image-guided surgery system (Philips Medical Systems, Best, The Netherlands) was designed for stereotactic neurological surgery. The system is composed of dedicated software running on a SUN Sparc hardware platform and a

Philips Medical Systems Corporation, Philips Bldg., 2-Chome, Minato-ku, Tokyo 108, Japan.

Fig. 1. EasyGuide Neuro: combination of an optical three-dimensional (3-D) localization system and a digital workstation

20-in. video display mounted on a mobile trolley (Fig. 1). The 3-D optical position digitizer is a single unit (6 × 50 × 9 cm) composed of two 2-D infrared-sensitive CCD (chargecoupled device) cameras. The camera array is mounted on the rails at the side of the operating table and connected to the computer trolley via a detachable coaxial cable. The surgical instruments are straight and bayonet-shaped pointers of different lengths and bipolar forceps, each featuring three nonlinear infrared light-emitting diodes that are connected to the digitizer by a coaxial cable. The pointers can by autoclaved and for this reason do not require special sterilization procedures.

The system tracks the pointer movement and the pointer's tip is indicated on the display, superimposed on 3-D images calculated from previously acquired computed tomography (CT) or magnetic resonance (MR) images. Under the condition that the CCD cameras are active and the line of sight is undisturbed, the pointer location is continuously updated. To manipulate images from the operation table, an infrared remote controller is provided. This device may be put into a sterile plastic bag for system manipulation even under sterile conditions.

Procedures

Several procedures, involving different departments in the hospital, must be carried out to ensure correct functioning and reliable performance of the IGS device.

Head Marker Placement

The EasyGuide Neuro system requires the use of fiducial markers glued on the patient's head. At least 5 markers are needed for successful registration, and usually 9 to 11 are applied to increase accuracy. For CT imaging, disk-shaped markers made of an aluminum alloy are used. These aluminum markers have the advantage that marker registration with the EasyGuide Neuro system is a fully automatic process, requiring user interaction only when a marker remains undetected behind or close to complex high-density structures. For MR imaging, copper sulfate hydrogel-filled, adhesive markers are utilized. For accurate matching of the patient images to the actual position during surgery, the markers are glued to the patient's skin and preoperative scans then are made with the markers in place. The markers are left in place until surgery.

Data Transfer

Preoperative-acquired CT or MR images can be transferred from the imaging modality to the operation room either via an existing DICOM-compatible network or via sneaker net by using optical disks.

Image Viewing and Surgery Planning

Before surgery, images are viewed and evaluated on the surgical navigation system. Different reconstruction planes (multiplanar reconstruction) allow for surgery and path planning. The size of the lesion, target points, entry points, and their distance can be established and quantified (Fig. 2). Preplanned trajectories can be stored in memory for later use during surgery if desired. Thereafter the adhesive markers must be identified in the preoperative image data. This is a manual process with MR markers and an automatic process with CT markers.

Marker Registration

Patient marker registration is carried out to match the image coordinates with those of the patient on the operation table. The patient's head is fixed in a head clamp and the navigation system is mounted. Next, each of the head markers is touched using the pointer tip, and the image markers and the pointer position are matched (Fig. 3).

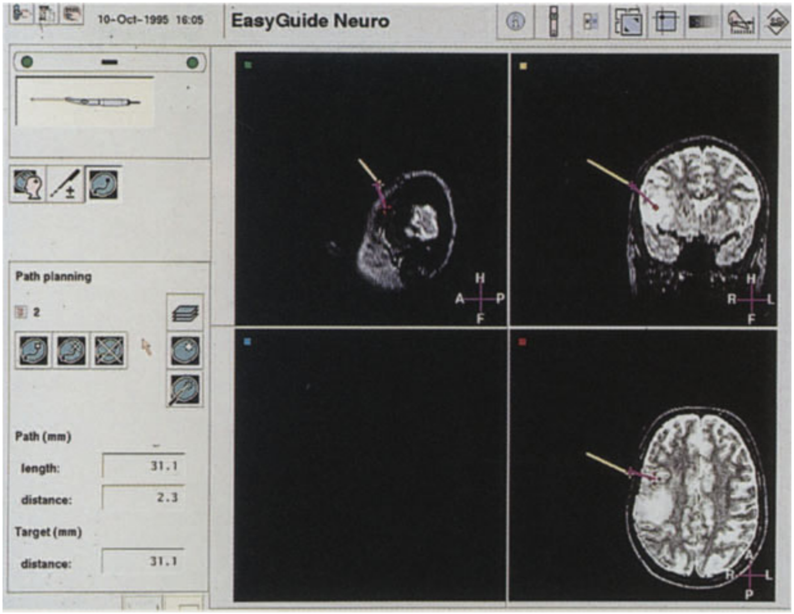

Fig. 2. EasyGuide Neuro display used for preoperative planning

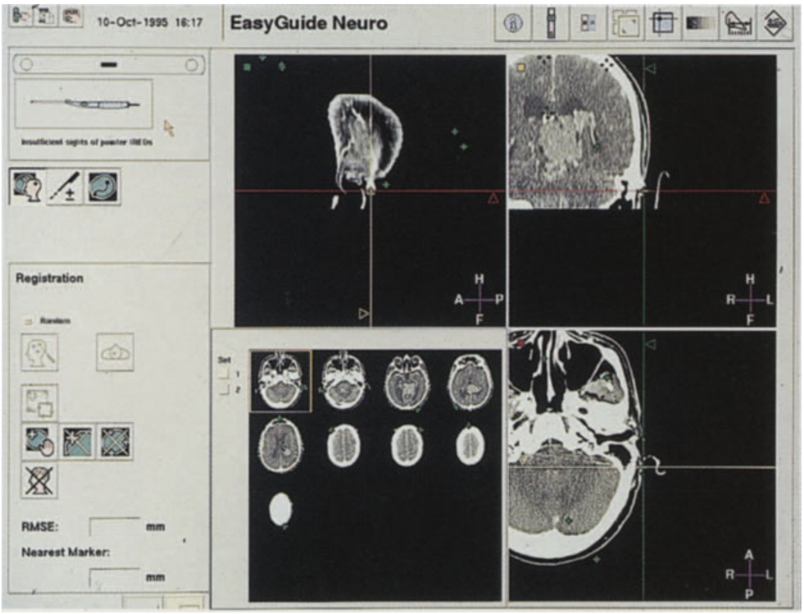

Fig. 3. EasyGuide Neuro display for marker registration

Surgical Planning and Intraoperative Navigation

After registration, the navigation system can be used interactively for viewing and for planning of the incision line, the craniotomy, and the burrholes. Because the fiducial markers are not readily accessible after the sterile drapes are in place, a number of anatomical landmarks or small holes drilled in the outer table of the exposed skull are identified and registered as additional checkpoints. These reference markers allow for easy reregistering during surgery. During surgery these checkpoints are touched with the pointer tip to check accuracy using the "distance-to-nearest-marker" value. If this value exceeds approrimately 2.5–3 mm, reregistration is required. During surgery the EasyGuide Neuro aids in navigation of instruments and tracking progress of the surgical procedure.

Conclusion

Philip's EasyGuide Neuro has been recognized by several authors as a navigation system that provides accurate, reliable, and valuable information in combination with a user interface that is very easy to learn.

Future Developments

Ongoing clinical studies indicate that image-guided or computer-assisted surgery will extend beyond neurological applications very soon. It is very likely that, among others, orthopedic and spine surgery will utilize navigation systems for the benefit of both surgeons and patients. In addition to the clinical advantages, the economical impact of shorter hospitalization time (as reported by several publications) on health care costs should not be ignored.

References

1. Watanabe E, Watanabe T, Manaka S, et al (1987) Three-dimensional digitizer (neuronavigator): new equipment for computed tomography-guided stereotaxic surgery. Surg Neurol 27:543–547
2 Adams L, et al (1990) Computer-assisted surgery. IEEE Comput Graphics Appl 10(3):43–51

Advanced Neurosurgical Navigation Using a Robotic Microscope Integrated with an Infrared-Based System

Lucia Zamorano, Federico C. Vinas, Razvan Buciuc, Zhaowei Jiang, and Fernando G. Diaz

Summary. Advanced neuronavigational techniques include the use of interactive image guidance during surgical procedures. Imaging data acquisition, software, and a digitizer device are the minimal requirements. We present our experience using a system in which a microscope was coupled to a robotic holder. Limitations encountered were related to the need to maintain the patient's head in a fixed position and to easy loss of registration in deep areas. These limitations were overcome by integrating an infrared system that allowed movement of the patient's head during surgery while tracking the accuracy of intraoperative registration. The optoelectronic integration of these two devices gives a "true" navigational system. The technical details of the system, methodology, and preliminary clinical experience are presented.

Key words. Stereotaxis—Brain tumor—Interactive image guided surgery—Computer-assisted surgery—Brain vascular malformation

Introduction

During the past few years, new neurosurgical techniques have been developed that facilitate surgical approaches, decrease the invasiveness of procedures, reduce postoperative complications, and shorten length of hospital stay. The emergence of minimally invasive neurosurgery and the evolution of image-guided and robotics-assisted procedures represent important developments in the treatment of patients with complex intracranial pathology [1]. Initially, robotic systems were cumbersome, nonintuitive, and time consuming to use; however, recent progress in industrial technology has led to further improvements in the mechanical precision and feasibility of robotic devices used for neuronavigation.

The MKM (Mehrkoordinaten Manipulator; multicoordinate manipulator) robotic microscope system (Carl Zeiss, Oberkochen, Germany) is specifically designed for image-guided procedures in neurosurgery. The purpose of this chapter is to describe the MKM robotic microscope system, emphasizing its applications to neuronavigation during surgery as well as its usefulness and limitations.

Department of Neurological Surgery, Wayne State University, 4160 John Road, Suite 930, Detroit, MI 48201, U.S.A.

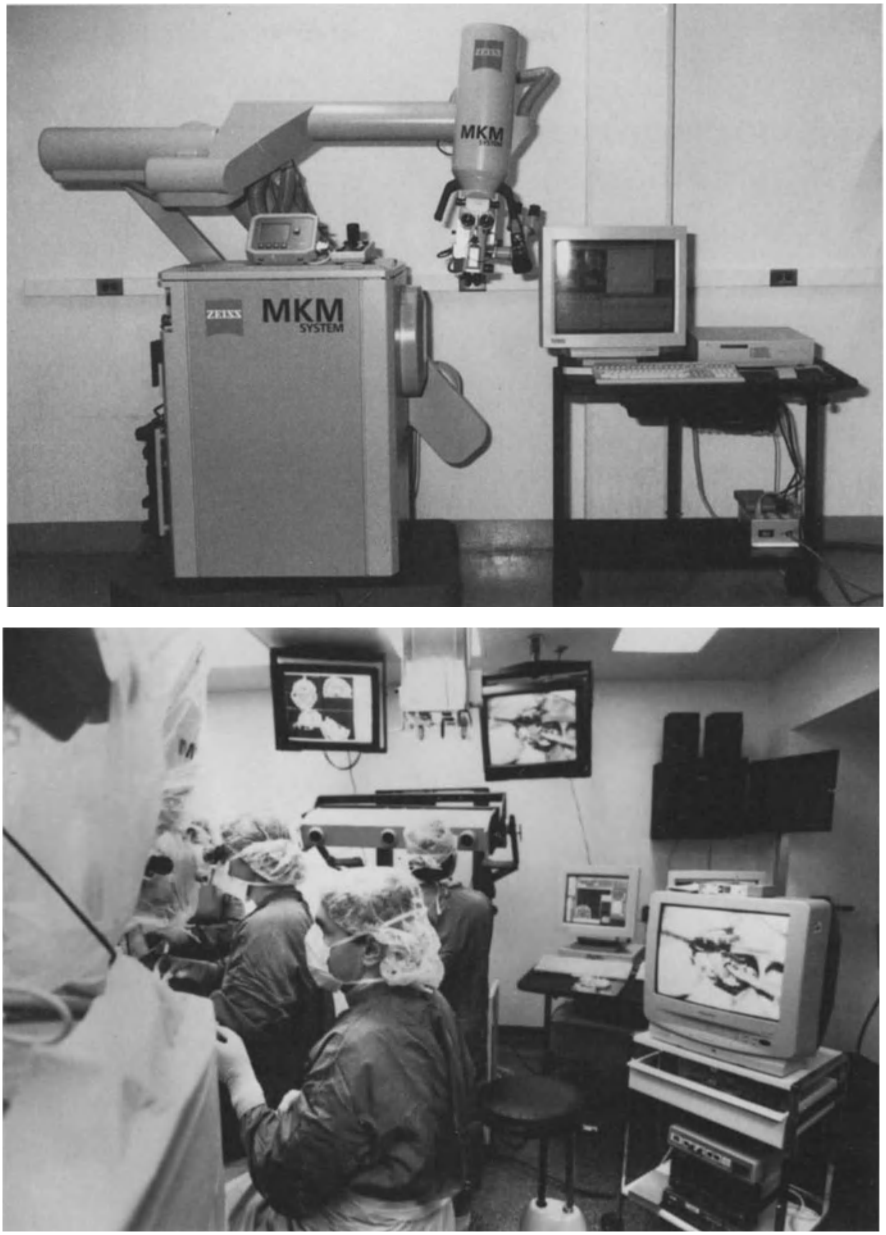

a

b

Fig. 1. **a** MKM (Mehrkoordinaten Manipulator; Zeiss, Oberkochen, Germany) stereotactic microscope system and planning workstation. **b** Intraoperative use of the MKM stereotactic microscope system in conjunction with the infrared digitizer developed at Wayne State University (Detroit, MI, USA). The integration of the infrared digitizer with the robotic microscope allows the real-time tracking of surgical instruments

Methodology

The MKM robotic microscope system consists of (1) a surgical microscope, (2) a robotic carrier system, and (3) a computer workstation that integrates the microscope with the robotic system (Fig. 1). We next briefly describe each component.

The Surgical Microscope

The surgical microscope is a standard OPMI ES (Zeiss OPMI-ES, Carl Zeiss, New York NY, USA), with a 1:6 ratio zoom system. The microscope has an autofocus feature with a digitally encoded zoom that selects the true focal plane. Also featured is a continuously variable focus length from 200 to 400 mm, illuminated by a xenon lamp.

The Robotic System

The robotic carrier system is motor-driven along six axes; by translational motion to different positions in space, pivot motion about a point in the focal plane of the microscope, and pivot motion about any point on the optical axis outside the focal plane of the microscope. This system is equipped with a sturdy motorized base that allows easy relocation of the system through a driveshaft [2].

Integration of the Microscope with the Robotic System

The surgical microscope and the robotic system are integrated by a portable computer workstation in the operative suite (see Fig. 1). A voice-recognition system activates important functions of the microscope and robotic system. For example, by using the microphone installed on the microscope, the surgeon can use voice commands to adjust the focus (i.e., "autofocus," "focus-defocus"), or position the microscope to different preset positions (i.e., "standby," "surgical position," "surgical trajectory," etc.).

The MKM robotic microscope system also has a data-superimposing monitor that projects the target contour and volume, as well as navigational information for the stereotactic procedure according to the surgical plan. Projections can also be oriented to the surgeon's perspective, making them intuitively easy to follow because of the heads-up display. A very useful feature of the MKM robotic microscope is the capacity to "preview" the surgery using focus-defocus, to bring perspective to the surgeon's eye view at different depths. During neuronavigation, the microscope's actual focal point serves as a virtual probe; therefore, no external pointing devices are needed [2].

The Surgical Procedure

To use the robotic microscope the following steps are required: image data acquisition, surgical planning, intraoperative registration, and intraoperative navigation by the robotic microscope during the surgical procedure.

Image Data Acquisition

The advent of digital imaging such as computed tomography (CT), magnetic resonance imaging (MRI), and positron emission tomography (PET) has resulted in images with exquisite detail. These images need to be registered with one another (multi-modality image registration) and with physical space (image-to-surgical space registration). Stereotactic frame systems and fiducial markers are the registration techniques most frequently used. The MKM robotic microscope system can be used with either frame-based and frameless techniques. For frame-based approaches, we use the Zamorano–Dujovny (Z-D) Stereotactic Unit (Fischer, Freiburg, Germany) [3]. For frameless approaches, we use fiducial markers attached to the skin or semipermanent implantable fiducial markers attached to the skull [4,5].

All patients in our series had gadolinium-enhanced MRI scans. Thereafter, the Z-D unit was put in place and patients underwent a CT scan with intravenous infusion of contrast. Both CT and MRI data were transferred directly to the computer workstation in the surgical suite.

Surgical Planning

The primary objective of surgical planning is to simulate and optimize the surgical approach. Surgical planning is performed using the Stereotactic Treatment Plan (STP) software (Leibinger-Fischer, Freiburg, Germany). After registering CT and MRI, the surgeon defines the target and other "volumes of interest" by manually delineating the contours of the lesion and other structures that the surgeon wants to identify intraoperatively.

Once a target has been defined, the surgeon defines the optimal trajectory. The approach can be a simple straight line (straight trajectory) or a more complex nonlinear approach along a curved line (curved trajectory). While conventional stereotaxis provides for a straight approach, the MKM robotic microscope allows for complex curved approaches, allowing access to deep targets using transulcal approaches. A straight trajectory is defined by two points, an entry and a target point. A curved trajectory is defined by multiple points along the planned approach. Both straight-line and curved approaches can be defined using computer visualization and manipulation tools. Information on multiple trajectories can be stored in the computer memory.

Intraoperative Registration

In the operative suite, the surgical procedure starts by mapping the image studies in the intraoperative space (intraoperative registration) by selecting reference points using the robotic microscope. Although the MKM robotic microscope system can define as many as 20 reference points, usually 3 or 4 points are sufficient. For intraoperative registration, the microscope is moved to the reference point to be selected (e.g., a fiducial marker). A visible cross is used to center the reference point in the microscope's field of view, with both focal distance and autofocus at maximal magnification. After the coordinates of all reference points have been stored, the system automatically loads the coordinates of the entry point from the computer workstation and performs a landmark test to analyze whether the system is correctly aligned with the coordinate system of the patient.

Intraoperative Guidance and Navigation

At the beginning of the surgical procedure, a "standby" and a "surgical" position are defined. The standby position is a defined position outside the surgical field to which the microscope can be moved at any time during the procedure. In the standby position, the robotic microscope will not interfere with the surgeon's movements during open craniotomies. The surgical position is used during the procedure to access the surgical field. The microscope can be moved from the standby position to the surgical position by a voice command whenever necessary.

Patients are positioned in the supine, semilateral, lateral, or prone position, according to the location of the lesion and surgeon's preference, with the head fixed to the operating room table using a Mayfield headholder. A standard centered craniotomy is then performed according to the surgical planning.

During surgery, the ability to remotely control the microscope position, the continuous display of contours from the surgeon's perspective, and the continuous display of the center of the focal point allow for true navigation and guidance. The data-superimposing monitor projects data from the workstation into the right eyepiece while the field of the surgery remains fully visible. Several types of data are displayed, including navigational aids showing the preplanned approach in relation to the current position, contours of tissue areas drawn during the surgical planning (i.e., target or structures to be preserved), and diagnostic images (MRI, PET).

The integration of the robotic system with the microscope also introduces a "keyhole feature" that consists of a pivot movement of the microscope with different focal lengths, allowing one to explore large cavities through a simple burrhole. As with other interactive image-guided systems, a continuous display is shown in the computer monitor in two-dimensional (2-D) multiplanar images with the center of reconstruction being the center of the focal point.

We have overcome the limitations of rigid fixation during surgery by using an infrared-based digitizing system developed at Wayne State University [3–6]. The surgical instruments are displayed on the computer images, and we have correlated the localization obtained with the robotic microscope with the infrared system. Consequently, the surgeon receives feedback regarding the depth of the instruments.

Preliminary Clinical Experience

During the past 4 months, we have performed 24 image-guided procedures using the MKM robotic microscope (Table 1). The patient population included 10 men and 9 women aged 25–77 years. The cases included surgeries for primary brain tumors (18), cavernous angiomas (2), third ventricular colloid cyst (1), arteriovenous malformation (1), and metastatic lesions (2). Surgical approaches included 3 intraventricular, 7 frontal, 3 deep parietal, 1 midline interhemispheric, 2 posterior fossa, 6 deep tempo-

Table 1. Characteristics of patients undergoing image-guided surgeries

Case	Sex	Age (yr)	Pathology	Location
1	F	38	Cavernous angioma	Deep intraventricular
2	F	35	Metastasis, melanoma	Deep parietal
3	F	39	Brain lesion	Frontal/motor cortex
4	M	42	Left temporal	Left temporal
5	F	65	Herniated disc	L2–L3 (lumbar spine)
6	M	3	Ependymoma	Brainstem/cerebellum
7	M	35	Colloid cyst	Third ventricle
8	M	45	Cavernous angioma	Deep left temporal
9	M	60	Astrocytoma	Temporal
10	F	32	Astrocytoma	Temporal
11	F	32	Astrocytoma	Frontal
12	M	77	Glioblastoma multiforme	Temporal
13	F	25	Cavernous angioma	Deep frontal
14	M	37	Glioblastoma multiforme	Frontal
15	F	48	Choroid plexus papilloma	Intraventricular
16	M	45	Astrocytoma	Right frontal
17	M	45	Metastasis, ovary	Deep temporal
18	M	25	Glioblastoma multiforme	Parietal
19	F	26	Astrocytoma	Left temporal
20	F	48	Glioblastoma	Left occipital
21	F	27	Meningioma	Left parietal
22	M	40	Glioblastoma	Right frontal
23	F	36	Arteriovenous malformation (AVM)	Posterior fossa
24	F	27	Astrocytoma	Deep midline

ral, and 1 spinal lumbar posterior approach. In each case, computer-assisted surgical planning was used to identify neighboring vital structures and to contour these structures with the pathology, to assist the surgeon in their identification and preservation. All results were clinically satisfactory. Postoperative CT and MRI studies showed total or subtotal resection.

Comparison Accuracy

In all cases, a second type of localizing technology was available; i.e., stereotactic ring or infrared digitizer MKM localization of the entry was accurate in all cases. However, in some instances localization was lost because of movements of the patient. The dural opening and the superficial part of the surgery were clearly performed with accurate navigation. However,at deeper levels it was difficult to achieve an exact focus for display of the contours, resulting in a loss of accuracy.

Representative Clinical Cases

Case 1

A 38-year-old woman with a history of chronic headache was evaluated in an emergency room after experiencing an episode of paresthesia and pain in the left-upper extremity. A CT scan revealed a left parietooccipital mass with intraventricular extension. A subsequent MRI scan showed signal characteristics compatible with a cavernous angioma (Fig. 2). She underwent a centered craniotomy and resection of the malformation using the MKM robotic microscope. The procedure was performed using both a stereotactic frame and implantable fiducial markers to compare and verify intraoperatively the surgical trajectories displayed by the microscope and ster-

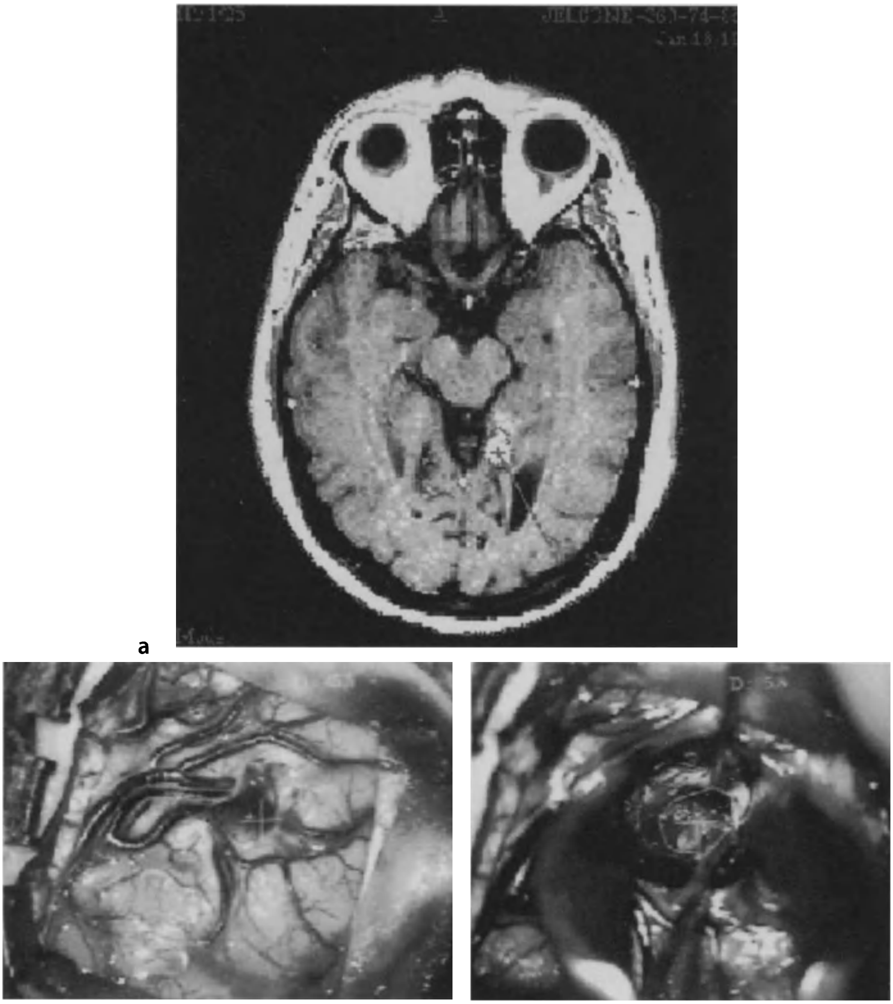

Fig. 2a–d. A 38-year-old patient with a cavernous angioma with intraventricular extension. The lesion was approached through the left parietal lobe through the precuneus (**a**) using the robotic microscope. **b** Intraoperative view through the entry point at the cortical level (*cross*). **c** Surgical corridor. The *circle* represents the contour of the lesion at the deepness indicated (*small arrow*). The heads-up display keeps the surgeon oriented thoroughout the surgical procedure. **d** Postoperational scan after resection of the lesion

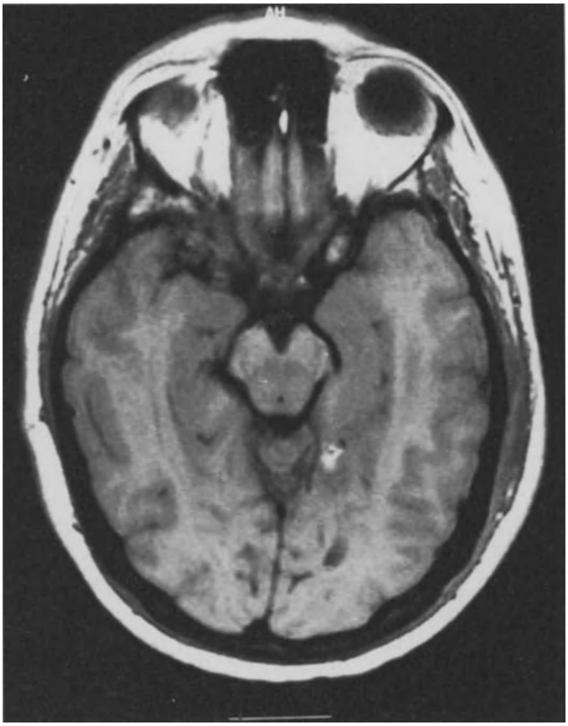

d

Fig. 2a-d. (*Continued*)

eotactic arc. In this case, the MKM robotic microscope selected the entry point for the centered craniotomy, which was displayed in the surgeon's right ocular.

On completion of a 4-cm-diameter craniotomy, the microscope was again brought into the operative field to locate the entry point on the cortical surface so as to perform a minimal corticotomy in an avascular area. The surgical corridor was developed using stereotactic brain retractors mounted on the stereotactic arc. Under continuous guidance by the microscope, the margins of the malformation were visualized at different depths for evaluation of possible difficulties during resection. The MKM microscope was also useful in identifying the vascular pedicle, which was situated posteriomedially. After resection, the keyhole feature of the microscope was used to verify the accuracy of the resection and to rule out any residual malformation. The patient tolerated the procedure well and was discharged home after 3 days.

In this particular case we believe the robotic microscope increased safety by providing continuous intraoperative guidance. At no time did we have to stop the surgical procedure for verification of position.

Case 2

A 35-year-old woman in apparent good health was admitted to an outside facility after an acute episode of headache and anomia. A diagnostic evaluation revealed two

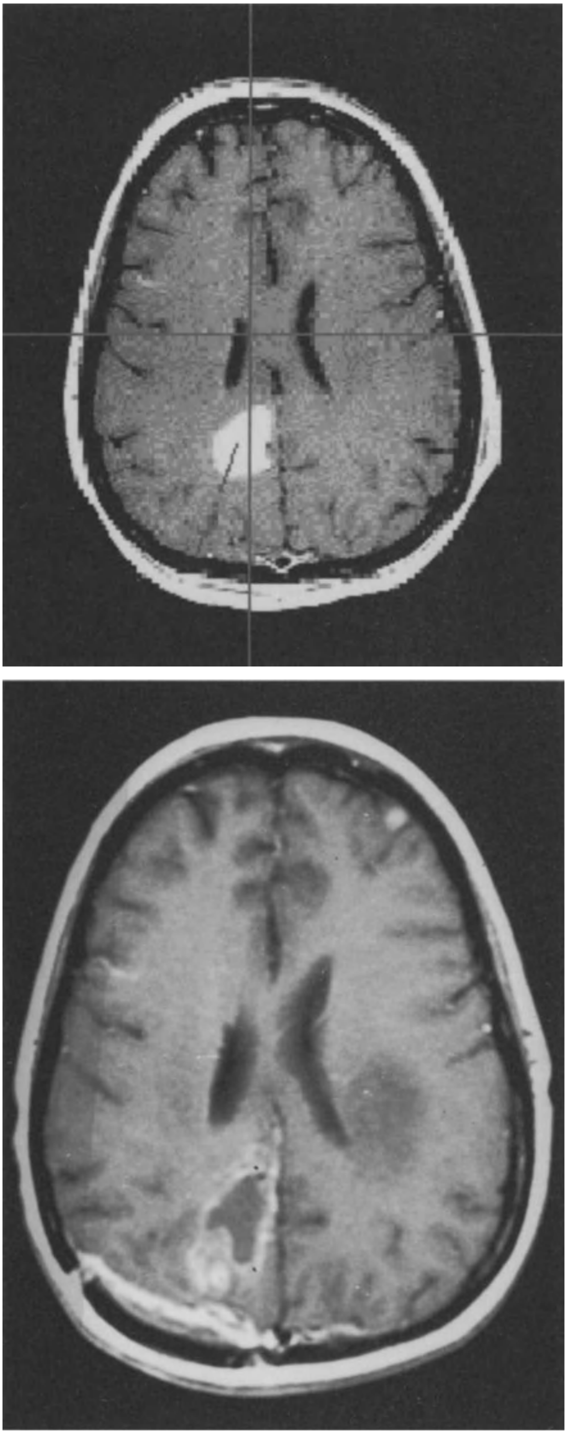

a

b

Fig. 3a,b. A 35-year-old woman with a right parafalcine and a left thalamic mass. The right parafalcine lesion (**a**) was approached initially with the robotic microscope. The pathology was consistent with a metastatic tumor. After a total resection of the right parafalcine lesion (**b**), she underwent external beam radiation therapy and radiosurgery for the left thalamic lesion masses, a right parietal parafalcine and a left thalamic (Fig. 3). Further workup revealed a lung mass, which proved to be a metastatic lesion from a melanoma. Her intracranial lesions were approached in a stepwise fashion consisting of a craniotomy and resection of the right metastasis followed by radiosurgery for the left thalamic lesion.

Five implantable fiducial markers were placed on areas of the head where they would not interfere with the surgical corridor. Before surgery, an MRI and a CT scan were done for surgical navigation. After positioning and draping, three fiducial points were digitized using the microscope (image-space registration). The entry point (according to the preoperative planning of the surgical corridor) was visualized through the right ocular and marked on the skin. A centered craniotomy was done based on the defined entry point. After opening of the dura, the surgical resection proceeded under the guidance of the microscope.

During the resection, the surgical trajectory was displayed, and as the surgical corridor was developed the tumoral contour was continuously shown while the resection was in progress. In parallel on the computer workstation, a continuous display of the surgical position of the focusing point was also available to further orient the surgeon. A complete resection of the metastasis was possible through a minimal-size craniotomy. At the end of resection, the keyhole feature of the microscope was used to evaluate the tumoral bed and the completeness of resection. The postoperative course of the patient was uneventful, and after 4 days she was discharged home.

Discussion

During intracranial surgery, the use of a robotic microscope during neurosurgical interventions offers several advantages over conventional stereotaxis. First, image-guided craniotomies can be done without a localizing arch and aiming needle. Second, during the approach to deep, complex lesions, the MKM robotic microscope enables guidance with the best possible trajectory without the need to follow a straight line (conventional stereotaxis requires a straight trajectory). For example, the MKM allows a curved trajectory to approach an insular lesion through the sylvian fissure, minimizing damage to normal brain. In addition, the heads-up display shows the volume and contours of the lesion or anatomical landmarks to be preserved, and the computer can display the exact location of the target, including distances, axes, pivot point, and a keyhole approach. The MKM robotic microscope system can be utilized during the surgical resection of tumors or vascular malformations, for epilepsy surgery, and for other interactive image-guided procedures [5].

The MKM is valuable during the resection of superficial, subcortical, and deeply located tumors. For the resection of cortical or subcortical tumors, the MKM can help minimize the size of the craniotomy, which we believe contributes to decreased operative morbidity.

During the surgical resection of deep-seated tumors located in the basal ganglia or thalamus, neurological complications are primarily related to problems of localization, exposure, and extent of resection [7,8]. The optimal surgical approach depends on the location of the tumor. For example, anterior thalamic tumors can be approached transfrontally, while posterior dorsal thalamic lesions can be approached through the temporooccipital junction.

Intraventricular tumors are deeply situated, surrounded by vital neurological and vascular structures, and often have irregular geometrical configurations, posing particular difficulty for the surgeon in maintaining orientation during surgery. Conventional neurosurgical techniques can lead to an incomplete or suboptimal resection of these masses. During their resection, the MKM provides an interactive display of the geometry of the tumor, margins of the surgical resection, vascular structures, and relationship of the tumor with surrounding brain structures that need to be preserved. The proximity of skull-base tumors to vital areas of the brain, major blood vessels, and cranial nerves poses a variety of obstacles [9]. During surgical exposure and resection of skull-base tumors, the MKM robotic microscope provides intraoperative visualization of the tumor geometry, allowing the surgeon to maintain orientation even with irregularly shaped tumors. Furthermore, the MKM shows the position of blood vessels and cranial nerves, often displaced from their usual anatomical position.

During the surgical treatment of temporal and extratemporal epilepsy, the MKM robotic microscope allows for localization of normal anatomical structures and abnormalities defined by imaging studies. For example, during callosotomies, the MKM defines the extent of the corpus callosum section; during resection of a temporal lobe epileptic focus, the MKM is useful in judging the posterior margin of anterior temporal lobe resection.

The MKM is also useful for locating deep small lesions such as deep cavernous angiomas. During the resection of complex arteriovenous malformations, the MKM can show the localization of feeders, nidus, and draining veins and the relationships between the vascular malformation and surrounding vital structures, allowing a safer and more effective resection.

An important disadvantage encountered with the surgical robotic microscope is that it required a fixed position of the patient in relation to the microscope and robot base. A sudden movement of the patient could disrupt an accurate intraoperative localization. Also, in many instances, the surgeon desires to change the position of the patient's head. This problem is solved by integration of the robotic microscope with an infrared digitizer. The integration of the robotic system with dynamic reference (provided by the infrared digitizer) allows intraoperative movements of patient position, which is sometimes necessary to access deep, complex lesions. In addition, it allows the simultaneous interactive display of the position of surgical instruments such as bipolar, dissectors, etc.

From the collaboration of Zeiss–Leibinger–Fisher and Wayne State University came the concept of advanced neurosurgical navigation using three tools: (1) the infrared-based system alone (STN; surgical tool navigator); (2) the infrared-based system coupled to a standard microscope (SMN; surgical microscope navigation); and (3) infrared-MKM. Some intracranial or spinal procedures may require only STN, others SMN. Infrared-MKM provides a "true" navigational system for application in intracranial procedures. MKM without the infrared system is especially useful to center the craniotomy for superficial and subcortical lesions. For deep lesions, the main limitation of the MKM is its inability to precisely determine the accurate depth to display the contours. The "autofocus" feature attempts to perform this function but becomes ambiguous. In the deeper portions of the brain it is difficult to use the focal point as the virtual probe. We overcame this problem by integrating the microscope with the infrared digitizer.

In summary, we believe that the MKM robotic microscope offers the surgeon an intuitive navigational guidance. The combination of the MKM microscope with the infrared digitizer becomes fast and reliable because it allows continuous registration. Because it is an intuitive system, it is easy to operate. Although the microscope requires some time to set up, it does not prolong the surgical procedure; in fact, during the approach of deep, complex lesions, it can decrease the overall duration of the procedure. It is reliable, especially in combination with the infrared digitizer; as demonstrated in previous in vitro studies, accuracy was 0.7 mm.

Conclusion

The combination of the MKM robotic microscopic system with an infrared digitizer represents an application of image guidance techniques to modern neurosurgery. Because of its utility, precision, and minimum addition to procedure length, this system can be used in a whole range of indications of frame-based and frameless stereotaxis.

In the near future, we plan to automatically and continuously update the control of the robotic microscope with the continuous registration generated by the infrared-based system. Furthermore, methods of continuous intraoperative image acquisition such as intraoperative MRI will allow the continuous intraoperative updating of the image data set to reflect changes in brain position during the resection of an intracranial mass. These new techniques may add precision and safety, especially for deep lesions and those located near eloquent areas, and contribute to the optimization of the surgical procedure.

References

1. Watanabe E, Mayanagi Y, Kosugi Y, et al (1991) Open surgery assisted by the neuronavigator, a stereotactic, articulated, sensitive arm. Neurosurgery 28:792–800
2. Zeiss (1996) MKM system: manual and instructions for use. Revision 2.X. Carl Zeiss, Geschaftsbereich, Germany
3. Zamorano L, Kadi M, Jiang Z, Diaz FG Zamorano-Dujovny (1994) Multipurpose neurosurgical image-guided localizing unit: experience in 866 consecutive cases of "open stereotaxis." Stereotactic Funct Neurosurg 63:45–51
4. Zamorano L, Nolte LP, Kadi AM, Jiang Z (1994). Interactive intraoperative localization using an infrared-based system. Stereotactic Funct Neurosurg 63:84–88
5. Zamorano L, Vinas FC: Intraoperative digitization: computer-assisted neurosurgery using a surgical wand. In: Advances in technical standards in neurosurgery, vol 24, Springer-Verlag, Berlin Heidelberg New York Vienna (in press)
6. Zamorano L, Nolte L, Kadi M, Jiang Z (1993) Interactive intraoperative localization using an infrared-based system. Neurol Res 15:290–298
7. Salcman M (1993) Intrinsic cerebral neoplasms. In: Apuzzo M (ed) Brain surgery complication avoidance and management. Churchill Livingstone, New York, pp 379–461

8. Vinas FC, Zamorano L, Lis-Planells M, Buciuc R, Diaz FG (1996) Interactive intraoperative localization during the resection of intraventricular lesions. Minim Invasive Neurosurg 39:65–70
9. Sekhar LN, Goel A (1993) General considerations in skull base surgery. In: Apuzzo M (ed) Brain surgery complication avoidance and management. Churchill Livingstone, New York, pp 2167–2174

Part 2
Various Applications of Computer-Assisted Systems

Application of the ISG Viewing Wand for Endoscopic Procedures

Michael W. McDermott and Alan Jacobs

Summary. The use of intracranial endoscopy for operative procedures is increasing. Navigation within the ventricular system is straightforward, using known anatomical landmarks. Interactive image-guided surgical systems are helpful for defining the trajectory to the ventricular system and for performing endoscopy within cystic cavities where there are no landmarks for orientation. We have used the Viewing Wand system, a passive mechanical arm, with rigid endoscopes for the following applications: (1) defining the trajectory to the frontal horn for endoscopic III ventriculocisternostomy, colloid cyst removal, arachnoid cyst fenestration, or external ventricular drain placement ($n = 5$); (2) defining the trajectory to the ventricle from the occipital region for ventriculoperitoneal or cyst-peritoneal shunts ($n = 4$); (3) defining the trajectory to the frontal horn for shunt placement in cases of benign intracranial hypertension ($n = 3$); (4) fenestration of multiloculated parenchymal cysts occurring post brachytherapy ($n = 3$); and (5) placement of an Ommaya reservoir into a parenchymal cyst ($n = 1$). The system requires the use of rigid lens or fiberoptic endoscopes, custom measuring probes, and adapters to connect different endoscopes to the Viewing Wand. The operating room setup, probe adapters for rigid endoscopes with the Viewing Wand, and a single surgeon experience are presented.

Key words: Viewing Wand—Endoscopy—Image-guided surgery (IGS)

Introduction

The application of interactive image-guided technology for ventricular access may seem unecessary given the well-defined anatomical landmarks used for orienting the surgeon to the ventricular system for passage of a catheter or endoscope. In the operating room under sterile draping, however, the orientation of the head and the position of surface landmarks used for ventricular access may be obscured [1]. In adult patients there is no window through which the intracranial contents can be imaged with ultrasound, in contrast to the fontanelles of infants. In pathological

Department of Neurological Surgery, University of California, 533 Parnassus Avenue, Suite U-126, San Francisco, CA 94143-0350, U.S.A.

Table 1. Procedures using Viewing Wand/endoscope combination

Description	No. of cases	Endoscope
Ventriculoperitoneal (VP) shunt		
Frontal	3	Fiberoptic (1.2-mm outer diameter)
Occipital	4	Fiberoptic
Frontal horn access		
Colloid cyst	1	Rod lens (4.2-mm outer diameter)
III ventriculostomy/EVD	2	Fiberoptic (1); rod lens (1)
Arachnoid cyst	2	Rod lens
Parenchymal cyst fenestration, frontal lobe	3	Rod lens
Placement of Ommaya reservoir, frontal lobe	1	Fiberoptic
Total:	16	

EVD, external ventricular drain.

conditions in which the ventricles are small, deformed, or contain a cyst that the surgeon does not want to enter first, standard landmarks and approaches may be inappropriate. Interactive image-guided systems provide a new noninvasive method of orienting the surgeon to the intracranial contents imaged immediately preoperatively [2–9]. Methods for adapting these systems to endoscopy are straightforward.

The main indications for which the authors have combined use of an interactive image-guided system with endoscopes are accessing small ventricles in the setting of benign intracranial hypertension; occipital passage of a ventricular catheter; fenestration of parenchymal or intraventricular cysts; and accurate access to the frontal horn for drainage of a colloid cyst or for third ventriculostomy (Table 1). This chapter briefly summarizes our experince using the ISG/Elekta Viewing Wand (ISG, image-guided surgery) with both small fiberoptic and larger rod lens endoscopes for intracranial procedures.

Materials and Methods

Hardware

The ISG/Elekta Viewing Wand has been in use at the University of California, San Francisco (UCSF) since 1993 for more than 500 intracranial cases. Applications for endoscopic procedures began in 1994. The system incorporates a passive mechanical arm with electropotentiometers at six joints that relate angular information to probe position in imaging space after registration [10]. The arm has a 60-cm reach and the tip position is updated 30 times per minute. Custom probes were designed for both our own rod lens endoscope and a fiberoptic 1.2-mm endoscope (Neuronavigational Corporation, Costa Mesa, CA, USA). These probes were measured during the setup procedure and were equivalent in length to the endoscopes mounted to custom adapters. When the endoscope "probes" were selected using the software interface with the endoscope now attached to the Viewing Wand, the tip of the endoscope became the virtual probe tip on the computer screen.

Scanning Requirements

The imaging study selected for use was dependent on whether the ventricle or a cyst was to be accessed. Computed tomographic (CT) studies were used where ventricular access was needed and magnetic resonance (MR) imaging when parenchymal cysts were entered. CT data were obtained by scanning the entire head with 3-mm-thick slices, with 3-mm interval spacing and a field of view of 25 cm with a 512 × 512 matrix. For MR imaging a volumetric 124-slice, 1.5-mm-thick SPGR (spoiled gradient recall) axial study was obtained with no interslice spacing. Vitamin E capsules were used for MR fiducials and lead shots for CT.

Operating Room Setup

The positions of patient, surgeons, and monitors are outlined in Fig. 1. All patients must be placed in rigid pin fixation, which can create some problems with positioning for ventricular or cyst-to-peritoneal shunting. Most important is that the monitors be placed such that the surgeon can look directly up from the operating field to the monitors without having to turn his or her head. This is especially important for

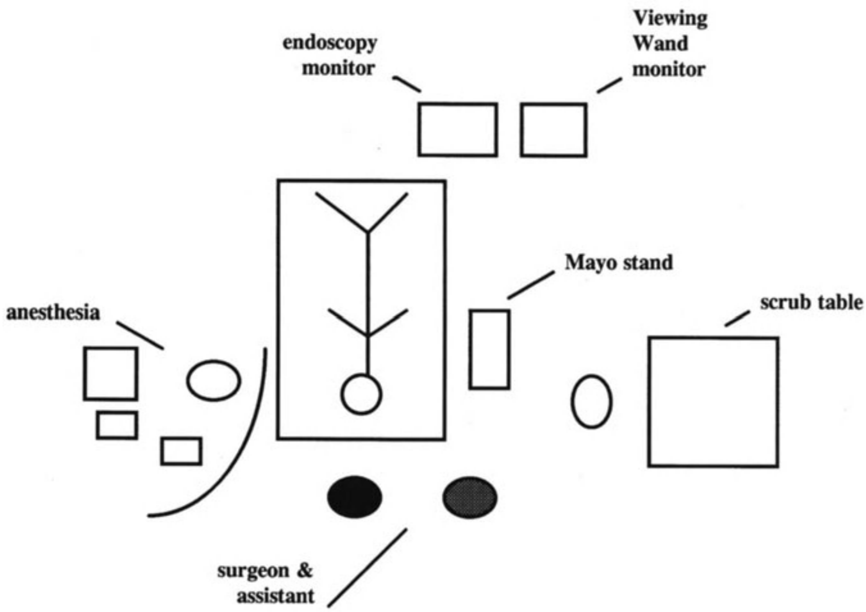

Fig. 1. Operating room setup for combined endoscopy–interactive image-guided surgical procedure. The endoscope video monitor and Viewing Wand monitor are placed at the foot of the bed, allowing the surgeon to look straight up without turning. In endoscopic procedures, one surgeon navigates and another operates

parenchymal cyst septae fenestration where there are no anatomical landmarks to direct the surgeon and only the crosshair on the Viewing Wand screen tells the surgeon which portion of the cyst has been reached.

When using the Viewing Wand–endoscope combination for occipital horn access, the Viewing Wand should be placed at a position much further away from the head than is used normally or the endoscope cannot be laid down in the desired trajectory. Fiducials are placed in a "half-and-half" position, front and back, ipsilateral to the side of the ventricular puncture (Fig. 2). The patient's head is turned parallel to the floor and the shoulder bolstered with a rolled flannel. For ventricular catheter placement, the 1.2-mm endoscope is used and the tip of the catheter is cut longitudinally at the tip ("fish-mouth" opening) so that the endoscope can be passed through the tip when the ventricle is reached (Fig. 3). The catheter is cut at the 10-cm mark, similar to the mark on the endoscope. Before attaching the endoscope the standard short probe is used to confirm the position of the burrhole and the trajectory to the ventricle. After the pial surface has been opened, the endoscope is attached to the arm and the probe designation in the software program changed to "endoscope."

Watching the Viewing Wand screen, using the trajectory view oriented in the axial plane, the tip of the endoscope is observed passing to the ventricle (Fig. 4). The length of catheter needed to reach the frontal horn can be confirmed using displayed depths beyond the endoscope tip from 1 to 5 cm (Fig. 5). When the computer images indicate an intraventricular location, the endoscope is advanced through the tip of the cut catheter and the ventricular location confirmed. The endoscope is withdrawn while holding the catheter position with a rubber-shod forceps and then the endoscope is

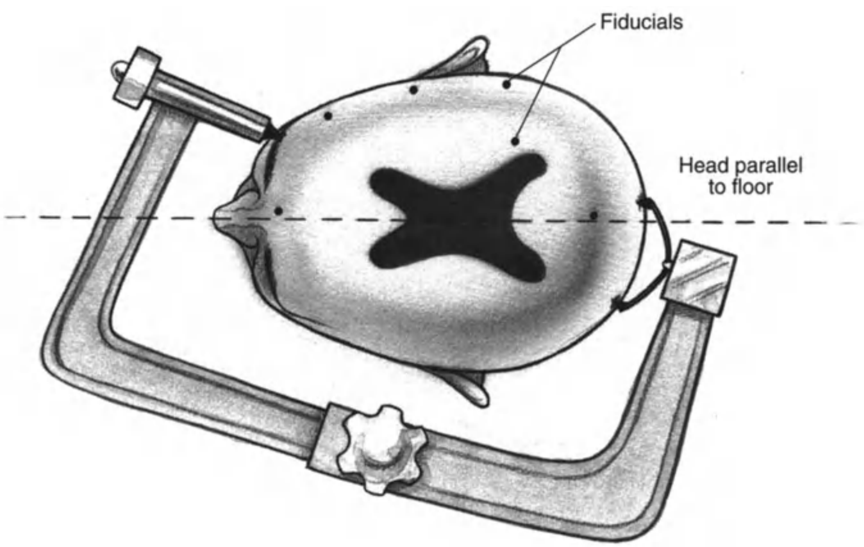

Fig. 2. Head and fiducial position for occipitoparietal approach to ventriculoperitoneal shunt; the ipsilateral shoulder is bolstered with a rolled flannel. Rigid pin fixation is necessary to maintain accuracy of registration but renders subcutaneous tunneling somewhat more difficult. Of the six fiducials, one is reserved for the postregistration accuracy check

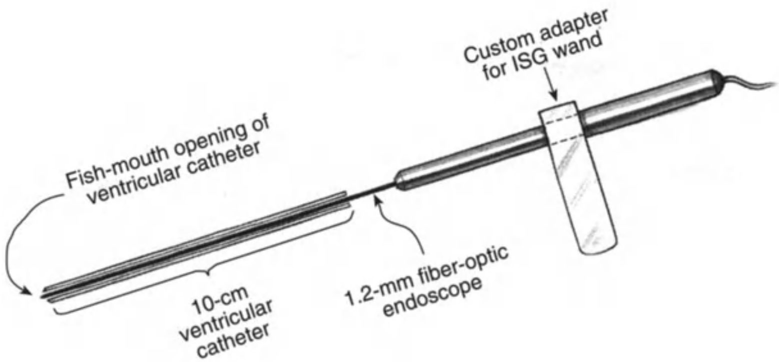

Fig. 3. Using the 1.2-mm endoscope for ventriculoscopy during catheter placement, the endoscope is attached to the Viewing Wand with a special adapter. The ventricular catheter is cut at 10 cm and the distal end cut in the long axis of the catheter with a no. 11 blade, producing a "fish-mouth" opening

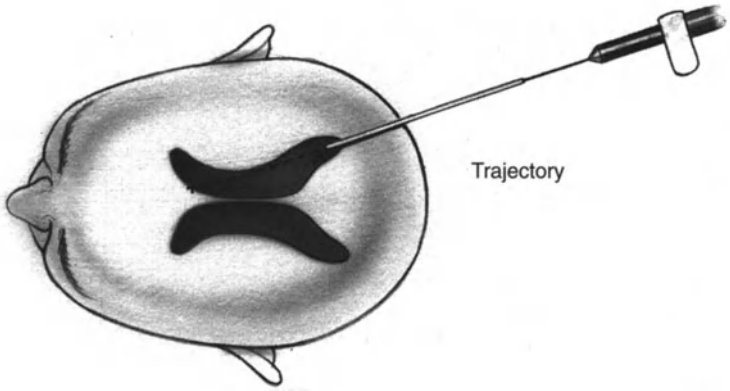

Fig. 4. Watching the trajectory view, the endoscope within the catheter is advanced into the ventricle. Once the ventricle is entered as indicated by the Viewing Wand, the endoscope is removed while holding the catheter in place. If cerebrospinal fluid (CSF) is observed, the endoscope is detached from the Viewing Wand and endoscopic guidance of the ventricular catheter is carried out in the usual manner

detached from the Viewing Wand for easier use. The endoscope is reintroduced down the ventricular catheter and just beyond its end into the ventricle. Then, under direct vision the endoscope–catheter combination is advanced to the frontal horn. Once there, the distance to the outer table of the skull is noted as marked on the catheter, the catheter secured, and the endoscope removed. The valve is then connected to the catheter, taking into account the additional length with the valve attached and cutting this length from the ventricular catheter.

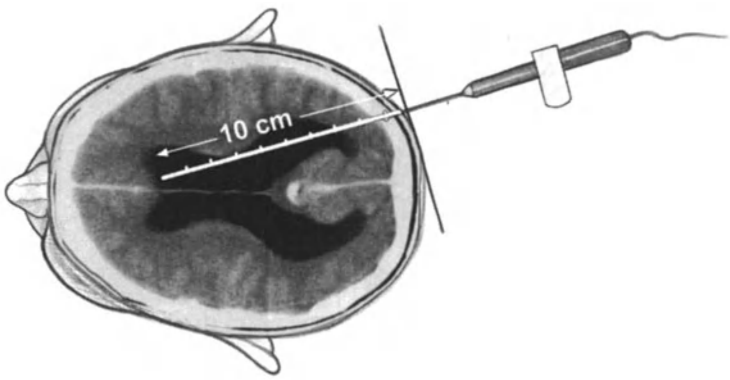

Fig. 5. Another advantage of image-guided insertion of the ventricular catheter is that length needed can be estimated from the ray projection on the Viewing Wand screen, which is marked at 1-cm increments to 5 cm from the tip of the catheter. From the occipitoparietal approach, a 10-cm catheter length is adequate to reach the frontal horn

Results

There have been no complications or adverse patient events directly related to applying endoscopic and image-guided technologies together. Rather, as one would predict, in each case the ventricle or cyst was entered on the first passage through brain tissue. Although some time is added to the setup before patient general anesthesia, as our experience increased the limited additional time required intraoperatively seemed offset by the success of reaching the desired target on the first pass.

Shunts

There were three frontal horn ventricular catheter placements, two in patients with small ventricles and benign intracranial hypertension, and one in a patient with slit ventricle syndrome who required a ventricular catheter revision. In the three occipitoparietal approach cases, two patients had tumors in the body of the lateral ventricle and one patient had a huge corpus callosum arteriovenous malformation. In two of these cases, the final catheter tip position was in the contralateral frontal horn, but both these catheters worked well. Positioning in the contralateral ventricle likely resulted from applying too much force to the 1.2-mm fiberoptic endoscope when it was attached to the viewing wand, resulting in some bending of the endoscope in a real trajectory different from that defined by the image-guided system. In another case, a cerebellar posthemorrhagic encephalomalacic cyst communicating with an isolated fourth ventricle, there were no defined external landmarks for the passage of this cyst catheter, and in such a case the image-guided system was ideal. A small dural opening through a large craniectomy defect from previous surgery allowed the accurate placement of this catheter, and the median raphe of the fourth ventricle was clearly visualized with the endoscope.

Frontal Horn Access

In one case of an incompletely drained colloid cyst where the ventricles were only slightly enlarged, a precoronal approach was used, and the projection of the probe tip seen on the trajectory view, marked out at 1-cm increments, prevented the inadvertent puncture of the cyst with a passage of the endoscope that was too deep. MR imaging was used in another case to allow biopsy of a dural-based lesion of less than 1-cm-diameter convexity in a patient with postviral meningitis and a suspected leptomeningeal process. After the biopsy of this lesion and just anterior to it, the image-guided system was used to pass an external ventricular drain. In two cases of intraventricular arachnoid cysts of the body and atrium of the lateral ventricle, the frontal horn was accessed first with the 4.2-mm endoscope. This allowed identification of the normal ventricular anatomy followed by the cyst wall seen more posteriorly in the ventricle. Fenestration of both the front and back walls of these arachnoid cysts was then accomplished with electrocautery.

Parenchymal Cyst Fenestration

The problem with parenchymal cysts that contain multiple septations is that there are no intracystic landmarks to orient the surgeon. Thus the image-guided systems are invaluable in determining position within each loculated compartment and allowing safe passage through septa into the next accompanying cyst. Irrigation within the cyst compartment allows for clear visualization with the endoscope. The associated gliosis of surrounding brain in our two cases of radiation-induced cystic necrosis prevented brain or cyst collapse with lysis of the various septations. This is one of the most helpful settings for the combination of direct imaging via endoscopy and image-guided systems.

Placement of Ommaya Reservoir

In the single case in which there was a recurrent solitary parenchymal cyst following radiosurgical treatment of a recurrent malignant glioma, CT-based imaging was used to place the Ommaya reservoir within the central portion of the cyst. The image-guided system allowed direct measurement of the depth of penetration into the cyst, and under direct visualization the catheter tip was placed 1 cm back from the medial wall of the cyst so that if the cyst collapsed, the catheter would not penetrate the brain parenchyma. While there was some additional setup time, the surgical procedure itself required only 30 min.

Discussion

Catheter access to the ventricular system is a basic neurosurgical technique, but the incidence of improperly placed or passaged catheters remains unacceptably high [11]. The most common sites on the surface of the skull used for ventricular access are the precoronal frontal site (Kocher's point) and the occipitoparietal site [1]. Traditionally, Kocher's point is defined as 2–3 cm lateral to the midline, just in front of the coronal suture, and the occipitoparietal site as 4 cm from the midline and 6 cm above the inion. From Kocher's point, a trajectory in the sagittal plane passing through the middle ipsilateral canthus, and in the coronal, plane passing through the external auditory canal, have been used. The Gjhar guide has been devised to ensure the appropriate passage and success with hitting the frontal horn of the lateral ventricle from this point [12]. Using freehand techniques from the anatomical landmarks, failure to hit the correct target is more common than it should be. Multiple blind passes toward the ventricle are associated with increased neurological morbidity, although little is published about this fact. From the occipitoparietal approach, an all-too-common error in trajectory results in passage through the centrum semiovale of the thalamus or placement of a catheter into he temporal horn of the lateral ventricle. In all seven of our cases in which a combination of endoscopy and image-guided techniques was used for ventricular access, the ventricle was accessed in each case on the first pass. Once the ventricle was accessed, direct vision of the ventricular cavity with the endoscope was used for final positioning of the ventricular catheter. In two cases, the ventricular catheter tip was positioned in the contralateral ventricle, likely related to the flexibility of the 1.2-mm fiberoptic endoscope. These two events occurred during the third and fourth cases in which we used the combination of endoscope and the viewing wand, and we have not had a recurrence.

Rhoten et al. [7] have described using a much larger broad lens endoscope for ventricular fenestration and shunting. A ventricular catheter in their cases was placed after ventricular septi were fenestrated with the rigid rod lens scope; a ventricular catheter was placed independent of the image-guided system and the catheter location was then confirmed with the endoscope. For simple shunting procedures in which no fenestration is necessary, the very narrow fiberoptic endoscopes are used as the shunt catheter stylet and larger rod lens scopes are not necessary. Drake et al. [2] described the use of the Viewing Wand in nine pediatric patients, four with aqueductal stenosis and 5 with loculated ventricles. In a similar fashion, their endoscope was attached to the articulated arm by modifying the probe attachment apparatus. We believe that for occipitoparietal approaches in particular, the interactive image-guided systems are the safest way to access the ventricle with certainty.

The problem with fenestration of intraventricular cysts and intraventricular septations that occur after meningitis is well known, and endoscopy and the image-guided system have been used more extensively for treatment of this condition. While the advantage of converting multiloculated compartment to a single one is obvious and eliminates the needs for multiple shunts, orientation within these multiple compartments is the problem. The image-guided systems are indispensable in these cases. While in adults we had no cases of multiple ventricular septations, two of our patients had intraventricular arachnoid cysts, and the image-guided system allowed us to access the frontal horn of the lateral ventricle in front of the cyst itself. This allowed us to visualize the cyst wall anteriorly, fenestrate it widely, pass through the cyst, and fenestrate the back wall as well. Again, once the normal ventricle is accessed, the intraventricular anatomy is used primarily for orientation.

In a similar fashion, but a different location, cystic radionecrosis seen after high-dose interstitial brachytherapy or radiosurgery is a confounding problem for neurooncologists. These cysts frequently recur after stereotactic aspiration and usually have multiple septations. The key to eliminating early cyst recurrence is breaking down the septations between these separate cysts. Again, the image-guided systems are invaluable. As the fluid in these cysts tends to be xanthochromic or even frankly hemorrhagic, copious irrigation of the cavity is necessary before a good endoscopic visualization can be achieved. Even then, a clear view of a featureless white wall of the cyst provides no help to the navigating surgeon as to where the next cyst lies. The side-by-side endoscopic and image-guided systems display therefore allows the surgeon to watch the tip of the probe and orient its position relative to these septations and distal compartments. Fenestrations in the septa then allow communication from one cyst to another with collapse and decompression.

Previously, when small cysts or ventricles were to be accessed with a catheter, frame-based stereotactic systems were used [13]. Target-centered systems are particularly versatile in this respect, allowing some freedom of the entry point for deeply located cysts and the ability to access very superficial cysts quickly. However, this technique is somewhat invasive, requiring the application of a stereotactic frame under local or intravenous anesthesia, and requires that the patient wear the frame until after the surgical planning and the operative procedure itself are completed. With the interactive image-guided systems, only skin-based fiducials are used, and for relatively large cysts, the ones most likely to be clinically symptomatic, the accuracy of the image-guided systems suffices to assist with placement of these catheters and reservoirs. Depth projections in the axis of the probes beyond its tip allow surgeons to calculate the depth and length of catheter needed from the outer table of the skull, as opposed to using the ventricular catheter itself as a depth gauge and then having to subtract additional distance added by connecting the reservoir. In our first experience with the use of the ISG viewing wand for replacement of an Ommaya reservoir into multiply recurrent radionecrotic cysts, the interactive system allowed planning the most beneficial position of the entry point where the cyst was closest to the brain surface and did not compromise previous skin incisions.

The issue of the accuracy of the various image-guided systems is definitely overrated when the system is applied for open procedures in an intraaxial location where tumor tissue and or brain tissue is removed and the three-dimensional shape of the surrounding brain changes. Drainage of cerebrospinal fluid (CSF) also shifts the brain, affecting superficial structures more than deep ones, so that submillimeter accuracy is a nonissue in practical application. For burrhole techniques and ventricular access, little CSF escapes, and at the point of access of these cavities, the accuracy of the system is somewhat more important. Golfinos et al. [3] found that the actual error for the ISG viewing wand just after registration was judged by the operating surgeon to be less than 2 mm in 92% of MR and 82% of CT cases. The accuracy of the system degraded during the operation, so that by the third assessment of error it was estimated to be less than 2 mm in 72% of MR and 62% of CT imaging cases. In their study of 325 cases, in 12 the system was used for assistance with a ventriculoperitoneal shunt. They described one case in which the viewing wand was used to position a plastic peel-away sheath on the walls of the various cysts within the ventricle; the probe was then exchanged for an endoscope, and in this way each of the cyst walls was fenestrated. Sipos et al. [8] evaluated the viewing wand in 250 patients undergoing a wide range of procedures, and in a subset of 45, tests of the accuracy were made before and during the surgery. Using fiducial fit initial registration and CT scans, the geometric mean error was 2.26, and using magnetic resonance, 2.81. In none of their cases was the system used for shunting or cyst fenestration.

Conclusions

Interactive image-guided systems are a useful adjunct to the surgical armamentarium, particularly for endoscopic applications. Through custom adaptors, endoscopes can be attached to the ISG viewing wand to assist with finding the trajectory to the ventricle, to the frontal horn, occipital horn, or body of the ventricle for shunt procedures, for parenchymal or intraventricular cyst fenestration, and for the placement of reservoir systems. Interactive image guidance is necessary only for selected cases. Although there are additional costs associated with preoperative imaging, the benefits to the operating surgeon and the patient seem real. We are now retrospectively evaluating the morbidity associated with multiple attempts at ventricular access during ventriculoperitoneal shunting procedures so as to attempt to quantify some of the benefits that may be realized using interactive image-guided systems.

Acknowledgements. We wish to thank Christine Gralapp for creating the art work in this chapter.

References

1. Mapstone TB, Ratcheson RA (1996) Techniques of ventricular puncture. In: Wilkins RH, Rengachary SS (eds) Neurosurgery. Williams and Wilkins, New York, pp 179–183
2. Drake JM, Prudencio J, Holowka S, et al (1994) Frameless stereotaxy in children. Pediatr Neurosurg 20:152–159
3. Golfinos JG, Fitzpatrick BC, Smith LR, et al (1995) Clinical use of a frameless stereotactic arm: results of 325 cases. J Neurosurg 83:197–205
4. Kato A, Yoshimine T, Hayakawa T, et al (1991) A frameless, armless navigational system for computer assisted neurosurgery. J Neurosurg 74:845–849
5. Koivukangas J, Louhisalmi Y, Alakuijala J, et al (1993) Ultrasound-controlled neuronavigator-guided brain surgery. J Neurosurg 79:36–42
6. Kondziolka D, Lunsford LD (1995) Guided neurosurgery using the ISG Viewing Wand. Contemp Neurosurg 17:1–6
7. Rhoten RLP, Luciano MG, Barnett GH (1997) Computer-assisted endoscopy for neurosurgical procedures: technical note. Neurosurgery 40:6332–6338
8. Sipos EP, Tebo SA, Zinreich SJ, et al (1996) In vivo accuracy testing and clinical experience with the ISG Viewing Wand. Neurosurgery 39:194–202
9. Watanabe E, Mayanagi Y, Kosugi Y, et al (1991) Open surgery assisted by the navigator, a stereotactic, articulated, sensitive arm. Neurosurgery 28:792–799
10. McDermott MW, Gutin PH (1996) Image-guided surgery for skull base neoplasms using the ISG Viewing Wand. Neurosurg Clin N Am 7:285–295
11. Drake JM, Sainte-Rose C (1995) The shunt book. Blackwell, Ann Arbor, p 142
12. Drake JM, Sainte-Rose C (1995) The shunt book. Blackwell, Ann Arbor, p 118
13. McDermott MW, Ciricillo SF, Gutin PH, et al (1995) Stereotactic insertion of an Ommaya reservoir: technical note. Can J Neurol Sci 22:235–238

Computer-Assisted Endomicroscopic Surgery

Takayuki Ohira[1], Masato Ochiai[1], Takeshi Kawase[1],
Masatoshi Wada[2], and Katsushige Nakamura[2]

Summary. Conventional neuroendoscopic surgery using a stereotaxic frame has two important problems: difficulty of holding the lenscope and loss of orientation. To solve these problems, we developed a new type of endoscopic surgery, computer-assisted endomicroscopic surgery. Computer-assisted endomicroscopic surgery was performed using the "navigated endomicroscope," consisting of a lenscope, a neuronavigation system, and a mechanical holding system. A three-dimensional (3-D) video system is also available. The motion of the system is smooth, and the endoscope can easily be set at any position and to any direction and also held very firmly. The position of the endoscope in the brain was continuously monitored throughout the operations. This configuration resembles a small system of a microscope equipped with neuronavigation. We believe the endomicroscope provides one means of minimally invasive neurosurgery.

Key words. Neuroendoscope—Neuronavigation—Minimally invasive neurosurgery—Computer-assisted neurosurgery—Mechanical holding system—3-D endoscope

Introduction

Neuroendoscopic surgery by a lenscope with multichannel ports such as the endoscope designed by Dr. Caemart [1] enables us to perform both-hands manipulation similar to that of microscopic surgery. However, this kind of conventional neuroendoscopic surgery with a stereotaxic frame has two important problems: the difficulty of holding the lenscope and loss of orientation.

To solve these problems, we developed a new type of endoscopic surgery that we named computer-assisted endomicroscopic surgery.

[1] Department of Neurosurgery, Keio University, 35 Shinano-machi, Shinjuku-ku, Tokyo 160, Japan.
[2] Mitaka Kohki Co., Ltd., 5-1-4 Ohsawa, Mitaka-shi, Tokyo 181, Japan.

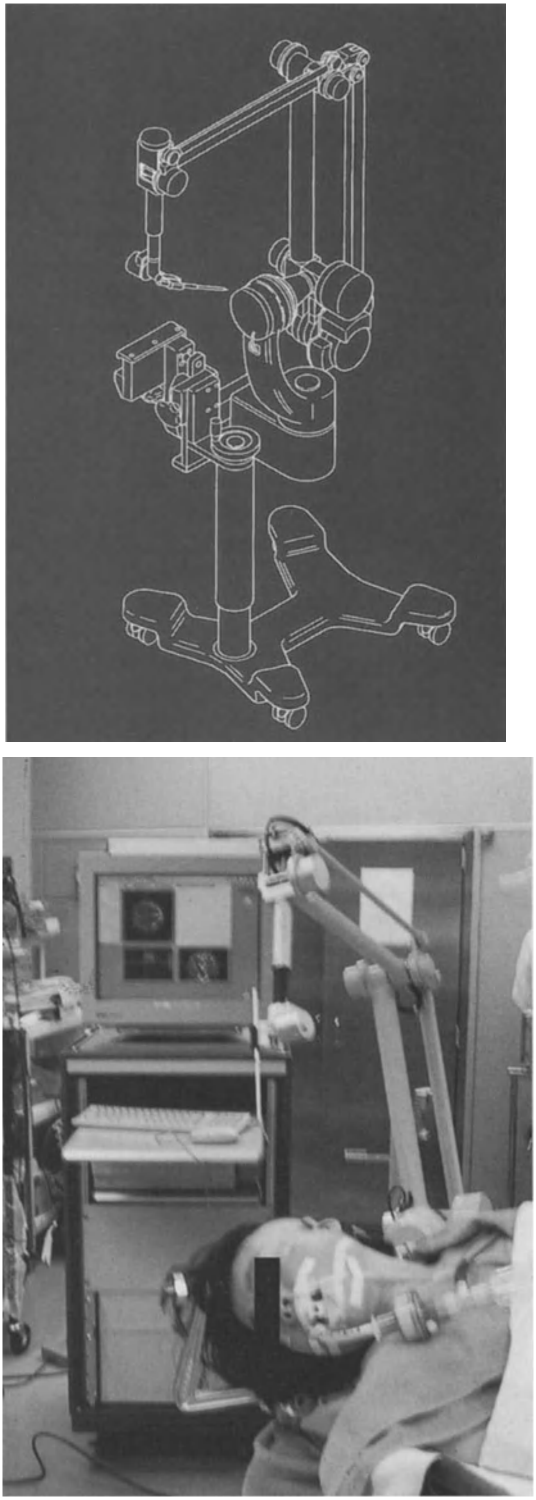

Fig. 1. The Brain Pointer is the neuronavigation system we developed for the navigated endomicroscope (*top*). The Brain Pointer is an arm-type neuronavigation system; the arm has a balancing and locking mechanism that enables the arm stay firm, allowing surgeons to have both hands free even under navigation (*bottom*)

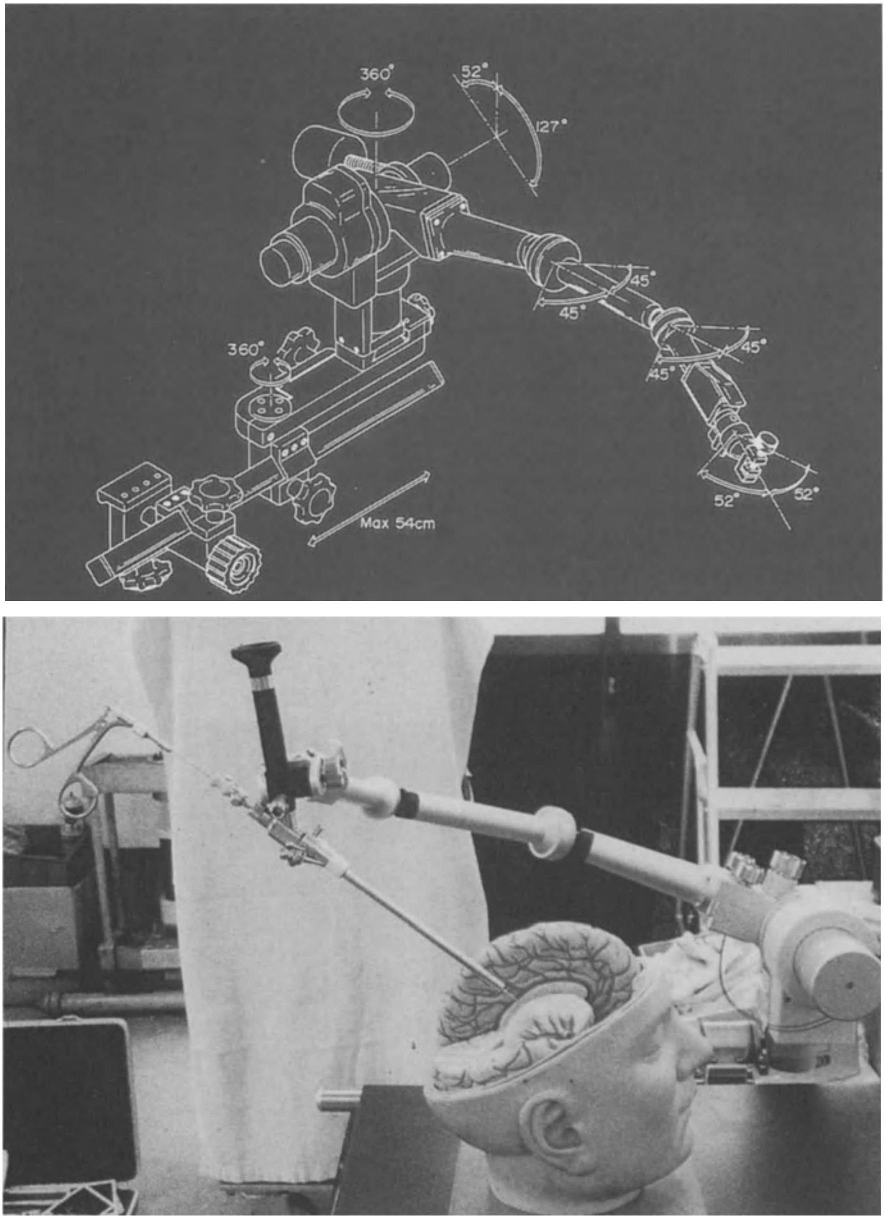

Fig. 2. The Point Setter is the mechanical holding system developed and modified for holding an endoscope (*top*). The system has an arm with multicubic joints, locked by a mechanical brake driven by oil pressure, that can hold as much as 2 kg of weight. The endoscope can be held by the Point Setter, and the position of the scope can easily and instantly be changed and fixed by this holding system (*bottom*)

Method and Results

Computer-assisted endomicroscopic surgery was performed using the "navigated endomicroscope," which consists of a lenscope, a neuronavigation system, and a mechanical holding system.

The neuronavigation system we developed for the navigated endomicroscope is the "Brain Pointer." The Brain Pointer is an arm-type neuronavigation system. Its arm has many characteristics: (1) a multijointed (seven joints) arm for free positioning; (2) high precision (2 mm; system precision, 3 mm) with seven encoders; (3) a balanced arm for easy handling and an open surgical field; and (4) a locking mechanism using electromagnetic clutches to retain arm direction and to hold 200 g of weight (Fig. 1). This balancing and locking mechanism enables the arm stay firm, allowing surgeons to have both hands free even under navigation.

The mechanical holding system is the "Point Setter," developed and modified for holding an endoscope. The system has an arm with multicubic joints locked by a mechanical brake driven by oil pressure that can hold as much as 2 kg. The endoscope can be held by the Point Setter, and the position of the scope can easily and instantly be changed and fixed by this holding system (Fig. 2).

We usually used a lenscope of the Gaab [2] or Caemaert [1] type because these lenscopes have multi-channel ports for irrigation and suction and also for surgical

Fig. 3. The three-dimensional (3-D) video system has two charge-coupled device (CCD) cameras, which can be attached to the conventional 2-D lenscope. The system can convert the two-dimensional (2-D) image from the endoscope to the 3-D image. The 3-D image is delivered to the surgeons through eyeglasses

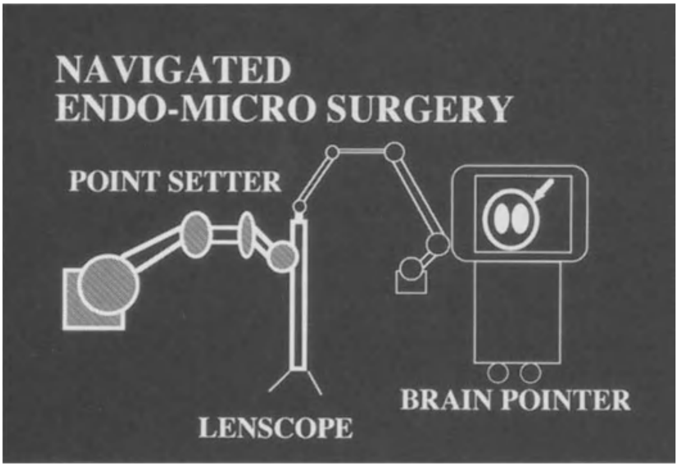

Fig. 4. The navigated endomicroscope consists of a lenscope, the Point Setter, and the Brain Pointer (*top*). A 3-D video system is also sometimes used. The motion of the system is smooth, and the endoscope can easily be set at any position and to any direction and also held very firmly (*bottom*)

Fig. 5. Computer-assisted endomicroscopic surgery is performed with the navigated endomicroscope. The position of the endoscope in the brain is continuously monitored throughout surgery. Surgeons can see the image from the endoscope and that from the navigation system simultaneously. This setup is just like a small system of a microscope equipped with a neuronavigation system

instruments. A three-dimensional (3-D) video system is also available. The system has two charge-coupled device (CCD) cameras that can be attached to a conventional two-dimensional (2-D) lenscope. The system can convert the 2-D image from the endoscope to a 3-D image. This 3-D image is delivered to surgeons through special eyeglasses (Fig. 3).

The endoscope is held by the Point Setter. The Brain Pointer is then attached to the endoscope to show the position of the tip of the endoscope in the brain on the CRT screen of the Brain Pointer's computer system. This setup—the endoscope, the Brain Pointer, and the Point Setter—was named the "navigated endomicroscope" (Fig. 4). The motion of the system is smooth, and the endoscope can easily be set at any position and pointed to any directions and also held very firmly. The position of the endoscope in the brain is continuously monitored throughout operations. Surgeons can see the image from the endoscope and that from the navigation system simultaneously. This setup resembles a small system of a microscope equipped with neuronavigation.

We have already used this system in 15 cases of intraventricular or cystic lesions and found it to be very useful (Fig. 5).

Discussion

As we have mentioned, problems of conventional neuroendoscopic operations include the difficulty of holding the endoscope and loss of orientation. Endoscopic operations are completely different from microsurgical operations. Surgical instruments are fixed in position and do not move within the operative field in endoscopic operations, because these instruments are introduced through the channel ports of the endoscope. Therefore, the endoscope must frequently change its position during an operation. In the conventional type of endoscopic operation, an endoscope was held by free-hand. However, free-hand holding of an endoscope interferes with two-handed manipulation such as microscopic operations and fine manipulations because the endoscope with its CCD camera system is heavy. The mechanical holding system, the Brain Pointer, is the key to solving these problems.

Because of the limited viewing field, loss of orientation is another important problem during neuroendoscopic operations. Identification of landmark structures in the ventricles, such as the foramen of Monro and mammary bodies, is very important to determine position during endoscopic operations. However, in cystic lesions, especially multicentric cystic lesions, no landmarks exist, and it is hard to know in which part of a cyst or in which one of multicentric cysts the endoscope has been placed. For these situations, a neuronavigation system is very helpful. A similar approach was tried with an armless-type neuronavigation system [3]. Conjunction of lenscopes and an arm-type navigation system is easy because both the lenscope and the arm end are straight.

We consider our system "endomicroscope" as a small microscope that can be introduced into the brain through a burrhole. We have already added a 3-D imaging system for an endoscope that gives us a 3-D view as in microscopic operations. We believe the endomicroscope to be one way of performing minimally invasive neurosurgery.

References

1. Caemaert J, Abdullah J, Calliauw L (1994) A multipurpose cerebral endoscope and reflections on technique and instrumentation in endoscopic neurosurgery. Acta Neurochir Suppl (Wien) 61:49–53
2. Schroeder HW, Gaab MR, Niendorf WR (1996) Neuroendoscopic approach to arachnoid cysts. J Neurosurg 85(2):293–298
3. Manwaring KH, Manwaring ML, Moss SD (1994) Magnetic field guided endoscopic dissection through a burr hole may avoid more invasive craniotomies. A preliminary report. Acta Neurochir Suppl (Wien) 61:34–39

Precisely Targeted Tumor Biopsy and Marking under CT-Fluoroscopy

Kazuhiko Nonomura[1], Tetsuo Kanno[1], Kazuhiro Katada[2], Masato Abe[3], Tsukasa Kawase[1], Isao Okuma[1], Nobuo Kiya[1], Motoharu Hayakawa[1], Katsuhiko Akashi[1], Ryoichi Kato[2], and Yoshihiro Ida[2]

Summary. An innovative imaging procedure, computed tomographic (CT) fluoroscopy, was recently developed by Katada and Toshiba Medical Corporation in Japan [1,2]. This procedure permits sequential display of computed tomograms in real time. CT-fluoroscopy has been found to be extremely useful for real-time monitoring, which ensures the safety and accuracy of invasive techniques such as punctures in the neurosurgical field [3]. We recently, attempted targeted needle biopsy at three points, the subcortex near the lesion and the lateral side and center of the lesion, under CT-fluoroscopy. We then attempted to precisely place a marker at the inner border of the lesion near the internal capsule. A round mini-coil was used as the marker. Two weeks later we succeeded in extensively resecting the tumor lesion without producing motor weakness because the marker's shadow on an ultrasonic image allowed navigation to the bottom of the lesion very precisely by showing where the eloquent area was located. A neuronavigation system using preoperative images was used simultaneously. There was a difference of 10 mm between the point indicated with the navigator and the actual position of the marker. This difference is considered to reflect brain shift caused by intraoperative leakage of cerebrospinal fluid. Thus, the computer-aided neuronavigation system appears to require a feedback technique for intraoperative brain shift that would enhance precision, reliability, and safety. In this respect, CT-fluoroscopy combined with intraoperative CT is considered to play a potentially very important role.

Key words. CT-fluoroscopy—Computer-assisted neurosurgery—Open MRI—Neuronavigation—Ultrasonography—Astrocytoma

---

[1] Department of Neurosurgery, [2] Department of Radiology, [3] Department of Pathology, Fujita Health University School of Medicine, 1-98 Dengakugakubo, Kutsukake-cho, Toyoake, Aichi 470-11, Japan.

Introduction

Computed tomographic (CT)-fluoroscopy was applied clinically in the field of neurosurgery for the first time in 1993. Early clinical application has since been carried out in the following 12 patients: 9 with brain hemorrhage, 1 with an intraventricular hematoma caused by moya-moya disease, 1 who was undergoing neuroendoscopic observation of a cystic brain tumor, and 1 requiring cisternal drainage of a subarachnoid hemorrhage [4,5]. The result of this early clinical application to cerebrovascular disease was mainly aspiration of brain hemorrhage. CT-fluoroscopy appears to be a very important imaging procedure in attempts to achieve minimally invasive neurosurgery.

Keyhole surgery, interventional techniques, and neuroendoscopic procedures have recently become widely used in the field of neurosurgery. With such new techniques, navigation systems or real-time monitoring instead of information from direct observation is needed. Moreover, computer technology has made great progress and its cost has fallen remarkably in recent years. Thus, numerous neuronavigation systems have been developed [6–8] that are very useful, but it is still impossible to track a target which shifts intraoperatively [9].

CT-fluoroscopy is a real-time monitoring method that allows the correspondence of intraoperative cerebral changes with display information from areas other than the restricted operative field. Visualizing modalities similar to this method include ultrasonic tomography and open magnetic resonance imaging (MRI), but these have not yet been perfected in terms of precision of coordinates, objectivity, and resolution and have not become well established with the exception of a few areas of use. Some attempts to conduct open MRI without radiation exposure have also recently been initiated. This is a noteworthy modality but at present there are several complex prablems, such as distortion and magnetic field leak, as compared to CT-fluoroscopy. Furthermore, there are also many restrictions on open MRI; the application of open MRI as an intraoperative monitor has only recently begun [10–12].

With the clinical application of CT-fluoroscopy, radiation exposure to surgeons and patients is a major concern. Strict evaluation in this regard and innovations in reducing the exposure dose are essential. Based on the aforementioned consideration, the usefulness and possibilities of CT-fluoroscopy in the neurosurgery field, particularly computer support techniques, were investigated.

Clinical Materials and Methods

Data sampled by the high-speed CT scanner were transferred to the memory field through a preprocessor. The raw data stream was calculated with deletion and addition employing a new partial reconstruction algorithm and displayed through the monitor simultaneously. The first image displayed was input into the data stream of the memory field and the other images were continuously renewed. Thus, CT-fluoroscopy provided real-time reconstruction and display of CT images during scanning at a rate of 6 images per second with a 0.64-s delay. The delay in image reconstruction is less than 0.25 s, which is nearly within real time (Fig. 1). Thus, we can obtain real-time images and ascertain what is happening in the brain at the time of imaging.

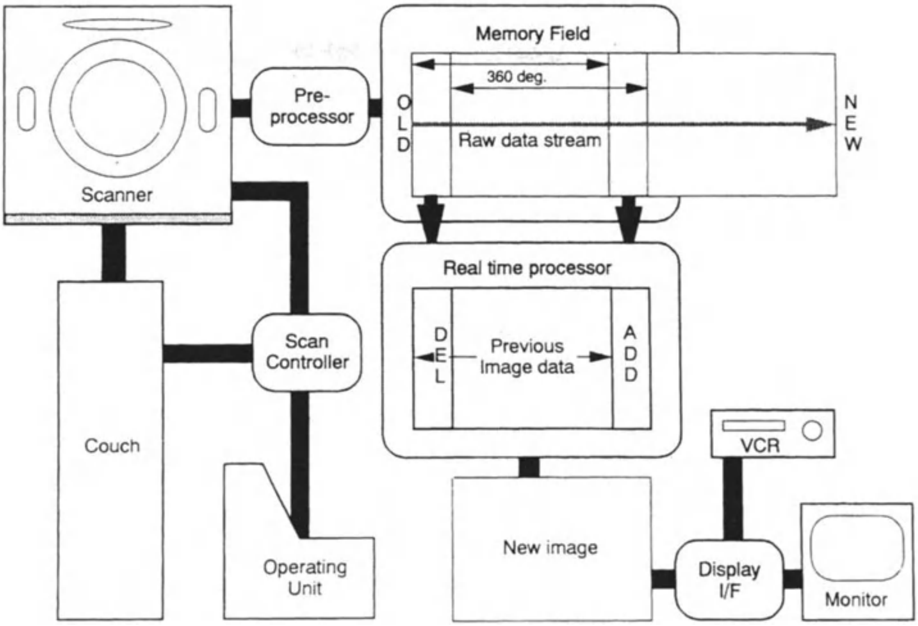

Fig. 1. Computed tomographic fluoroscopy (CT-fluoroscopy) system. *deg.*, degree; *DEL*, delete; *I/F*, interface; *VCR*, videocassette recorder

We recently applied CT-fluoroscopy to biopsy and marker installation for a case of intraaxial tumor. The patient was a 55-year-old woman with right hemisensory disturbance and mild dysarthria caused by an astrocytoma. CT revealed a low-density area in the left basal ganglia without enhancement by contrast medium (Fig. 2), and MRI also revealed a T_1-weighted image of low intensity, a T_2-weighted image of high intensity, and a proton image of high intensity (Fig. 3). Angiography revealed an avascular area without tumor staining.

On July 8, 1996, we attempted targeted needle biopsy using a radiolucent framed stereotaxy type SBD-03 (Tokai Rika, Japan) at three points: the subcortex near the lesion, the lateral side of the lesion, and the center of the lesion. These biopsies were done under real-time CT-fluoroscopic observation (Fig. 4).

The first targeted biopsy was performed at the subcortex near the lesion, easily and precisely. The specimen was consistent with a subcortical structure which included an edematous portion, but there was no evidence of malignancy with hematoxylin-eosin (H-E) staining (Fig. 5A). Next, the lateral side of the lesion was sampled, which showed some nuclear atypism, but neither mitosis nor endothelial proliferation was seen in the specimen with H-E staining (Fig. 5B). Finally, the center was precisely biopsied, allowing visualization of the biopsy forceps opening and closing in real time (Fig. 4).

Pathological findings appeared the same as those of the lateral side specimen. They were diffusely stained with glial fibrillary acidic protein (GFAP) (Fig. 5C), and the

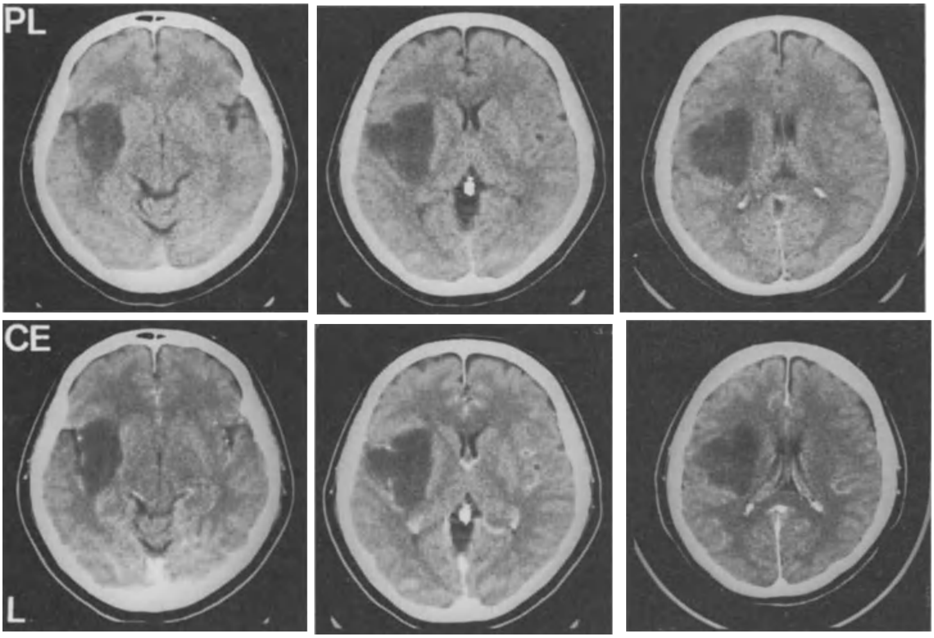

Fig. 2. CT revealed low-density area in the left basal ganglia without enhancement following injection of contrast medium. Lesion was almost uniformly low in density, but some areas indicated partial isodensity

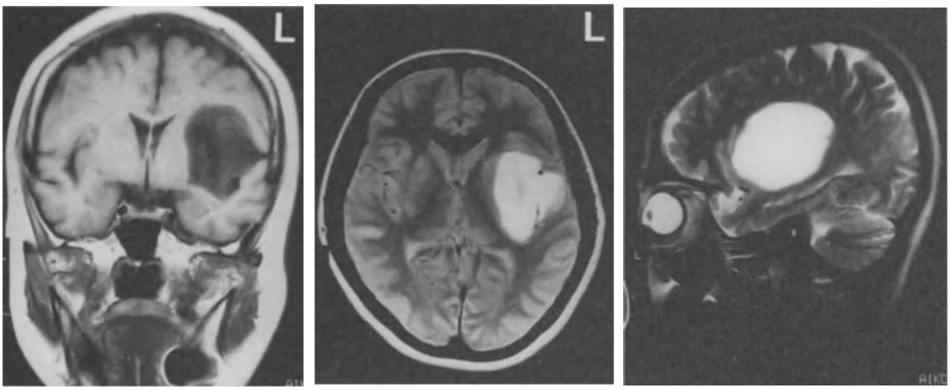

Fig. 3. MRI revealed T_1-weighted image of low intensity (*left*), proton image of high intensity (*center*), and T_2-weighted image of high intensity (*right*)

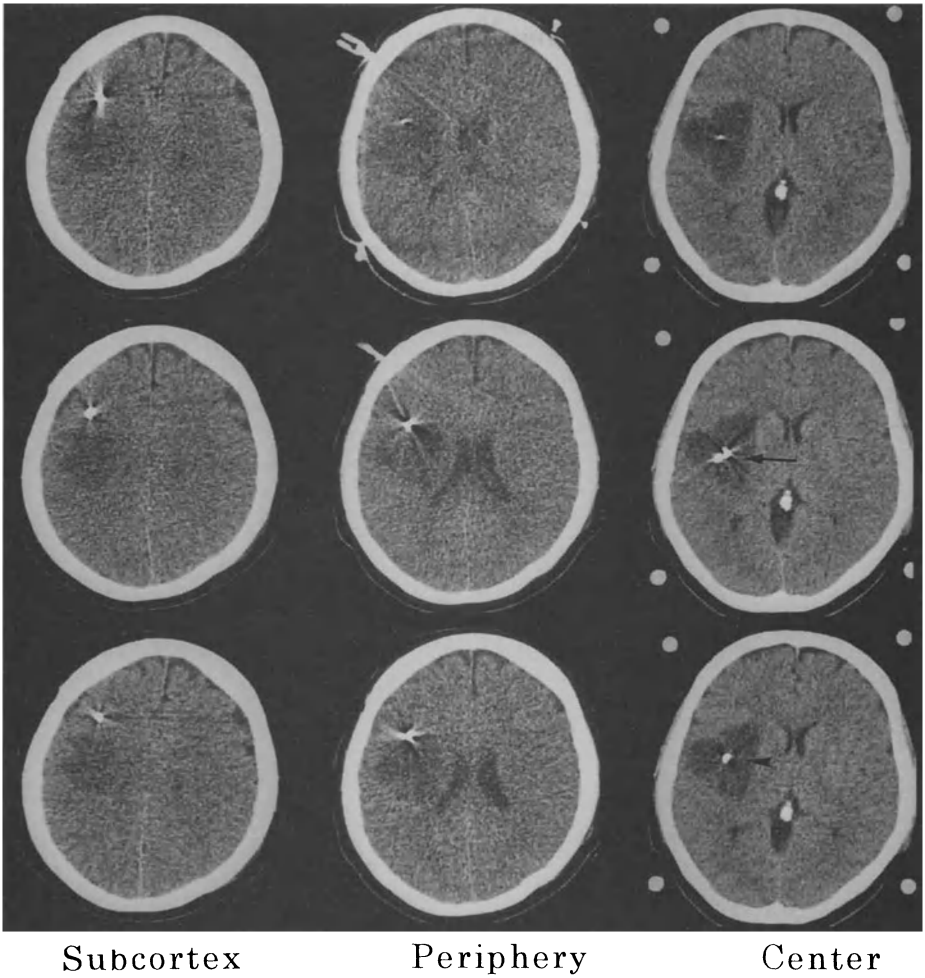

Fig. 4. *Left*: CT line shows first target biopsy at *subcortex* near the lesion under CT-fluoroscopic guidance. Artifacts caused by the biopsy needle metal disturbed the CT-fluoroscopic images but the margin of the lesion can be precisely detected. *Center*: CT line shows second target biopsy under CT-fluoroscopy. *Right*: CT line reveals last target biopsy. We can detect exactly the biopsy forceps just opening (*arrow*) and closing (*arrowhead*) in real time

MIB-1 (Fig. 5D) expression rate was approximately 1.38%. The lesion was thus diagnosed as a low-grade astrocytoma (grade 2). After the report from the neuropathologist on the frozen section, we attempted as the next step to place a marker precisely at the inner border of the lesion near the internal capsule. A round mini-coil made of platinum (0.46-mm diameter, single coil; Hilar Cook), covered with a feather, was used as the marker (Fig. 6). This marker has been widely used for embolization in endovascular surgery.

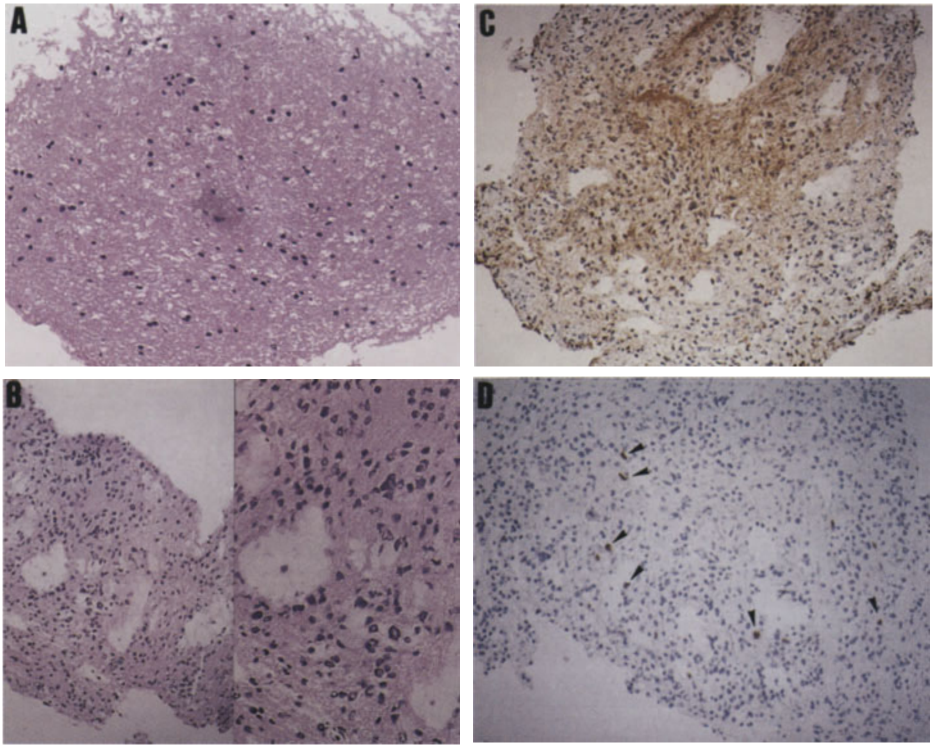

Fig. 5. **A** The first target biopsy done at the subcortex near the lesion showed normal structure with minimal edematous findings with hematoxylin-eosin (H-E) stain. There was no evidence of malignant cells. **B** The third target biopsy at the center of the lesion revealed some nuclear atypism, but neither mitotic findings nor endothelial proliferation was seen. The lateral side of the lesion produced the same findings. **C** The specimen shown in **B**, stained with glial fibrillary acidic protein (GFAP). **D** The positivity index of the specimen stained by MIB-1 antigen was 1.38%; brown stain (*arrowheads*), cells positive by MIB-1

Upon completion of the biopsy and marking procedure, the patient had no neurological deficits such as motor weakness or speech disturbance. Postoperative CT revealed no bleeding, and the marker had been placed at the targeted point with great precision (Figs. 6, 7).

Two weeks later, tumor resection was performed via the left transsylvian approach. We also used intraoperative ultrasonography and the navigation system termed the Brain Pointer, an articular frameless system (Mitaka Koki, Mitaka, Japan). The navigation system, which consists of preoperative digital images only, had indicated the exact point until extradural manipulation. Through navigation guided by the marker's shadow in ultrasonic images, we could find the bottom of the lesion very precisely, showing where the eloquent area was located. However, this point gradually shifted after opening the dura.

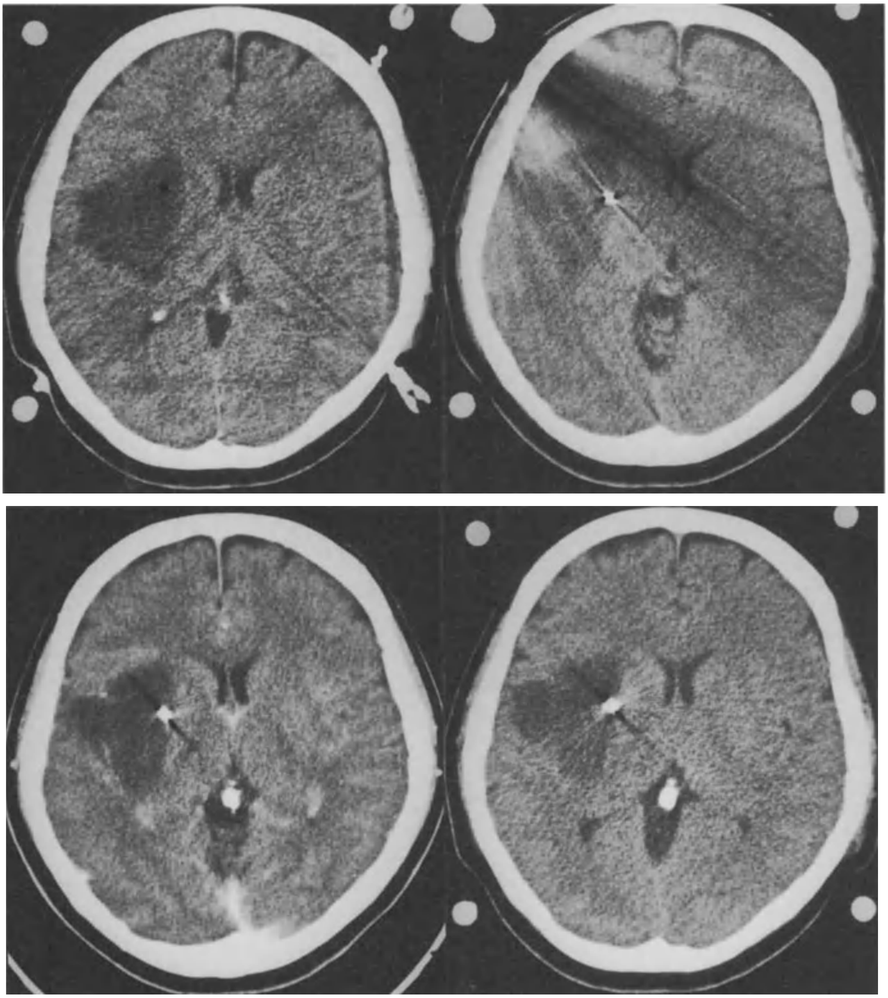

Fig. 6. Placement of the marker, a round platinum mini-coil (Hilar Cook; 0.46-mm diameter, 3-mm length, for endovascular embolization), under CT-fluoroscopic guidance to the deep site of the lesion

The discrepancy between the marker that was installed by CT-fluoroscopic guidance before tumor resection and the point indicated by the Brain Pointer finally reached 10 mm (Fig. 8), suggesting brain shift during the operation. Just after the marker was removed, dyed oxycel cotton was placed at the same depth; furthermore, the tumor was extracted to the depth of the marker level. Thus, we succeeded in extensive resection of the tumor without producing motor weakness or other deficits (Fig. 9).

Fig. 7. After the targeted tumor biopsy and marking, CT revealed no bleeding in the lesion, along the needle trajectory, or near the lesion

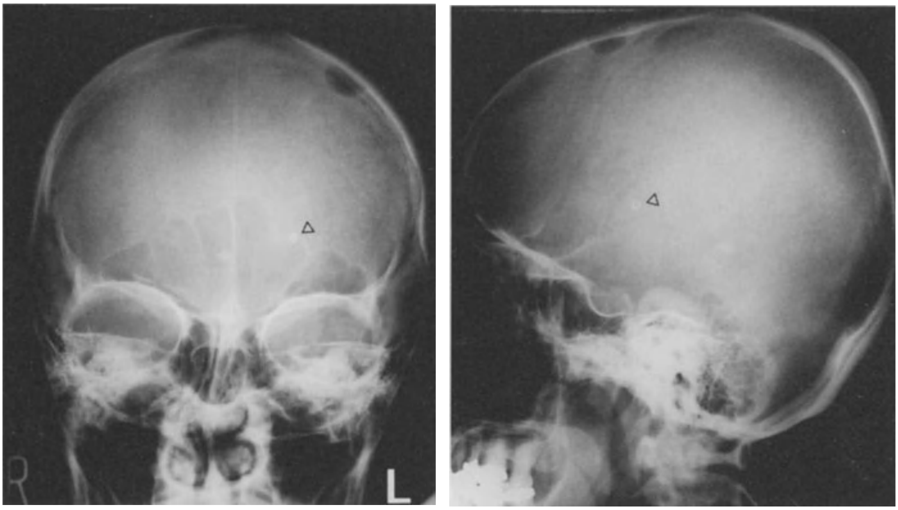

Fig. 8. After marker installation, plain cranial skull X-ray showed the marker placed accurately in the target (*arrowheads*)

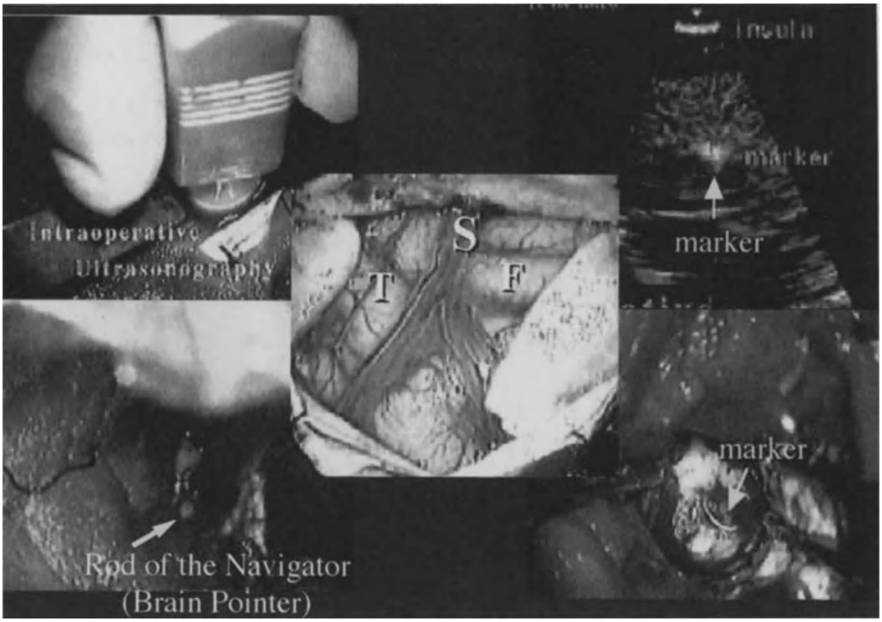

Fig. 9. The platinum marker was detected by a high echogenic shadow with low echo tail by intraoperative ultrasonography (*upper left*). The operation used the transsylvian fissure (*TSF*) approach (*inset, center*). We also used the Brain Pointer (*lower left*) and intraoperative ultrasonographic guidance. When the marker was exposed in the microscopic field (*upper* and *lower right*), the discrepancy was 10 mm from the point indicated by the arm (*arrow*) of the navigation system

Conclusions

1. Brain tumors at the targeted sites could be biopsied precisely and safely by CT-fluoroscopy.
2. CT-fluoroscopic techniques, even at their present stage of development, are extremely useful for procedures such as puncture and biopsy.
3. Marks were made in the vicinity of the deep eloquent area of an astrocytoma of the basal ganglia under CT-fluoroscopic observation. This marking was extremely useful for the subsequent extensive resection used concomitantly with intra-operative ultrasonic tomography within the range at which neurological deficits would not be produced.
4. When the frameless neuronavigation system based on preoperative image information was used with tumor resection, a shift of approximately 10 mm from the marker occurred.

References

1. Katada K, Anno H, Koga S, et al (1993) Initial trial with CT fluoroscopy. Radiology 190:662
2. Katada K, Anno H, Ogura Y, et al (1994) Early clinical experience with real-time CT fluoroscopy. Radiology 193(suppl):339

3. Kanno T, Nagata J, Nonomura K, et al (1993) New approaches in the treatment of hypertensive intracerebral hemorrhage. Stroke 24(suppl)12:96–100
4. Nonomura K, Kanno T, Katada K (1995) Clinical application of CT fluoroscopy to the treatment of hypertensive intracerebral hemorrhage. In: Kanno T (ed) Proceedings of ICH 95. Neuron, Tokyo, pp 155–167
5. Katada K, Kato R, Nonomura K (1996) Guidance with real-time CT fluoroscopy: early clinical experience. Radiology 200:851–856
6. Iseki H, Masutani Y, Nishi Y, et al (1996) Neurosurgical operation under volume-graphscope. In: Lumke HU, Vannier MW, Inamura K, Farrman AG (eds) Computer and communication systems for image-guided diagnosis and therapy, CAR 96. Elsevier, Amsterdam
7. Cinquin P, Baville E, Barbe C, et al (1995) Computer assisted medical interventions. Robots in surgery. IEEE Trans Med Biol 14(3):254–263
8. Renhardt H (1995) Neuronavigation: a ten years review. In: Taylor R, Laval'ee S, Burdea G, Mosges R (eds) Computer-integrated surgery. MIT Press, Cambridge
9. Buchols RD, Yeh DD, Trobaugh J, et al (1997) The correction of stereotactic inaccuracy caused by brain shift using an intraoperative ultrasound device. In: Proceedings, CVRMED-MRCAS-97, Grenoble, France, pp 459–466
10. Lens GW, Dewey C (1995) An open MRI system used for interventional procedure: current reserch and initial clinical results. In: Proceedings, Computer-assisted radiology (CAR), Berlin, pp 1180–1187
11. Schenck JF, Jolesz FA, Romer PB, et al (1995) Superconducting open-configuration MR imaging system for image-guided therapy. Radiology 195:805–814
12. Moriatry TM, Kikinis R, Joles IA, et al (1996) Magnetic resonance imaging therapy. Clin Front Interact Image-guided Neurosurg 7(2):323–331

Interactive Image-Guided Surgery Using an Infrared-Based System

Lucia Zamorano, Razvan Buciuc, Federico C. Vinas, and Fernando G. Diaz

Summary. The surgical management of intracranial tumors has always been a challenge for the neurosurgeon, from the dual perspective of acquiring a complete resection on one hand and maintaining neurological function on the other. Stereotactic technology followed by computer-assisted neuronavigation has markedly changed the outcome of these operations. It has improved the accuracy of resection, diminished the neurological complication rate, and decreased the length of hospital stay and costs. Interactive image-guided surgery has extended its applications to other fields such as epilepsy and skull-base and spine surgery, and is even used in brain trauma. From December 1991 to December 1996, we used an infrared-based system for intraoperative image-guided resections; in 1995 we began using the same system for spinal applications as well. Our patient group includes 464 patients treated for intracranial pathology and 27 for spinal lesions. In this chapter we discuss our system, protocols used for different applications, and preliminary results in patient care. From our experience with this system we conclude that the infrared-based neuronavigator is a very useful technology that increases accuracy and the safety of surgical resection.

Key words. Computer-assisted—Image-guided—Infrared—Interactive—Resection

Introduction

Surgery in brain parenchyma is often difficult because of the lack of identifiable boundaries between the mass to be resected and the adjacent functional tissue [1–3]. The need for localization and orientation in a "sea" of tumor and brain has generated the development of neuronavigational instruments. The origin of interactive image-guided neurosurgery stems from the classic stereotactic, frame-based technique. From point-target localization to surface and volume navigation, significant steps have developed from several technological advancements: (1) computed tomographic

Department of Neurological Surgery, Wayne State University, Harper Professional Building, Suite 930, 3900 John Road, Detroit, MI 48201, U.S.A.

Table 1. Detailed pathology of the cases operated using interactive image guidance at Wayne State University

Location	Pathology type	Gross pathology	Fine pathology	Number of cases
Brain	Tumors	Glioma	Low-grade astrocytoma	27
			Oligodendroglioma	8
			Ependymoma	6
			Subependymoma	4
			Anaplastic astrocytoma	51
			Anaplastic oligodendroglioma	4
			Anaplastic ependymoma	2
			Glioblastoma	82
			Ganglioglioma	3
		Meningioma		24
		Choroid plexus	Papilloma	2
			Carcinoma	2
		Pituitary tumor		3
		Pineal tumors		3
		Craniopharyngioma		3
		Dermoid		2
		Acoustic neuroma		2
		Cholesterol granuloma		1
		Medulloblastoma		3
		Glomus jugulare		2
		Hamartoma		2
		Chordoma		2
		Hemangioblastoma		1
		Metastases		95
		Unclassified		24
	Vascular malformations	Arteriovenous malformations (AVM)		8
		Cavernomas		14
		Venous malformations		1
	Abscess			3
	Aspergilloma			1
	Tuberculoma			1
	Epilepsy			37
	Radiation necrosis			14
	Colloid cysts			5
	Other cysts			5
	Trigeminal neuralgia			1
	Unclassified lesions			14
Spine	Fractures	Cervical		1
		Thoracic		5
		Lumbar		1
		Sacropelvic		5
	Lumbar stenosis			6
	Lumbar disk			1
	Lumbar tumor			3
	Lumbar osteomyelitis			1
	Spondilolystesis			3

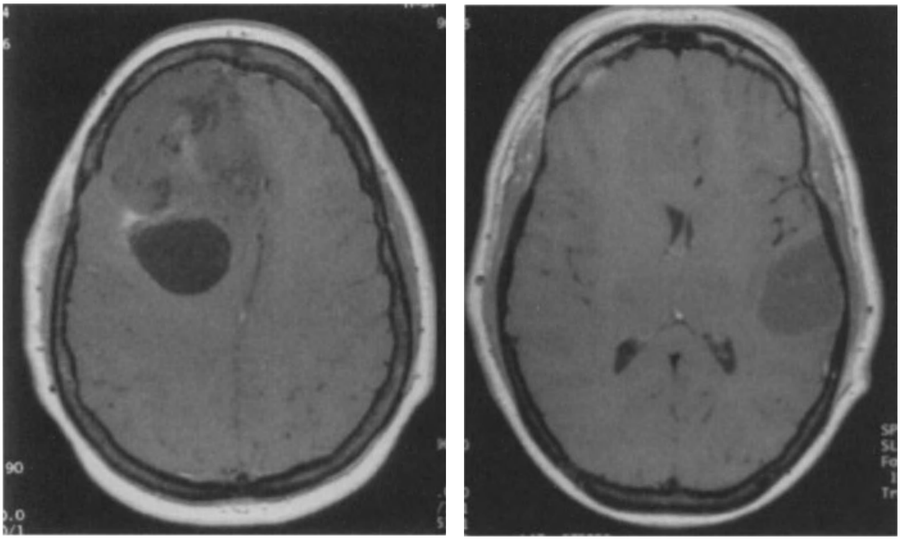

a b

Fig. 1a,b. Case example, preoperative MRI: T_1-weighted axial scans through areas with tumor. **a** Scan through right frontal region. **b** Scan through left temporal region

(CT) scan technology with direct visualization of brain parenchyma, followed by (2) improvements in the fine-scan table movements, and finally (3) the development of several types of three-dimensional (3-D) digitizers [4–7]. Concomitantly neurosurgeons as well as computer scientists have developed multiple ways of registering the CT and later magnetic resonance imaging (MRI) coordinates (image coordinates) with the patient's anatomy, initially through frame-based systems and later through frameless ones [4,8,9]. The final step to the current state of intraoperative neuronavigation consisted of introducing the 3-D digitizer which, after registering different image modalities with real anatomical structures, displays the real position of a pointer on a preoperative MRI or any other type of image. The real-time track of the pointer's position makes possible precise navigation within preplanned volumes. In this way the surgeons can orient themselves to the lesion's margins as well as protect eloquent areas in the brain.

Used initially in the resection of brain tumors, this technology has been extended to other areas as well, such as epilepsy, vascular surgery for malformations, spine surgery, and even trauma.

In December 1991 we began using an infrared-based digitizer for interactive image-guided resections. Among the many available 3-D digitizers we have chosen the infrared type for several reasons: (1) the infrared system has a greater accuracy than other similar digitizers; (2) its design makes it flexible when attaching different surgical instruments; (3) it gives a real-time display of the surgical position; and finally (4) it may be used in both frame-based and frameless environments.

In the following sections we describe the components of the infrared system we use, the methodology of image-guided neurosurgical navigation, and our preliminary experience with its use.

Materials and Methods

From December 1991 until December 1996 we treated 491 patients with intracranial and spinal lesions using the infrared localizer. There were 201 females and 290 males in our study; their ages ranged from 1 year to 89 years, with mean age of 44.5 years. In this patient group, 361 patients had brain tumors; 37 were treated for epilepsy, 23 for vascular malformations, 3 for brain abscesses, 2 for granulomatous lesions, 14 for radiation necrosis, 5 for colloid cysts, 5 for other cysts, 14 for other intracranial lesions, and 27 for spinal pathology. The detailed pathology is presented in Table 1.

Each patient underwent preoperative CT (and MRI) scanning, and in those operated for intracranial pathology, postoperative imaging studies including a noncontrast CT scan. After surgery all patients with intracranial lesions had a noncontrast CT scan to evaluate grossly the accuracy of resection and to rule out postoperative bleeding. After the CT was completed all patients spent 1 night in the intensive case unit (ICU) and were transferred to a neurosurgical floor the next day. After 3–5 days of hospital stay the uncomplicated cases were discharged home. In addition, all patients were evaluated neurologically preoperatively and postoperatively to assess improvement, new deficit, or residual deficit.

Applications of Interactive Image Guidance and Preliminary Results

Primary Intraaxial Tumors

Low-grade intraaxial tumors have a good long-term prognosis; the main factor of prognosis is the extent of the resection. Frequently their margins may have texture and coloration similar to that of the surrounding brain, which makes an accurate resection difficult. The issue is complicated even further when such tumors are situated in the vicinity of eloquent areas such as the motor or speech cortex. In such situations the extent of resection is important for the survival prognosis as is confinement within the margins of resection for the functional result. Intraoperative image guidance increases the accuracy of these resections and identifies the eloquent areas, thereby increasing the safety of surgery.

For more malignant tumors, patient survival is also dependent on the extent of resection although in a different fashion. By obtaining a reduction of 90% or more in the tumoral mass, the tumoral bed is better prepared for further therapy such as external radiation or placement of radioactive implants.

During the period 1991–1996 we operated on 47 low-grade gliomas and 139 glioblastomas using interactive image guidance and cortical functional mapping where tumors have been located in eloquent areas. We believe that the infrared system has been most helpful in acquiring volumetric resection and, together with cortical functional mapping, in defining the areas to be spared.

Brain Metastases

The use of an infrared localizer for brain metastases has proven to be useful, especially when the tumors have an irregular shape or when the plane of cleavage is not defined (as in the case of melanomas) when again the localizer orients the surgeon for an accurate volumetric resection. For well-defined lesions, the system still plays a role in diminishing the size of the craniotomy size and providing a good orientation for deep-seated lesions.

During the time of this study we have used the infrared system in 95 cerebral metastases. In all cases we have succeeded in completely resecting the tumoral mass and, again as in the case with intraaxial tumors, we could identify and eventually spare the eloquent cortex. In all metastases there have been no complications related to infrared use. The operative time has been minimized to an average of 2.5–3 h, and the size of craniotomy has been reduced to a minimum by the accurate preoperative localization of the tumor margins.

Vascular Malformations

The surgical approach to a vascular malformation is a challenging one. The difficulty of distinguishing the arterial feeders from passing vessels, the complicated shape of the malformation, and the arterialized venous outflow, as well as the size, location, and other associated factors, may confuse the surgeon and increase the difficulty of the operation. The infrared localizer has proven in our experience to be an excellent tool for approaching these lesions. When its use is combined with a preoperative stereotactic angiogram, we have been able to identify the arterial feeders in most cases and by this means to increase the safety of the surgical procedure and reduce its length. As of December 1996 we have operated on 23 patients with vascular malformations using intraoperative image guidance. For cavernous angiomas, the infrared system contributes (as in the case of metastases) to the reduction of the surgical approach as well as to the delimitation of the malformation's margins.

Epilepsy

The use of infrared guidance in epilepsy has a significant value. In the evaluation of temporal focus, the system may be utilized to guide the application of subdural electrodes over the suspected epileptogenic focus or over certain anatomical areas or lesions hidden to the craniotomy site. Also, with the infrared localizer electrocorticographic epileptogenic areas may be registered and further resected.

For the surgical treatment of intractable seizures, the main usefulness of the system is to guide the extent of resection be it in the extended or reduced temporal lobectomies or in the extratemporal approaches [5,10]. We have used the infrared system mainly in guiding the extent of surgical resection, and again the results have been gratifying in both the safety of resection as well as of the seizure control. In interactive image guidance for epilepsy we routinely use preoperative positron emission tomography (PET) scans with both glucose and flumezanil for coregistration with MRI and CT scan images. So far 28 cases of intractable epilepsy have been approached by intraoperative image guidance.

Particular Locations

Intraventricular and skull-base pathology represent particular areas that deserve special consideration. The lengthy aspect of skull-base surgery as well as the complicated anatomical details in the vicinity of or inside skull-base tumors may tax the neurosurgeon and create confusion in key moments. A good orienting tool in an often-distorted environment may significantly reduce the morbidity of these procedures together with the surgical time. On the other hand, intraventricular lesions often have irregular shapes and are surrounded by important vessels that must be spared. Identification of such structures is of great help during resection of an intraventricular tumor.

Within our study period we have resected 23 skull-base tumors and 18 intraventricular lesions.

Spine Lesions

The use of neuronavigation in spine surgery was triggered by the relatively high number of misplaced pedicle screws and the morbidity associated with this complication. This application was started at Wayne State University initially as a lab project in which two groups of pedicle screws were inserted with and without infrared guidance. Thereafter cadaveric spines were sectioned in thin slices and a comparison done. The result was a significant difference in accuracy for the group in which the screws were inserted with guidance [11–13]. The application was further refined for intraoperative use and since September 1995 we have provided technical support for the use of infrared localizer-based guidance in spine applications.

We recently redesigned the Neurological Planning System (NSPS) software as a single program with applications for both intracranial and spinal surgery. In our institution the spine application of the infrared localizer has been used mainly for posterior surgical approaches. However there have been several cases in which the system proved useful even for anterior lesions. We have operated on 26 patients with spine lesions using this technology. In all spine cases the image guidance has been useful in "giving" the optimal point of entry in the pedicle as well as the surgical trajectory. However, compared with the intracranial navigation, for spine surgery we have noticed that registration accuracy is somewhat more difficult to maintain during the procedure and that at times it is also hard to maintain the angle of drilling during the initial foraminal canal in a fixed position without rigid stabilization.

Discussion

The Infrared Digitizer

The infrared digitizer is an optoelectronic system based on a 3-D motion analysis system (Optotrak 3D Bar, Northern Digital, Waterloo, IA, USA) [4,14]. The system uses three infrared cameras, each of which employs a 2048 linear charge-coupled device (CCD) array and a cylindrical lens. The cameras continuously track the position of up to 256 light-emitting diodes (LEDs) during the surgical procedure. The LEDs can be mounted on different surgical instruments, on the patient's body (attached to the skull by a headframe, or to the spine), and on the surgeon's headlight.

When the LEDs are mounted on the patient's anatomy in a fixed way, this is referred to as the "patient rigid body." Once the image coordinates from the LEDs to the camera are registered with the patient's body, the system will remain in registration regardless of repositioning the patient, so long as the rigid relationship between the head or spine and the reference points is maintained.

When the LEDs are included in a probe that may be further attached to surgical instruments, this will represent the neuronavigator as such. Given the significant flexibility of the system, the LEDs may be included in a single probe and different surgical instruments may be attached to it interchangeably (as is the case for brain applications), or multiple LEDs may be attached to multiple instruments that are used and displayed separately as, for example, in the spine surgical unit. Finally, the LEDs may be attached to the surgeon's headlight and display the surgeon's position in relation to the areas of interest.

With software developed at Wayne State University, the calibration of the infrared digitizer is possible within minutes as well as recalibration for different instrument use. The pointer used for intracranial applications contains 20 LEDs mounted in different coordinates so that continuous display is possible independent of the surgical instrument's position; only 3 LEDs are necessary at one time for maintaining an accurate position. Given the frame rate of the system (3500Hz/number of markers) it is possible to have real-time anatomy reconstruction and display.

There are two main advantages of the infrared digitizer, when compared to the sonic digitizer or articulated arm; one is the accuracy of the system, which is 0.1 mm in an operating volume of 1×1 m at a distance of 2 m from the infrared cameras. As compared with other systems the infrared seems to be the most accurate, which increases the range of surgical techniques to more delicate areas like the posterior fossa, skull-base regions, and the intraventricular environment. The second advantage is flexibility when using a variety of tools and its accuracy in either a frame-based or frameless environment. One disadvantage is the fact that there must be unobstructed space between the LEDs and the camera. This limitation is overcome by placing multiple LEDs in different coordinates so that regardless of surgical instrument position a minimum of three LEDs are still "seen" by the camera.

The Neurosurgical Planning System

To be able to preoperatively plan a surgical strategy based on recently acquired images, a computer environment is necessary. In the Detroit Medical Center (DMC) this consists of a local network of workstations connected through a central network to the imaging suites, which includes CT, MRI, PET, or any other imaging modality deemed necessary by the neurosurgeon [14]. Our imaging suite is located adjacent to the operating room and is easily accessible by both the surgical and computer team. The images acquired under specific protocols are then registered with the frame-based or frameless systems to be used in the preplanning stage and intraoperatively.

To use the data collected from the imaging scans, we use a software program developed at our institution, the NSPS. The software was initially developed mainly for intracranial procedures but is currently being used for spinal cases as well. As mentioned earlier, the software is used specifically for defining a surgical corridor to a target point or area, and is also used for superimposing and comparing actual patient data with anatomical atlases and for interactive intraoperative image guidance with the use of an infrared system.

Image Acquisition

In principle any image modality may be used for intraoperative navigation provided that the images generated can be correlated to other imaging studies, to the anatomical atlas resident in the computer, and to the patient's actual anatomy. Registration techniques most frequently involve two kinds, surface and point registration. Surface registration uses attachments to the skin surface that serve as markers; these markers show up on the imaging studies. Although the use of implantable fiducial markers is more comfortable for the patient and allows imaging to be done at any time before the surgical procedure (as opposed to using coordinates on a headframe, which means imaging must be done the day of surgery to maintain coordinate consistency), it is more time consuming and less accurate. Fiducial marker registration is most often used for co-registration of PET images with other image modalities. Point registration is the most accurate and most frequently used method of image registration. In terms of coordinate systems used for registration there are two known such systems, frame-based and frameless.

At Wayne State University we use both systems as each has its own advantages. For frame-based registration we use the Zamorano–Dujowny (Z-D) headframe and for the frameless system we have recently introduced a system of implantable fiducial markers compatible with both MRI and CT imaging. The most common type of imaging in neuronavigation is MRI. The current capabilities of obtaining visual data in the MRI include a large spectrum that can be used for different purposes. The type of images, image thickness, field of view, magnification, and plane of acquisition all can be tailored to the specific requirements of a particular case. We have developed protocols of MRI image acquisition for different pathologies, and for each patient the neurosurgeon is consulted regarding the specific sequence to be obtained in the MRI. We routinely obtain a preoperative MRI and CT scan, which are thereafter transferred to the computer room and processed while the patient is being prepared for surgery.

Surgical Planning

In our study, all patients underwent imaging studies that included CT and MRI, and in selected cases patients had functional positron emission tomography (PET), angiography. For spinal patients a CT scan with 1-mm-thick slices and bone windows was sufficient. The data from imaging studies for each patient were then run through a transformation matrix that converts the data to 3-D images to be used by the NSPS software for preplanning.

The NSPS is a multimodular software program specifically designed for manipulating large amounts of data [15,16]. After initial processing of image information, the

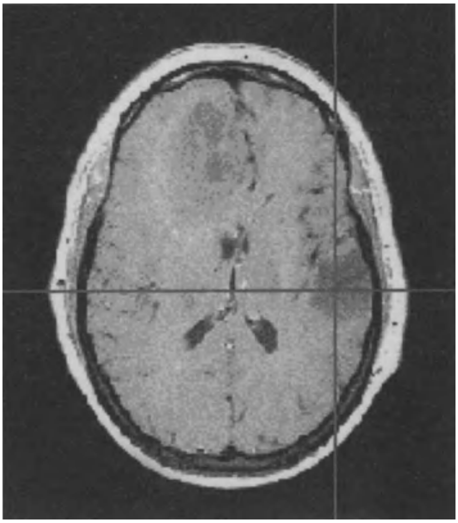

Fig. 2. Intraoperative interactive image guidance. The localizer's tip is in the planned target

software defines a target or target volumes and creates an optimal pathway to the target area. This plan is used intraoperatively to guide the infrared digitizer as it moves toward the lesion or tumor.

Using the NSPS software, after coregistration of CT and MRI (for intracranial surgery) preoperative surgical planning is done. The main goal of the planning is to define an optimal surgical corridor. The surgical trajectory is defined so that it accomplishes several criteria: it is the shortest route to the target, it avoids eloquent areas, it avoids major vessels, it provides an optimal angle of attack for the lesions, and if possible it uses predefined anatomical pathways (subarachnoid space). Creating the surgical corridor involves several steps: defining an entry point and a target, defining an initial surgical trajectory, and reconstructing an anatomical corridor with the surgical perspective. Once the surgical trajectory has been obtained, the NSPS reorganizes image data into a surgical perspective. In this way the neurosurgeon can review the surgical pathway.

The next step in planning is simulation. In this step the surgeon visualizes, in the workstation, each of the reconstructed slices with the surgical perspective and evaluates the anatomical structures that may be encountered on the way and may need to be spared. During the optimization step, based on the information obtained from the simulation the surgical corridor is adjusted so that it meets optimally all the requirements for a safe and complete resection of the lesion.

Intraoperative Interactive Image Guidance

Interactive image guidance is an advanced function in computer-assisted surgery. Based on preoperative registration of images and intraoperative coregistration with the patient's anatomy, different digitizers can be used to display the surgeon's position during intracranial or spinal operations. Once the patient is positioned and draped the digitizer is initially used to coregister the patient's anatomical structures with the preoperative images. In this sense, if a frame-based system is used concomitantly different preselected points on the frame may be used for coregistration. For the frameless systems, the implantable fiducials constitute the points of coregistration. Generally is agreed that a minimum of three points are necessary for an accurate registration and an optimum of four gives the best accuracy. Five points or more actually decrease registration accuracy [16–18].

For intracranial procedures there is only one mobile component of the infrared system that may be used interchangeably with different surgical instruments such as dissectors, bipolar forceps, and endoscope. For each of these the system must be recalibrated and reregistered before use. For the spinal component there are several mobile components mounted rigidly on several surgical instruments, and each of these must be registered before use.

Once the process of coregistration is completed the system is ready for use. The tip of the surgical instrument is displayed on preoperative images as a red cross-hair. In our operating suite we use ceiling-mounted monitors installed in front and at the surgeon's right so that the position of the infrared pointer is visible from almost any angle. The surgical trajectory is also displayed on the monitor superimposed on the images. Finally, the surgical perspective is also shown in one separate window, and the tip of the infrared localizer is viewed as a small circle.

a 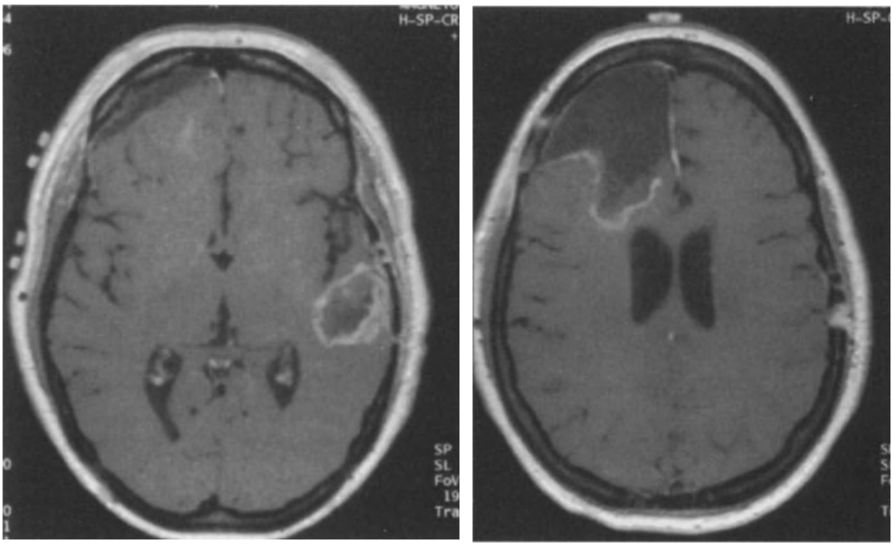 b

Fig. 3a,b. Postoperative MRI: T_1-weighted axial scans through (**a**) left temporal region and (**b**) right frontal region

The entry point on the patient's skull is touched by the probe of the digitizer and marked on the scalp. Before making an incision the craniotomy size and shape is determined by localizing the margins of the lesion as well as important anatomical structures such as the motor cortex, superior sagittal sinus, etc. After the dural opening is made, the entry point is verified again and if necessary modified so that the corridor to the target proceeds through a relatively avascular area. For superficial lesions the surgical corridor is easily defined, and the localizer is used for intracerebral guidance to achieve a volumetric resection with minimal collateral damage. For deeper lesions the surgical corridor is established with the aid of a stereotactic retractor in conjunction with the frame-based system. In spine surgery, the infrared digitizer is used for pedicle screw placement.

The main use of interactive image-guided technique in spine surgery is currently for the pediclescrew insertion. The initial steps of the procedure are the same, the only major differences being that the fiducial system is represented by bone landmarks selected preoperatively and the intraoperative coregistration is done separately for each vertebra.

Case Example

A 32-year-old woman had a past medical history of headaches for approximately 2 years that became progressively worse in the 6 weeks before she came to our hospital. Imaging studies revealed two masses, one right frontal and a second left temporal. She underwent a biopsy of the right frontal mass; it was determined to be a glioblastoma.

At the time of referral we evaluated the case and on the basis of on her clinical condition, long history of headache, and MRI tumor appearance we decided to redo the surgery in a staged fashion. First we approached the left temporal tumor. The surgery was performed under interactive image guidance using the frameless implantable marker fiducial system. Pathological findings indicated a low-grade astrocytoma. As mentioned earlier, an accurate volumetric resection is essential for the survival prognosis and in this sense the infrared localizer was very helpful in defining the tumor margins. On the other hand the tumor location was close to speech areas so that a strict limitation to the tumor volume was essential. The patient tolerated the procedure very well, and she was released home with the fiducial implants in place.

In the second stage, using the same fiducial system, we approached the right frontal tumor again using interactive image guidance. Pathological findings again indicated a low-grade astrocytoma but with anaplastic features. At this point the volumetric resection still remained the main goal because the next contemplated stage postoperatively was the placement of radioactive implants. In achieving the volumetric resection the infrared system was the most useful, especially for the posterior contour as the major limitation so as to spare the adjacent frontal lobe.

Conclusion

Interactive image-guided surgery is an advanced level in computer-assisted volumetric resection. From its single use in neurooncology, this technology has rapidly been extended to a wide range of surgical procedures, both intracranial and spinal. The infrared digitizer has proven to be the most accurate system among those currently in use. Its accuracy as well as its flexibility have made it a very valuable surgical instrument.

Future directions for the system include application as a feedback system for passive and active robots, extension into spinal surgery in anterior and endoscopic approaches, respectively, and possible use in vascular surgery, at least for its localization value in aneurysm surgery.

References

1. Barnett GH, Kormos DW, Steiner CP, et al (1993) Use of a frameless, armless stereotactic wand for brain tumor localization with two-dimensional and three-dimensional neuroimaging. Neurosurgery 33:674
2. Kadi AM, Zamorano L, Jiang Z, Nolte LP (1993) Intraoperative real-time localization of brain tumors. Proc Clin Applic Mod Imaging Technol 1894:279–291
3. Kelly PJ (1986) Computer-assisted stereotaxis: new approach for the management of intracranial intraaxial tumors. Neurology 36:535–541
4. Kadi AM, Zamorano L, Jiang Z (1993) Stereotactic brain surgery: instrumentation, automation, and image guidance. Proc Clin Applic Mod Imaging Technol 1894:216–228
5. Kondziolka D, Lundsford LD (1995) Guided neurosurgery using the ISG Viewing Wand. Contemp Neurosurg 17(8):1–6
6. Maciunas RJ, Galloway RL, Fizpatrick JM, et al (1992) A universal system for interactive image-directed neurosurgery. Stereotactic Funct Neurosurg 58:108–113
7. Maurer CR Jr, Fizpatrick JM (1993) A review of medical image registration. In: Maciunas R (ed) Interactive image-guided neurosurgery. AANS Publications, Park Ridge (IL) pp 17–44
8. Galloway RL Jr, Berger MS, Bass WA, et al (1993) Registered intraoperative information: electrophysiology, ultrasound and endoscopy. In: Maciunas R (ed) Interactive image-guided neurosurgery. AANS Publications, Park Ridge (IL), pp 247–258
9. Rohling R, Munger P, Hollerbach JM (1995) Comparison of relative accuracy between a mechanical and an optical position tracker for image-guided neurosurgery. J Image-Guided Surg 1:30–44
10. Bucholz RD, Baumann CK (1994) The use of image-guided frameless stereotaxy during epilepsy surgery. Scientific program for the 62nd annual meeting of the American Association of Neurological Surgeons, p 348
11. Nolte LP, Zamorano.L, Jiang Z (1995) Image-guided insertion of transpedicular screws: a laboratory setup. Spine 20:497–500
12. Zamorano L, Nolte LP, Kadi AM (1993) Interactive intraoperative localization using an infrared-based system. Neurol Res 15:290–298
13. Zamorano L, Nolte LP, Kadi AM (1994) Interactive intraoperative localization using an infrared-based syslem. Stereofactic Funct Neurosurg 63:84–88
14. Zamorano L, Jiang Z, Kadi AM (1994) Computer-assisted neurosurgery system; Wayne State University hardware and software configuration. Comput Med Imaging Graphics 18:257–271
15. Zamorano L, Nolte LP, Jiang Z (1993) Image-guided neurosurgery: frame-based and frameless approach. Neurosurg Operative Atlas 3:403–422

16. Bucholz RD, Smith KR (1993) A comparison of sonic digitizers versus light emitting diode-based localization. In: Maciunas R (ed) Interactive image-guided neurosurgery. AANS Publications, Park Ridge (IL), pp 179–200
17. Guthrie BL, Adler JR Jr (1992) Computer-assisted preoperative planning, interactive surgery, and frameless stereotaxy. Clin Neurosurg 38:112–131
18. Maciunas RJ, Galloway RL Jr, Latimer J (1994) The application accuracy of stereotactic frame systems. Neurosurgery (Baltim) 35:682–695

Part 3
Advanced Neurosurgical Planning Using Computer-Assisted Systems

Computer-Aided Surgery

Kintomo Takakura[1], Hiroshi Iseki[1], and Takeyoshi Dohi[2]

Summary. Minimally invasive surgery promises to speed patient recovery, as measured by such indices as duration of confinement to bed, hospitalization, postoperative outpatient visits, and rehabilitation. The shortening of the operation itself and elimination of unnecessary procedures reduce surgical bleeding and complications. It also reduces total medical costs and it might be beneficial for the care of aged patients. Minimally invasive surgery is based on preoperative and an intraoperative strategy system for surgical planning and on the volumegraph (augmented reality) navigation system. The purpose of computer-aided surgery (CAS) is to assist in minimally invasive surgery by the integration of medical images and information. This augmented reality and Hivision computer-aided surgery (HivisCAS) system provides a means of realization of minimally invasive surgery.

Key words. Computer-aided surgery (CAS)—Hivision—Volumetric ultrasonogram—Volumegraph—Photon radiosurgical system (PRS)

Introduction

Minimally invasive surgery aims to avoid large and hazardous surgical methods and to do a small dissection only as is necessary for the disease. This type of procedure promises a speedy recovery, as measured by such indices as the duration of confinement to bed, hospitalization, postoperative outpatient visits, or a long-term rehabilitation. This method also reduces total medical costs and is especially the best choice for those in an aging society.

Minimally invasive surgery is based on preoperative planning and an intraoperative navigation system. The purpose of computer-aided surgery is to assist minimally invasive surgery by the integration of medical images and information. This augmented reality and the Hivision computer-aided surgery (HivisCAS) system are necessary for realizing the minimum intervention [1]. Hivision

[1] Department of Neurosurgery, Neurological Institute, Tokyo Women's Medical College, 8-1 Kawada-cho, Shinjuku-ku, Tokyo 162, Japan.
[2] Faculty of Engineering, The University of Tokyo, 7-3-1 Hongo, Bunkyo-ku, Tokyo 113, Japan.

is an advanced video format developed by NHK (Japan Broadcasting Corporation, Tokyo, Japan), with approximately six times the bandwidth of National Television System Committee (NTSC). Volumegraph is a new three-dimensional format developed by Victor Company of Japan (Tokyo, Japan).

Medical Images for Strategy of Computer-Aided Surgery

The computerized automobile navigation system is widely known. This surgical system is similar to driving on a unknown road from starting point to goal (target point) with indices of the best and shortest course and the most accurate procedure. For this purpose, it is important to evaluate and estimate the location of the target and the neighboring areas preoperatively. Selection of the best access based on this evaluation method is necessary. During the surgical procedure, several kinds of medical images and reconstructed operative field images such as CT scan or MRI are similar to a road map and a bird's-eye view of a geographical field. Medical images indicate the location of the lesion and the objects, and simulation of the surgery can assist in determing the best approach. To give information about navigation to surgeons, registration of image information regarding the location of the operative field and simulation is needed [2].

The Volumegraph

Three-dimensional computer graphics are expected to be very helpful for such medical applications as well as clinical practice. However, display by existing output devices such as the CRT (cathode ray tube) is still limited in two-dimensional space and does not clarify three-dimensional information. As a realistic three-dimensional output medium, we have developed a novel system (Volumegraph) to visualize exact spatial information such as organ shapes during surgery. Volumegraph visualizes three-dimensional internal organ objects for a surgical procedure. An imaging plate is set by the surgical bed, and a half-mirror is used for optical image overlay. Preoperatively, the surgeon draws and determines the area of craniotomy to fit the virtual objects [3].

Intraoperative Monitoring and Navigation by Volumetric Ultrasonogram

The volumetric ultrasonogram (V-US) is basically composed of a rotatory ultrasound sector-type probe (5 MHz, 20 mm in diameter), a personal computer for reconstruction, a rotating stepping motor, and a stepping-motor control system. After an ultrasonogram at each 1.4° interval, V-US images are available in about 25 s. The target area (optional distance) in multi-slices can be determined on the ultrasonogram at any time. The location of a lesion is well displayed for operative procedures. It is important and useful practically to observe every anatomical structure during the operation as far as possible and also to correct the final target point by using the three-dimensional ultrasonogram [4,5].

Photon Radiosurgery System

In our clinic, focused radiation to the intracranial lesion is delivered by two different systems, a collimated cobalt-60 source (gamma knife) and a new interstitial radiation source (soft X-rays). The photon radiosurgery system (PRS) device is a lightweight, handheld, battery-powered photon generator. The tip of the probe is 3 mm in diameter and 10 cm in length. The energy of X-rays generated decreases sharply with distance from the probe, carrying the potential to effectively irradiate a lesion as large as 3.5 cm in diameter at a time. This system can be used without any special radioprotective shielding in an operating theater or a ward [6].

We treated 27 patients with cerebral lesions with a single fraction of interstitial irradiation by PRS after surgery including stereotactic biopsy and partial removal of the tumor. Dose rates of 200 cGy per minute are possible, allowing for the administration of 15 Gy to a lesion 2 cm in diameter in less than 10 min. All patients tolerated the procedure well. No neurological deficits were noted after surgery and irradiation. The clinical efficacy of PRS is now under investigation, but it appears quite promising.

HivisCAS System

Hivision computer-aided surgery (HivisCAS) offers to surgeons and medical staff accurate information regarding the brain map based on the integration of several medical images and information coordinately. Using the brain map information the surgeons can plan a safe and precise trajectory and evaluate the location of the target and the neighboring anatomical structures during the procedure. During the operation, HivisCAS can show every information image to the surgeon in a small craniotomy the same as in a large craniotomy. It demonstrates for the surgeon the accurate location of the tumor or other lesions and the important eloquent areas.

It is obviously important to control registration between the intraoperative location in the brain and the simulation images based on preoperative medical images. From the results of this registration these intraoperative images such as microscopic images and ultrasonograms have the same coordinate axis as the simulation images. With the ability to integrate all these data, the surgeon can perform a less invasive operation while maintaining a high standard of accuracy. This system is capable of overlaying various types of medical data or stored images on the image captured via the microscope, and can open the way for precise surgical simulation that will help surgeons to reduce the invasiveness of procedures. The surgeon sees and uses the images on the Hivision monitor during the operation rather than directly through the microscope.

The monocamera Hivision stereoscopic microscope system with two divided wide-vision views has a function in which the images of digital subtraction angiography (DSA), CT, MRI, and other medical information are superimposed (three-dimensional simulation images, the navigation image of the ultrasonogram, and the endoscopic image). The object of this system is to provide the surgeon with all information about the functions and spatial arrangement of the surgical site by superimposing pertinent imaging information over the microscopic image [3,7]. The graphical overlay might suggest the best incision line based on careful measurements taken beforehand. Doctors can discuss with each other the operative procedures in an operating theater, and they can select and perform the best surgical procedure by the same stereoscopic images.

Expectation and Development of Our System

The project in future is an application of this system for an automatic surgery with the development of a micromanipulator. It will be possible to perform telesurgery and finer surgery by micromachine by using the robotics technology of a micromanipulator and our system.

Acknowledgments. Our project was supported in part by the Proposal-Based Advanced Industrial Technology R&D program of the New Energy and Industrial Technology Development Organization (NEDO), the "Research for the Future" program of the Japanese Society for the Promotion of Science, a grant-in-aid for Scientific Research on Priority Areas of the Ministry of Education, Science, Sports, and Culture of Japan, and the Terumo Life Science Foundation.

References

1. Iseki H, Takakura K, Dohi T (1994) New technology of neurosurgical fields (in Japanese). Clin Neurosci 12:611–614
2. Iseki H, Takakura K, Dohi T, Nambu K (1994) Computer-aided surgery in the neurosurgery: about virtual hospital. Image Technol Information Display 26(20):1143–1147
3. Iseki H, Masutani Y, Iwahara M, et al (1996) Volumegraph (three-dimensional image-guided navigation): clinical application of augmented reality. In: Proceedings of international conference on Virtual Systems and Multimedia, VSMM '96, in Gifu, pp 97–100
4. Iseki H, Kawamura H, Tanikawa T, et al (1992) Image-guided stereotactic surgery: perioperative image and treatment. In: Oka M, Reutern GM, Furuhata H, Kodaira K (eds) Recent advances in neurosonology. Elsevier, Amsterdam, pp 493–500
5. Iseki H, Takakura K (1993) Intraoperative ultrasound monitoring (in Japanese). Clin Neurosci 11(4):112–113
6. Cosgrove G, Hochberg F, Zervas N, et al (1997) Interstitial irradiation of brain tumors, using a miniature radiosurgery device: initial experience. Neurosurgery, 40(3):518–525
7. Mochizuki R, Iseki H (1994) Hivision single-camera 3D imaging system for microscopic surgery. Adv Med 4:101–104

Surgical Simulation in an Anatomical/ Functional Atlas with HyperCAS

Kiyoyuki Chinzei[1], Takemasa Kawamoto[2], Takaomi Taira[2], Hiroshi Iseki[2], and Kintomo Takakura[2]

Summary. Surgical simulation in an anatomical/functional atlas was examined. The atlas of the hypothalamus region, constructed by referencing the standard brain atlas of Schaltenbrand and Wahren, had irregular slice thickness. Newly modified software, "HyperCAS for Neurosurgery," could work correctly with this irregularity. Simulations of two scenarios of thalamotomy and pallidotomy were performed, and the invasion trajectories of these cases were demonstrated. Simulation on the anatomical/ functional atlas could supply detailed information.

Key words. HyperCAS—Schaltenbrand-Wahren atlas—Irregular slice thickness—Punctuation simulation—Thalamotomy—Pallidotomy

Introduction

Surgical Planning and Brain Atlas

In conventional stereotactic neurosurgery, an atlas of the anatomical and functional segmentation of the brain has been an essential tool to determine and navigate the strategy of the operation. The *Atlas for Stereotaxy of the Human Brain* by G. Schaltenbrand and W. Wahren [1], known as the Schaltenbrand-Wahren atlas (abbreviated as the S-W atlas in this chapter), has been the most popular atlas for this purpose. In accord with the evolving image-guided surgeries, many attempts at an electronic atlas, such as segmented CT (computed tomography) or MR (magnetic resonance) images, have been reported. However, these images have certain limits of spatial resolution; they can visualize at best 0.5 mm, and only 1 mm for most clinically and routinely used images. On the other hand, stereotactic surgery of the hypothalamus region, e.g., thalamotomy and pallidotomy, requires accuracy better than 1 mm.

---

[1] Biomechanics Division, Mechanical Engineering Laboratory, MITI, 1-2 Namiki, Tsukuba, Ibaraki 305, Japan.
[2] Department of Neurosurgery, Neurological Institutes, Tokyo Women's Medical College, 8-1 Kawada-cho, Shinjuku-ku, Tokyo 162, Japan.

Simulation in the anatomical/functional atlas is promising because the atlas has better resolution. In this chapter, initial study of the electronic anatomical/functional atlas, simulation for surgical planning using this atlas, and the newly improved software tool are reported.

HyperCAS for Neurosurgery

"HyperCAS for Neurosurgery" is a preoperative/intraoperative surgical planning/assistance software for stereotactic neurosurgery developed by the authors [2,3] (Fig. 1). HyperCAS runs on Macintosh personal computers including old or notebook models that are equipped with very limited resources—slow processor, small memory, small hard disk, etc. Because HyperCAS runs comfortably on notebook computers, it is easily usable in the operating room.

HyperCAS has already been used clinically in several hospitals. The authors have distributed it through the Japanese Society of Computer Aided Surgery since 1994

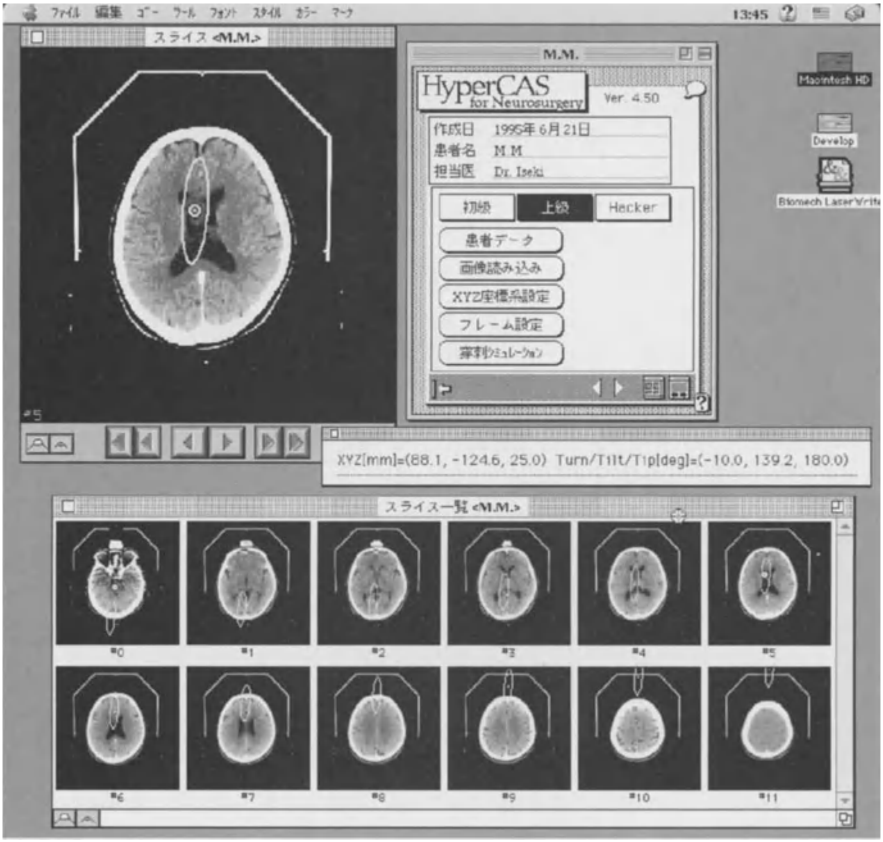

Fig. 1. HyperCAS for Neurosurgery. The trajectory of the virtual catheter is drawn as an ellipse

(see http://www.iscas.pe.u-tokyo.ac.jp/hypercas.html). In this chapter, the main features of HyperCAS for Neurosurgery are briefly introduced.

Image Display

HyperCAS can use axial, sagittal, or coronal sectioning slices, but the current version does not allow mixing these sections in one series of data. Image data are acquired from PICT format files as well as some X-ray, CT, or MRI raw data files. The latest version, used for this chapter, accepts irregular slice thickness. This function is necessary to perform simulation in the atlas based on the S-W atlas.

The image is compressed into 4-bit pixel depth. We determined the compressed depth from clinical experiments so that the image quality is sufficient for browsing. The display is limited to two-dimensional (2-D) slice images: one reason is to provide quick response, and another is fidelity to the original images.

Stereotactic Frame Setting

HyperCAS can calculate stereotactic frame settings. The operator must specify the target lesion and the insertion point on the skull surface. (HyperCAS does not offer automatic lesion detection or automatic determination of optimal invasion trajectory.) By specifying these two points, the frame settings can be determined in principle. Some frames have a redundant degrees of freedom. In such case, the operator must specify the redundant part of the freedom.

Catheter Insertion Simulation

By specifying the diameter of a cylindrical catheter, HyperCAS displays the simulation of a virtual catheter insertion. The trajectories on the slices are drawn as a series of ellipses (the intersection of an inclined cylinder on a planar slice will be an ellipse) that indicate the invaded region on each slice.

Cooperative Processing with NIH Image

HyperCAS itself is designed to be a compact program, but it can enhance the image-processing and simulation capabilities by cooperatively working with "NIH Image" (freely distributed by National Institutes of Health, Bethesda, MD, USA), an image-processing software widely available on Internet. HyperCAS can pass necessary data to NIH Image to produce the ultrasound imaging-like sectioning view, which is perpendicular to the virtual insertion trajectory.

Methods

Constructing the Anatomical/Functional Atlas

The electronic anatomical/functional atlas was constructed by referencing the information in the S-W atlas. Each page of the S-W atlas contains a picture of a cadaver dissection and the corresponding anatomical/functional segmentation map on transparent overlay sheets. We digitized the overlay maps of the sagittal myelin series (plates 34–49). We then deleted unnecessary parts and corrected lost and incorrect information.

A flatbed scanner machine (GT9000, Seiko Epson, Suwa, Japan) was used. This scanner is a popular type and is widely available. The scanner is controlled by PhotoShop (Adobe Systems, Seattle, WA, USA) on Apple Computer's Power Macintosh 8500/120 with 80 MB memory (Apple Computer, Cupertino, CA, USA).

However, the scanned pictures were not free from spatial distortion. We found that the distortion is not reproducible and is not simple as linear distortion (the distortion may be caused by the cheap and inaccurate mechanism, which is driven by a rubber belt). Elimination of this kind of distortion requires complicated nonlinear warping. We avoided the complicated method because the line drawings in the S-W atlas were not spatially precise (one finds that there is not a smooth connection between the consecutive slices).

It was still necessary to maintain the consistency of the origin and rotation. Each map of the S-W atlas has reference axes. One axis indicates the anterior–posterior commissura (AC-PC) line, another axis is perpendicular to the first, and they cross at the midpoint of the AC-PC line. We used these as the 2-D coordinate reference. The actual processes were as follow.

1. A transparent sheet was fixed on the scanner bed. Two crossing lines were drawn on it to serve as the reference axes.
2. The segmentation map was placed on the scanner and aligned to the reference axes.
3. The map was then digitized. The spatial resolution was 144 dpi (dots per inch), which is twice as dense than the displaying resolution, and the color resolution was in 256 grayscale. All necessary slices were scanned accordingly.
4. The scanned pictures were then trimmed. The trimming area should be aligned with respect to the scanned reference axes.
5. The picture foreground and background colors were reversed so that the background color was blue. This step is not essential, but it provides better visibility.
6. Unnecessary parts were deleted and lost or incorrect information was corrected.
7. The spatial resolution was reduced to 72 dpi, and the color resolution was reduced to 16 colors in the indexed color model.
8. The pictures was saved in PICT format files.

All these image-processing steps were done using PhotoShop.

Constructing HyperCAS Data

Before the simulation, we prepared the HyperCAS data file according to the following procedures.

1. Select "New Slicestack . . ." command from the HyperCAS menu. A vacant file was produced.

Table 1. Displacement from the midline and slice thickness of the slices in the Schaltenbrand–Wahren atlas, plates 35–49 [1]

Slice number	1	2	3	4	5	6	7	8	9	10	11	12	13	14	15	16	17
Displacement (mm)	1.5	2.5	3.5	5.0	5.5	6.5	9.0	10.5	12	13.0	14.5	16.0	17.0	20.0	22.0	24.5	27.5
Slice thickness (mm)	1.5	2.5	1.0	1.5	0.5	1.0	2.5	1.5	1.5	1.0	1.5	1.5	1.0	3.0	2.0	2.5	3.0

2. Load the scanned pictures. After this was finished, the first slice was displayed in a window.

3. Set the coordinate origin. Usually this is determined by clicking three fiducial markers in the CT or MR image. In the S-W atlas, there is no such marker. Instead, the reference axes are already drawn on the maps. We specified the crossing point of the reference axes, which is the midpoint of the AC-PC line, on the first slice as the coordinate origin. Before specifying the origin, one must type in the size of one pixel and the slice thickness. In this case, slice thickness is used as a temporal initial value.

4. Set the slice thickness for each slice piecewise. In the S-W atlas, the distance of each slice from the midsagittal line is indicated, shown as column 2 of Table 1. HyperCAS requires the slice thickness; thus the differential of these, shown in column 3 of Table 1, were typed in.

5. Specify the diameter of the virtual catheter. If this was omitted, the center of incision trajectory was displayed.

6. Specify the target and the start of insertion points. After doing so, the program is ready to start the simulation. (We discuss the selection of the target and insertion points in the next section.)

Simulations

We here demonstrate two scenarios, one thalamotomy and one pallidotomy. To perform punctuation simulation by HyperCAS, the user needs to specify the target point (=the lesion) and the insertion point on the image. Usually the insertion point is placed on the surface of the brain as the actual surgery is thus performed. In this case, the image of brain surface was not available. Therefore, we set the insertion point adjacent to the thalamus. Both the target and the insertion points were referenced relative to the AC-PC line. The diameter of the virtual catheter was set to 2 mm.

Thalamotomy

The target was set on the nucleus ventrointermedius (Vi.m.) in the thalamus. In the atlas, it was 5 mm anterior from the PC point and on the slice 14.5 mm lateral from the midsagittal line (Fig. 2). The insertion direction was chosen 45° superioanterior from the target (Figs. 3, 4). The insertion point was set adjacent to the surface of the ventriculus lateralis (Ve.l) on the slice 20 mm external from the midsagittal line (Fig. 5).

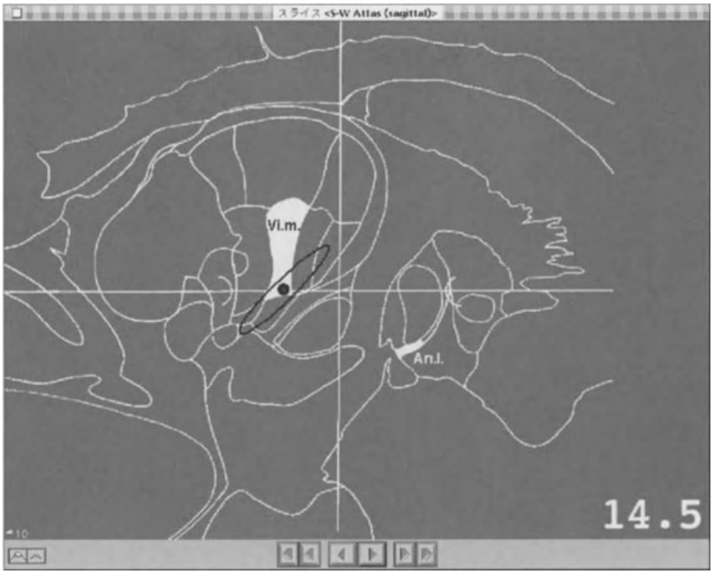

Fig. 2. Simulation of thalamotomy: target (*center of the ellipse*), nucleus ventrointermedius (*Vi.m.*), and calculated trajectory (*ellipse*) on sectioning 14.5 mm from the midsagittal line. (From [1], with permission)

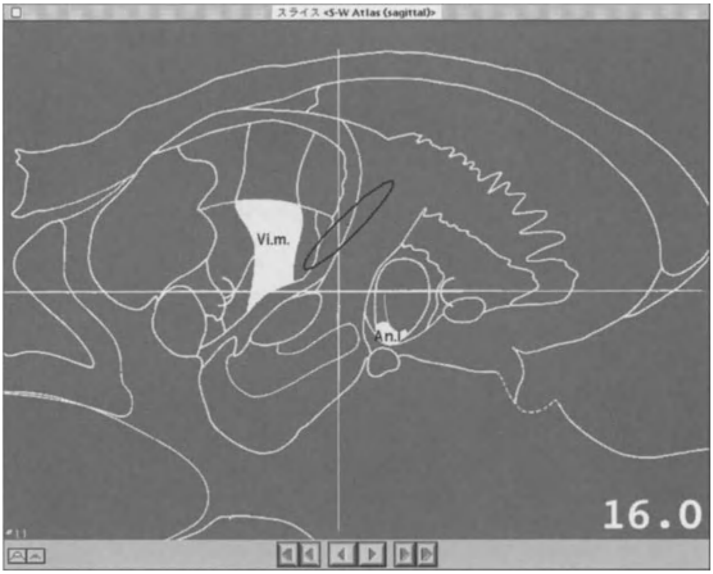

Fig. 3. Trajectory on sectioning 16.0 mm from the midsagittal line. (From [1], with permission)

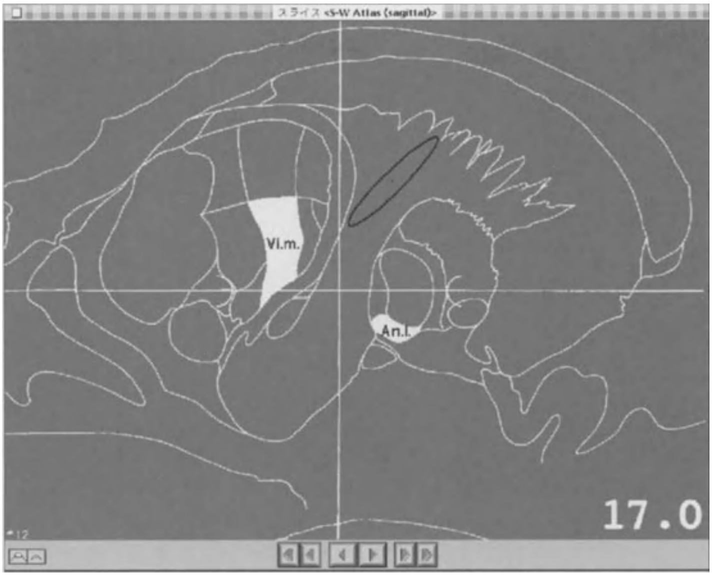

Fig. 4. Trajectory on sectioning 17.0 mm from the midsagittal line. (From [1], with permission)

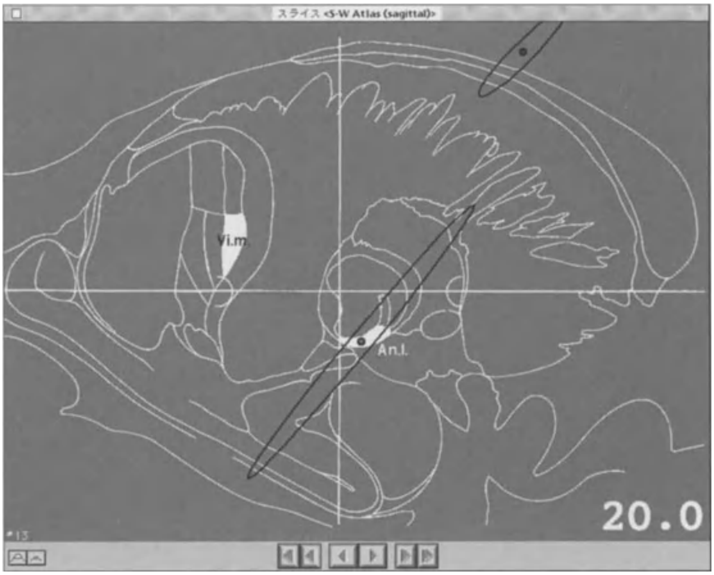

Fig. 5. Virtual insertion point for thalamotomy (*center of right-upper ellipse*), trajectory, and pallidotomy: target (*center of the ellipse*), ansa lenticularis (*An.l*), and calculated trajectory (*ellipse*) on sectioning 20.0 mm from the midsagittal line. (From [1], with permission)

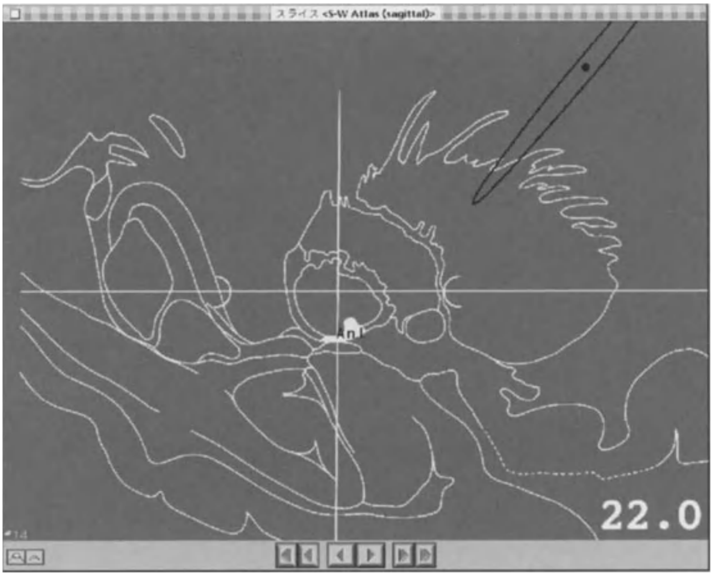

Fig. 6. Virtual insertion point for pallidotomy (*center of right-upper ellipse*) and trajectory. (From [1], with permission)

Pallidotomy

The pallidotomy target was placed on the ansa lenticularis (An.l) in the pallidum, 2 mm anterior and 4 mm inferior from the midpoint of the AC-PC line, on the slice 20 mm lateral from the midsagittal line (Fig. 5). The insertion direction was set 65° superioanterior from the target. The insertion point was selected on the stratum subcallosum, on the slice 22 mm lateral from the midsagittal line (Fig. 6).

Results

Figures 2–6 show the atlas, thalamus, pallidum, and the trajectories of the two scenarios.

The relation between the virtual invasion trajectories and the anatomical/functional sectioning was clearly visualized. It supplied much denser information than common surgical simulation attempts using X-ray, CT, or MR images.

Discussion

This simulation was not a clinical case from a particular patient or a particular disease. Thus we do not discuss the feasibility of the simulation in terms of its strategy decision.

Simulation in the Anatomical/Functional Atlas

The surgical simulation performed in this work was based on the standard atlas of anatomical/functional segmentation. Although the simulation was not a clinical case, it demonstrated the possibility of anatomical/functional simulation. It supplied much more useful and denser information than common surgical simulation attempts using X-ray, CT, or MR images.

The anatomical segmentation of the brain stem region requires good tissue contrast as well as high spatial resolution, of the order of a few millimeters or less. Clinically common X-ray, CT, or MRI cannot routinely acquire images having such high spatial resolution and tissue contrast.

The Advantages of HyperCAS

Support of irregular slice thickness is required to use the anatomical/functional atlas because its slice thickness varies from 0.5 to 3 mm. As far as the authors know, there is no other software for surgical simulation that allows the user to change the slice thickness for individual slices piecewise. Interpolating slices to regulate the slice thickness may work for normal X-ray, CT, or MR images. However, it usually assumes pixel-based representation. Therefore this function does not work for this atlas, which has been constructed by line drawings.

HyperCAS accepts the standard picture file format (PICT) as its input images. This allowed us to acquire images not only from CT scanners also from other sources such as the PC's image scanner. We could flexibly edit the scanned pictures using the general photo retouch software PhotoShop.

We also found that the simulation procedure of HyperCAS was simple and thus flexible. It only required information about the coordinate origin, the pixel size, slice thickness, and the position of the insertion and target points. During atlas construction, the authors noticed that the line drawing maps in the S-W atlas do not connect smoothly between adjacent slices. If one tries to visualize the 3-D volumetric graphics from such data, the surface drawing will appear miserably jagged. HyperCAS uses 2-D view only and is free from this cosmetic problem.

Future Work

The inaccuracy of the original atlas data certainly limits the accuracy of the simulation. For improving the accuracy of the anatomical atlas, there is hope that the Visible Human Project [4] of the U.S. National Library of Medicine (Bethesda, MD, USA) and its satellite works (see [5], for example) may provide the necessary information in digital format. It may also help the copyright issue that prohibits the distribution of the data derived from the S-W atlas. Apart from the accuracy issue, the segmentation should be referenced to the individual patient's anatomy, which includes individual variance.

Kuroki proposed the determination of distance between the AC-PC line to the pallidum by measuring the distance in the S-W atlas multiplied by the ratio of the

AC-PC line in the atlas and the patient's MR image [6]. However, the individual variance is probably not isotropicly linear and thus will require nonrigid registration, which is still an ongoing technical research topic.

Conclusion

The anatomical/functional atlas was constructed by referencing the segmentation information of the standard brain atlas (the Schaltenbrand-Wahren atlas). Two scenarios of thalamotomy and pallidotomy were simulated. The virtual invasion trajectories of these cases were visualized with respect to anatomical/functional sectioning. It was indicated that the simulation in the anatomical/functional atlas could supply rich and dense information. The pre/intraoperative surgical planning/simulation software "HyperCAS for Neurosurgery" could support the irregular slice thickness and effectively visualized the invasion trajectories.

References

1. Schaltenbrand G, Wahren W (1977) Atlas for stereotaxy of the human brain. Thieme, Stuttgart
2. Chinzei K, Dohi T, Iseki H, et al (1994) Surgical assistance tool HyperCAS. Video J Jpn Neurosurg 2(3)
3. Chinzei K, Masutani M, Dohi T, et al (1996) PC-based surgical planning tool for stereotactic neurosurgery, HyperCAS. In: Proceedings of conference in computer-assisted radiology (CAR 96), Paris, p 1045
4. Ackerman MJ (1991) The visible human project. J Biocommun 18(2):14
5. Schiemann T, Nuthman J, Tiede U, et al (1996) Segmentation of the visible human for high quality volume-based visualization. In: Höhne KH, Kikinis R (eds) Lecture notes in computer science proceedings of a conference in visualization in biomedical computing (VBC 96), Hamburg. Springer, Heidelberg, 1131:13–22
6. Kuroki A, Saito S, Nakai O, et al (1995) Measurement of the target for stereotactic pallidotomy with 3-dimensional MRI (SPGR method) (in Japanese). In: Proceedings of the 4th conference of the Japanese Society for Computer-Aided Surgery, Tokyo 83

Preoperative Simulation and Intraoperative Navigation with Three-Dimensional Computer Graphics

Nakamasa Hayashi, Shunro Endo, and Akira Takaku

Summary. We present a preoperative simulation and intraoperative navigation system (AdVANS) with three-dimensional computer graphics (3D-CG). The system consists of a graphics workstation and a three-dimensional digitizer for neuronavigation. At the workstation, the data were subjected to image-processing and volume-rendering manipulations to produce 3D-CG. The 3D-CG created by this system enabled surgeons to visualize lesions via the semitransparent scalp surface and the brain. Because the 3D-CG could be explored from any angle of view, the surgeons could accurately assess optimal head position, craniotomy placement, and trajectory to the target lesion on the computer display preoperatively. The three-dimensional digitizer, composed of a mechanical arm and a laser pointer, could monitor the intraoperative location illuminated by the laser pointer in real time on 3D-CG. Thus, this system is helpful in localizing the lesions and determining the extent of resection by preoperative simulation and intraoperative navigation with 3D-CG.

Key words. Computer-assisted neurosurgery—3-D computer graphics (3D-CG)—Simulation—Navigation—Stereotaxis

Introduction

Three-dimensional reconstruction techniques from magnetic resonance (MR) images offer significant advantages over cross-sectional tomographic images in comprehending the relationship of a lesion to surrounding brain structures [1]. In this chapter, we present a preoperative simulation and intraoperative navigation system with three-dimensional computer graphics (3D-CG). The system used here is described in detail elsewhere [2]. The 3D-CG created by our system enables surgeons to visualize lesions through semitransparent images of the scalp surface and brain. Using this system, the surgeon can accurately estimate the optimal head position, craniotomy placement, trajectory to the target lesion, and the extent of resection possible without damage to the normal area of brain on the computer display. Furthermore, to integrate the

Department of Neurosurgery, Toyama Medical and Pharmaceutical University, 2630 Sugitani, Toyama 930-01, Japan.

information obtained in the preoperative simulation into the surgical field, we developed a three-dimensional digitizer that incorporates a mechanical arm and a laser pointer. This system increased the safety of surgery in the brain.

Methods

Magnetic Resonance Imaging Data

MR imaging was carried out with three markers (cotton balls soaked in oil, 3-mm diameter) in the region surrounding the surgical field to determine reference coordinates for intraoperative navigation. These sites were labeled with India ink for use in image registration at surgery. Imaging was conducted using a whole-body, 1.5-tesla MR imaging system with a volumetric gradient echo-pulse sequence (FLASH) with TR of 40 ms, TE of 5 ms, and flip angle of 40°. The image acquisition time was about 20 min, and 120 contiguous sagittal sections (1.5 mm thick, 256×256 matrix of 1.1-mm pixels) were depicted.

Three-Dimensional Computer Graphics

The system (AdVANS, Tomiki Medical Instrument Co., Kanazawa, Japan) (Fig. 1) used to generate the 3D-CG consisted of a graphics workstation (Indy, Silicon Graphics, Mountain View, CA, USA) and an image scanner (GT-6500, Epson, Suwa, Japan). The software is implemented in the "C++" programming language under the UNIX operating system. Images were entered into the graphics workstation using an image scanner that reads film. Digital image data from sources such as MR imaging can also be transmitted to the graphics workstation using magnetooptical disks or floppy disks. The original cross-sectional images were interpolated to obtain image volume with cubic voxels.

At the graphics workstation, the data were subjected to image-processing and volume-rendering manipulations to produce three-dimensional views of the skin surface, brain, and region of interest traced out of the boundary on serial slices utilizing a mouse-controlled cursor before volume-rendering manipulations. Segmentation of the gross constituents such as the skin surface and brain was conducted semiautomatically based on the minimum and maximum gray values in the 8-bit image.

Three-Dimensional Digitizer

The three-dimensional digitizer (AdVANS, Tomiki), which incorporates a mechanical arm and a laser pointer, is used in integrating information obtained in the preoperative simulation into the surgical field. The mechanical arm consists of three joints mounted with rotary encoders forming an isocenter system. The arm is interlinked with the base ring of the stereotactic frame by the base table, allowing three-dimensional movement from the origin. The center of the arm is moved in relation to the Cartesian coordinates (x, y, and z) by the superior-inferior movement (y) of the base table and the right-left (x) and anterior-posterior (z) movement of the

a

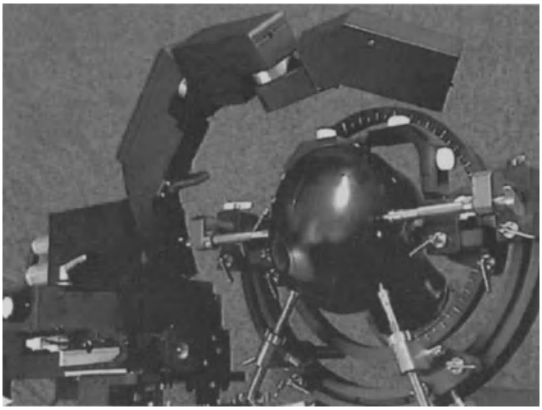

b

Fig. 1a,b. AdVANS (preoperative simulation and intraoperative navigation system). **a** Graphics workstation. **b** Three-dimensional digitizer

proximal end of the arm along the base table. The center is aligned with that of the stereotactic frame to fix the patient's head when the coordinates are 0, 0, and 0. All that is needed is to match the center of the arm with a target point on the Cartesian coordinate system.

The distal end of the arm has a laser pointer. In this apparatus, the laser beam is always oriented at the center of the orb formed by this arm in composite rotation of the three joints. Therefore, when the center of the arm is aligned with a target point on the Cartesian coordinate system, the position illuminated by the laser pointer indicates the trajectory to the target point. The laser pointer has a charge-coupled device (CCD) to measure the distance between the outlet of the laser beam and the position illuminated by the laser pointer. The point at which the distance measured by the CCD coincides with the radius of the orb formed by this arm (180 mm) corresponds to the target point. The geometrical data from the rotary encoders mounted in the joints of the arm and the CCD in the laser pointer are entered into the graphics workstation, where the position illuminated by the laser pointer is calculated and superimposed on the 3D-CG. Thus, the intraoperative location can be monitored in real time on the computer display.

At surgery, after the patient's head is fixed using the stereotactic frame, the three-dimensional digitizer is operated to read the three markers placed on the region surrounding the surgical field. These three points on the patient's head are illuminated by the laser pointer of the three-dimensional digitizer, and their Cartesian coordinates are measured. The coordinates of these markers on the patient's head are automatically entered into the graphics workstation and matched with those on 3D-CG. Thus the coordinates of the patient's head are aligned with the coordinate system of the three-dimensional digitizer and those of each cubic voxel composing an image volume at the graphics workstation.

The center of the arm of the three-dimensional digitizer is then matched with a target point on the Cartesian coordinate system. The position illuminated by the laser pointer on the patient's scalp indicates the trajectory to the target point. Because this point can be monitored on 3D-CG, the surgeon can accurately estimate the craniotomy placement, the trajectory to the target lesion, and the boundaries of the lesion preoperatively on the patient's scalp and then intraoperatively on the skull, dura mater, and brain surface.

Results

Figure 2 shows three-dimensional views of the region of interest seen through the semitransparent views of the scalp surface and brain. These three-dimensional views can also be explored from any angle of view using image rotation, and the expected operative field can therefore be visualized preoperatively on the computer display. When the user outlines the portion to be uncovered using the mouse-controlled cursor on the opaque skin surface, the brain surface and the region of interest become visible through the semitransparent brain image on the computer display. At surgery, the operator outlines the portion that he or she wishes to uncover using the three-dimensional digitizer on the patient's head in the same manner as using the mouse-controlled cursor and assesses the simulated craniotomy on the computer display. Therefore, the surgeon can accurately assess optimal head position, craniotomy placement, and trajectory to the target lesion. Intraoperatively, by survey on the brain surface using the three-dimensional digitizer, the surgeon could accurately estimate the boundaries of the lesion. The optimal trajectory to the target lesion through the patient's anatomy was delineated as well as the extent of resection of the lesion that is sufficient without damaging the surrounding healthy brain.

Discussion

In patients with intraaxial space-occupying lesions, which frequently have irregular three-dimensional spatial configuration [3], three-dimensional reconstructions allow surgeons to easily comprehend the three-dimensional surgical orientation. Hu et al. showed that three-dimensional views of the brain surface derived from MR images could be used in the preoperative assessment of the relationship between a lesion and anatomical landmarks such as the pre- and postcentral gyrus [4]. We have shown that the system enables surgeons to visualize the lesions in their three-dimensional rela-

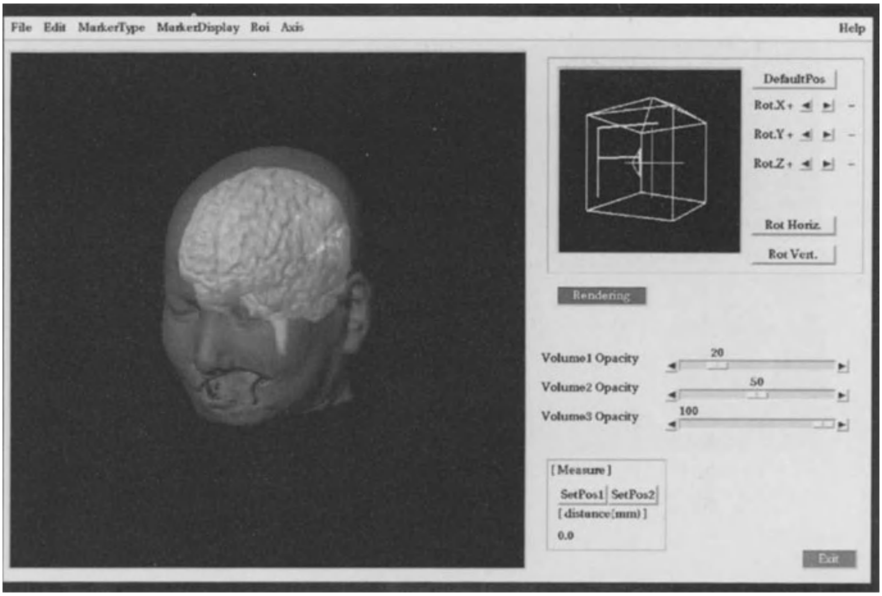

Fig. 2. Three-dimensional computer graphics. The three-dimensional view of the region of interest, which was colored red on the computer display, can be seen through the semitransparent views of the scalp surface and brain using the mouse-controlled cursor (*lower right*). The three-dimensional computer graphics can also be explored from any angle of view using image rotation (*upper right*)

tionship to the surrounding brain structures. It delineates the optimal trajectory to the lesion through the patient's anatomy as well as sufficient extent of resection of the lesion without damage to the surrounding structures.

Integration of preoperative imaging information into the surgical field has conventionally been an intuitive process on the part of the operating surgeon [5]. Various devices for neurosurgical stereotactic localization have been devised [5–17]. Because the arm of the present three-dimensional digitizer forms an isocenter system, the beam of the laser is always oriented via the trajectory to the lesion. The position illuminated by the laser pointer indicates the trajectory to the target point, and this position is monitored intraoperatively in real time on the computer display. Thus, our system can be used for intraoperative localization.

In conclusion, this system allows safe surgery by precise preoperative simulation and reliable intraoperative navigation with three-dimensional computer graphics.

References

1. Kikinis R, Gleason PL, Moriarty TM, et al (1996) Computer-assisted interactive three-dimensional planning for neurosurgical procedures. Neurosurgery (Baltim) 38:640–651
2. Hayashi N, Endo S, Kurimoto M, et al (1995) Functional image-guided neurosurgical simulation system using computerized three-dimensional graphics and dipole tracing. Neurosurgery 37:694–703

3. Kelly PJ, Kall BA, Goerss S (1984) Computer simulation for the stereotactic placement of interstitial radionuclide sources into computed tomography-defined tumor volumes. Neurosurgery 14:442–448
4. Hu X, Tan KK, Levin DN, et al (1990) Three-dimensional magnetic resonance images of the brain: application to neurosurgical planning. J Neurosurg 72:433–440
5. Roberts DW, Strohbehn JW, Hatch JF, et al (1986) A frameless stereotaxic integration of computerized tomographic imaging and the operating microscope. J Neurosurg 65:545–549
6. Watanabe E, Watanabe T, Manaka S, et al (1987) Three-dimensional digitizer (Neuronavigator): new equipment for computed tomography-guided stereotaxic surgery. Surg Neurol 27:543–547
7. Reinhaltd HF, Mayer H, Amerein E (1988) A computer-assisted device for the intraoperative CT-correlated localization of brain tumors. Eur Surg Res 20:51–58
8. Reinhaltd HF, Zweiful HJ (1990) Interactive sonar-operated device for stereotactic and open surgery. Stereotactic Funct Neurosurg 54/55:393–397
9. Gurthrie BL, Adler JR (1991) Frameless stereotaxy: computer interactive neurosurgery. Neurol Surg 2:1–22
10. Kato A, Yoshimine T, Hayakawa T, et al (1991) A frameless, armless navigational system for computer-assisted neurosurgery: technical note. J Neurosurg 74:845–849
11. Laborde G, Glisbach J, Harders A, et al (1992) Computer-assisted localizer for planning of surgery and intra-operative orientation. Acta Neurochir 119:166–170
12. Takizawa T (1993) Isocentric stereotactic three-dimensional digitizer or neurosurgery. Stereotactic Funct Neurosurg 60:175–193
13. Tan KK, Grzeszczuk R, Levin DN, et al (1993) A frameless stereotactic approach to neurosurgical planning based on retrospective patient-image registration: technical note. J Neurosurg 79:296–303
14. Drake JM, Prudencio J, Holowka S, et al (1994) Frameless stereotaxy in children. Pediatr Neurosurg 20:152–159
15. Olivier A, Germano IM, Cukiert A, et al (1994) Frameless stereotaxy for surgery of the epilepsies: preliminary experience: technical note. J Neurosurg 81:629–633
16. Golfinos JG, Fitzpatrick BC, Smith LR, et al (1995) Clinical use of a frameless stereotactic arm: results of 325 cases. J Neurosurg 83:197–205
17. Reinhardt HF, Trippel M, Westermann B, et al (1996) computer-assisted brain surgery for small lesions in the central sensorimotor region. Acta Neurochir (Wien) 138:200–205

Part 4
Intraoperative Imaging and Brain Shift

Three-Dimensional Image-Guided Navigation with Overlaid Three-Dimensional Image (Volumegraph) and Volumetric Ultrasonogram (V-US)

Hiroshi Iseki, Nobuhiko Hata, Yoshitaka Masutani, Makoto Iwahara, Tomoya Ono, Hiroyuki Kataoka, Ken Masamune, Takeyoshi Dohi, and Kintomo Takakura

Summary. Augmented reality is necessary for minimally invasive surgery. Recent medical imaging technology developments, such as X-ray, computed tomography (CT), and magnetic resonance imaging (MRI), have changed the methods and the dimensions of observation of the human body. Such image data are required for preoperative investigation to recognize the structure of organs and tumors three-dimensionally. Three-dimensional images seen in the air by means of a beamed light have been reported previously. The images are superimposed on the patient's head and body via a semitransparent mirror. We have applied these techniques to the navigation system for neurosurgical operations. The three-dimensional data obtained from CT and MRI before the operation were processed by a computer. This reconstructed three-dimensional image was superimposed and registered at the patient's head according to fiduciary markers (registration). The application of augmented reality in the surgical field makes it possible to do a neurosurgical intervention more easily. The surgeon can operate by this three-dimensional image-guided navigation system easily and accurately. In the development of volumetric ultrasonogram (V-US) navigation, the distortion of the brain during surgery is the key problem for truly accurate and effective guidance.

Key words. Ultrasonography—Image-guided navigation—Volumegraph—Volume scan—Augmented reality

Introduction

In the field of surgery, minimally invasive surgery without a large craniotomy or laparotomy has recently been developed. Surgical navigation is a key technique for reduction of surgical intervention in the narrowing operative field. This technique

[1] Department of Neurosurgery, Neurological Institute, Tokyo Women's Medical College, 8-1 Kawada-cho, Shinjuku-ku, Tokyo 162, Japan.
[2] 3D Project, Victor Company of Japan Limited, 2969-2 Ishikawa-cho, Hachioji, Tokyo 192, Japan.
[3] School of Engineering, The University of Tokyo, 7-3-1 Hongo, Bunkyo-ku, Tokyo 113, Japan.

makes exact the direct correlation between preoperative imaging by CT or MRI and the reality of the operating field (augmented reality) and is recognized as a tool that provides surgeons with, as it were, a "new eye." Navigation important to the operating neurosurgeon superimposes the navigational image on the surgical field accurately so that the correlation between both is easy to understand.

Volumegraph is an integrated photography-based optical recording system [1] with multiple microlens and a multiexposable sensitizer and display, which allows truly three-dimensional images to be observed by means of a beamed light without any special eyeglasses. The images are superimposed to the patient's head and body via a semitransparent mirror. We applied these techniques to the navigation system of neurosurgical operations. The three-dimensional data obtained from CT and MRI before the operation were processed by a computer. Such image data are applied for preoperative investigation so as to recognize the three-dimensional structure of organs and the tumor. Brain deformation as seen on the neuronavigation system is mainly caused by cerebrospinal fluid drainage and tumor resection. The use of intraoperative CT and MR imaging for navigation is one of the best means of observing deformation occurring during surgery. Compared to these modalities, ultrasonography is a more suitable imaging modality for intraoperative use given the space restrictions in the operating room.

In this chapter, the newly developed overlaid three-dimensional image (Volumegraph) navigation system and volumetric ultrasonogram (V-US) are presented with some clinical applications. These systems introduce the concept of three-dimensional image-guided surgery based on preoperative MR/CT images and real-time volumetric ultrasonography, which can encompass deformations of the tumor caused by surgical maneuvers.

Material and Methods

Registration Technique of the Volumegraph

Before obtaining preoperative MR imaging, three fiducial markers are attached to the patient's head. For preoperative image registration of the patient, we have developed a original triangular-shaped marker system. The location of three fiducial markers is based on our marker system. The coordinates of the markers are determined from multiple slices of MR images. Intraoperatively, after the patient and the supporting pole for the Volumegraphscope are rigidly fixed to the operating table with a Mayfield head clamp and a clamp, respectively, the triangular marker system is attached to the patient's head.

Before scrubbing and draping, the position of the markers on the patient and the three-dimensional triangular marker of the Volumegraph are registered manually. After draping, the supporting pole of the Volumegraphscope fixes the position and orientation of the Volumegraph. The Volumegraphscope is rigidly fixed to the operating table and the patient's position is maintained. Therefore, the position and orientation of Volumegraph with respect to the patient's brain can be registered throughout the operation. The purpose of the system (Volumegraphscope) is to register preoperative and intraoperative images (operative field) so as merge to the three-dimensional image (from the Volumegraph) of the patient with segmented preoperative MRI or CT images and to display it in the operating theater.

Principle of the Volumegraph

X-ray, CT, and MRI image data are required for the preoperative study so as to identify the structure of organs and tumors three-dimensionally. Three-dimensional computer graphics especially is expected to be very helpful for such medical applications as well as in the clinical setting. However, existing output devices like the CRT (cathode ray tube) display, which are still limited to two-dimensional space, distort three-dimensional information. As a realistic three-dimensional output medium, we have developed a novel system "three-dimensional (3-D) plotter" to visualize real spatial information such as organ shapes (Fig. 1).

Image Display of the Volumegraphscope

A three-dimensional view of the overlaid image can also be displayed via a transparent mirror. The Volumegraphscope consists of a carrier system, a half-mirror, which is used for optical image overlay, the Volumegraph (a thin plate of three-dimensional recorded medium) with back-lighting, and a freely adjustable arm with a determined position from one unit. The superimposition of three-dimensional navigation data (Volumegraph) is done through a half-mirror, implemented with a built-in Volumegraphscope (Fig. 2) [2,3].

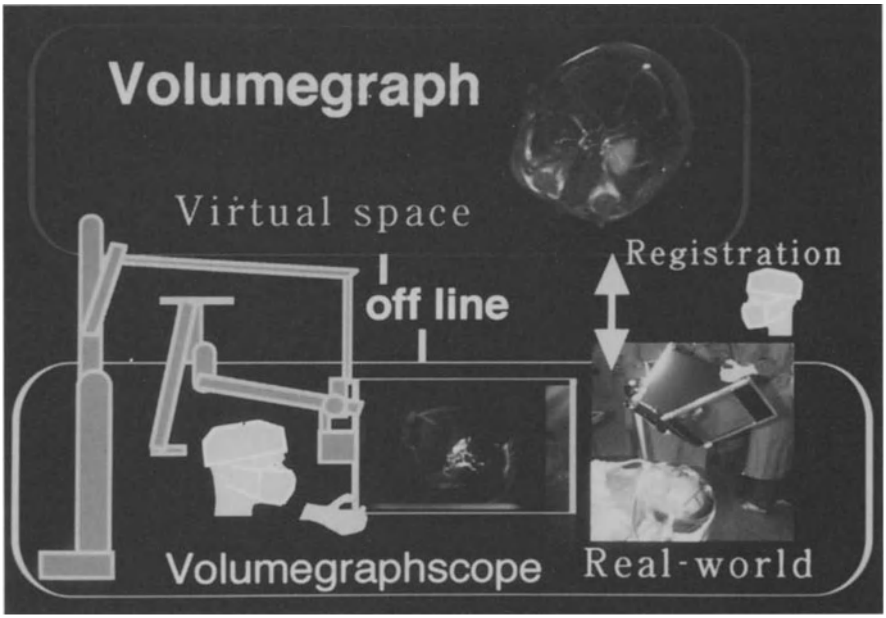

Fig. 1. Concept of the Volumegraphscope (augmented reality)

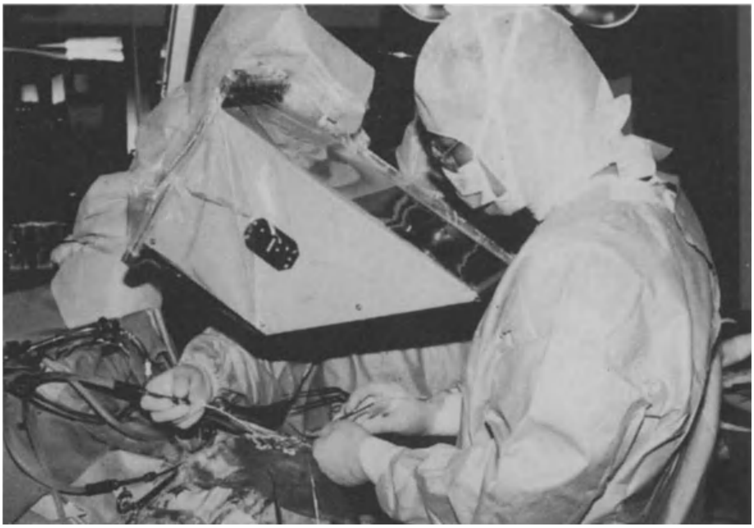

Fig. 2. Surgeon operating under the Volumegraphscope

Intraoperative Monitoring and Navigation of the Volumetric Ultrasonogram

The volumetric ultrasonogram (V-US) is basically composed of a rotatory ultrasound sector-type probe (Aloka, Tokyo, Japan; 5 Mhz, 20-mm-diameter-sector), a rotating stepping motor, and a personal computer for reconstruction and stepping-motor control (Fig. 3). After an ultrasonogram is taken for each 1.4°, V-US images are available in about 25 s. Target area (optional distance) for multislices can be determined on the ultrasonogram at any time. The location of a lesion is often displaced by surgical procedures. Therefore, it is important to observe the intraoperative environment directly as much as possible and also to correct the final target point by means of the ultrasonogram, the multislices of V-US (Fig. 4) [4,5].

Results

In a preliminary study, the Volumegraph system was applied to seven cases. In this chapter, a case of left meningioma (a 48-year-old woman) is presented. The preoperative MRI image was obtained with the fiducial markers attached. Before surgery, the location of each marker, the target tumors, and essential brain structures were extracted from MRI. At the initial stage of surgery, the triangular marker system was attached to the patient's head, which is located by three fiducial markers. After manual registration, surgery begins. With the help of the superimposed navigation system, the surgeon can recognize the three-dimensional localization of a tumor and the cortical sulci and other organs important for neurosurgery on the scalp easily, and thus decide the target volume of tumor, scalp incision, and craniotomy (Fig. 5).

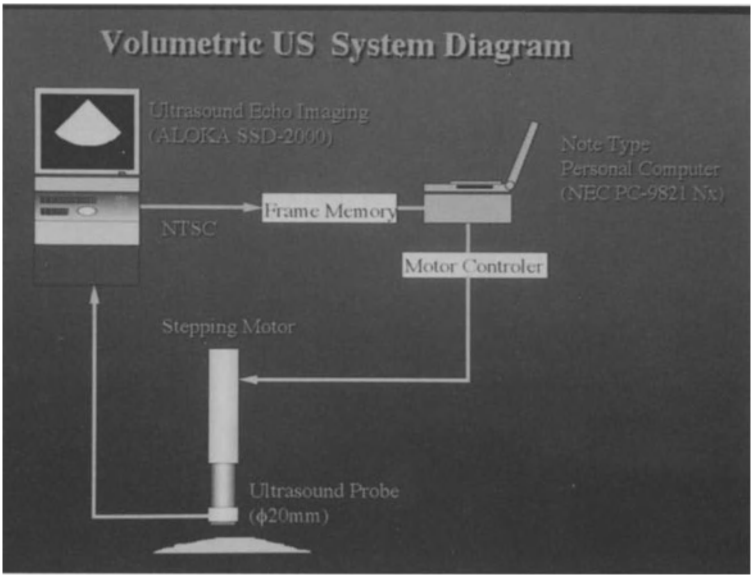

Fig. 3. Volumetric US (ultrasonography) system diagram

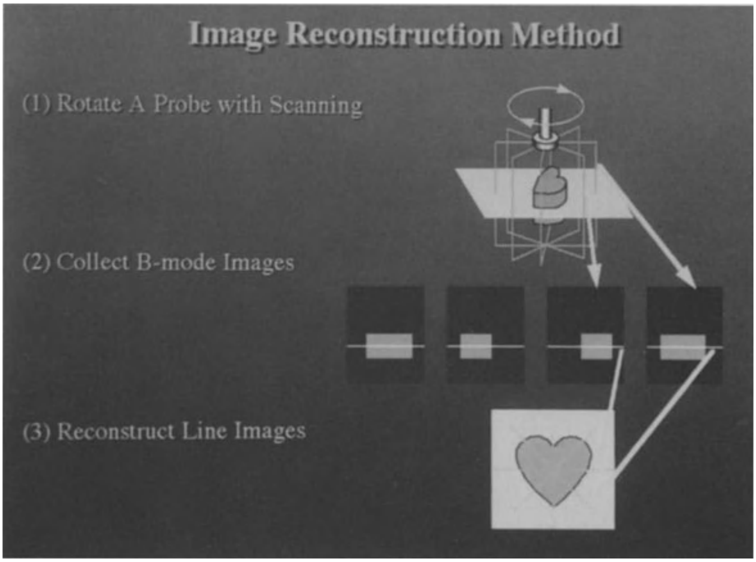

Fig. 4. Image reconstruction method of volumetric US

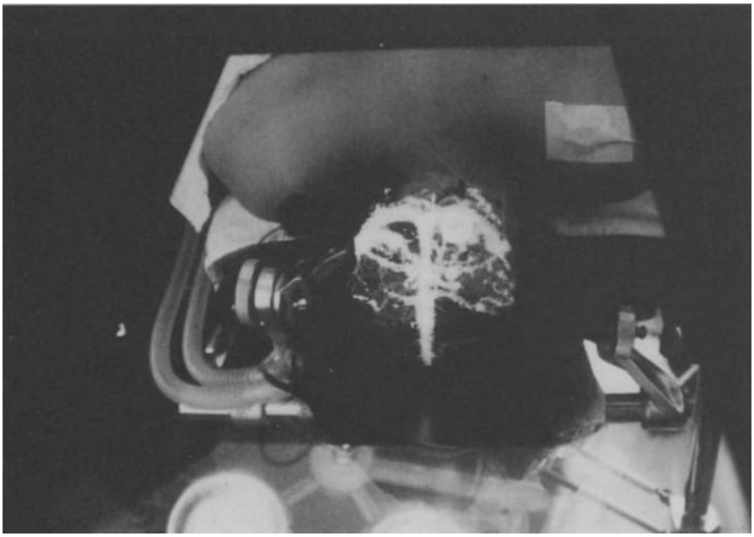

Fig. 5. During surgery, the surgeon observes the volumegraph overlaid on the patient's head and is able to recognize easily the three-dimensional invisible organ

The other system (V-US) was applied to ten cases. A case of right astrocytoma (a 35-year-old man) is presented here. During surgery, the multislice ultrasonography image was transferred to the personal computer (Fig. 6). Then, the axial reformatted ultrasonography image (C-mode) was displayed on the monitor screen. The tumor and neighboring structures were identified in both the three axial images of the ultrasonography image (C-mode) and the multiplane of the sector ultrasonography (B-mode), which was obtained at any location of standard ultrasonography in the window of the computer by moving the cursor. The surgeon can easily recognize the localization of the tumor and any deformity of the structure in real time (Fig. 7).

Discussion

Advantages

Clinical application demonstrated several advantageous aspects of the system. The Volumegraph can be observed truly three-dimensionally without eyeglasses. After a small craniotomy suitable for minimally invasive surgery, the neurosurgeon can observe a location of the whole brain as a virtual operative field under the Volumegraphscope without a making large craniotomy.

The V-US is a frameless navigation system with three-dimensional US-CT monitoring. V-US can be used to observe the intraoperative distortion of brain structures in real time.

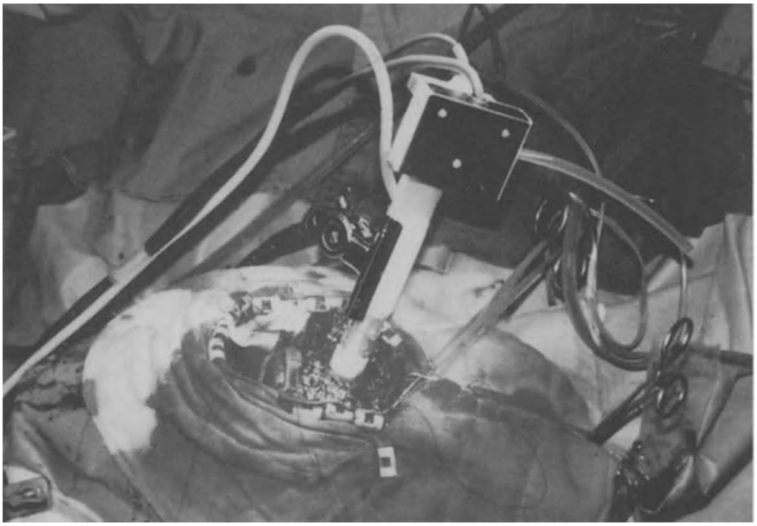

Fig. 6. The volumetric ultrasonogram (V-US) probe was maintained by a self-retractor during surgery

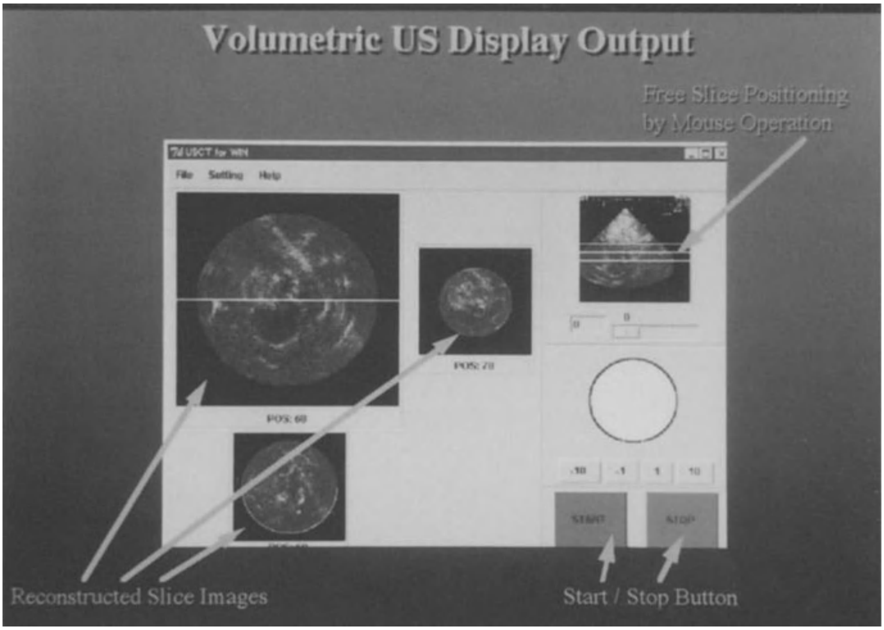

Fig. 7. The LCD display shows the three slices by V-US (C-mode) and sector US (B-mode)

Disadvantage

The principal disadvantage is that the Volumegraph, based on preoperative images of CT/MRI, cannot follow the intraoperative distortion of brain during surgical procedures.

Future Developments

The functional areas of the brain may often shift with respect to the location of the normal structures when the tumor is located near the eloquent areas. Before surgery, the distorted location of the eloquent area can be determined accurately by preoperative functional imaging. Missing components in the anatomical navigation can be supplemented with preoperative functional imaging (functional MRI and magnetic electroencephalography). The Voumegraph can easily offer a three-dimensional view of the integrated image based on anatomical MR image data and functional MR image data.

Acknowledgments. Our project was partly suported by the Proposal-Based Advanced Industrial Technology R&D Program of the New Energy and Industrial Technology Development Organization (NEDO), the "Research for the Future" Program of the Japan Society for the Promotion of Science, a grant-in-aid for scientific research on priority areas from the Ministry of Education, Science, Sports and Culture of Japan, and the Terumo Life Science Foundation.

References

1. Masutani Y, Iwahara M, Samuta O, et al (1995) Development of integral photography-based enhanced reality visualization system for surgical support. In: Proceedings of ISCAS '95, Labo-kikaku, Tokyo, pp 16–17
2. Iseki H, Masutani Y, Nishi Y, et al (1996) Neurosurgical operation under volumegraphscope. In: Lemke HU, Vannier MW, Inamura K, Farrman AG (eds) Computer-assisted radiology, proceedings of the international symposium on computer and communication systems for image-guided diagnosis and therapy, CAR '96. Elsevier, Amsterdam, p 1046
3. Iseki H, Masutani Y, Iwahara M, et al (1996) Volumegraph (three-dimensional image-guided navigation): clinical application of augmented reality. In: Proceedings of international conference on virtual systems and multimedia, VSMM '96, Gifu, pp 97–100
4. Iseki H, Kawamura H, Tanikawa T, et al (1992) Image-guided stereotactic surgery: perioperative image and treatment. In: Oka M, Reutern GM, Furuhata H, Kodaira K (eds) Recent advances in neurosurgery. Elsevier, Amsterdam, pp 493–500
5. Hata N, Dohi T, Iseki H, Takakura K (1997) Development of a frameless and armless stereotactic neuronavigation system with ultrasonography registration. Neurosurgery (Baltim) 41:608–614

Consideration of Intraoperative Brain Shift for Frameless Stereotaxy

Hiroshi Okudera, Shigeaki Kobayashi, Hisashi Nagashima,
Toru Koyama, and Susumu Oikawa

Summary. Brain shift during open neurosurgery is a major factor causing errors in intraoperative neuronavigation based on preoperative neuroradiological images. Under the observation of intraoperative CT images provided by the operating CT scanner system in Shinshu University Hospital, the causes of intraoperative brain shift were analyzed. As direct surgical factors of intraoperative brain shift, decompressive effects by craniotomy, dural opening, and suction of cerebrospinal fluid may play a significant role on intraoperative shift. Also, surgical procedures including brain retraction and dissection significantly affect intraoperative CT findings. Furthermore, changes of brain volume by administration of anesthetic and osmotic agents and intraoperative management of respiration and blood pressure may be important indirect factors in intraoperative brain shift affecting neuronavigation.

Key words. Navigation—Image-guided surgery (IGS)—Computer-assisted surgery—Frameless stereotaxy—Intraoperative CT scanning—Brain shift—Open neurosurgery

Introduction

The concept of neuronavigation was evolved with the development of frameless stereotaxy [1]. Recently, with the development of computer and associated device technology, several frameless stereotaxic systems have been designed by means of ultrasound [2], a mechanical sensing arm [3], magnetic field [4], and infrared light [5]. We have developed an intraoperative computerized tomographic (CT) scanner system [6,7] for intraoperative CT scanning. Intraoperative CT scanning reveals significant brain shift during open neurosurgery [8]. Therefore, in our University Hospital, we have used the open stereotaxy system with the Sugita multipurpose head frame based on intraoperative CT images [9]. In this chapter, the significance and several

Department of Neurosurgery, Shinshu University School of Medicine, Asahi 3-1-1, Matsumoto, Nagano 390, Japan.

causes of intraoperative brain shift based on intraoperative CT scanning are discussed.

Materials and Methods

Intraoperative CT images are obtained by the operating CT scanner system in the neurosurgical operating theater [7]. The system consists of a mobile CT scanner gantry [6], digitally controlled operating table [10], and head fixation exclusively designed for intraoperative scanning [11,12]. We usually perform intraoperative CT scanning for deep-seated lesions, locating basal ganglia and the paraventricular region. Postoperative immediate scan under general anesthesia on the digitally controlled operating table is a routine procedure in our University Hospital [13]. We perform retrograde analysis of all images obtained intraoperatively with special reference to possible causes of intraoperative brain shift.

Results

The mechanism of intraoperative brain shift is extremely complicated. During open neurosurgery, many factors may affect the shape and volume of the brain (Fig. 1). As direct factors of intraoperative brain shift, decompression caused by surgical procedures in open neurosurgery may be the most important mechanism [8]. At the time of craniotomy, dural opening, and suction of cerebrospinal fluid, significant sinking of the cortex has been observed on several occasions (Table 1). Microsurgical procedures including brain retraction and dissection also affect intraoperative CT findings. General management under anesthesia plays a significant role in the mechanism of intraoperative brain shift. Selection of anesthetic agent, osmotic agent, and respiratory management are key factors in controlling brain volume (Table 2).

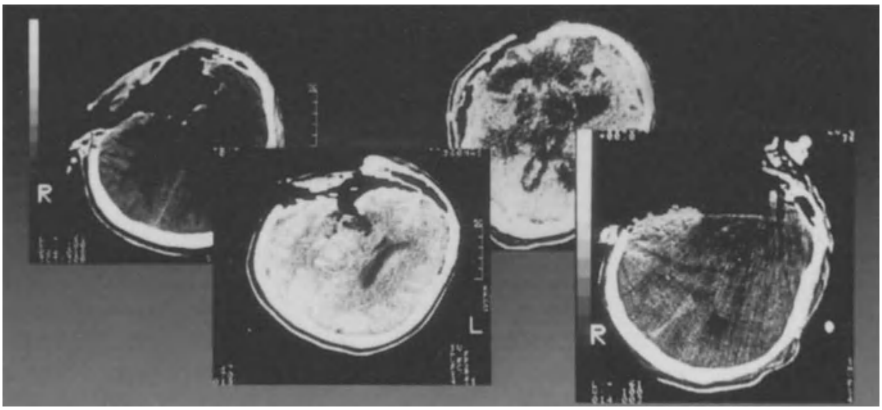

Fig. 1. Intraoperative CT images in various lesions during open neurosurgery obtained by the operative CT scanner system in Shinshu University Hospital

Table 1. Direct factors causing intraoperative brain shift

Decompressive effect
Craniotomy
Dural opening
Suction of cerebrospinal fluid
Surgical procedures
Brain retraction
Dissection

Table 2. Factors changing brain volume during surgery

Anesthesia
Anesthesic agent
Osmotic agent
General management
Respiration
Blood pressure
Cerebral perfusion pressure

Intraoperative positioning of the patient is a well-known factor for the control venous pressure.

Discussion

In modern neurosurgery, introduction of frameless stereotaxy is a major trend to realize minimally invasive surgery. New frameless methods have succeeded another [14–16]. Recently, smaller workstations have provided refinement of data management, especially in registration and integration of multiple preoperative images [17–20]. However, in conjunction with an increasing number of cases [21,22], questions as to the accuracy and error of frameless stereotaxy have been raised as a controversial point in managing intracranial lesions [23–27]. Zinreich et al. [23] has evaluated the spatial accuracy of a rapid interactive method of transferring CT information between the computer screen and the operating field with a multidimensional computer combined with a six-jointed position-sensing mechanical arm. The median error value between image and real location was 1–2 mm. However, they reported that accuracy was increased with the selection of widespread registration points, and 95% of all errors were less than 3.70 mm.

In the review by Kitchen et al. [24], the frame-based systems are reported to have the advantage of proven clinical utility and instrument carriage with a high degree of mechanical stability and accuracy. On the other hand, frameless methods are more complex, but also more flexible, and may have wide applications in general neurosurgery if clinical efficacy is confirmed. Sipos et al. [25] presented an in vivo accuracy test with the ISG Viewing Wand. They used this system in 250 patients undergoing a wide range of neurosurgical procedures to assess its clinical usefulness and safety. In a subset of 45 neurosurgical patients, a battery of objective accuracy measurements was obtained before and during surgery. In their series, there were no instances of adverse outcomes attributable to the use of this system. A comparison of two alternative patient image registration techniques established that the fiducial-fit method was slightly more accurate than the surface-fit method.

Nauta studied error assessment during "image-guided" and "imaging-interactive" stereotactic surgery and reported that neither the image accuracy nor the mechanical accuracy of the instrument is the limiting factor in the usefulness of the guidance based on clinical experiences [26]. The author pointed out that the errors encountered in actual use result from tissue position changes which occur during the procedure, and that the need for intraoperative update of the guidance image is obvious if greater accuracy is required.

Ryan et al. [27] introduced frameless stereotaxy with real-time tracking of patient head movement and retrospective patient image registration. The average distance and standard deviation between the actual position of the mass and its stereotactically predicted location was 4.8 ± 3.5 mm. The authors concluded that frameless stereotaxy can be used for accurate localization of intracranial masses without resorting to use of fiducial markers during presurgical imaging and without immobilizing the patient's head during surgery.

Although there have been several attempts to improve the accuracy of frameless stereotaxy in open neurosurgery, intraoperative brain shift still remains the major factor of error. On the other hand, frameless stereotaxy is useful in skull base surgery [28] and extracranial applications including spinal lesions [29–31] because of the lack of intraoperative structural shift.

Conclusion

We have studied intraoperative brain shift during open neurosurgery. In neuronavigation by frameless stereotaxy, intraoperative CT scanning realizes intraoperative update of the image for registration.

References

1. Watanabe E, Mayanagi Y, Kosugi Y, et al (1991) Open surgery assisted by the neuronavigator, a stereotactic, articulated, sensitive arm. Neurosurgery 28:792–799
2. Roberts DW, Strohbehn JW, Hatch JF, et al (1986) A frameless stereotaxic integration of computerized tomographic imaging and the operating microscope. J Neurosurg 65: 545–549
3. Watanabe E, Watanabe T, Manaka S, et al (1987) Three-dimensional digitizer (neuronavigator): new equipment for computed tomography-guided stereotaxic surgery. Surg Neurol 27:543–547
4. Kato A, Yoshimine T, Hayakawa T, et al (1991) A frameless, armless navigational system for computer-assisted neurosurgery. Technical note. J Neurosurg 74:845–849
5. Zamorano L, Jiang Z, Kadi AM (1994) Computer-assisted neurosurgery system: Wayne State University hardware and software configuration. Comput Med Imaging Graphics 18:257–271
6. Okudera H, Kobayashi S, Sugita K (1989) Mobile CT scanner gantry for use in the operating room. AJNR (Am J Neuroradiol) 12:131–132
7. Okudera H, Kobayashi S, Kyoshima K, et al (1991) Development of the operating computerized tomographic scanner system for neurosurgery. Acta Neurochir (Wien) 111:61–63

8. Okudera H, Kyoshima K, Kobayashi S, et al (1994) Intraoperative CT scan findings during resection of glial tumours. Neurol Res 16:265–267
9. Okudera H, Kobayashi S, Sugita K (1989) Computer-assisted three-dimensional surgical guide system using a laser guide arm based on intraoperative computerized tomography. In: Brock M, Banerji AK, Sambasivan M (eds) Modern neurosurgery, vol 2. WFNS (World Federation of Neurosurgical Societies), Trivandrum, pp 471–477
10. Okudera H, Kobayashi S, Kanemaru K, et al (1990) Digitally controlled neurosurgical operating table. Technical note. Neurol Med Chir (Tokyo) 30:201–203
11. Okudera H, Kobayashi S, Kyoshima K, et al (1992) Modified head fixation system for intraoperative CT scanning. Technical note. Neurol Med Chir (Tokyo) 32:38–39
12. Okudera H, Kobayashi S, Kyoshima K, et al (1994) New radiolucent head fixation made of engineering plastics for intraoperative CT scanning. Acta Neurochir (Wien) 127:121–123
13. Harada T, Okudera H, Kobayashi S, et al (1991) [Computerized tomography immediately after surgery in the neurosurgical operating theater] (in Japanese). Neurol Surg 19:415–419
14. Reinhardt HF, Horstmann GA, Gratzl O (1993) Sonic stereometry in microsurgical procedures for deep-seated brain tumors and vascular malformations. Neurosurgery 32:51–57
15. Barnett GH, Kormos DW, Steiner CP, et al (1993) Intraoperative localization using an armless, frameless stereotactic wand. Technical note. J Neurosurg 78:510–514
16. Takizawa T (1993) Isocentric stereotactic three-dimensional digitizer for neurosurgery. Stereotactic Funct Neurosurg 60:175–193
17. Tan KK, Grzeszczuk R, Levin DN, et al (1993) A frameless stereotactic approach to neurosurgical planning based on retrospective patient-image registration. Technical note. J Neurosurg 79:296–303
18. Barnett GH, Kormos DW, Steiner CP, et al (1993) Use of a frameless, armless stereotactic wand for brain tumor localization with two-dimensional and three-dimensional neuroimaging. Neurosurgery 33:674–678
19. Smith KR, Frank KJ, Bucholz RD (1994) The NeuroStation—a highly accurate, minimally invasive solution to frameless stereotactic neurosurgery. Comput Med Imaging Graphic 18:247–256
20. Sandeman DR, Patel N, Chandler C, et al (1994) Advances in image-directed neurosurgery: preliminary experience with the ISG Viewing Wand compared with the Leksell G frame. Br J Neurosurg 8:529–544
21. Golfinos JG, Fitzpatrick BC, Smith LR, et al (1995) Clinical use of a frameless stereotactic arm: results of 325 cases. J Neurosurg 83:197–205
22. Kondziolka D, Lunsford LD (1996) Intraoperative navigation during resection of brain metastases. Neurosurg Clin North Am 7:267–277
23. Zinreich SJ, Tebo SA, Long DM, et al (1993) Frameless stereotaxic integration of CT imaging data: accuracy and initial applications. Radiology 188:735–742
24. Kitchen ND, Lemieux L, Thomas DG (1993) Accuracy in frame-based and frameless stereotaxy. Stereotactic Funct Neurosurg 61:195–206
25. Sipos EP, Tebo SA, Zinreich SJ, et al (1996) In vivo accuracy testing and clinical experience with the ISG Viewing. Neurosurgery 39:194–202
26. Nauta HJ (1994) Error assessment during "image guided" and "imaging interactive" stereotactic surgery. Comput Med Imaging Graphics 18:279–287
27. Ryan MJ, Erickson RK, Levin DN, et al (1996) Frameless stereotaxy with real-time tracking of patient head movement and retrospective patient-image registration. J Neurosurg 85:287–292
28. Okudera H, Takemae T, Kobayashi S (1993) Intraoperative computed tomographic scanning during transsphenoidal surgery. Technical note. Neurosurgery 32:1041–1043
29. Brodwater BK, Roberts DW, Nakajima T, et al (1993) Extracranial application of the frameless stereotactic operating microscope: experience with lumbar spine. Neurosurgery 32:209–213

30. Kalfas IH, Kormos DW, Murphy MA, et al (1995) Application of frameless stereotaxy to pedicle screw fixation of the spine. J Neurosurg 83:641–647
31. Glossop ND, Hu RW, Randle JA (1996) Computer-aided pedicle screw placement using frameless stereotaxis. Spine 21:2026–2034

Clinical Application of CT-Fluoroscopy

Tetsuo Kanno[1], Kazuhiko Nonomura[1], Krupa Shanker[1], and Kazuhiro Katada[2]

Summary. Computed tomography (CT)-guided intervention has been a common procedure during the past 10 years, but real-time monitoring with CT images has not previously been available. We have developed real-time CT-fluoroscopy, of which the initial trial was reported in 1993. This chapter describes the early clinical experience with this system. A third-generation scanner equipped with a slip ring was used. Images were reconstructed and displayed at a rate of six per second with a 0.83-s delay time using a newly designed array processor. CT-fluoroscopy was carried out in 12 cases (10 brain hemorrhage, 2 tumor). Good quality fluoroscopic images were obtained in all cases. Real-time monitoring with CT-fluoroscopy of needle placement and advancement was useful for accurate puncture needle biopsy and evacuation of the lesions. No serious complication was recognized in this series. These preliminary results suggest that CT-fluoroscopy offers improved accuracy and safety in neurosurgery as a new neuronavigation system and makes it possible to do freehand puncture without stereotactic procedures.

Key words. CT-fluoroscopy—Brain hemorrhage—Tumor biopsy—Minimally invasive neurosurgery—Real-time CT

Introduction

Computed tomography (CT)-guided intervention has become a common procedure in the field of neurosurgery in the past 10 years. Rapid advances are being made in CT techniques, largely as a result of the development of a variety of hardware and software in the computer field. An example is the development of the spiral scanner (helical CT). On the other hand, many attempts have been made to apply diagnostic methods using digital images such as MRI and CT to guide noninvasive techniques such as tumor biopsy, along with the development of interventional surgery. However, conventional CT-guided biopsy has the disadvantage that real-time image

[1] Department of Neurosurgery and [2] Department of Neuroradiology, Fujita Health University School of Medicine, 1-98 Dengakugakubo, Kutsukake-cho, Toyoake, Aichi 470-11, Japan.

monitoring is impossible and in fact is even inferior to ultrasonic tomography in this respect.

Recently, keyhole surgery, or interventional techniques in neuroendoscopic procedures, have become popular because the main idea behind them is minimally invasive surgery of the brain. This has resulted in the production of neuronavigation systems. However, these navigation systems provide information from direct observation, producing only fixed images; real-time monitoring with a CT image is not yet available. We have developed real-time CT fluoroscopy, which has made it possible to track target shifts during surgical procedures [1,2]. With this instrumentation, we believe that we can really achieve the ultimate aims of minimally invasive surgery, that is, precise target localization and surgical procedures with no injury to surrounding brain tissue.

Materials and Methods

System

The system used is a high-speed, third-generation CT machine, the Toshiba (Japan) X-vigor prototype [1,2]. It is equipped with a serial spin mechanism by means of a high-pressure slip ring, a large-capacity X-ray tube (6.5 mega-heat units), and a highly sensitive detector with 896 channels. It has a rapid scan time of 100 s (1 s per rotation). The image-processing method, with a new imaging arithmetic alogrithm (real-time reconstruction unit, RTRU), was applied to high-speed CT. This enables sequential display of any CT slice surface for a maximum of 100 s with a temporal resolution of six images per second at 120 kV and a low dose of 50 mA.

The raw data stream obtained by high-speed sequential scanning is recorded in order in the memory after preprocessing. Immediately after recording, convolution and back projection are performed with an RTRU, and the data are gradually transmitted to the display. When data for 360° accumulate in the memory, the first image is displayed on the CRT. When the raw data transmitted suquentially at the same angle accumulate, the results of processing for that angle are superimposed on the image, and the results of processing of the old data at the same angle are removed simultaneously. By repeating this process, serial CT images are obtained with minimal delay.

Artifacts such as afterimages sometimes occur when motion is fast, but a sufficient sense of real time is provided. CT images similar to images seen in routine fluoroscopic examinations are obtained.

Clinical Experience

CT-fluoroscopy has been so far carried out in 12 cases, 10 cases of brain hemorrhage and 2 tumors [3].

Clinical Experience with Brain Hemorrhage and CT-Fluoroscopy

All the patients with brain hemorrhage underwent a freehand surgical aspiration of the hematoma under CT-fluoroscopy (CT-F) guidance (Fig. 1).

Fig. 1. Freehand hematoma aspiration under CT-fluoroscopy (CT-F)

The instruments used for head immobilization and puncture were radiolucent (an Argyle 12-Fr. thoracocentesis needle was temporarily used as a puncture needle). The gantry can be tilted and the table (couch) can be moved with a control unit separate from the CT scan while viewing the same monitor as the surgeon's.

Two mode combinations were used according to the shape and extension of the hematoma and the required trajectory path for aspiration: (1) Still Mode and Tilt Mode, and (2) Slide Mode and Tilt Mode.

Still Mode and Tilt Mode
In four patients with putaminal hemorrhage of the extended type, in which the long axis of the hematoma extended sagittally, the trajectory of the puncture needle was matched to the CT plane by appropriately tilting the gantry. The insertion pathway was confirmed by CT-F, and the hematoma was punctured and aspirated.

Slide Mode and Tilt Mode
In two patients having a subcortical hematoma in the parietal region, the patients's head was immobilized by adjusting the settings for the trajectory of the puncture pathway so that it would parallel the axis along which the table moved as much as possible.

With the gantry tilted and the table appropriately moved under CT-F guidance, the CT planes were moved distal to the tip of the puncture needle, based on planning the trajectory of the puncture needle on the helical scans and multiplanar reconstruction data before puncture. Thus, the planes were adjusted until the target site was reached.

External Ventricular Drainage

One of the patients with a brain hemorrhage had moya-moya disease with intraventricular hemorrhage. This patient underwent ventricular puncture and insertion of a drainage tube, which could be done very precisely under CT-F guidance.

Practical Experience with Precise Targeted Tumor Biopsy and Marking under CT-F Guidance

CT-fluoroscopy was applied for biopsy and marker installation for an intraaxial tumor.

Miscellaneous Uses

Apart from these major procedures, CT-F was also used for repositioning a cisternal drainage tube following aneurysm surgery and for tapping a subdural effusion.

It was also useful for pain relief in two cases of advanced malignancy. One was a case of renal cancer in a 71-year-old man who had a paraaortic ganglion block under CT-F guidance. The second case was a 54-year-old man with advanced cancer who underwent a CT-F-guided celiac ganglion block.

Results

Brain Hemorrhage

1. It was possible to evacuate and flush out a cerebral hematoma in deep basal ganglia extremely safely and precisely by freehand under CT-F guidance and also to place an indwelling drainage tube.
2. CT-F enabled serial assessment of the status of hematoma removal by evacuation and checking for rebleeding; cerebral deformation and changes in target position associated with intraoperative cerebrospinal fluid (CSF) leakage and hematoma removal were also detected by CT-F.
3. Intraoperative helical scanning was possible. The state of the brain on planes other than the involved slices could also be determined. Planning could be performed, again intraoperatively.
4. Insertion pathways trajectoried at various angles are needed for clinical application to the spherical skull. The prototype CT unit is designed for frequent diagnostic use. The insertion pathways for matching the trajectory to the CT plane are restricted to the frontal approach because of the width of the gantry and restriction of the tilt angle.
5. Puncture approaches in the parietal and temporal regions were possible in the moving mode by tilting the gantry and adjusting the table or in the still mode in which gantry and table are fixed. Puncture sites other than the tip could be targeted by tilting the gantry and moving the table.

A typical case encountered (case 1) was a 74-year-old man with a right putaminal hemorrhage. He presented clinically with right hemiplegia (1/5) and dysarthria. Five days after onset of symptoms, the hematoma was punctured via the right frontal region under CT-F guidance. This was done very easily and accurately.

The hematoma cavity was flushed out with physiological saline solution as the puncture needle was gradually moved under CT-F guidance. Decrease in the size of the hematoma and cerebral changes around the hematoma were confirmed in real time, and it was possible to remove about 60% of the hematoma during a CT-F time of about 200 s (Fig. 1). After the hematoma had been removed, helical scanning was performed again; because residual hematoma was found at the bottom of the hematoma cavity, it was punctured again under CT-F guidance. Ultimately, about 90% of the hematoma was safely removed. A drainage tube was then accurately positioned at a target site in the hematoma cavity (see Fig. 1).

Tumor Biopsy

Using the CT-F multiple site, freehand biopsy of a tumor could be done very precisely. Also, a marker could be placed to delineate the tumor, which was useful during open excision of the tumor. This was done without injuring the surrounding normal brain and without producing any postoperative deficit in the patient.

A typical case encountered (Figs. 2, 3) was a 55-year-old woman with right hemisensory disturbance and mild dysarthria. CT revealed a low-density area at the left insula with no enhancement with contrast. MRI showed a hypo- and hyperintense area in T_1 and T_2-weighted images, respectively, with no enhancement with

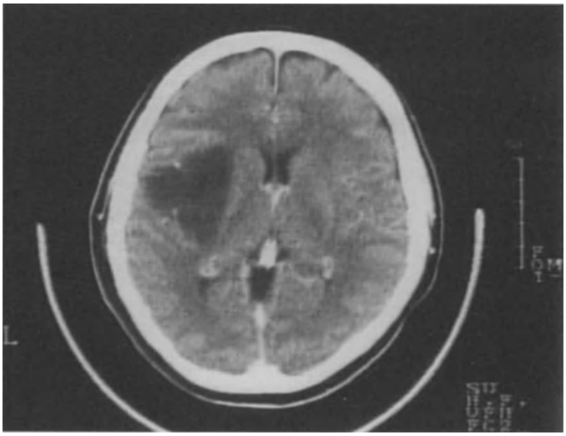

Fig. 2. A case of left insular glioma shown on CT-F

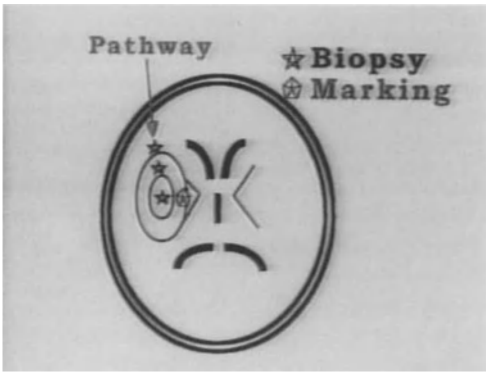

Fig. 3. Planning of trajectory pathway sites of biopsy and marker installation under CT-F

gadopentate-tetradecanoylphorbol acetate (Gd-TPA). The angiogram showed avascularity. Using a radiolucent framed stereotaxy (SBD-03, Tokai-rika, Japan), a needle biopsy was done under real-time CT-F guidance at three points: the subcortex near the lesion, the lateral side of the lesion, and the center of the lesion (see Fig. 3).

The first target biopsy was performed at the subcortex near the lesion, which was done easily and precisely. Hematoxylm-eosin (H-E) stain showed no evidence of malignancy. The next site was the lateral side of the lesion; H-E stain now showed unclear atypism but no mitosis or endothelial proliferation. The last site was at the center; during the procedure we could see the biopsy forceps opening and closing under real-time imaging. Histopathology was the same as that of the lateral portion; the tissue was stained with glial fibrillary acidic protein (GFAP), and the MB-1 expression rate was about 2%–7%. A diagnosis of low-grade astocytoma (grade 2) was made.

After confirming the report from the neuropathologist, a marker was installed at the inner border of the lesion adjacent to the internal capsule under CT-F guidance. A round mini-coil made of platinum (0.46-mm diameter, single coil; Hilar Cook) and covered by feathers was used as the marker. After these procedures, the patient recovered very well with no fresh deficits. Postoperative CT revealed no bleeding, and the marker had been placed at the target point very precisely.

Two weeks later, tumor resection was performed by the transsylvian approach using frameless armed navigation (Brain Pointer, Mitaka, Japan). This navigation system, which is based on preoperative digital images, is accurate only up to the extradural plane. After the opening of the dura the accuracy declines because of lack of real-time imaging. We found that the discrepancy between the marker, which was instilled under CTF guidance before tumor resection, to the point indicated by the Brain Pointer was 100 mm, which is explained by the brain shift that takes place during surgery. The tumor resection was carried on until the marker and stopped at that level, which was the internal capsule. Thus we could do an extensive resection of the tumor without causing any postoperative deficits in the patient.

Discussion

The new digital image-processing method is very useful in designing minimally invasive neurosurgery. A neuronavigation system using digital images such as CT-MRI has recently been attempted, consisting of navigation on reconstructed images based on images collected preoperatively. The intraoperative changes could be seen only by CT-F observation and open MRI. It is worthy to mention that the disadvantage of other navigation systems is compensated for by CT-F.

Ultrasonic tomography is another method of imaging that offers similar possibilities, but ultrasonic tomograms of deep sites in the brain are poorer than CT images in terms of accuracy, the objectivity of coordinates, and the field of images. As a result, ultrasonic tomography has not come into widespread use.

Extremely useful neuronavigation systems can be constructed by overlaying CT-F as a real-time monitor on a navigator using digital images and the planning system and by optimizing their combined use. In addition to puncture aspiration and biopsy, functional procedures for fragmentation such as thalmotomy and pallidotomy, neuromodulation, drug infusion, and cell implantation are expected to be widely applied clinically using CT-F guidance. However, there are still some problems to be solved in the future.

Detailed assessment of the radiation dose to which surgeons and patients are exposed during CT-F is required. A model that takes into account the gantry, shape and size of the slip ring, capacity, weight, and proper cost of the X-ray tube, on the assumption that it is going to be installed in an operation room, should be developed. Radiolucent equipment for immobilizing the head and radiolucent surgical instruments would be better for working with CT-F.

Finally, the difficulty of using CT-F with a microscope should be overcome.

References

1. Katada K, Anno H, Koga S, et al (1993) Initial trial with CT fluoroscopy. Radiology 190:662
2. Katada K, Anno H, Ogura Y, et al (1995) Development and early trials of real-time CT fluoroscopy. Neuroradiology 37:587–588
3. Kanno T, Nonomura K (1996) Hyperbaric oxygen therapy to determine the surgical indication of moderate hypertensive intracerebral hemorrhage. MIN (Minim Invasive Neurosurg) 39:56–59

Image-Guided Neurosurgery at Brigham and Women's Hospital

Shin Nakajima[1,6], Ron Kikinis[1,6], Peter McL. Black[2,6], Hideki Atsumi[1,6], Michael E. Leventon[3], Nobuhiko Hata[1,6], David C. Metcalf[1,4], Thomas M. Moriarty[2,6], Eben Alexander III[2,6], and Ferenc A. Jolesz[5,6]

Summary. We have been conducting various forms of image-guided neurosurgery for several years. Our image-guided therapy program includes surgical planning, intraoperative guidance using preoperative images, and intraoperative guidance using real-time magnetic resonance (MR) images. In the Surgical Planning Laboratory, we produce three-dimensional (3-D) images by reconstructing image data from computed tomograms (CT), MR imaging, and MR angiograms (MRA). These images are transferred through a network to SUN workstations in the Surgical Planning Laboratory. Registration between each modality is performed using the maximization of mutual information method. After the segmentation of each anatomical structure, such as brain, tumor, ventricles, or vessels, a 3-D model is constructed and displayed using surface rendering. We can rotate, translate, change color, and make translucent each structure on the computer display. Presurgically, this 3-D model is used to evaluate the surgical risks, choose the best method of intervention, and select the most appropriate surgical approach. In the operating room, either the video registration method or a frameless stereotaxic system is used for navigation. The 3-D model is superimposed onto the surgical field using a video mixer for the video registration system. The surgical navigator displays the tip of the probe on the 3-D model and original MR images for frameless stereotaxy. The other image-guided neurosurgery project involves the open-configuration intraoperative MR imaging system. This system produces MR scans of the patient during various types of neurosurgical procedures. Two surgeons can obtain access to the patient through a 56-cm space in the 0.5-tesla superconducting magnet. They can look at frequently updated MR images

[1] Image-Guided Therapy Program and Surgical Planning Laboratory, Department of Radiology, Brigham and Women's Hospital, 75 Francis Street, Boston, MA 02115, U.S.A.
[2] Division of Neurosurgery, Brigham and Women's Hospital, 75 Francis Street, Boston, MA 02115, U.S.A.
[3] Artificial Intelligence Laboratory, Massachusetts Institute of Technology, 545 Technology Square, Cambridge, MA 02139, U.S.A.
[4] Department of Computer Science, Boston University, 111 Commington Street, Boston, MA 02215, U.S.A.
[5] Department of Radiology, Brigham and Women's Hospital, 75 Francis Street, Boston, MA 02115, U.S.A.
[6] Harvard Medical School, 25 Shattuck Street, Boston, MA 02115, U.S.A.

during surgery. So far this system has been used for frameless stereotaxic brain biopsies, for tumor or arteriovenous malformation (AVM) resection, and for various shunting or cyst-draining procedures.

Key words. 3-D reconstruction—Computer-assisted neurosurgery—Image-guided surgery (IGS)—Intraoperative magnetic resonance image (MRI)—Surgical navigator

Background

Image-guided, computer-assisted neurosurgery has emerged as an alternative to conventional frame-based stereotaxy and the traditional surgical approach. Improved localization and targeting, better anatomic definition of the surgical field, and decreased invasiveness can result from the extensive use of image-based information. The increased use of computer-assisted frame-based stereotactic systems [1–5], surgical navigators [6–13], three-dimensional (3-D) models [14–24], and surgical simulations [25–28] have resulted in substantial changes in neurosurgery. Further transformation of conventional neurosurgery is anticipated from the use of computer-assisted stereotaxic microscopes [29–31], intraoperative computed tomography (CT) fluoroscopy [32], and open-configuration magnetic resonance (MR) imaging systems [33–43]. Behind these revolutionary changes are computers that are playing more and more consequential roles in the field of neurosurgery.

We have been involved in various forms of "image-guided neurosurgery" and the use of high-performance computing in medical imaging. Our image-guided therapy program includes surgical planning using 3-D reconstructed models, intraoperative navigation using preoperative MR images, and intraoperative navigation within an open-configuration MR imaging system with near real-time image update. Our working hypothesis is that for optimal image-based guidance the integration of preoperative planning and simulation with registration techniques is necessary to utilize image data intraoperatively. In addition, these preoperative image-based techniques could be combined into a fully integrated intraoperative guidance system in which frequent image update can account for changes during surgery. In this chapter, we introduce our activities in image-guided neurosurgery at Brigham and Women's Hospital of Harvard Medical School and discuss the future directions of computer-assisted neurosurgery based on our experiences.

Introduction

Brigham and Women's Hospital is one of the affiliated hospitals of Harvard Medical School, which is located in Boston, MA, USA. It is also a research institute awarded the nation's second largest grants from the National Institutes of Health, $97.6 million. The Brigham and Women's Hospital is known to neurosurgeons as the place where modern neurosurgery was started by Harvey Cushing, who served as Surgeon in-Chief from 1913 to 1932.

The Image-Guided Therapy Program of the MRI Division consists of three main projects. The Surgical Planning Laboratory (SPL) is investigating and developing techniques for computerized image processing, surgical planning, and intraoperative navigation, and the Intraoperative MRI project is advancing the use of real-time MR imaging during surgery and interventional radiology procedures. The third project, MR-Guided Focused Ultrasound Surgery, is investigating the use of acoustic energy for noninvasive thermal tumor ablations, vascular occlusions, and targeted drug delivery.

In 1990, the SPL was initiated within the framework of the MRI Division in the Department of Radiology. It now contains 50 SUN workstations and four supercomputers. There are more than 200 regular users, consisting of medical doctors, biological scientists, radiological physicists, engineering scientists, and others (Table 1). The active research and clinical projects in the laboratory include surgical planning and simulation [16,18,19], intraoperative image guidance [14,15,17], longitudinal study using computerized image processing for the analysis of multiple sclerosis [44], the study of morphologic abnormalities in schizophrenia [45], virtual endoscopy [46], intracranial compartment volume analysis [47,48], and numerous other studies related to medical image processing. These research projects are supported by both commercial software and an extensive library of in-house software.

The purpose of the neurosurgical planning is to make 3-D MR- or CT-based reconstructions for preoperative planning and intraoperative navigation. The clinically relevant surgical planning team consists of two to five professionals including at least two neurosurgeons. At the moment, four persons, including two neurosurgeons, are working on neurosurgical cases. In addition, an orthopedic surgical planning team has just started.

The Intraoperative MRI project is based on a prototype open-configuration MR imaging system that was developed in collaboration with GE Medical Systems (Milwaukee, WI, USA), and was installed at the Department of Radiology, Brigham and Women's Hospital in March 1994. Two surgeons are able to obtain simultaneous access to a patient during MR scanning (Fig. 1). They can operate on the patient while monitoring the patient with the MR scanner. The first neurosurgical case, brain biopsy, was performed within this unit in 1995. The intraoperative MRI is now used as one of the operating rooms, and there are four to five surgeries per week. Three radiology technologists, four nurses, and one MR engineer are working full time in the open MR unit. Multiple projects and clinical trials using this unit include craniotomies, biopsies, endoscopies, thermal ablations with laser, and

Table 1. The backgrounds of active users in the Surgical Planning Laboratory

Users	Background
Physicians	Radiology, neurosurgery, psychiatry, orthopedics, neonatology, internal medicine, public health, plastic surgery, otolaryngology
Medical scientists	Psychology, cognitive science, MR physics, anthropology, neuroscience, biomechanics
Engineering scientists	Computer science, medical image processing, mechanical engineering, mathematics, information science, electrical engineering
Students	Medicine, computer science, nuclear engineering, health science and technology, mathematics, psychology, neuroscience
Outside collaborators	University, institution, company, hospital

a

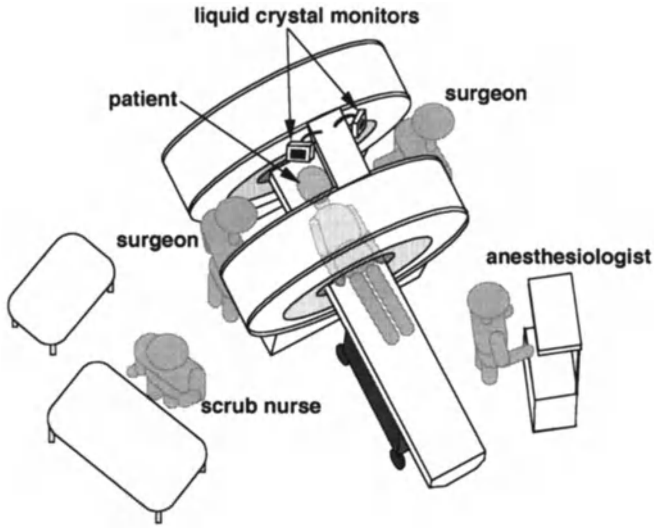

b

Fig. 1a,b. Open-configuration magnetic resonance (MR) imaging system. **a** Neurosurgical procedure in the open MRI. **b** Schema of the open-configuration MR imaging system for neurosurgery. Surgeons have access to the patient through the 56-cm space between the two magnetic coils. Surgeons can see the images using two liquid crystal monitors during the procedure. All surgical and anesthesiological equipment is MR compatible cryoprobes as well as other percutaneous or open surgical procedures. The project has funding from industry, government, and private foundations. Research involves the development and testing of new dynamic MR imaging sequences, MR-compatible surgical instruments, and several new procedures for minimally invasive treatment including laser thermal ablations, cryosurgery, and MR-guided focused ultrasound surgery [49–52].

Surgical Planning Using Three-Dimensional Models

We have completed a network from the MR/CT scanners to the 3-D reconstruction algorithms in the SPL to the display in the operating room. Using this system, we have made more than 200 3-D models and used them for presurgical planning and intraoperative navigation. The profiles of these cases from July 1994 to March 1997 are summarized in Table 2.

The Standard Method of 3-D Reconstruction

We have a special MR protocol for 3-D reconstruction that includes a series of 124 postcontrast spoiled gradient recalled acquisition (SPGR) MR images of 1.5-mm thickness. This sequence is a T_1-weighted gradient echo with 3-D data acquisition that is obtained with a 1.5-tesla superconducting MR imaging system (Signa, GE Medical Systems, Milwaukee, WI, USA). Because left–right distance is the shortest of the three orthogonal coordinates in a human head, we usually use the sagittal plane so that the 3-D slab can cover the whole head.

After transferring the MR data, we segment all 124 images into the skin, brain, tumor, ventricles, vessels, and any other necessary anatomical structures. The segmentation is based on thresholding of signal intensities [53,54]. Then, each object is modeled using the marching cubes algorithm by a polygon mesh, which consists of between several hundred and 100 000 triangles [55–57]. All anatomical structures are put together to produce a complete model.

This model is displayed with a 3-D display program (LAVA, Sun Microsystems, Mountain View, CA, USA) on which each object can be colored or made translucent. The total 3-D model can be rotated, translated, and zoomed as a viewer wishes. A

Table 2. How three-dimensional models were used (July 1994–March 1997)

Field	Method	No. of cases
Neurosurgery	Video registration	38
	Surgical navigator	29
	Displayed in the OR only	34
	Surgical planning only	40
	All	141
Otolaryngology, etc.	All	9
Total		150

OR, operating room.

stereoscopic view is also available. We use this model for presurgical planning and intraoperative navigation.

Special Techniques for 3-D Reconstruction

We also have special techniques to improve the model quality. For the 3-D models to be more than just a beautiful picture, they must include information needed during surgery. We use a morphologically based, interactive segmentation tool with volumetric renderer that works on a supercomputer (CM-2, Thinking Machines, Cambridge, MA, USA) to manually edit images. We can update the volume rendering within 20 s after an editing operation. For simple segmentation of the skin and brain, this technique is precise and sufficient. For ventricles, it is necessary to separate them into three or four parts to complete segmentation because it is difficult to distinguish the ventricles from cisterns by only thresholding and connectivity.

It is relatively easy to segment a high signal intensity or a well-enhanced tumor on T_1-weighted images. However, it is difficult to segment nonenhanced tumors with low signal intensity on T_1-weighted images. For those tumors that are isointense with normal gray matter, we can apply another segmentation technique: we register images with different contrast mechanisms and select from these the anatomical structures

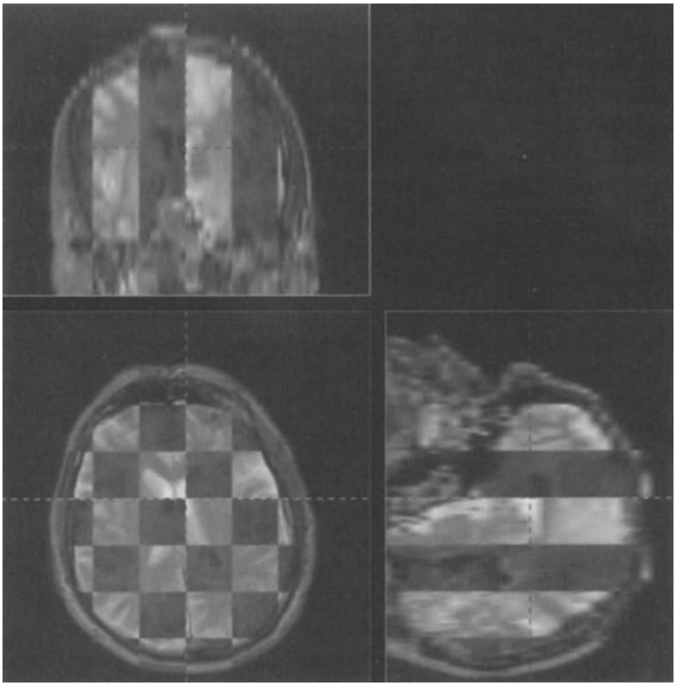

Fig. 2. Registration between the spoiled gradient recalled (SPGR) and T_2-weighted images. The *dark squares* of the checkerboard show the SPGR images; the *light squares* are the T_2-weighted images. Note the consistency of the two types of data

that are expressed best. For example, T_2-weighted images sometimes show better contrast than postcontrast SPGR images to define the tumor. In those cases, we register the T_2-weighted images to SPGR images and reformat them to match the image formats (same slice thickness and field of view in the same plane). Similarly, we register and use a 3-D phase-contrast MR angiogram for vessels and CT scanning for bony structures [17,58] (Fig. 2).

We regard vessels as very important structures for image-guided neurosurgery, because the cortical vessels are good landmarks for the brain surface and are used for video registration. Thus, we chose a 20 cm/s venc (velocity-encoding value) to visualize the veins in a 3-D phase-contrast MR angiogram. To improve segmentation of the vasculature, we use a couple of line-filtering techniques for particular cases [59,60].

For vascular diseases, we obtain the vector of the blood flow from the 3-D phase-contrast MR angiogram with 60 cm/s venc. This information is then available for vascular flow analysis [18,61]. One possible problem with the flow analysis is phase wrapping, which disturbs flow vectors greater than 60 cm/s of blood flow. One of our projects has solved this problem by detecting and unwrapping this phase wrapping [62].

Because we have an established pipeline for 3-D reconstruction, outside collaborators sometimes request a 3-D model from their own data. One such collaborator transferred MR data to us from eight neurosurgical cases. We made the 3-D models and transferred them back to the site through the Internet to be used for their surgical planning (Table 3).

Presurgical Planning with 3-D Models

Before surgery, we use the 3-D model for surgical planning. For brain tumor cases, the main issues are the tumor location and the spatial relationship between the tumor and surrounding normal structures. Therefore, the important anatomical structures that should be reflected on the 3-D model are the cortical anatomy (i.e., central sulcus, superior temporal gyrus, frontal operculum), major arteries, cortical vessels, ventricles, cranial nerves, and bony structures, although some of them are difficult to distinguish (Fig. 3).

We sometimes use cortical mapping during surgery under local anesthesia to localize the motor and sensory areas. This procedure becomes more efficient and precise with the presurgical identification of pre- and postcentral gyrus [17]. For cerebrovascular cases, a 3-D model is used for decision making in various steps of

Table 3. Telecollaborated three-dimensional reconstruction cases through the Internet

Category	Disease
Brain tumor	Anaplastic astrocytoma, pineal tumor, DNT, astrocytoma, pilocytic astrocytoma
Vascular disease	Cavernous angioma
Congenital anomaly	Encephalocele

DNT, dysembriogenic neuroepithelial tumor.

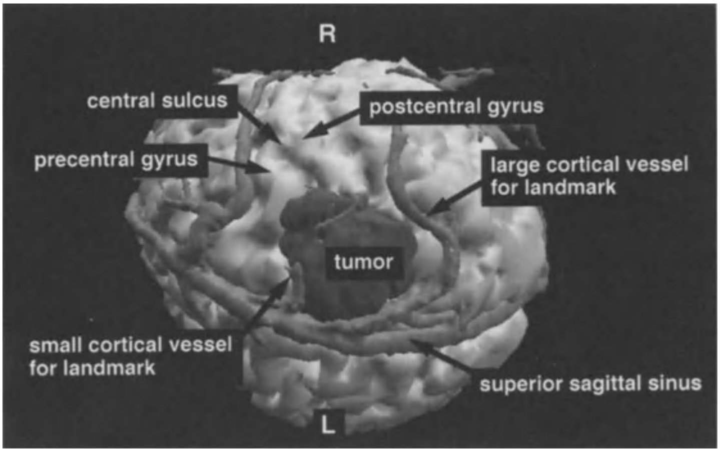

Fig. 3. Surgical planning with three-dimensional (3-D) reconstruction. Each structure (*arrows*) was morphologically identified on the 3-D model

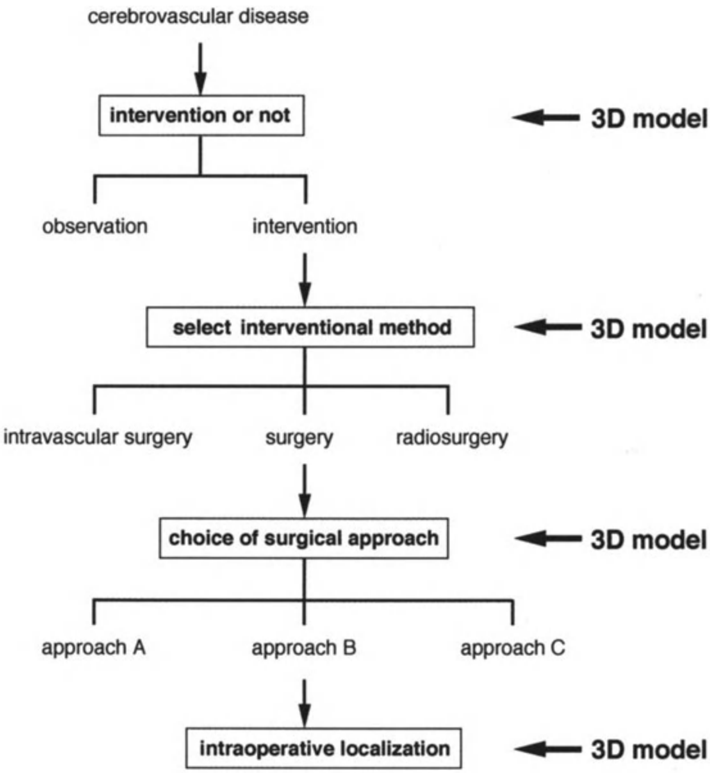

Fig. 4. Three-dimensional models are used for various stages of decision making, presurgical planning, and intraoperative navigation for cerebrovascular diseases

surgical planning as well as for intraoperative navigation (Fig. 4) [18]. For example, the flow analysis tool detects the flow direction [61], which distinguishes arteries from veins in arteriovenous malformation (AVM) cases and contributes to deciding the Spetzler–Martin grade for selecting the interventional method [63].

Intraoperative Navigation Using Preoperative MR Images

The 3-D model is also used for intraoperative surgical navigation in the operating room. We have two methods for lesion localization and surgical navigation: video registration [15,17], and laser registration with a surgical navigator [14].

Video Registration

For cortical or subcortical superficial lesions, a video registration technique is useful for lesion localization. A video camera is positioned to have a view of the surgical field similar to that of the surgeon. The 3-D model is overlaid onto the video image using a video mixer. The images are manually registered by rotating, translating, and zooming the 3-D model to match the video image. For initial approximate alignment, we use a "skin-to-skin" registration technique, which fits the skin contour of the 3-D model to that of the patient's head. However, this registration technique does not achieve sufficient accuracy because the lack of prominent landmarks. Therefore, after opening the dura mater, we refine our registration using a "vessel-to-vessel" technique. This technique aligns the unique curve of the cortical vessel of the 3-D model onto that of the actual surgical field. This refinement has been shown by a phantom study to improve accuracy in a 2-D plane from 8.9 ± 5.3 mm to 1.3 ± 1.4 mm [17].

Illustrative Case of Video Registration

A 46-year-old man presented with generalized seizures. An MR scanning showed a $6.5 \times 4.5 \times 4$ cm tumor in the left frontal lobe. A 3-D model reconstructed from both SPGR MR images and an MR angiogram showed that the tumor was anterior to the precentral sulcus and did not invade the precentral gyrus. During surgery, the brain surface was well described by the 3-D model. The tumor resection was performed using the "vessel-to-vessel" video registration method (Fig. 5; see the end of this chapter). The patient showed temporary motor aphasia for 4 weeks after gross total resection.

Surgical Navigator

While video registration works well to localize the lesion and to define the boundary of the tumor in the cortical and subcortical region, it does not include depth information. Thus we developed our surgical navigator using infrared light-emitting diodes (LEDs) and sensors. The two flashing infrared LEDs on a probe are detected by three cameras positioned above the surgical field. Then the tip of the probe is localized and displayed on a 3-D model as well as on MR images in three orthogonal planes (Fig. 6;

see the end of this chapter). This 3-D model can be rotated, translated, and zoomed independently from the original MR images. Each object in the model can be colored or made translucent arbitrarily.

In the operating room, we use an automated technique, either a laser scanning or a skin-tracking method, for the registration between the 3-D model and the patient's head (Fig. 7). One of the advantages of this system is that the patient does not require fiducials during MR/CT scanning [14]. Having a 3-D model in addition to the original MR images provides intuitive information to the surgeon. For example, before planning the skin incision, we use the surgical navigator to outline the tumor contour on the skin. We found this easier to do by referring to the 3-D model than by referring to the MR images of the three planes.

Besides intraoperative navigation, we also use this surgical navigator for pre-, intra-, and postoperative registration and navigation. As it does not require fiducials, it is possible to register the result of preoperative transcranial magnetic stimulation to the intraoperative surgical field or to register the position of the grid of the surgery to the preoperative MRI (Fig. 8; see the end of this chapter).

One problem when using preoperative radiological data for intraoperative surgical navigation is brain shift after removal of the cerebrospinal fluid. The brain shift is estimated to be as much as 17.3 mm [64] and 14 mm [65] on the brain surface. To overcome this source of error, our surgical navigator has a function for updating registration during surgery. If the surgeon identifies some particular anatomical structures, such as cortical vessel branches, the registration will be updated using the corresponding points on the original MR images. Although it is not a perfect solution to the brain shift problem, it is a useful first step.

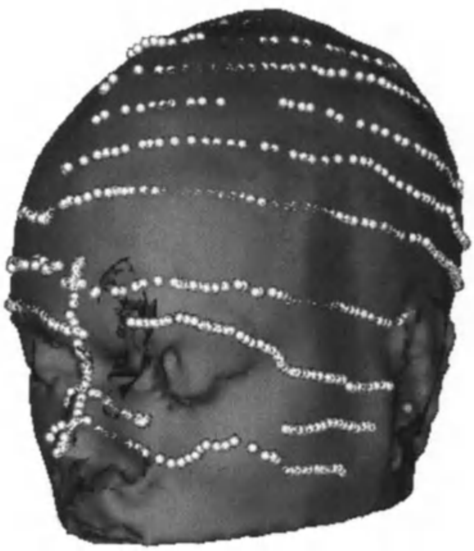

Fig. 7. Registration with instrument tracking. The head of the patient was tracked with the probe, and the surface contours thus shown (*white lines*) were automatically matched with the contour of the three-dimensional model

Illustrative Case of the Surgical Navigator

This patient was a 44-year-old man who presented with headache. The MR images showed a $7 \times 6 \times 6$ cm tumor in his left parietal lobe. The biopsy in another hospital proved it to be glioblastoma. Then, the surgical navigator was used with a 3-D model for accurate resection (Fig. 9; see the end of chapter). The patient's neurological status was monitored under local anesthesia during surgery. There was no postoperative neurological deficit after gross total resection.

Intraoperative Navigation Using Real-Time MR Images

Overview of Open MRI

The open-configuration MR imaging system at Brigham and Women's Hospital is the first clinical interventional MR unit produced by GE Medical Systems (Signa SP Intraoperative MRI). This unit consists of two vertical components that provide a 0.5-tesla magnetic field between them. The height of the coils are 184 cm and the space between these coils where a physician can have access to the patient is 56 cm. There are two liquid crystal monitors so that surgeons can see the MR images during procedures [33–36].

Many MR sequences are available in this system, including T_1-weighted spin echo, T_2-weighted spin echo, and T_1-weighted gradient echo. From the surgical viewpoint, there are two categories of scanning procedures. One is the "intraoperative" mode, which is the same scanning method as an ordinary MR unit. It takes a few minutes to generate a series of 10–15 slices. For example, a neurosurgeon can obtain MR images after tumor removal by scanning the patient's brain. Usually, the necessary slab is just an abnormal part of the brain. This mode is useful to check for a residual tumor. The other category is the "real-time" mode, in which the scanner obtains a 2-D image every 1.5 s. Therefore, a neurosurgeon can see his procedure in a 2-D plane almost immediately. This mode is useful for tracking the needle tip during tumor biopsy.

This unit has the capability for surgical navigation. A 3-D digitizer (Flashpoint, Pixsys, Boulder, CO, USA) is installed in this system, so the probe tip is displayed on the intraoperative MR images. Because three cameras for infrared detection are fixed on the ceiling of the unit and the near-real-time image is used, it is not necessary to register the MR image to the patient's head. The accuracy of the navigation system has been strictly calibrated and maintained in the working space.

It is also possible to specify a scan plane with the probe. There are three options: one plane vertical to the probe and two planes along the probe (Fig. 10). Therefore, the surgeon can select the scanning plane using the probe. With "real-time" scan mode, surgeons feel as if they are using a extremely high-contrast, high-resolution echo ultrasound probe during surgery.

All surgical and anesthesiological instruments used in this unit must be MR compatible. Among them are a high-speed drill, a surgical microscope, an anesthesia machine, and patient monitoring devices with which microsurgery under general anesthesia can be performed. With all these capabilities, this unit is a powerful tool for precise localization of lesions, total removal of tumors, and avoidance and "real-time"

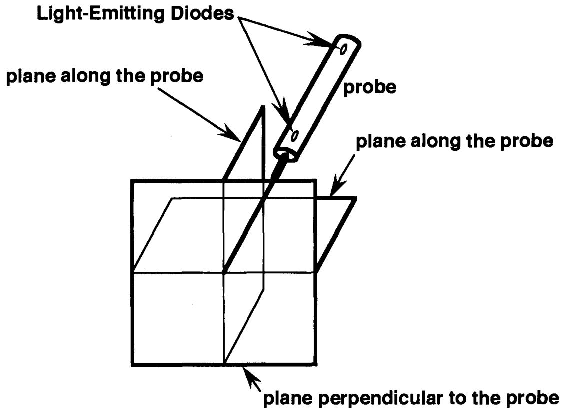

Fig. 10. The probe for the 3-D digitizer system specifies three imaging planes, two along the probe and one perpendicular to the probe

Table 4. Neurosurgical cases performed in the open-configuration MR imaging system

Surgery	No. of cases
Stereotactic biopsies	48
Craniotomies	34
Cyst manipulations	6
Laser hyperthermia cases	3

detection of surgical complications, such as intracerebral hemorrhage. So far, more than 100 operations have been performed in this MR unit including biopsy, tumor removal, and cerebrovascular cases (Table 4).

Illustrative Case

This 49-year-old woman had a resection of left temporal glioblastoma and external radiation therapy 1 year ago. Although stereotactic radiosurgery and the second surgical resection were performed for the recurrence, she experienced increased confusion and urinary incontinence 1 month ago. The MR images showed regrowth of the mass with a cyst and increased edema. Therefore, the third resection was performed in the open-configuration MR imaging system to achieve complete tumor removal. Intraoperative MR image showed no enhanced area after the tumor resection (Fig. 11).

The Advantages of Open MRI

With the three-dimensional digitizer system and intraoperative MR images, the open-configuration MR imaging system is appropriate for surgery for deep lesions needing

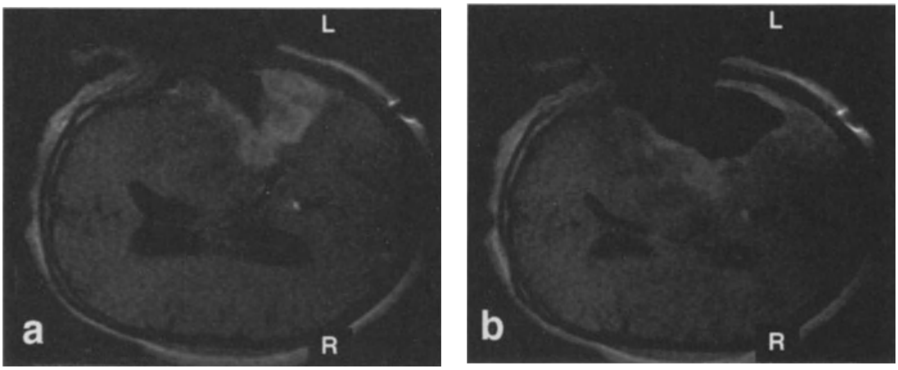

Fig. 11a,b. Tumor resection using the open-configuration MR unit. **a** The intraoperative MR image showed the residual tumor. The surgeon continued removing the tumor after the scanning. **b** No residual tumor was visible in the intraoperative MR image

biopsy, lesions needing accurate stereotactic guidance, and lesions requiring total removal. In particular, this system is powerful for intraventricular tumor cases, or tumors with a cystic component. During surgery, the lesion is shifted after fluid removal, but it is possible to monitor the tissue deformation in the open-configuration MR imaging system.

The real-time monitoring capability is also used to perform dynamic or motion scanning. Because the patient can move their cervical or lumbar spine, knee, or elbow in the magnet, it is possible to acquire a series of images from the flexion position to the extension position. Thus, the open-configuration MR imaging system is useful for diagnosis as well as intervention.

The open-configuration MR imaging system is the combination of a surgical navigator with a real-time imager. Additional integration with cortical mapping, functional MRI, and other imaging modalities (SPECT, PET) will improve its effectiveness for intractable epilepsy cases or tumor removal close to the primary motor cortex or language cortex.

The Future of Image-Guided Surgery

In our Image-Guided Therapy Program we have combined navigational tools with registration techniques and with real-time imaging to achieve image-guided neurosurgery. However, there are still many problems and questions. One of those problems is practicality. We are frequently asked, "How long does it take to complete a 3-D model of one case?" "How many cases do you process per week?" "How much will it cost if we want to have the same 3-D reconstruction system?" Initially, a 3-D model required approximately 30 h of processing time, but it takes only 3 h now. We used to process two or three cases per month, but now we can handle as many as five cases per week. However, our 3-D reconstruction system is still in the experimental stage. It is necessary to have a stable and standardized system before we can apply these technologies to routine clinical work.

The next and most important question is, "Does image-guided neurosurgery really improve the patient's outcome?" There are a few "benchmarks" to evaluate the usefulness of image-guided surgery, such as hospital length of stay, hospital charges, extent of tumor resection, postoperative functional status, symptom-free period, and survival period [66–69]. We have completed a preliminary review of image-guided surgical cases and are currently designing a formal study to compare the success rates of conventional neurosurgery and image-guided neurosurgery.

Acknowledgments. The authors gratefully acknowledge the support of the NIH (grant P01 CA67165-02). We also acknowledge many of our colleagues for their help and support in this work. In particular we thank Mark Anderson, Marianna Jakab, William Wells, Gil Ettinger, Eric Grimson, Yoshinobu Sato, Nobuyuki Shiraga, Abhir Bhalerao, Kazue Nakajima, Jens Licholt, Fatma Ozlen, Alexandra Chabrerie, and Mary Knapman.

References

1. Shelden CH, McCann G, Jacques S, et al (1980) Development of a computerized microstereotaxic method for localization and removal of minute CNS lesions under direct 3-D vision. Technical report. J Neurosurg 52:21–27
2. Kelly PJ (1986) Computer-assisted stereotaxis: new approaches for management of intracranial intra-axial tumors. Neurology 36:535–541
3. Roberts DW, Strohbehn JW, Hatch J, et al (1986) A frameless stereotaxic integration of computerized tomographic imaging and the operating microscope. J Neurosurg 65:545–549
4. Hsiang JNK, Liang EY, Lam JMK, et al (1996) The role of computed tomographic angiography in the diagnosis of intracranial aneurysms and emergent aneurysm clipping. Neurosurgery 38:481–488
5. Gibson S, Samosky J, Mor A, et al (1997) Simulating arthroscopic knee surgery using volumetric object representations, real-time volume rendering, and haptic feedback. In: Troccaz J, Grimson E, Mösges R (eds) CVRMed-MRCAS'97. Springer, Berlin Heidelberg New York, pp 369–378
6. Watanabe E, Watanabe T, Manaka S, et al (1987) Three-dimensional digitizer (neuronavigator): new equipment of CT-guided stereotaxic surgery. Surg Neurol 27:543–547
7. Watanabe E, Mayanagi Y, Kosugi Y, et al (1991) Open surgery assisted by the neuronavigator, a stereotactic, articulated, sensitive arm. Neurosurgery 28:792–800
8. Kato A, Yoshimine T, Hayakawa T, et al (1991) A frameless, armless navigational system for computer-assisted neurosurgery. Technical note. J Neurosurg 74:845–849
9. Barnett GH, Kormos DW, Steiner CP, et al (1993) Intraoperative localization using an armless, frameless stereotactic wand. J Neurosurg 78:510–514
10. Tan KK, Grzeszczuk R, Levin DN, et al (1993) A frameless stereotactic approach to neurosurgical planning based on retrospective patient-image registration. Technical note. J Neurosurg 79:296–303
11. Reinhardt HF, Horstmann GA, Gratzl O (1993) Sonic stereometry in microsurgical procedures for deep-seated brain tumors and vascular malformations. Neurosurgery 32:51–57
12. Barnett GH, Kormos DW, Steiner CP, et al (1993) Use of a frameless, armless stereotactic wand for brain tumor localization with two-dimensional and three-dimensional neuroimaging. Neurosurgery 33:674–678
13. Golfinos JG, Fitzpatrick BC, Smith LR, et al (1995) Clinical use of a frameless stereotactic arm: results of 325 cases. J Neurosurg 83:197–205

14. Grimson WEL, Ettinger GJ, White SJ, et al (1996) An automatic registration method for frameless stereotaxy, image-guided surgery, and enhanced reality visualization. IEEE Trans Med Imaging 15:129–140
15. Gleason PL, Kikinis R, Altobelli D, et al (1994) Video registration virtual reality for nonlinkage stereotactic surgery. Stereotactic Funct Neurosurg 63:139–143
16. Kikinis R, Gleason PL, Moriarty TM, et al (1996) Computer-assisted interactive three-dimensional planning for neurosurgical procedures. Neurosurgery 38:640–651
17. Nakajima S, Atsumi H, Kikinis R, et al (1997) Use of cortical surface vessel registration for image-guided neurosurgery. Neurosurgery 40:1201–1208
18. Nakajima S, Atsumi H, Bhalerao AH, et al (1997) Computer-assisted surgical planning for cerebrovascular neurosurgery. Neurosurgery 41:403–409
19. Kettenbach J, Richolt JA, Hata N, et al (1997) Surgical Planning Laboratory: a new challenge for radiology? In: Computer-assisted radiology. Elsevier, Amsterdam
20. Hu X, Tan KK, Levin DN, et al (1990) Three-dimensional magnetic resonance images of the brain: application to neurosurgical planning. J Neurosurg 72:433–440
21. Aoki S, Sasaki Y, Machida T, et al (1992) Cerebral aneurysms: detection and delineation using 3-D-CT angiography. AJNR 13:1115–1120
22. Schwartz RB, Jones KM, Chernoff DM, et al (1992) Common carotid artery bifurcation: evaluation with spiral CT—work in progress. Radiology 185:513–519
23. Castillo M, Wilson JD (1994) CT angiography of the common carotid artery bifurcation: comparison between two techniques and conventional angiography. Neuroradiology 36:602–604
24. Schwartz, RB (1994) Neuroradiological applications of spiral CT. Semin Ultrasound CT MR 15:139–147
25. Koyama T, Okudera H, Kobayashi S (1995) Computer-assisted geometric design of cerebral aneurysms for surgical simulation. Neurosurgery 36:541–547
26. Tampieri D, Leblanc R, Pleszek J, et al (1995) Three-dimensional computed tomographic angiography of cerebral aneurysms. Neurosurgery 36:749–755
27. Kelly PJ, Kall BA, Goerss SJ (1988) Results of computed tomography-based computer-assisted stereotactic resection of metastatic intracranial tumors. Neurosurgery 22:7–17
28. Kelly PJ (1988) Volumetric stereotactic surgical resection of intra-axial brain mass lesions. Mayo Clin Proc 63:1186–1198
29. Kelly PJ, Kall BA, Goerss S, et al (1986) Computer-assisted stereotactic laser resection of intra-axial brain neoplasms. J Neurosurg 64:427–439
30. Hata N, Wells WM III, Halle M, et al (1996) Image-guided microscopic surgery system using mutual-information based registration. In: Proceedings of 4th international conference on visualization in biomedical computing (VBC '96), Hamburg, Germany, pp 307–316
31. Pillay PK (1997) Image-guided stereotactic neurosurgery with the multicoordinate manipulator microscope. Surg Neurol 47:171–177
32. Katada K, Kato R, Anno H, et al (1996) Guidance with real-time CT fluoroscopy: early clinical experience. Radiology 200:851–856
33. Jolesz FA, Blumenfeld SM (1994) Interventional use of magnetic resonance imaging. Magn Reson Q 10:85–96
34. Schenck JF, Jolesz FA, Roemer PB, et al (1995) Superconducting open-configuration MR imaging system for image-guided therapy. Radiology 195:805–814
35. Silverman SG, Collick BD, Figueira MR, et al (1995) Interactive MR-guided biopsy in an open-configuration MR imaging system. Radiology 197:175–181
36. Moriarty TM, Kikinis R, Jolesz FA, et al (1996) Magnetic resonance imaging therapy: intraoperative MR imaging. Neurosurg Clin North Am 7:323–331
37. Kaufman L, Arakawa M, Hale J, et al (1989) Accessible magnetic resonance imaging. Magn Reson Q 5:283–297
38. Gronemeyer DH, Kaufman L, Rothschild P, et al (1989) New possibilities and aspects of low-field magnetic resonance tomography. Radiol Diagn 30:519–527

39. Gronemeyer DHW, Seibel RM, Kaufman L, et al (1991) Low-field design eases MRI-guided biopsies. Diagn Imaging 47:139–143
40. Gronemeyer DHW, Seibel RM, Schmidt A (1995) Image-guided access techniques. Endosc Surg 3:69–75
41. Ortendahl DA, Kaufman L (1995) Real-time interactions in MRI. Comput Biol Med 25:293–300
42. Lu DSK, Lee H, Farahani K, et al (1997) Biopsy of hepatic dome lesions: Semi-real-time coronal MR guidance technique. AJR (Am J Roentgenol) 168:737–739
43. Anzai Y, Desalles AA, Black KL, et al (1993) Interventional MR imaging. RadioGraphics 13:897–904
44. Guttmann CRG, Ahn SS, Hsu L, et al (1996) The evolution of multiple sclerosis lesions on serial MR. AJNR 16:1481–1491
45. Shenton ME, Kikinis R, Jolesz FA, et al (1992) Abnormalities of the temporal lobe and thought disorders in schizophrenia. A quantitative magnetic resonance imaging study. N Engl J Med 327:604–612
46. Jolesz FA, Lorensen WE, Shinmoto H, et al (1997) Interactive virtual endoscopy. AJR (Am J Roentgenol) (in press)
47. Matsumae M, Kikinis R, Mórocz IA, et al (1996) Intracranial compartment volumes in patients with enlarged ventricles assessed by MRI based image processing. J Neurosurg 84:972–981
48. Matsumae M, Kikinis R, Mórocz IA, et al (1996) Age-related changes in intracranial compartment volumes in normal adults assessed by magnetic resonance imaging. J Neurosurg 84:982–991
49. Matsumoto R, Oshio K, Jolesz FA (1992) Monitoring of laser and freezing-induced ablation in the liver with T_1-weighted MR imaging. J Magn Reson Imaging 2:555–562
50. Matsumoto R, Selig AM, Colucci VM, et al (1993) MR monitoring during cryotherapy in the liver: predictability of histologic outcome. J Magn Reson Imaging 3:770–776
51. Cline HE, Schenck JF, Hyṅynen K, et al (1992) MR-guided focused ultrasound surgery. J Comput Assist Tomogr 16:956–965
52. Darkazanli A, Hynynen K, Unger EC, et al (1993) On-line monitoring of ultrasonic surgery with MR imaging. J Magn Reson Imaging 3:509–514
53. Cline HE, Dumoulin CL, Lorensen WE, et al (1989) 3D reconstruction of the brain from magnetic resonance images using a connectivity algorithm. Magn Reson Imaging 5:345–352
54. Cline HE, Lorensen WE, Kikinis R, et al (1990) Three-dimensional segmentation of MR images of the head using probability and connectivity. J Comput Assist Tomogr 14:1037–1045
55. Cline HE, Lorensen WE, Ludke S, et al (1988) Two algorithms for the three-dimensional reconstruction of tomograms. Med Phys 15:320–327
56. Lorensen WE, Cline HE (1987) Marching cubes: a high resolution 3D surface construction system. Comput Graphics 21:163–169
57. Cline HE, Lorensen WE, Souza SP, et al (1991) 3D surface rendered MR images of the brain and its vasculature. Technical note. J Comput Assist Tomogr 15:344–351
58. Wells WM III, Viola P, Atsumi H, et al (1996) Multi-modal volume registration by maximization of mutual information. Med Image Anal 1:35–51
59. Koller T, Gerig G, Székely G, et al (1995) Multiscale detection of curvilinear structures in 2-D and 3-D image data. In: Proceedings of fifth international conference on computer vision (ICCV '95). IEEE Computer Society Press, Los Alamitos, pp 864–869
60. Sato Y, Nakajima S, Atsumi H, et al (1997) 3D multi-scale line filter for segmentation and visualization of curvilinear structures in medical images. In: Troccaz J, Grimson E, Mösges R (eds) CVRMed-MRCAS'97. Springer, Berlin Heidelberg New York, pp 213–222
61. Bhalerao AH, Summers PE (1995) A multiresolution approach to flow feature extraction from phase contrast MRA. In: Bizais Y, Barillor C, Paola RD (eds) Proceedings of 14th international conference of information processing in medical imaging. Kluwer, Dordrecht, pp 397–398

62. Bhalerao A, Westin C-F, Kikinis R (1997) Unwrapping phase in 3D MR phase contrast angiograms. In: Troccaz J, Grimson E, Mösges R (eds) CVRMed-MRCAS'97. Springer, Berlin Heidelberg New York, pp 193–202
63. Spetzler RF, Martin NA (1986) A proposed grading system for arteriovenous malformations. J Neurosurg 65:476–483
64. Hill DLG, Aurer CR, Wang MY, et al (1997) Estimation of intraoperative brain surface movement. In: Troccaz J, Grimson E, Mösges R (eds) CVRMed-MRCAS'97. Springer, Berlin Heidelberg New York, pp 449–458
65. Bucholz RD, Yeh DD, Trobaugh J, et al (1997) The correction of stereotactic inaccuracy caused by brain shift using an intraoperative ultrasound device. In: Troccaz J, Grimson E, Mösges R (eds) CVRMed-MRCAS'97. Springer, Berlin Heidelberg New York, pp 459–466
66. Nazzaro JM, Neuwelt EA (1990) The role of surgery in the management of supratentorial intermediate and high-grade astrocytomas in adults. J Neurosurg 73:331–344
67. Curran WJ Jr, Scott CB, Horton J, et al (1992) Does extent of surgery influence outcome for astrocytoma with atypical or anaplastic foci (AAF)? A report from three Radiation Therapy Oncology Group (RTOG) trials. J Neuro-Oncol 12:219–227
68. Albert FK, Forsting M, Sartor K, et al (1994) Early postoperative magnetic resonance imaging after resection of malignant glioma: objective evaluation of residual tumor and its influence on regrowth and prognosis. Neurosurgery 34:45–61
69. Kowalczuk A, Macdonald RL, Amidei C, et al (1996) Quantitative postoperative imaging study of the effect of surgical resection of malignant astrocytomas on survival. In: Poster program of the 64th annual meeting of the american association of neurological surgeons. American Association of Neurological Surgeons, Park Ridge, pp 304–305

Fig. 5a–d. Tumor resection with vessel-to-vessel video registration. **a** The tumor was in the left frontal area. **b** A 3-D model was made from the SPGR-MR images and the MR angiogram; the tumor is colored in *green* and the vessels in *red*. There were unique cortical vessels (*arrow, double arrows, long arrow*), which would be used as landmarks for "vessel-to-vessel" registration. **c** The brain surface was consistent with the 3-D model. The unique cortical vessels (*arrow, double arrows, arrowhead*) for registration were identified. **d** The vessel-to-vessel video registration was used for tumor resection. The cortical vessels (*arrow, double arrows, long arrow*) were used for registration, and the tumor boundary was easily defined on the overlaid image

Fig. 6. The interface of the surgical navigator with the 3-D model (*upper left*) as well as three orthogonal MR images. The *yellow line* on the 3-D model shows the position and direction of the probe. *White crosses* on the MR images show the tip of the probe

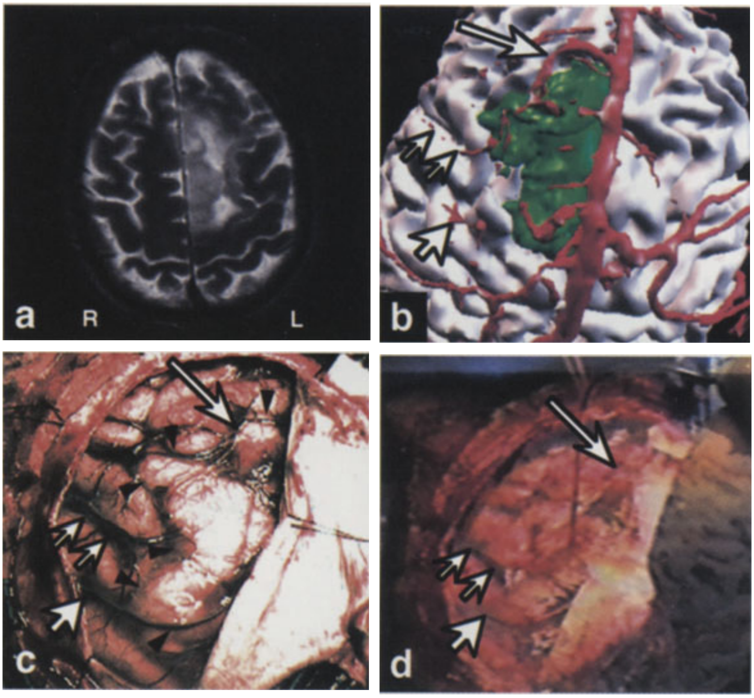

5

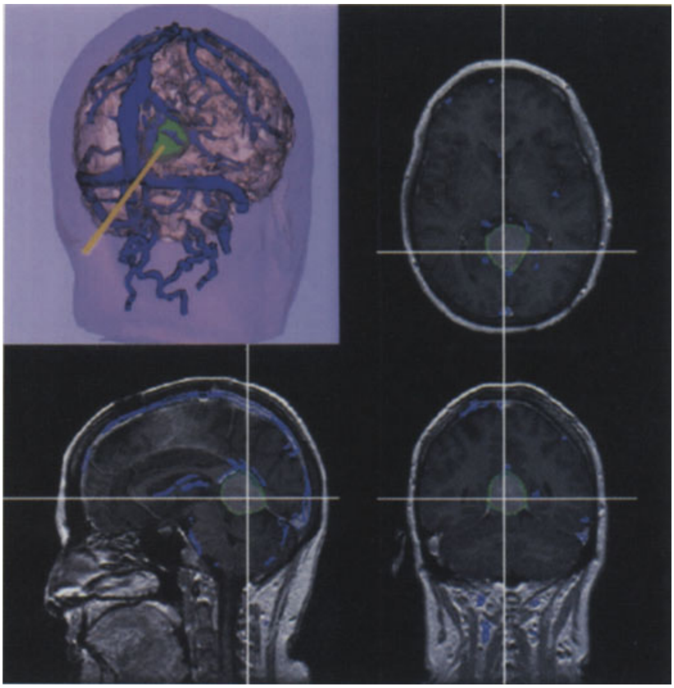

6

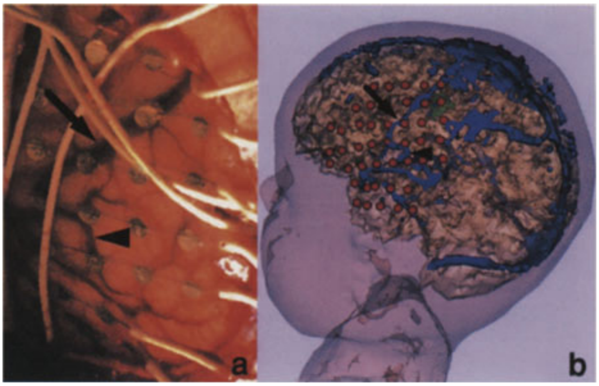

Fig. 8a,b. An intractable epilepsy case. **a** A subdural grid was placed on the brain surface. Each electrode was localized with the surgical navigator. There were unique cortical vessels (*arrow*, *arrowhead*). **b** The electrode positions were displayed on the 3-D model. The tumor, electrodes, and vessels were colored in *green*, *red*, and *blue*, respectively. The cortical vessels were well described on the 3-D model

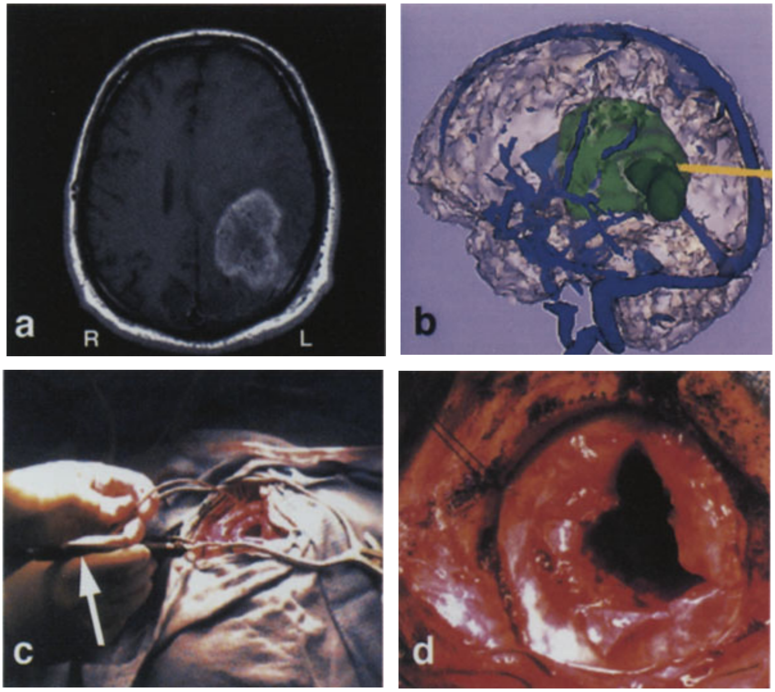

Fig. 9a–d. Resection of glioblastoma with the surgical navigator. **a** The postcontrast T_1-weighted MR image showed a 7 × 6 × 6 cm mass in the left parietal lobe. **b** Left lateral view of the 3-D model. The tumor, vessels, and ventricles are colored in *green*, *blue*, and *light blue*, respectively; the *yellow line* shows the position and direction of the probe. **c** The surgeon confirmed the boundary of the tumor with the probe (*arrow*). **d** The tumor was gross totally resected

Part 5
Computer-Assisted Neurosurgery of Difficult Lesions

Surgical Management for Gliomas Around the Motor Strip: Preoperative Anatomical and Functional Imaging

Toshihiro Kumabe[1], Nobukazu Nakasato[1], Teiji Tominaga[1], Shuichi Higano[2], Shoki Takahashi[2], and Takashi Yoshimoto[1]

Summary. Improvement of the prognosis of gliomas around the motor strip requires that maximum tumor resection be achieved while preserving motor function. Preoperative assessment of the anatomical relationship between the tumor and the motor strip was attempted by correlation of functional and anatomical imaging. The operative field was simulated by superimposing the superficial venous image obtained by magnetic resonance (MR) using a three-dimensional phase-contrast technique on the surface anatomy scan (SAS) obtained by the multiple-slice SAS method for surface anatomical images of the brain. A MR imaging-linked whole-head magnetoencephalography (MEG) system, which consists of an array of 66 MEG sensors uniformly distributed over the whole head, was used to localize the central sulcus. Combination of these preoperative anatomical and functional images enabled us to project the best surgical management and to resect tumors around the motor strip without additional motor deficit.

Key words. Anatomy—Glioma—Magnetoencephalography (MEG)—Motor strip—Surface anatomy scan

Introduction

More aggressive surgical resection of gliomas has been advocated to potentiate adjuvant therapy and improve overall survival [1]. However, maximal tumor resection is difficult to achieve when the tumor involves, or is adjacent to, eloquent brain regions such as the sensorimotor pathways, language cortex, and descending motor pathways. Surgical management of these lesions involves a significant risk of functional morbidity. Therefore, accurate preoperative and intraoperative localization of the eloquent regions is essential to minimize such morbidity.

[1] Department of Neurosurgery and [2] Department of Radiology, Tohoku University School of Medicine, 1-1 Seiryo-machi, Aoba-ku, Sendai 980-77, Japan

Preoperative visualization of the surface of the brain is extremely helpful in surgical planning for gliomas. Surface anatomy scan (SAS), a magnetic resonance (MR) imaging technique for direct visualization of the gyral patterns, can be performed without a craniotomy [2,3]. A relief image of the cerebral surface is constructed by employing a thick-slice, spin-echo imaging sequence and using the cerebrospinal fluid in the subarachnoid space as a natural contrast medium. The multiple-slice SAS method provides surface anatomical images of the brain by maximum intensity projection of thin-section, heavily T_2-weighted images using a gradient echo sequence [4]. In addition, imaging of the superficial venous system is a very useful marker to decide the border of the resection. The large cortical veins appear as white areas on the SAS images, but the smaller cortical veins cannot be identified [3]. SAS images with superimposed MR angiograms of the cortical veins are useful for this purpose [4].

Magnetoencephalography (MEG), the measurement of weak magnetic fields generated by intracerebral electric currents, is applicable to functional brain mapping. MEG can achieve accurate source localization because the inhomogeneous conductivity of the head has little influence. The advantages of MEG include its noninvasive nature and high spatial and temporal resolution. We have previously described our MR imaging-linked whole-head MEG system for noninvasive functional mapping of the central sulcus [5–7].

We describe here our method for the integrated anatomical and functional localization of the central sulcus using the superficial venous image superimposed on the SAS with MR imaging-linked MEG and its use in surgical treatment of glioma located near the motor strip.

Materials and Methods

Superficial Venous Image Superimposed on the SAS

MR imaging was performed with a 1.5-T superconducting MR unit (Siemens-Asahi, Tokyo, Japan) using a circular polarized head coil. The surface anatomical images of the brain were reconstructed by maximum intensity projection of thin-section, heavily T_2-weighted images. The heavily T_2-weighted images were obtained using the fast spin-echo sequence. Other parameters were repetition time (TR)/echo time (TE) of 9000/259 ms, 3- or 4-mm section thickness with no interslice gap, 256×162 matrix, 20-cm field of view (FOV), signal acquisition three, and echo train length 27. The imaging plane angle was selected to provide a reconstructed surface image similar to the surgical view expected in the planned surgical approach. The image obtained was reversed to show the cerebrospinal fluid in black. MR angiography of the surface cortical veins was obtained with the three-dimensional phase-contrast technique using the gradient echo sequence (TR/TE/flip angle = 104/14/12) with 64-mm slab thickness, 48 partition, and a low velocity encoding value of 5 cm/s. The angle of plane, FOV, and matrix size were identical to those for the heavily T_2-weighted imaging. The final images were formed by superimposing the MR angiograms on the reversed surface cerebral MR images.

Magnetoencephalography

The MEG measurements were performed in a magnetically shielded room according to our previously reported method [5–7]. The nasion and preauricular points were marked with small oil-containing capsules to provide three fiduciary points. Three-dimensional MR images were obtained, digitally transferred to a graphics workstation, and transformed to the MEG coordinate system. MEG used our "whole-cortex MEG system," which consists of an array of 66 MEG sensor sites uniformly distributed over the whole head (CTF Systems, Port Coquitlam, BC, Canada). The position of the subject's head relative to that of the MEG sensors was determined using three coils attached to the same three fiduciary points used for the MR imaging.

The somatosensory evoked responses were obtained by unilateral electrical stimuli delivered to the median nerve or the posterior tibial nerve. The first prominent peaks with a clear dipole pattern contralateral to the stimulated nerve were employed for analysis. These correspond to the N20m peak for the median nerve stimulation and the P38m response for the posterior tibial nerve stimulation. The source of the tibial P38m is at the medial end of the central sulcus, and the source of the median N20m is on the posterior bank of the lateral central sulcus. Combination of these data allows easy tracing of the central sulcus from medial to lateral on the MR images.

Intraoperative Identification of the Central Sulcus

The central sulcus was identified intraoperatively by somatosensory evoked potential (SEP) recordings. Briefly, the contralateral median nerve was electrically stimulated at the wrist. Cortical evoked potentials were directly recorded by contact strip electrodes placed over the exposed cortex in a direction orthogonal to the central sulcus. The central sulcus was identified by phase reversal.

Case Studies

Case 1

A 36-year-old left-handed man developed generalized seizure activity 2 months before admission. Neurological examination was normal. MR imaging revealed a gadolinium-enhanced lesion in the mesial posterior portion of the left frontal lobe (Fig. 1). The superior frontal sulcus appeared to split the motor cortex. MR imaging-linked MEG showed that the somatosensory evoked field (SEF) dipoles of both N20m and P38m were localized on the posterior bank of the central sulcus, so the tumor was located one gyrus apart from the motor cortex (Fig. 2).

A frontoparietal craniotomy was performed. The superficial venous image superimposed on the SAS was apparently identical to the intraoperative view (Fig. 3). SEP identified the central sulcus as the same shown by MR imaging-linked MEG. The entire lesion was resected. Pathological results were consistent with a glioblastoma. Postoperatively, the patient was hemiparetic on the right. However, the hemiparesis disappeared within 2 days. MR imaging obtained 4 days after the operation revealed

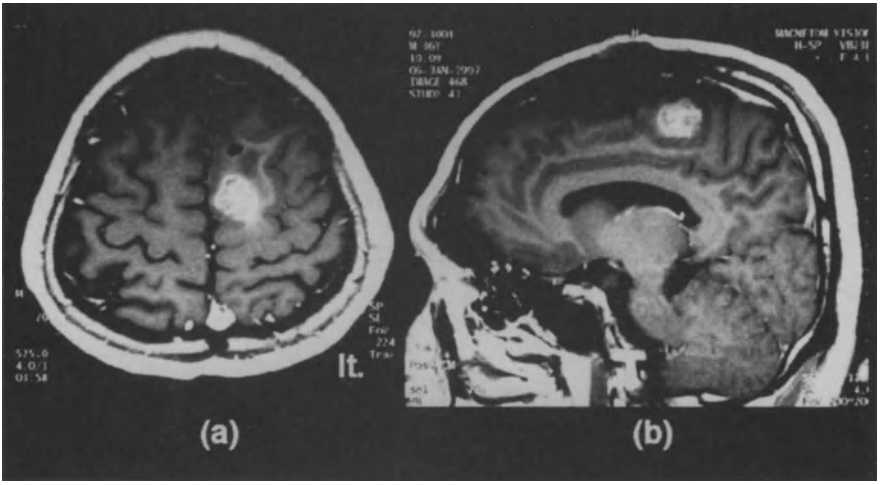

Fig. 1a,b. Case 1. Preoperative gadolinium- (Gd-) enhanced magnetic resonance (MR) images of a 36-year-old man with a glioblastoma. **a** MR image revealed a Gd-enhanced lesion in the mesial posterior portion of the left frontal lobe. **b** Slightly parasagittal midline section MR image shows the motor cortex as the gyrus anterior to the marginal sulcus, which might be mistaken as adjacent to the tumor

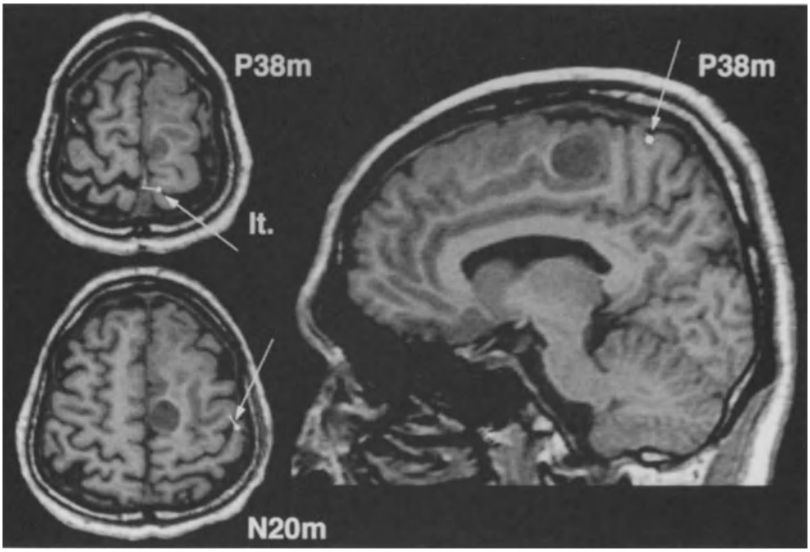

Fig. 2. Case 1. MR imaging-linked magnetoencephalography (MEG) image of the dipole positions of the somatosensory evoked fields (SEFs) for the median (*N20m*) and the posterior tibial nerves (*P38m*) indicates the posterior bank of the central sulcus. Note that there was one gyrus between the tumor and the motor cortex. *Circles* and *bars*, dipole position and orientation, respectively; *arrows*, central sulcus

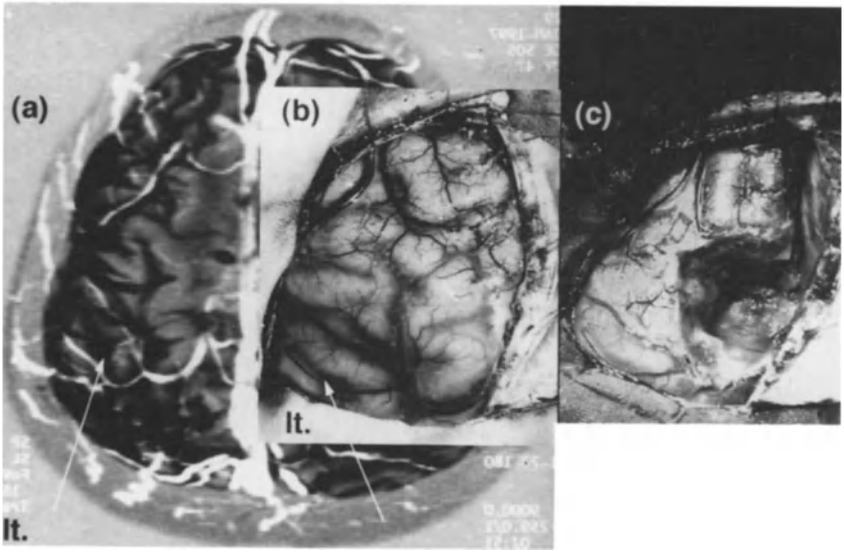

Fig. 3a–c. Case 1. Superficial venous image obtained by MR angiography superimposed on (**a**) the surface anatomy scan (SAS): (**b**) preoperative view; (**c**) postoperative view. *Arrows* indicate the same positions of the central sulcus

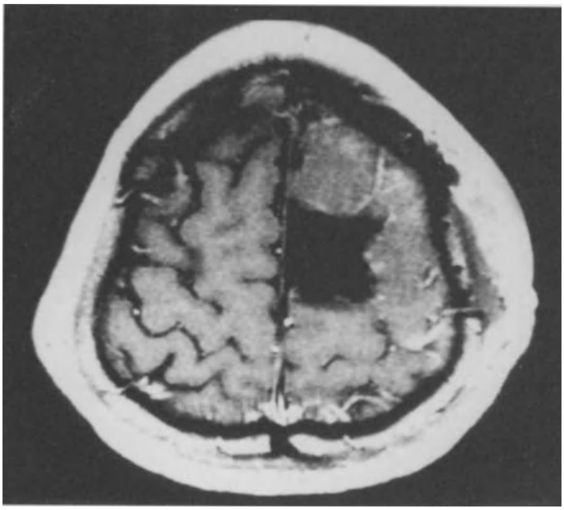

Fig. 4. Case 1. MR image obtained 4 days after the operation; the tumor had been completely resected

the tumor was resected completely (Fig. 4). The patient received postoperative radiochemotherapy.

Case 2

A 29-year-old right-handed man developed generalized seizure activity 2 weeks before admission. Neurological examination was normal. T_2-weighted MR imaging revealed a hyperintense lesion in the mesial posterior portion of the left frontal lobe that had compressed the corpus callosum downward (Fig. 5a). There was no contrast enhancement with gadolinium. MR imaging-linked MEG revealed that the tumor was located just anterior to the precentral sulcus (Fig. 6a).

A frontoparietal craniotomy was performed. The superficial venous image superimposed on the SAS was apparently identical to the intraoperative view (Fig. 7). Most of the lesion was resected. The pathology was consistent with an anaplastic astrocytoma. Postoperatively, the patient was mute and hemiplegic on the right. One day later, spontaneous speech returned but with difficulty in word-finding. Four days later, no neurological deficits were detected. MR imaging obtained 7 days after the operation demonstrated the tumor had been resected almost completely and that the

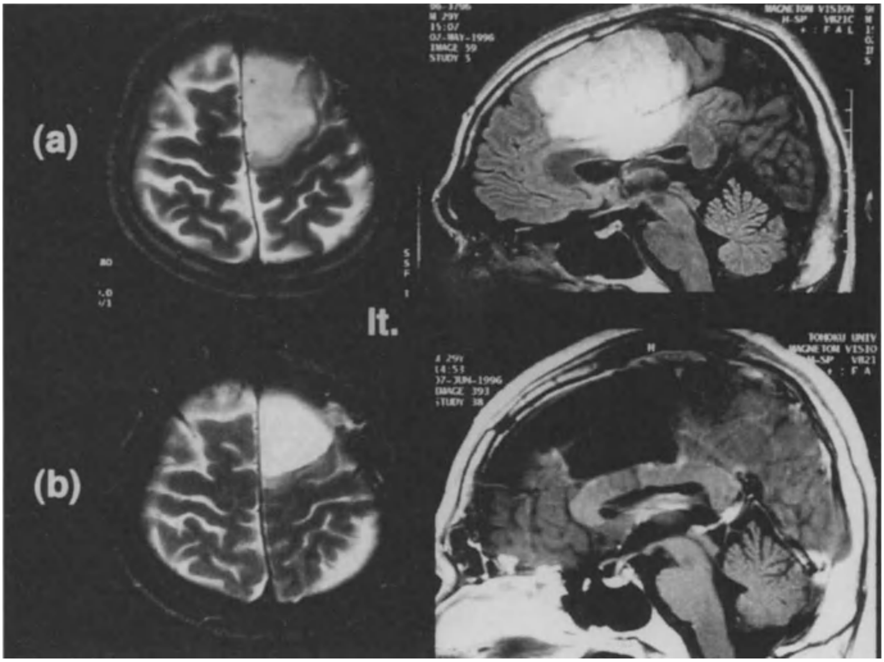

Fig. 5a,b. Case 2. Preoperative (**a**) and postoperative (**b**) MR images of a 29-year-old man with an anaplastic astrocytoma. **a** T_2-weighted MR image showed that a hyperintense lesion in the mesial posterior portion of the left frontal lobe had compressed the corpus callosum downward. **b** MR image 7 days after the operation; the tumor was resected almost completely and the corpus callosum had recovered its normal shape

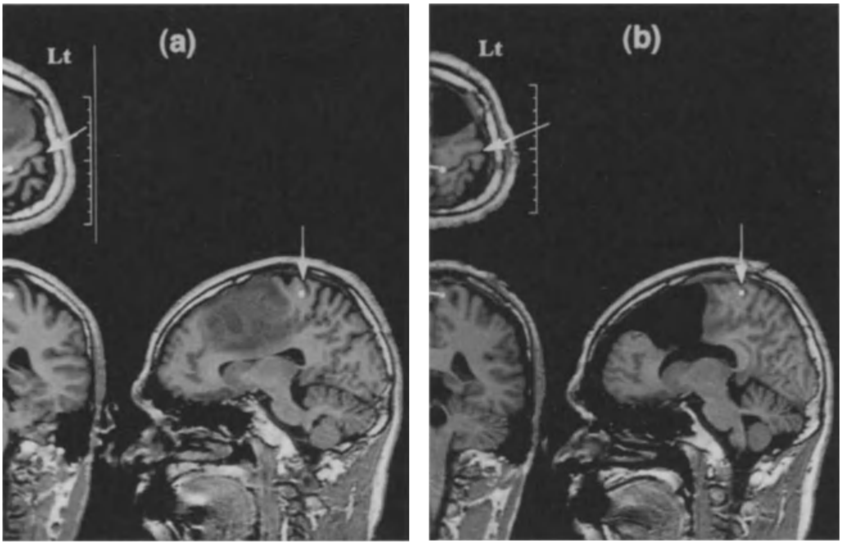

Fig. 6a,b. Case 2. **a** Preoperative MR imaging-linked MEG image of the SEF indicates the tumor was located just anterior to the precentral sulcus. *Circles* and *bars*, dipole position and orientation, respectively; *arrows*, central sulcus. **b** Postoperative image shows normal SEF findings including peak latency, peak amplitude, and dipole patterns

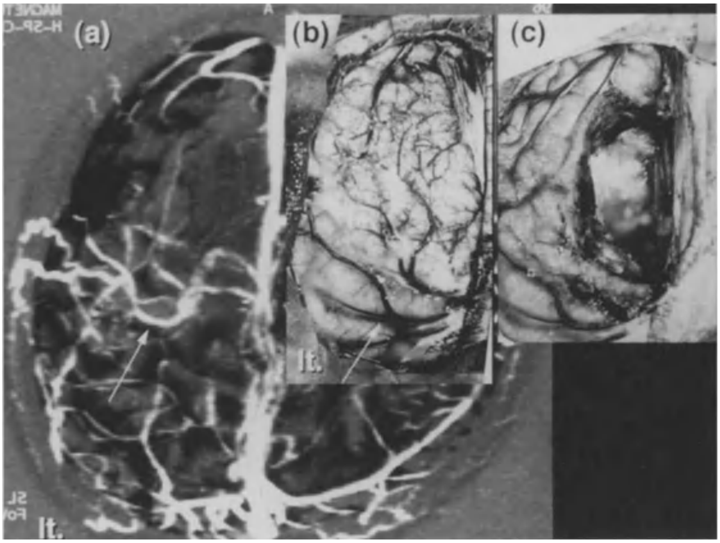

Fig. 7a–c. Case 2. Superficial venous image obtained by MR angiography superimposed on (**a**) the SAS: (**b**) preoperative view; (**c**) postoperative view. *Arrows* indicate the same positions for the central sulcus

corpus callosum had recovered its normal shape (Fig. 5b). Postoperative MR imaging-linked MEG showed the peak latency and amplitude of all the SEF components were normal. Reproducible dipole localization indicated the central sulcus (Fig. 6b). The patient received postoperative radiochemotherapy.

Discussion

Presurgical localization of the central sulcus is essential in neurosurgical planing, to avoid injury to the primary sensorimotor cortices during procedures. The typical sulcal pattern of the medial central region has been described previously [8,9]. Conventional MR imaging can provide enough information for the identification of sensory and motor cortices. The central sulcus can be identified as a mirror-image pair of distinctly transverse sulci, on the most rostral vertex T_2-weighted axial MR images. The motor cortex can be identified as the gyri directly anterior to the marginal sulcus, which is the terminal continuation of the cingulate sulcus on sagittal or slightly parasagittal midline sections [10]. However, sole reliance on anatomical criteria is inadequate. The precentral sulcus connects with the central sulcus, as seen in our case 1, in 12% on the right and 28% on the left [9]. This connection is difficult to distinguish from the superior frontal sulcus. As a result, the motor cortex is sometimes improperly identified as the superior frontal gyrus. Additionally, large mass lesions and edema can significantly displace the anatomical structure and obscure the gyral pattern.

The clinical merits of our MR imaging-linked whole-head MEG system for neurological diseases include simultaneous measurement of whole-brain activity, rapid operation, and applicability to patients with neurological disease [6,7]. Linkage to three-dimensional MR imaging and the use of the best-fitting sphere for individual head shape result in a more accurate source position estimation. Mapping of the signal source positions onto the MR images enables direct comparison of the results of functional localization with the corresponding anatomy.

The preoperative superficial venous/SAS images obtained by our method were apparently identical to the intraoperative view. We used the multiple-slice SAS method, although the raw images were obtained by the fast-spin-echo technique. Unlike the original SAS thick-slice method, our method provides stereoscopic images and rotatory motion pictures of the surface of the brain. We applied a three-dimensional phase-contrast technique for MR angiography. Unlike the time-of-flight method, the phase-contrast method can directly measure flow, and thus demonstrates the angioarchitecture more clearly even if the vessels run transversely in the slice [11]. Also, the vessels are not hindered by surrounding tissues with short T_1 values, including subcutaneous fat. The superficial venous image superimposed on the SAS was extremely helpful to determine the limit of resection, even in the case of a large tumor with extensive surrounding edema that caused obscure gyral patterns. The functional mapping obtained by MR imaging-linked MEG traced on the anatomical imaging (superficial venous image superimposed on SAS) allowed planning of the best approach for tumor resection without damaging motor function.

Unfortunately, these preoperative anatomical and functional imagings do not allow achieving maximal tumor resection because of three problems. First, cortical surface recording of the SEP to identify the central sulcus is useful, but the phase reversal does not always cross the central sulcus [12], and likewise MEG alone may not correctly identify the central sulcus. Second, the exact relationship between an individual motor function area and tumors located within the motor strip is difficult to predict preoperatively, resulting in unsatisfactory resection of the tumor. Finally, the course of the pyramidal tract in the white matter cannot be visualized, so the depth of resection is determined by the surgeon's instinct. Therefore, intraoperative brain mapping techniques, including direct cortical and subcortical stimulation, are necessary to maximize tumor resection and minimize morbidity [1,13–17]. The combination of preoperative anatomical and functional imaging with intraoperative brain mapping techniques will facilitate the satisfactory resection of gliomas around or within the motor strip and enable preservation of motor function.

Conclusions

The superficial venous image obtained by MR angiography superimposed on the SAS provides an accurate simulation of the actual operative field. MR imaging-linked MEG indicates the central sulcus accurately. Combination of this functional localization of the central sulcus with superficial anatomical imaging allows safer resection of tumors located near the motor strip.

References

1. Berger MS, Deliganis AV, Dobbins J, et al (1994) The effect of extent of resection on recurrence in patients with low grade cerebral hemisphere gliomas. Cancer (Phila) 74:1784–1791
2. Katada K (1990) MR imaging of brain surface structures: surface anatomy scanning (SAS). Neuroradiology 32:439–448
3. Sumida M, Uozumi T, Kiya K, et al (1995) Surface anatomy scanning (SAS) in intracranial tumours: comparison with surgical findings. Neuroradiology 37:94–98
4. Ogura Y, Katada K, Imai F, et al (1994) Clinical application of synthesized brain surface imaging for preoperative simulation of brain biopsy under local anesthesia. Prog CI (Jpn) 16:119–124
5. Nakasato N, Seki K, Fujita S, et al (1996) Clinical application of visual evoked fields using an MRI-linked whole head MEG system. Front Med Biol Eng 7:275–283
6. Nakasato N, Seki K, Kawamura T, et al (1996) Cortical mapping using an MRI-linked whole head MEG system and presurgical decision making. Electroencephalogr Clin Neurophysiol Suppl 47:333–341
7. Nakasato N, Kumabe T, Kanno A, et al (1997) Neuromagnetic evaluation of cortical auditory function in patients with temporal lobe tumors. J Neurosurg 86:610–618
8. Ebeling U, Reulen HJ (1992) Subcortical topography and proportions of the pyramidal tract. Acta Neurochir (Wien) 118:164–171
9. Ono M, Kubik S, Obernathey CD (1990) Atlas of the cerebral sulci. Thieme, Stuttgart
10. Berger MS, Cohen WA, Ojemann GA (1990) Correlation of motor cortex brain mapping data with magnetic resonance imaging. J Neurosurg 72:383–387
11. Dumoulin CL (1995) Phase contrast MR angiography techniques. Magn Reson Imaging Clin N Am 3:399–411
12. Suzuki A, Yasui N (1992) Intraoperative localization of the central sulcus by cortical somatosensory evoked potentials in brain tumor. J Neurosurg 76:867–870

13. Berger MS, Kincaid J, Ojemann GA, et al (1989) Brain mapping techniques to maximize resection, safety, and seizure control in children with brain tumors. Neurosurgery 25: 786–792
14. Berger MS, Ojemann GA, Lettich E (1990) Neurophysiological monitoring during astrocytoma surgery. Neurosurg Clin N Am 1:65–80
15. Berger MS, Keles E, Geyer JR (1992) Cerebral hemisphere tumors of childhood. Neurosurg Clin N Am 3:839–852
16. Berger MS, Ghatan S, Haglund MM, et al (1993) Low-grade gliomas associated with intractable epilepsy: seizure outcome utilizing electrocorticography during tumor resection. J Neurosurg 79:62–69
17. Berger MS (1994) Malignant astrocytomas: surgical aspects. Semin Oncol 21:172–185

CANS Navigator for Skull Base Surgery: Usefulness of Successive Localizations and Surgical Track

Amami Kato[1], Toshiki Yoshimine[1], Masaaki Taniguchi[1], Masayuki Hirata[1], Toshiyuki Fujinaka[1], Norio Hirabuki[2], Takeshi Okumura[3], and Toru Hayakawa[1]

Summary. Detection of surgically manipulated extension is sometimes difficult during skull-base surgery. It is, however, essential to preserve important structures and to excise the lesion precisely. To solve this problem we developed a frameless, armless neurosurgical navigational system ("CANS navigator"). The CANS navigator utilizes electromagnetic coupling technology and detects the spatial position and orientation angle of a suction tube attached to a magnetic sensor. It displays the tip of the suction tube as well as its direction at a real-time basis on the preoperative images. Because the suction tube is continually directed toward the point of surgical manipulation, the navigator is able to demonstrate the extent of the surgical manipulation by accumulating the manipulation points on the display ("surgical track"). Before the skin incision is made, this system is useful in optimizing the patient's head-position and the microscope angle and in determining the extent of the skin incision. After the craniotomy, this system assists the operator in clarifying surgical orientation, in preserving important structures encased in the tumors, and in confirming the dissectable range of neoplasms with unclear or irregular margins. Surgical track display is especially powerful in recurrent surgery or staged surgery in which the normal anatomy has been destroyed. The CANS navigator introduces precise localization of CT or MR to conventional skull-base surgery without limiting the operative field or interfering with the surgical procedures and assists the surgeon in reducing surgical invasion.

Key words. Skull base surgery—Neurosurgical navigation—Image-guided surgery (IGS)—Computer-assisted neurosurgery—Surgical track—Electromagnetic tracking

[1] Department of Neurosurgery and [2] Department of Radiology, Osaka University Medical School, 2-2 Yamada-oka, Suita-shi, Osaka 565, Japan.
[3] Research and Development Department, CT Medical Systems Division, Shimadzu Corporation, 1 Nishinokyo-Kuwabara-cho, Nakagyo-ku, Kyoto 604, Japan.

Introduction

Surgical resection of skull-base tumors often presents technically challenging problems, partly because of the closeness of neurovascular structures and the complexity of local anatomy [1]. Loss of correct orientation during surgery may result in incomplete dissection or major morbidities [2,3]. To assist the surgeon with precise surgical orientation, we have developed a neurosurgical navigator (the CANS navigator) and applied it to skull-base surgery [4–6].

Method

Setup of the CANS Navigator

The CANS navigator (Fig. 1) utilizes a magnetic field for the detection of the spatial position of the suction tube and enables real-time display of surgical manipulation on the preoperative radiological images without the use of a frame or an arm [4]. It consists of a three-dimensional (3-D) digitizer, a computer, and a graphics unit.

Fig. 1. The CANS navigator

Before the operation, CT or MR images are transferred and stored in the computer. The 3-D digitizer utilizes a low-frequency magnetic field to determine a full 6 degrees-of-freedom, the position and orientation angles of the small magnetic field sensor. The magnetic source and the sensor are basically composed of three coils arranged

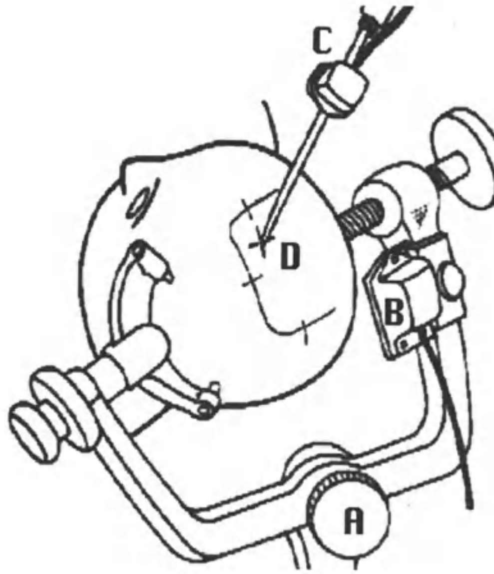

Fig. 2. Setup of the CANS navigator. The patient's head is fixed with a Mayfield skull clamp made of carbon fiber resin (*A*) to which the magnetic field source (*B*) is attached. The magnetic sensor (*C*) is mounted on a suction tube. Receiving the magnetic field from the magnetic source (*B*), the navigator calculates the tip position of the suction tube (*D*)

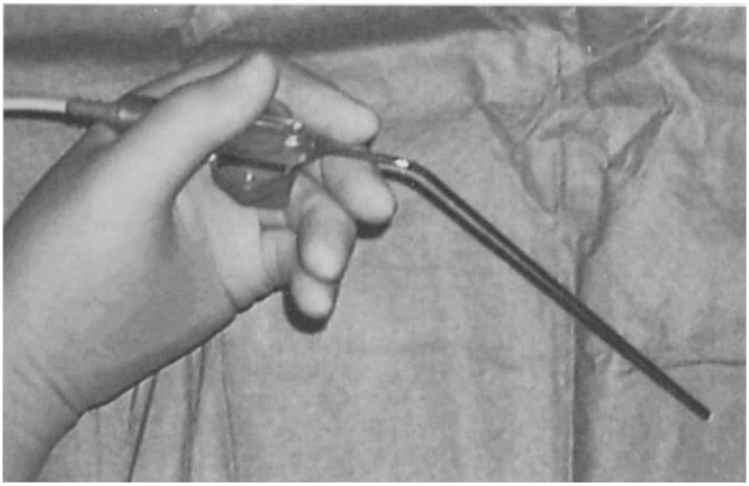

Fig. 3. The suction tube probe of the CANS navigator is made of resin and thin titanium tubing

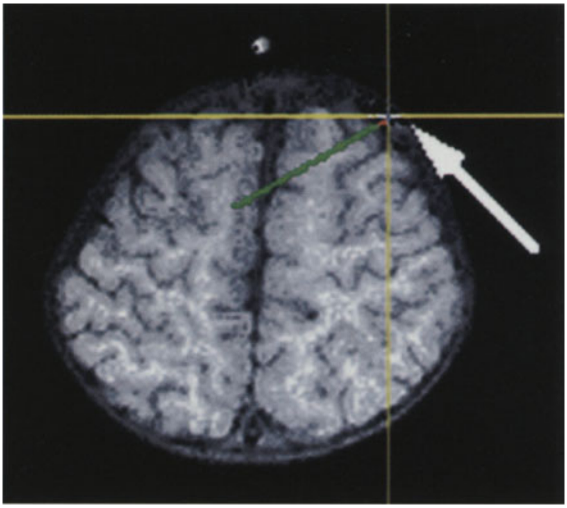

Fig. 4. Navigational display of the CANS navigator. The *yellow cross-hair cursor* indicates the position of the tip of the suction tube (*arrow*); the *green oblique line* indicates the probe direction

vertically to each other. The strength and the phase of the electromagnetic signals induced in all three antenna sensor coils are analyzed to calculate the spatial position of the sensor and sent to the computer.

In the operating room, the patient's head is fixed with a Mayfield skull clamp made of carbon fiber resin to which the magnetic field source is attached (Fig. 2). This skull clamp minimizes the pointing error from magnetic field turbulence. The magnetic sensor is mounted on a suction tube with resin screws and sterilized with ethylene oxide gas. The suction tube made with resin and thin titanium tubing is light and handy for use as an ordinary suction tube in standard microsurgery (Fig. 3). The tube, however, is not flexible to keep the precise spatial relationship with the magnetic sensor. Receiving the magnetic field from the magnetic source, the navigator calculates the position of the tip, as well as the orientation angles of the suction tube, and superimposes it on the patient's preoperative images with a cursor (Fig. 4).

Evaluation of System Accuracy

To evaluate the accuracy of this system, a model of a 3-D frame was made using acrylic resin plates (Fig. 5). This consisted of a horizontal plate having a lattice of 5-mm-interval lines and a vertical plate on which the magnetic field source was fixed. First, the position of each intersection of the lattice measured with this system was compared with the actual coordinates of each one to check the precision of the position data from the digitizer. Second, the direction of the probe was varied with its tip remaining fixed, to check the error from the drift of orientation angle data. The 3-D digitizer in this system was susceptible to interference by the

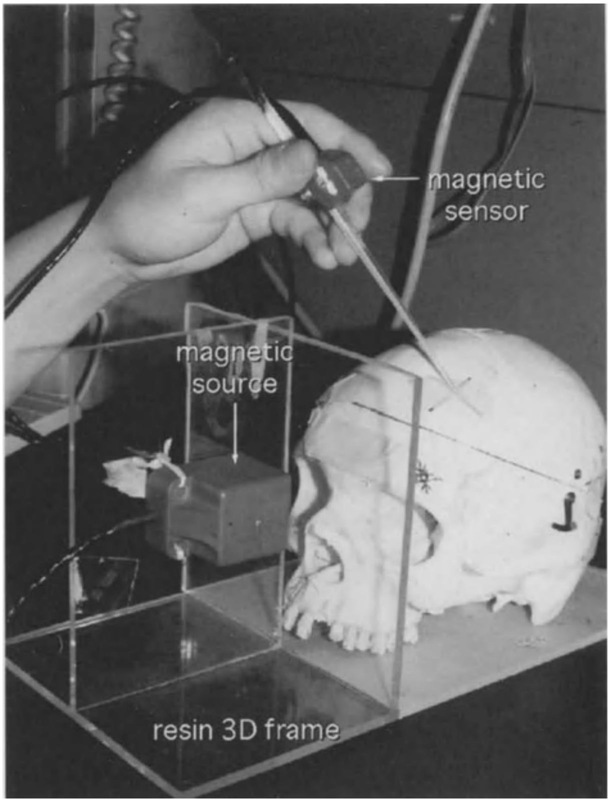

Fig. 5. Phantom study evaluating accuracy. A three-dimensional frame made of acrylic resin plates and a dried skull containing phantom targets were used. The frame consisted of a horizontal plate having a lattice of 5-mm-interval lines and a vertical plate on which the magnetic field source was fixed

conductors because of induced magnetism. To estimate this influence, we placed several metal pieces or surgical instruments between the fixed source and sensor and checked the changes in the measured coordinates of the sensor. Finally, a simulation study using a dried skull was performed. CT images of the dry skull with a phantom target inside were taken and stored in this system. Then, the discrepancy between the target positions measured with this system and those on the CT image was estimated.

Calibration of Head Position

Immediately before surgery, the position of the patient's head is calibrated by pointing to each scalp marker in sequence with the calibration probe (Fig. 6). Before CT or MR scanning, we select four points on the patient's head and mark these with an

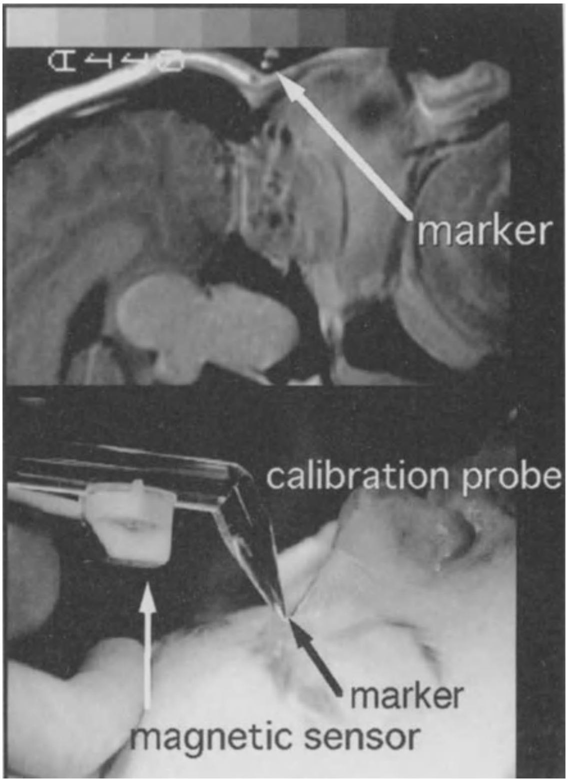

Fig. 6. Calibration of head position. One of the fiducial markers is shown on the nasion of the patient's MR image (*upper*). The head position is calibrated by pointing to each scalp marker in sequence with the calibration probe (*lower*)

indelible ink. Because the coordinates of those markers with respect to the CT or MRI reference frame are known, the equation converting the coordinates can be determined. This procedure requires about 5 min.

We use an affine instead of an orthogonal coordinate system. The spatial positions of the fiducial points are measured with CT or MRI in practice. The fiducial points, therefore, inevitably introduce errors into the calculation of the probe position because of limitation in slice thickness, distortion of the image, scalp movement, and pointing errors in calibration of the head position. In the orthogonal coordinate system, this error might be enhanced as the probe leaves the origin of the reference frame. In the affine coordinate system, however, the errors could be reduced inside the trigonal pyramid outlined by the fiducial points. The simulation study indicated that if the measuring errors for the fiducial points are reduced to less than 3 mm, the pointing errors around the center of the trigonal pyramid are evaluated as less than 1.5 mm. Pointing errors outside the head, however, would be larger than those in the orthogonal coordinate system.

Navigational Display

The navigational functions are activated immediately after calibration of the head position. The surgeon can consult the navigator alone by using the suction probe without changing the operative procedure (Fig. 7). In this system, a set of 12 arbitrarily arranged images can be displayed on the monitor at one time. This system accepts any image regardless of its mode if the coordinate system is properly determined. The images are changed automatically depending on the location of the tip of the suction tube.

On the navigational display, the cross-hair cursor indicates the position of the tip of the suction tube and the oblique line indicates the probe direction (see Fig. 4). The cursor mimics the movement of the suction tube on a real-time basis on the monitor screen like an animation.

Surgical Track

The position of the tip of the suction tube can be recorded in memory. The positions can then be accumulated to form the "surgical track." This is the extent of the surgical manipulation and can be shown simultaneously on the display. Thus, the surgical track, shown as an accumulation of red spots, indicates the extent of tumor resection (Fig. 8).

Fig. 7. Use of the CANS navigator in microsurgery. The suction tube attached to the small magnetic sensor is seen in the surgeon's left hand. This suction tube is light and handy for use as an ordinary suction tube in standard microsurgery

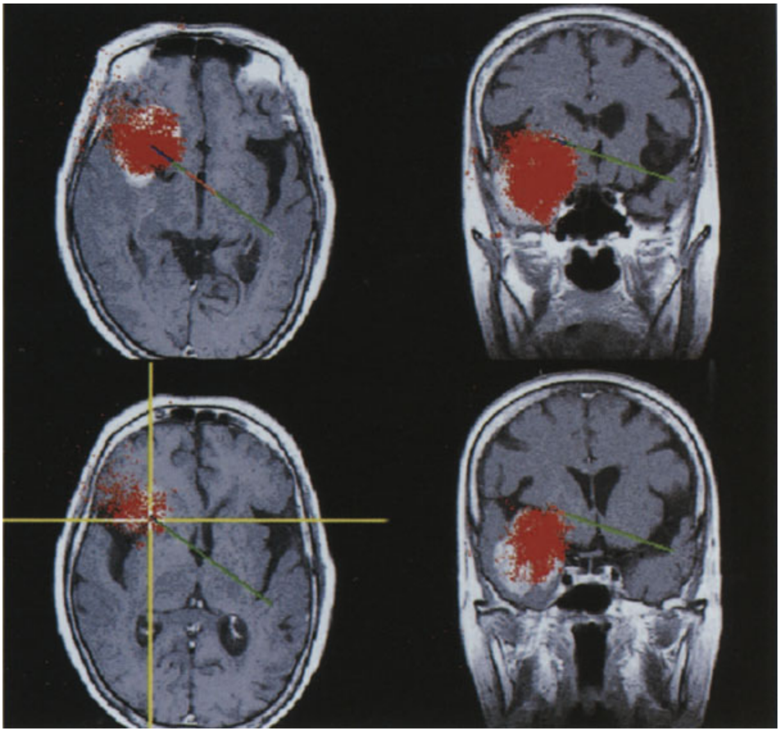

Fig. 8. A surgical track display (accumulation of *red spots*) in surgery of sphenoidal ridge meningioma is formed by plotting the positions of the suction tip and is regarded as being the extent of tumor removal

Table 1. Surgery on 30 skull-base lesions using the CANS navigator

Lesion	Number of surgeries
Meningioma	14
Clival tumor	7
Pituitary adenoma	3
Craniopharyngioma	2
Fibrous dysplasia	2
Epidermoid	1
Basilar aneurysm	1

Surgical Application

Surgery was performed on 30 skull-base lesions using the CANS navigator (Table 1). About half (14) of the lesions were meningiomas, 7 were clival tumors, and 3 were invasive pituitary adenomas; 18 patients were female, 6 were male, and 3 underwent a staged operation.

Results

System Accuracy

The positioning error using the 3-D frame model was 0.5 mm (256 trials). When the probe direction was varied with its tip fixed, the error increased up to 1.5 mm with the suction tube pointer (256 trials). Among the metals placed between the magnetic source and sensor, iron caused the greatest interference, followed by aluminum, brass, duralumin, and stainless steel in decreasing order. In the case of iron, the measured coordinates shifted as much as several centimeters. To reduce the error within 1 cm, it was necessary to keep iron at least 40 cm from the magnetic field source and sensor. The error tends to become larger in relation to metal volume. Among the surgical instruments, however, only the stainless steel plate for cottonoid placement, which was as large as 13×10 cm, produced noticeable error, and other instruments such as the bipolar coagulator, suction tubes, spatulas, or Greenberg's retractor did not interfere with the measurements unless they were placed between the magnetic source and the sensor. The simulation study using the dry skull revealed a 4-mm maximum error.

Surgical Application

Before the skin incision is made the CANS navigator is useful in optimizing patient's head-position and microscope angle and in determining the extent of the skin incision. After the craniotomy, this system assists the operator in clarifying surgical orientation, preserving important structures encased in the tumors, and confirming the dissectable range of the neoplasms with unclear or irregular margins. The surgical track display was especially powerful in the recurrent or staged surgery where the normal anatomy was destroyed.

According to the surgeons' impression, the CANS navigator was indispensable or useful in 18 of the 30 cases (Table 2). The reasons for indicating uselessness in 3 cases included 1 accidental slip of the patient's head from the skull clamp, 1 magnetic field turbulence by the Hardy's speculum in the transsphenoidal removal of the pituitary adenoma, and 1 clear orientation without the CANS navigator (in the case of a small craniopharyngioma).

Table 2. Clinical usefulness of the CANS navigator in skull-base surgery

Surgeons' impression	Number of surgeries
Indispensable	7
Useful	11
Advantageous	9
Useless	3

Illustrative Cases

Case 1

A fibrous dysplasia of the frontal base in a 15-year-old boy was operated on for unroofing of the optic canal. The MRI revealed remarkable thickening of the frontal base (Fig. 9a) and narrowing of the optic canal (Fig. 9b). The navigator was used to find and protect the optic nerve hidden under the osseous skull-base tissue and then to reconstruct the orbital roof symmetrically. Both axial and coronal CT images were used in the navigational display to find the optic nerve buried in the thick bony component (Fig. 9c). When the navigator indicated that the manipulation was

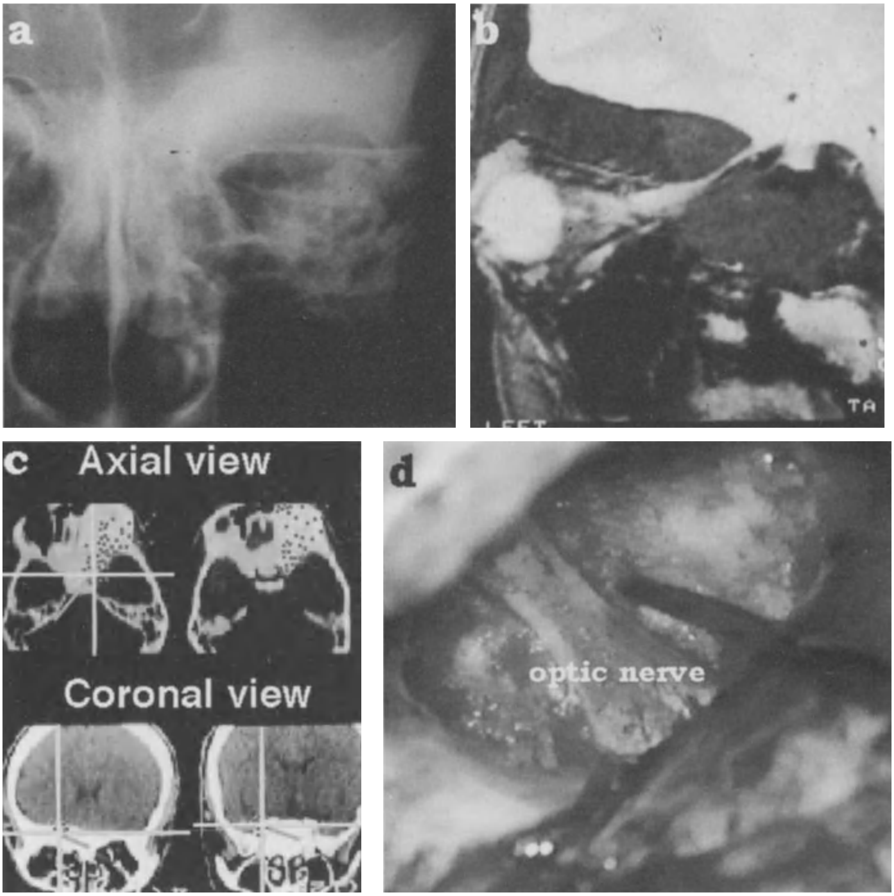

Fig. 9a–d. A fibrous dysplasia of frontal base in a 15-year-old boy (case 1). **a** Anteroposterior view of the skull X-ray image shows the remarkable thickening of the left frontal base. **b** The MRI section along the left optic nerve revealed marked narrowing of the optic canal. **c** Navigational display during unroofing of the optic canal. Both axial and coronal CT images were used to find and protect the optic nerve which was buried in the thick bony component. **d** Successfully exposed and decompressed optic nerve

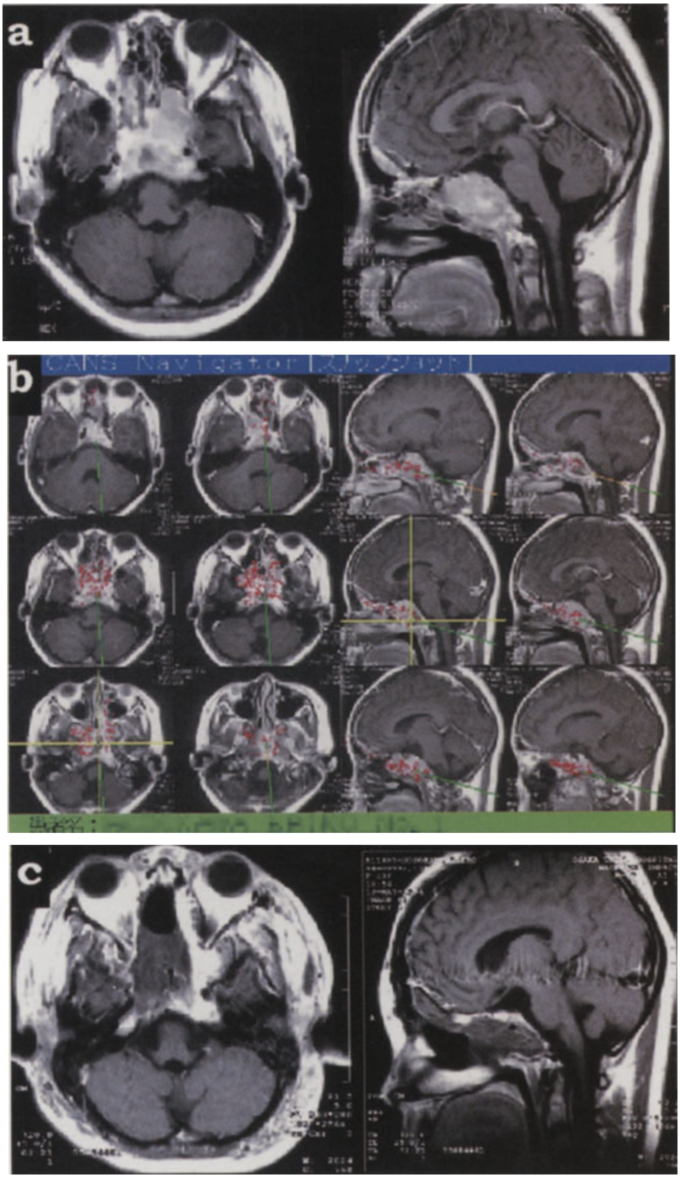

Fig. 10a–c. A recurrent giant cell tumor of skull base extending to the clivus in a 16-year-old girl (case 2). **a** Preoperative MRI shows the tumor extending to the clivus, both pyramidal apices, and the cavernous sinus. **b** The navigational display when the most of the tumor bulk had been removed. Both axial and sagittal MR images were used. **c** Postoperative MR images. Note the extent of the tumor removal is just as was shown by the surgical track during the operation

approaching close to the optic nerve, the nerve was found through the thin wall of the optic canal (Fig. 9d).

Case 2

A recurrent giant cell tumor of the skull base extending to the clivus in a 16-year-old girl was operated on using a frontobasal approach (Fig. 10a). In this case, the normal anatomical structures had been destroyed by repeated recurrence and previous operations. The CANS navigator was useful to avoid the risk of disorientation and to preserve the vital structures behind the thick tumor tissue because the tumor had invaded the cavernous sinus and involved the internal cartotid artery. Most of the tumor bulk was removed. The extension of tumor removal was displayed during the operation as shown by the surgical track (Fig. 10b) and was confirmed by the postoperative MRI (Fig. 10c).

Discussion

Skull-base surgery is characterized by deep-seated targets and complicated normal and pathological structures. Although preoperative high-definition imaging and the use of microsurgical techniques have improved intraoperative orientation, a large number of complications still are caused by localization problems [7]. Anatomical landmarks normally used to identify these vital structures [8], however, may be distorted by tumor involvement or previous operative dissection. In recent years, several neuronavigation systems have been developed for precise and objective localization [4, 9–17].

Several methods have been proposed to detect the spatial position of the probe. The multijoint arm system [10,16,17] is simple and may be reliable. It may, however, restrict the surgical field and the surgical procedure. In this system successive monitoring is not possible. The optical method [15] should be very accurate because it is based on the fact that light travels in a straight line. Spatial tracking, however, can be interrupted when the light is intercepted by the surgeon or by the instrumentation around the surgical field. This makes continuous monitoring of surgical instruments difficult. Moreover, the size of the sensing module cannot be minimized to less than several centimeters because the infrared elements need to be at a distance. Then, the system using infrared light could be suitable for tracking the microscope, endoscope, or pointing needle rather than a forceps or suction tube handled on the center of surgical field.

The CANS navigator uses a suction tube, the fundamental instrument in neurosurgery, for the principal probe and enables continuous and real-time monitoring throughout the operation [4,6]. The surgical track, the accumulation of the tip position of the suction tube, is then regarded as the extent of surgical manipulation, in other words, the extent of tumor removal [6]. Skull-base tumors usually have an irregular margin and penetrate into hard osseous tissue. The successive display of tumor removal makes it easier for the surgeon to grasp the extent of the residual tumor compared to intermittent localization. This then makes surgery more precise and efficient. To our knowledge, this function is available only in the CANS navigator.

The surgeons' impression indicated that the CANS navigator was useful for performing the operations strictly as planned preoperatively. The finest manipulation is possible in modern microsurgery if the lesion appears in the sight of the operator. Most of the surgical approaches developed recently intend to expose the lesion wider and safely by selecting the route that avoids the important structures. Then, the strictness of the approach route is very important to make the lesion accessible.

In case 2, the surgeon had to refer to the CANS navigator to identify the carotid artery behind the tumor bulk, because the normal anatomy had been destroyed by repeated previous operations. The risk of carotid injury is not negligible even in modern skull-base surgery. Inadvertent vascular injury may result in life-threatening bleeding or delayed neurological sequelae. Moreover, massive transfusion therapy may significantly alter the hemostatic mechanism in the perioperative period. This risk could be minimized by the use of MRI as the navigational images because the carotid artery is well distinguished on MRI.

The factors affecting accuracy include, first, the drift of the 3-D digitizer; second, electromagnetic noise surrounding the magnetic field source and sensor; and third, the poor spatial precision of the scalp marker in calibrating the head position. We expect that the system error can be decreased to 1 mm by improving the precision of the digitizer, using surgical instruments of titanium alloy or resin, and replacing the scalp markers with cranial screws. Because the precision of navigation does not reach that of conventional headframe systems and no rigid holder for the navigational probe has been developed, we have not used this navigational system for stereotactic biopsy of tumors or functional neurosurgery. The possibility of this system for such usage depends on future improvement of its accuracy.

Because this system indicates the relative position of the probe on the preoperative tomographic images, brain distortion during surgery could cause a problem. Special attention should be paid to interpreting the position of the probe displayed on the system when the brain is retracted, cerebrospinal fluid is lost, or a large mass of tumor is being removed. Several methods are proposed to evaluate intraoperative brain distortion, such as placing radiopaque markers around the lesion, simulating the distortion by a finite-element method, or combining the system with a real-time echogram. The intraoperative CT will add further data on brain distortion at various times during the surgery. This problem, however, may not be serious during the early stage of craniotomy or when dealing with lesions attached to the skull base. Actually, the distortion during skull-base surgery could be negligible in most cases. The navigation information would be most useful for debulking the tumors safely. After decompression was done and dissection of the tumor was started, when distortion of the tissue did occur the surgeon could usually approximate the orientation by direct inspection.

We expect the navigators will become indispensable in future neurosurgery. A qualified navigational map is important, which should be simple and easy but should contain all the information the surgeon requires. We recently developed a simple and fast image-processing method to reconstruct the image of the surgical field [18]. The surgeons themselves after a short training period can produce the image with most personal computers. This image is being used for the navigator after simulation to operate as precisely as planned.

One of the inconveniences in using the navigator is the need to change one's sight from microscope to look at the display. This could be dangerous because the surgeon may injure vital structures when the probe is inserted in the surgical field where it out of the range of sight. To avoid such a risk, we are developing an overlay display system for the microscope [19].

In conclusion, the CANS navigator introduces precise localization of neuroimaging to conventional skull-base surgery without limiting the operative field or interfering with surgical procedures and provides a powerful means for safer and less invasive skull-base surgery.

Acknowledgment. This work was supported in part by a grant-in-aid from the Ministry of Education, Science, Sports and Culture of Japan (no. 09220213).

References

1. Chang CY, O'Rourke DK, Cass SP (1996) Update on skull base surgery. Otolaryngol Clin N Am 29:467–501
2. Bogdasarian RS, Kwyer TA, Dauser RC, et al (1983) Internal carotid artery blowout as a complication of sphenoid sinus and skull-base surgery. Otolaryngol Head Neck Surg 91:308–312
3. Leonetti JP, Smith PG, Grubb RL (1989) Management of neurovascular complications in extended skull base surgery. Laryngoscope 99:492–496
4. Kato A, Yoshimine T, Hayakawa T, et al (1991) A frameless armless navigational system for computer-assisted neurosurgery. J Neurosurg 74:845–849
5. Kato A, Yoshimine T, Hayakawa T, et al (1991) Computer-assisted neurosurgery: development of a frameless and armless navigation system (CANS navigator). No Shinkei Geka (in Japanese) 19:137–142
6. Kato A, Yoshimine T, Nakajima S, et al (1994) Computer assisted neurosurgery based on individualized functional anatomy. No Shinkei Geka (in Japanese) 22:7–16
7. Klimek L, Mosges R, Laborde G, et al (1995) Computer-assisted image-guided surgery in pediatric skull-base procedures. J Pediatr Surg 30:1673–1676
8. Leonetti JP, Smith PG, Linthicum FH (1990) The petrous carotid artery: anatomic relationships in skull base surgery. Otolaryngol Head Neck Surg 102:3–12
9. Bucholz RD, Greco DJ (1996) Image-guided surgical techniques for infections and trauma of the central nervous system. Neurosurg Clin N Am 7:187–200
10. Golfinos JG, Fitzpatrick BC, Smith LR, et al (1995) Clinical use of a frameless stereotactic arm: results of 325 cases. J Neurosurg 83:197–205
11. Horstmann GA, Reinhardt HF (1994) Micro-stereometry: a frameless computerized navigating system for open microsurgery. Comput Med Imaging Graphics 18:229–233
12. Iseki H, Kawamura H, Tanikawa T, et al (1994) An image-guided stereotactic system for neurosurgical operations. Stereotactic Funct Neurosurg 63:130–138
13. Koivukangas J, Louhisalmi Y, Alakuijala J, et al (1993) Ultrasound-controlled neuronavigator-guided brain surgery. J Neurosurg 79:36–42
14. Manwaring KH, Manwaring ML, Moss SD (1994) Magnetic field guided endoscopic dissection through a burr hole may avoid more invasive craniotomies. A preliminary report. Acta Neurochir Suppl (Wien) 61:34–39
15. Reinhardt HF, Trippel M, Westermann B, et al (1996) Computer-assisted brain surgery for small lesions in the central sensorimotor region. Acta Neurochir (Wien) 138:200–205
16. Takizawa T, Soto S, Sanou A, et al (1993) Frameless isocentric stereotactic laser beam guide for image-directed microsurgery. Acta Neurochir (Wien) 125:177–180

17. Watanabe E, Mayanagi Y, Kosugi Y, et al (1991) Open surgery assisted by the neuronavigator, a stereotactic, articulated, sensitive arm. Neurosurgery (Baltim) 28:792–799
18. Nakajima S, Kato A, Yoshimine T, et al (1997) A reconstruction method of cerebral surface anatomical image for image guided localization. J Clin Neurosci 4:80–84
19. Taneda M, Kato A, Yoshimine T, et al (1995) Endoscopic-image display system mounted on the surgical microscope. MIN (Minim Invasive Neurosurg) 38:85–86

Navigational Surgery of the Skull Base and Other Vital Area Lesions Using the Mehrkoordinaten Manipulator (MKM) System

Mitsugu Nakamura, Norihiko Tamaki, Shogo Tamura, Hisahiko Suzuki, and Kazumasa Ehara

Summary. After introduction of the Mehrkoordinaten Manipulator (MKM; multicoordinate manipulator) system (Zeiss, Oberkochen, Germany) for frameless stereotactic microneurosurgery, we could determine the target point and the access route to the lesion preoperatively and outline the lesion and critical areas at a computer workstation. The system integrates stereotactically oriented computed tomography and magnetic resonance imaging with optical visualization by the microscope, displaying the spatial location of the point of focus in three sectional images. Additionally, the system superimposes the access route to the lesion, the target point with its location and direction, and the outline of the lesion and critical areas in the microscope. MKM-guided stereotactic microneurosurgery was performed in 14 patients with lesions involving the skull base, brain stem, and other deep sites. Because the lesion and surrounding structures of the skull base and brain stem maintained constant anatomical relationships during surgery, MKM-guided surgery provided easier access to the lesion, safer skull-base drilling, and better surgical results than classical microsurgical techniques. For small deep-seated lesions, the system could provide frameless stereotactic access to the lesion, but the outline of the lesion was not precisely superimposed because of displacement of the lesion and surrounding structures by cerebrospinal fluid outflow, brain retraction, and resection. The MKM system is very useful in its present configuration for lesions involving the skull base and brain stem. In the future, the MKM computer workstation should be given capability to interact with real-time intraoperative imagings to display small deep-seated lesions more accurately.

Key words. Navigation—Neurosurgery—Intraoperative monitoring—Mehrkoordinaten Manipulator (MKM; multicoordinate manipulator)—Skull base—Brain stem

Department of Neurosurgery, Kobe University School of Medicine, 7-5-1 Kusunoki-cho, Chuo-ku, Kobe 650, Japan.

Introduction

Microsurgical technique has long been used to treat lesions involving the skull base, brain stem, and other vital areas. To improve surgical results, we have sought to integrate neuroanatomy, surgical technique, neuroimaging, and neurological monitoring. Recent advances in electrophysiological monitoring, portable digital subtraction angiography, neuroendoscopy, and ultrasonography have contributed to the improvement of surgical outcome.

In addition, computed tomography (CT) and magnetic resonance imaging (MRI) provide precise preoperative information concerning the location, extent, characteristics, and nature of the lesion. Current technology makes it possible to integrate preoperative images with intraoperative monitoring. The Mehrkoordinaten Manipulator (MKM; multicoordinate manipulator) surgical microscope system represents a new generation of microscopes devised by Zeiss (Oberkochen, Germany) (Fig. 1). The computer workstation of the MKM system can memorize stereotactic CT and MRI images. We present our clinical experience using this system.

Fig. 1. The Mehrkoordinaten Manipulator (MKM) system created by Zeiss (Oberkochen, Germany) is one of a new generation of microscopes, incorporating a surgical microscope with a computer workstation

Subjects and Methods

Using the MKM system, we performed stereotactic microneurosurgery in the 14 patients profiled in Table 1. The day before surgery, four screws were introduced as bone markers under local anesthesia. The materials chosen for CT, for MRI, or for the operative microscope could be mounted on these screws. Both CT and MRI were taken in all 14 patients.

For stereotactic CT scan images, 60 axial images were taken as 1-mm slices. For skull-base lesions, bone windows also were obtained, and for brain tumors, contrast-enhanced imaging was performed. For stereotactic MR imagings the markers were filled with a solution of vitamin E acetate, and 120 axial images were taken of 1-mm slices. MR images were obtained according to a three-dimensional (3-D) fast low-angle shot (FLASH) sequence (repetition time, 30 ms; echo time, 11 ms; flip angle, 20°; base matrix, 512; field of view, 300 mm; pixel size, 1.17–0.59 mm) or a 3-D fast imaging with steady-state free precession (FISP) sequence (repetition time, 35 ms; echo time, 10 ms; flip angle, 20°; base matrix, 512; field of view, 300 mm; pixel size, 1.17–0.59 mm). In tumor cases, images enhanced with gadolinium diethylenetriamine pentaacetic acid (Gd-DTPA) (Schering, Berlin, Germany) also were obtained. The marker for CT showed a high density, and the marker for MRI appeared as a focus of high signal intensity (Fig. 2a,b).

Table 1. Case summaries

Case	Age (yr)	Sex	Diagnosis	Location of lesion	Surgery
1	16	Female	Glioma	Left putamen	Transcranial resection
2	48	Female	Aneurysm	Internal carotid-ophthalmic artery	Neck clipping
3	20	Male	Glioma	Brain stem	Transcranial resection
4	72	Female	Chordoma	Parasellar and cavernous sinus	Transcranial resection
5	62	Female	Facial spasm	Posterior fossa	Decompression
6	17	Male	Cavernous angioma	Subcortical	Transcranial resection
7	52	Female	Pituitary adenoma	Intrasellar	Transsphenoidal surgery
8	52	Male	Aneurysm	Anterior communicating artery	Neck clipping
9	8	Male	Arteriovenous malformation	Temporal	Transcranial resection
10	42	Female	Acoustic neurinoma	Cerebellopontine angle	Transcranial resection
11	24	Female	Pituitary adenoma	Intrasellar	Transsphenoidal surgery
12	54	Male	Aneurysm	Anterior communicating artery	Neck clipping
13	63	Male	Facial spasm	Posterior fossa	Decompression
14	22	Female	Pituitary adenoma	Intrasellar	Transsphenoidal surgery

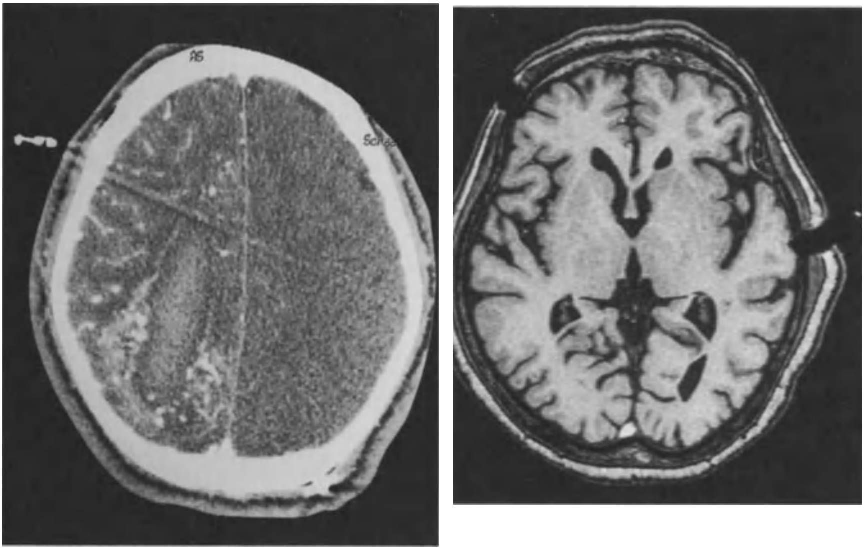

a b

Fig. 2a,b. The marker for computed tomography (CT) shows high density (**a**); the marker for magnetic resonance imaging (MRI) shows a focus of high signal intensity (**b**)

The next step was simulation of the surgical procedures on the MKM computer workstation. We determined the target point, surgical entry route, and outlines of the lesion as well as critical areas that had to be preserved. The target point was usually set at the center of the lesion. For skull-base lesions, we also determined outlines of bony structures to be drilled off. The risk zones included vascular structures, certain bony structures such as the labyrinth and cochlea, cranial nerves, and eloquent brain.

Before incision of the scalp, the MKM microscope autofocused on the four chosen markers. This encoding procedure memorized the precise spatial location of the markers. We then started the surgical procedure.

Illustrative Cases

Case 1

A 72-year-old woman had a chordoma. Preoperative MRI demonstrated tumor involvement of both cavernous sinuses, the sphenoid sinus, and the intrasellar and suprasellar regions (Fig. 3). A left fronto-orbito-zygomatic craniotomy was employed. The lateral wall of the cavernous sinus was exposed by the extradural microsurgical approach. The tumor involving the left cavernous sinus was resected through the anterolateral and anteromedial triangles. The MKM microscope superimposed the lesion located in the sphenoid sinus and intrasellar region. After drilling the sphenoid bone, the tumor in the sphenoid sinus and intrasellar region was resected. The lateral, anterior, and the medial margins of the tumor were correctly superimposed in the

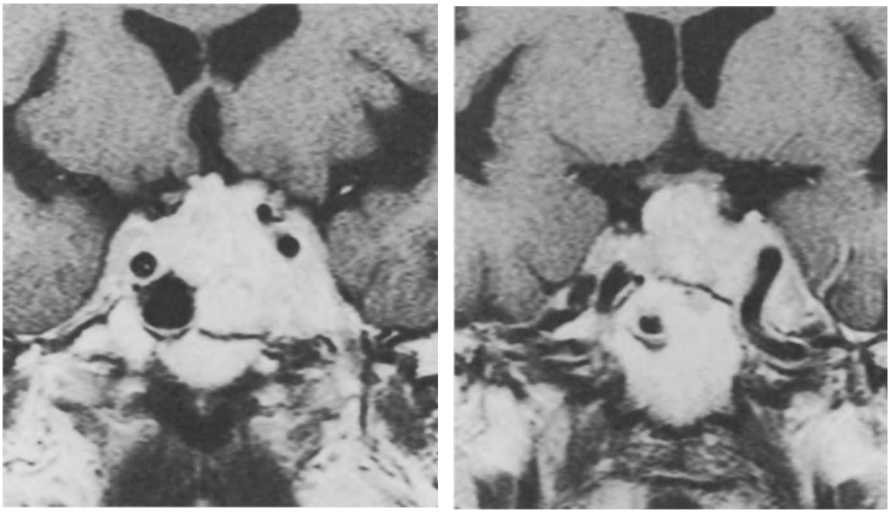

a b

Fig. 3a,b. Case 1. Preoperative gadolinium diethylenetriamine pentaacetic acid- (Gd-DTPA-) enhanced MRI (**a** and **b**) demonstrated the tumor involved both cavernous sinuses, sphenoid sinus, and intra- and suprasellar regions

MKM microscope. After we resected the tumor extradurally, the lesion extending to the intradural space was superimposed. The dura was incised, and the intradural tumor was dissected from the pituitary stalk and removed.

Postoperatively the patient developed only a transient oculomotor nerve palsy. Postoperative MRI demonstrated that the tumor involving the left cavernous sinus, the sphenoid sinus, and the intra- and suprasellar regions had been removed (Fig. 4).

Case 2

A 20-year-old man had a recurrent astrocytoma. Preoperative MRI demonstrated the tumor in the superior vermis and in dorsal portions of the midbrain and pons (Fig. 5). A combined occipital and suboccipital craniotomy was employed. Through the infratentorial supracerebellar approach, contours displayed in the MKM microscope correctly indicated the extent of tumor growth. The margin between the tumor and the brain stem was correctly superimposed in the microscope.

After incision of the tentorium from a suboccipital transtentorial approach, the lateral and posterior margins of the tumor were precisely superimposed in the MKM microscope. While resecting the tumor, surrounding normal structures easily could be preserved. The patient had only a mild cerebellar ataxia postoperatively. Postoperative MRI demonstrated near-total removal of the tumor (Fig. 6).

Case 3

A 47-year-old woman had a right internal carotid-ophthalmic artery aneurysm. The patient presented with progressive visual disturbance in the right eye. Right internal carotid angiograms demonstrated an internal carotid-ophthalmic artery aneurysm

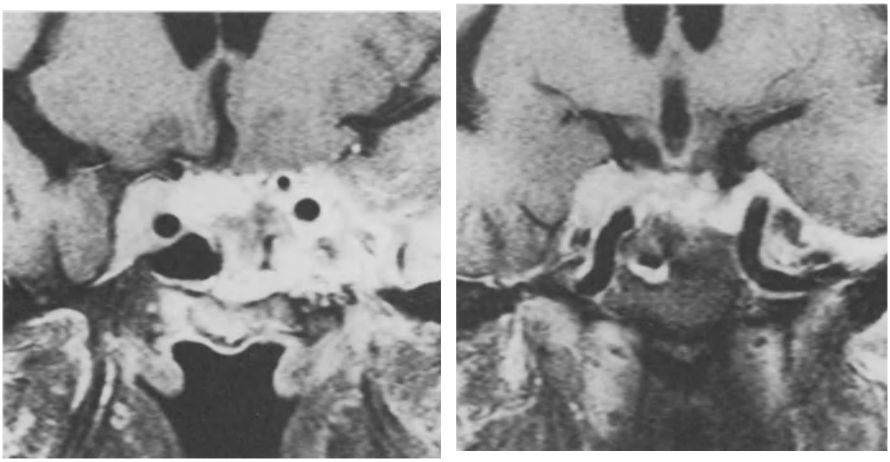

a b

Fig. 4a,b. Case 1. Postoperative fat-suppression Gd-DTPA-enhanced MRI (**a** and **b**) demonstrate resection of the lesion from the left cavernous sinus, sphenoid sinus, and intra- and suprasellar regions

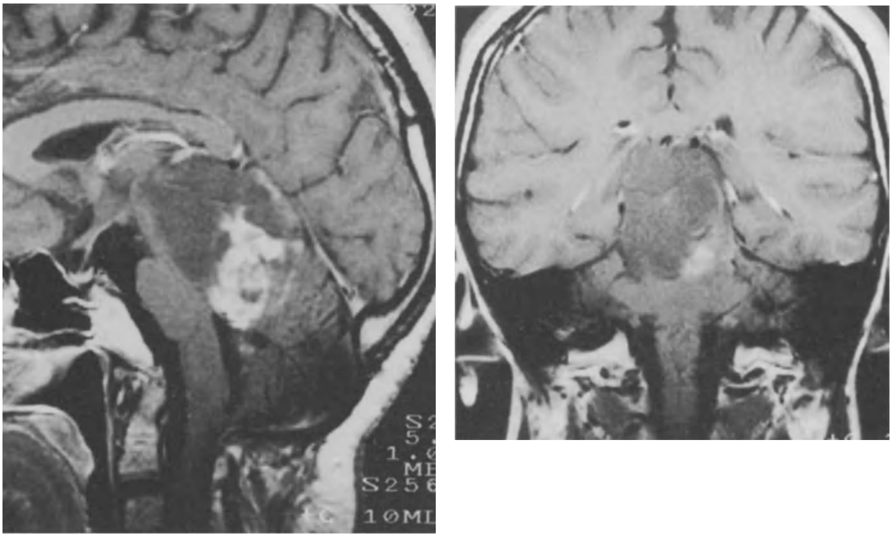

a b

Fig. 5a,b. Case 2. Preoperative Gd-DTPA-enhanced MRI (**a** and **b**) demonstrates tumor involvement of the upper vermis and the dorsal midbrain and pons

(Fig. 7). 3D-CT clearly showed anatomical relationships among the aneurysm, the anterior clinoid process, and the internal carotid artery (Fig. 8). We preoperatively determined a target point at the center of the aneurysm and outlined the aneurysm and the anterior clinoid process at the MKM workstation.

During surgery the outlines of the aneurysm and the anterior clinoid process were precisely superimposed in the MKM microscope. We could safely and easily drill the

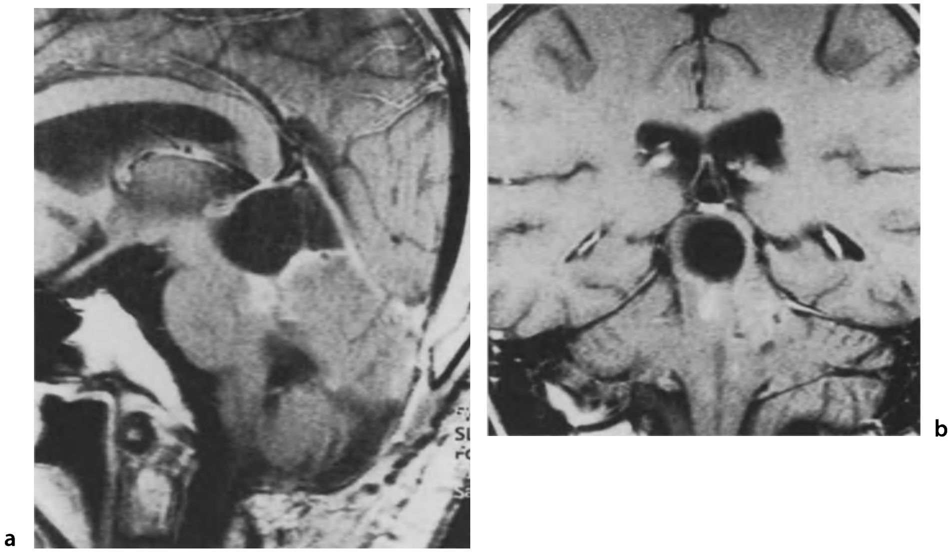

Fig. 6a,b. Case 2. Postoperative Gd-DTPA-enhanced MRI (**a** and **b**) show near-total resection of the lesion

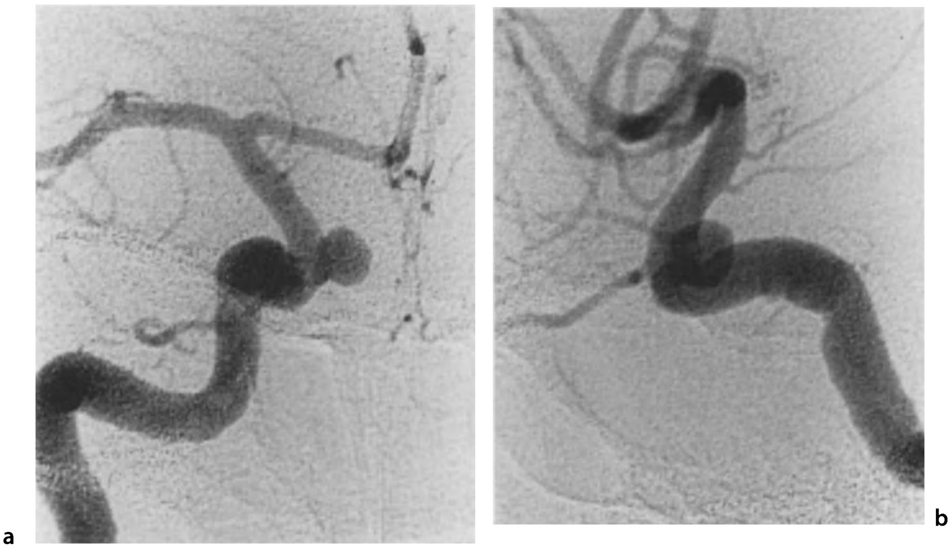

Fig. 7a,b. Case 3. Right internal carotid angiograms demonstrate a right internal carotid-ophthalmic aneurysm. **a** Anteroposterior view. **b** Lateral view

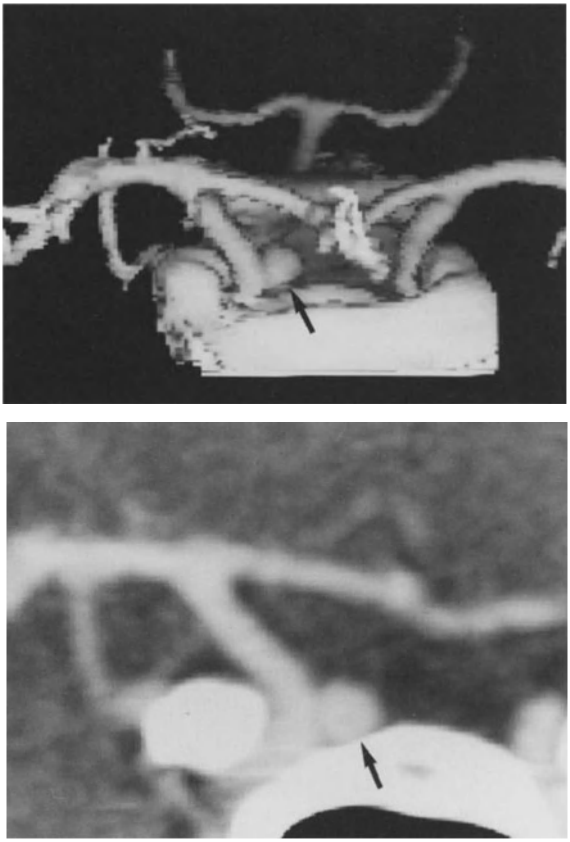

a

b

Fig. 8a,b. Case 3. Three-dimensional CT (**a** and **b**) demonstrates relationships among the aneurysm (*arrows*), the internal carotid artery, and the anterior clinoid process

anterior clinoid process by the extradural microsurgical approach (Fig. 9a). After opening the dura and exposing the neck of the aneurysm, successful clipping of the aneurysm was achieved (Fig. 9b,c). The postoperative course of the patient was uneventful.

Case 4

A 17-year-old man had a cavernous angioma. The patient presented with intractable seizures. Preoperative MR imaging demonstrated a subcortical lesion in the right frontal lobe (Fig. 10a). Frameless stereotactic access to the lesion was simulated (Fig. 10b,c).

After craniotomy and incision of the dura, the MKM microscope superimposed the entry sulcus (Fig. 11a). The arachnoid membranes surrounding the targeted sulcus were dissected. The lesion was exposed through an MKM-guided entry route and was

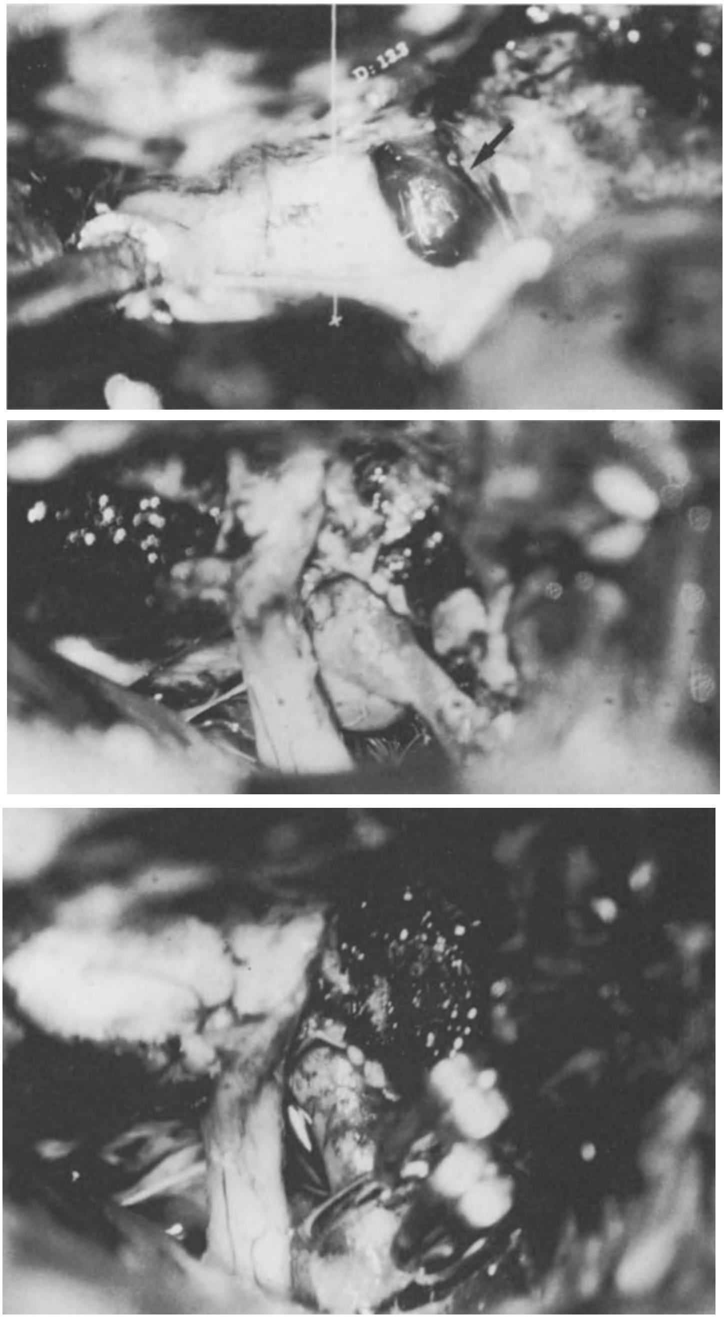

a

b

c

Fig. 9a–c. Case 3. **a** The anterior clinoid process was drilled off extradurally with superimposition of the center of the aneurysm (*small white cross*). The anterior loop of the internal carotid artery was exposed (*arrow*). **b** The aneurysm is exposed intradurally. **c** The aneurysm was obliterated with two fenestrated clips

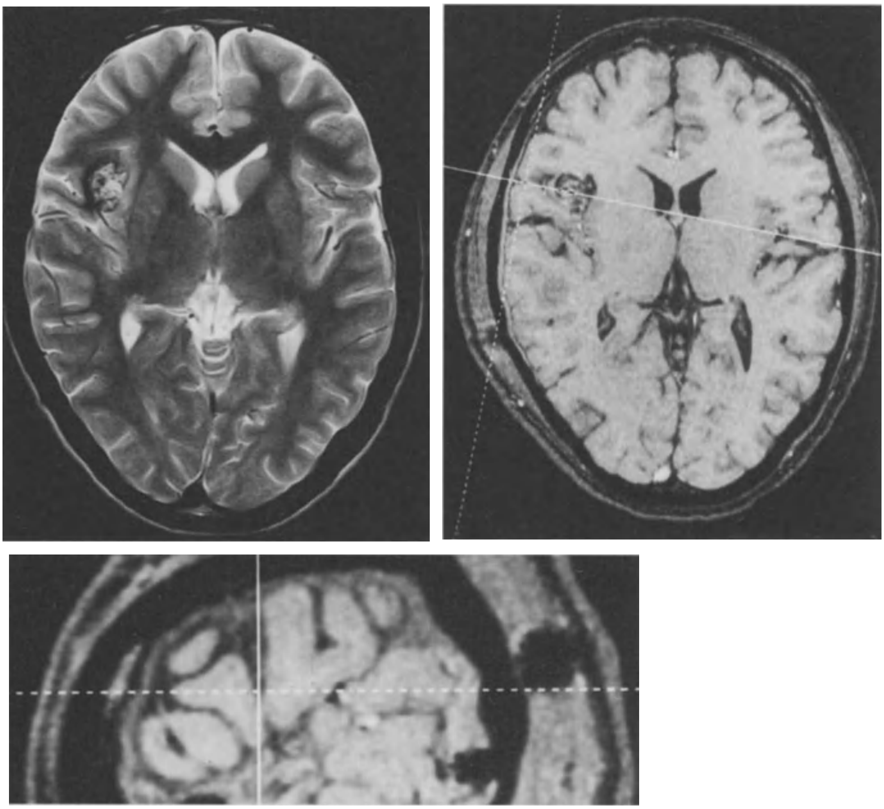

a b c

Fig. 10a–c. Case 4. **a** Preoperative T_2-weighted MRI demonstrates the subcortical lesion in the right frontal lobe. **b** and **c** Preoperative simulation using three-dimensional MRI (3-D MRI) shows the predetermined entry sulcus providing access to the lesion

removed through an area of gliosis between the lesion and the normal brain. MKM provided easy and accurate frameless stereotactic access to the lesion.

Postoperative MRI demonstrated total removal of the lesion (Fig. 11b). The entry sulcus navigated by the MKM system was the predetermined one (Fig. 11c). The patient's convulsions were controlled with anticonvulsant drugs, and he was discharged without any neurological deficit.

Results

Tolerance of the skull screws was good, and no bone or skin infection occurred. We could easily manipulate the MKM system and simulate the neurosurgical procedure at the computer workstation within 30–60 min depending on the number of image sequences.

We used both stereotactic CT and MRI for all 14 patients. For skull-base tumors, we monitored CT during a craniotomy and bone drilling of the skull base and Gd-DTPA-

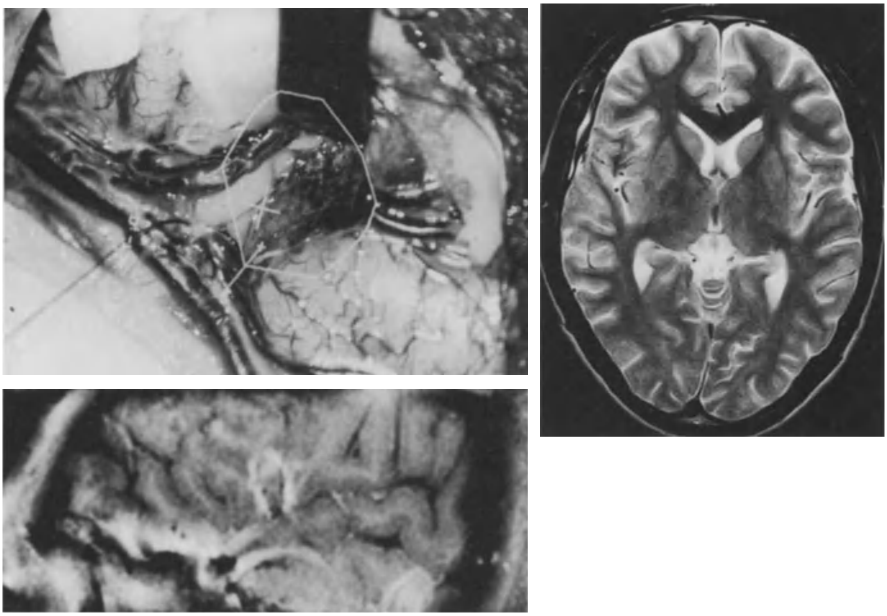

Fig. 11a–c. Case 4. **a** Intraoperative photograph shows the superimposed target point (*small white cross*), the access route to the target point, and the *outline* of the lesion. The *large white cross* indicates the center of the microscope. **b** Postoperative T_2-weighted MRI shows total resection of the lesion. **c** Postoperative 3-D MRI demonstrates the surgical entry sulcus corresponding to the predetermined one

enhanced MRI obtained by a FLASH sequence during tumor resection. Although FISP was available for MR angiography, which demonstrated the arteries and vascular diseases as high signal intensities, CT was more useful in monitoring during surgery of cerebral aneurysms and arteriovenous malformations than MRI. Consequently FISP imaging was used only for microsurgical decompression of the facial nerve. In the treatment of cavernous angioma, MRI of a FLASH sequence was used as intraoperative guidance because it clearly demonstrated the location and extent of the lesion.

As the lesion and surrounding structures located at the skull base, including the brain stem, did not shift significantly during surgery, the MKM system provided accurate stereotactic information. We could easily and safely drill the bone of the skull base, including the anterior clinoid process, the floor of the sella, and the internal auditory canal, with MKM guidance. MKM-guided microsurgery resulted in radical resection of tumors as well as preservation of normal structures. Postoperative MRI demonstrated the radical resection of these lesions, as shown for the illustrative cases.

For deep-seated lesions, we could perform a minimal scalp incision and craniotomy because we could see the outline of the lesion in the microscope before scalp incision. MKM-guided stereotactic access to the lesion helped to minimize brain retraction and damage. For small deep-seated lesions, MKM provided an accurate entry route, although the outline of the lesion was not precisely superimposed as a result of displacement of the lesion and surrounding structures following cerebrospinal fluid (CSF) outflow, brain retraction, and lesion resection.

Discussion

Microneurosurgery guided by imaging has been used for intracranial and spinal lesions. MRI, CT images, and sonograms have been used for intraoperative neuroimaging. Recent improvement of CT and MRI image quality as well as 3-D sequences permits preoperative simulation of neurosurgical procedures, including extent of craniotomy, the microsurgical approach, and relationships between the lesion and surrounding normal structures [1]. The MKM system, the viewing wand [2–7], NeuroSAT (neuronavigation by computer-assisted frameless stereotaxy) [8,9], and hyper-CAS (computer-assisted surgery) [10] all can utilize stereotactic CT and MR images.

The viewing wand (ISG Technologies, Mississauge, Ontario, Canada) has a multijointed mechanical arm and an analog/digital hybrid transducer to locate the spatial position of the probe tip. This apparatus is interfaced to a computer graphics workstation, and the surgeon can observe the 3-D position and direction of the tip of the instrument. Frameless stereotactic surgery with the viewing wand has been reported as useful for neurosurgical treatment of deep-seated or skull-base lesions [2–5] and for oral maxillofacial surgery [6,7]. NEURO-SAT is a frameless isocentric stereotactic system, designed by Takizawa et al., that provides accurate and reliable navigation in treating deep-seated brain tumors [8]. Kinjo et al. have reported osteoplastic petrosal craniotomy guided by NEURO-SAT [9]. With an image integration system developed by Iseki et al., hyper-CAS can provide for stereotactic craniotomy, the access route to the lesion, and the extent of the lesion during surgery [10].

Neuroimaging-guided surgical tools should provide us with two kinds of information; intraoperative orientation, displayed at the workstation where the observed field is; and intraoperative navigation, indicating where the surgeon should go. All systems can provide intraoperative orientation at the computer workstation using preoperative CT and MRI.

MKM is a new generation of microscopes created by Zeiss. This system integrates a robotic microscope with a computer workstation. The workstation can memorize spatial localization of the markers. MKM provides intraoperative orientation demonstrating the exact spatial location of the anatomical structure in focus in axial, sagittal, and coronal CT or MR images. Additionally, the MKM system has a navigation function, superimposing in the microscope the predetermined access route, the location of the target point with its distance and direction, and outlines of the lesion and critical areas that must be preserved. Using these MKM functions, we could perform stereotactic microneurosurgery via a small craniotomy, drill the skull-base bone safely, attain access to the lesion easily, and resect tumors more radically with minimal risk even if the lesion involved the skull base, brain stem, and other vital structures.

When the lesion, like the normal structures of the skull base and the brain stem, did not shift significantly during surgery, the system could provide accurate intraoperative orientation and navigation. On the other hand, small deep-seated lesions and surrounding structures tended to shift following CSF outflow, brain retraction, and resection, so in these cases the outline of the lesion could not be precisely superimposed. All the image-guided operative systems have this disadvantage. Real-time intraoperative image is also required for such cases.

Ultrasonography has been widely utilized for real-time intraoperative monitoring. Shkolnik and McLone have reported ultrasonic guidance of ventricular shunt placement in infants [11]. Tsutsumi et al. presented ultrasound-guided biopsy for deep-seated brain tumors [12], and Rubin et al. evaluated ultrasonography for intracranial mass lesions [13]. Knake et al. have demonstrated intraoperative sonographic delineation of low-grade brain neoplasms poorly defined by CT [14]. Takahashi et al. observed major intracranial vessels with intraoperative color-coded sonography [15]. Intraoperative ultrasound-guided surgery has been also useful for intramedullary spinal tumors, syringomyelia, and spinal cysts [16–18].

Although ultrasonography has been used intraoperatively to visualize deep-seated intracranial and spinal lesions, it has not achieved the same image quality as currently available CT and MRI. Recently, other real-time intraoperative imaging tools including intraoperative CT fluoroscopy, open MRI, and neuroendoscopy have been reported. Katada et al. have used real-time CT fluoroscopy for drainage and aspiration of intracranial hematomas [19]. Scholz et al. have studied open MRI combined with an endoscopic system in a human cadaveric model [20]. Although the surgeons are irradiated during CT fluoroscopy and surgical tools should be made of non-magnetic materials for intraoperative MRI, these modalities might be available in the future.

We have used ultrasonograms and neuroendoscopy combined with the MKM system. From our early clinical experience, we have concluded that the MKM microscope system with its present configuration is already very useful for skull base, brain stem, and other critically located lesions. We consider that it should have some interface with real-time imaging equipment, especially for small deep-seated lesions.

Conclusion

The MKM system proved useful in providing accurate stereotactic intraoperative orientation and navigation. MKM-guided neurosurgery resulted in easy access to the lesion, optimal exposure, and better surgical outcome. We could perform less invasive and more effective microsurgery for lesions of the skull base, brain stem, and other vital areas with the MKM system. For small deep-seated lesions, the MKM workstation should be integrated with intraoperative real-time imaging modalities.

References

1. Kikinis R, Gleason L, Moriarty TM, et al (1996) Computer-assisted interactive three-dimensional planning for neurosurgical procedures. Neurosurgery 38:640–651
2. McDermott MW, Gutin PH (1996) Image-guided surgery for skull base neoplasms using the ISG viewing wand. Anatomic and technical considerations. Neurosurg Clin N Am 7:285–295
3. Doshi PK, Lemmieux L, Fish DR, et al (1995) Frameless stereotaxy and interactive neurosurgery with the ISG viewing wand. Acta Neurochir Suppl (Wien) 64:49–53

4. Sandeman DR, Patel N, Chandler C, et al (1994) Advances in image-directed neurosurgery: preliminary experience with the ISG Viewing Wand compared with the Leksell G frame. Br J Neurosurg 8:529–544
5. Drake JM, Prudencio J, Holowaka S, et al (1994) Frameless stereotaxy in children. Pediatr Neurosurg 20:152–159
6. Carney AS, Patel N, Baldwin DL, et al (1996) Intra-operative image guidance in otolaryngology—the use of the ISG viewing wand. J Laryngol Otol 110:322–327
7. Hassfeld S, Muhling J, Zoller J (1995) Intraoperative navigation in oral and maxillofacial surgery. Int J Oral Maxillofac Surg 24:111–119
8. Takizawa T, Sato S, Sanou A, Murakami Y (1993) Frameless isocentric stereotactic laser beam guide for image-directed microneurosurgery. Acta Neurochir (Wien) 125:177–180
9. Kinjo T, Mukawa J, Tomiyama N (1996) Modified petrosal approach using cosmetic osteoplastic craniotomy with NEURO-SAT guidance. Neurol Med Chir (Tokyo) 36:310–313
10. Iseki H, Kawamura H, Tanikawa T, et al (1994) An image-guided stereotactic system for neurosurgical operations. Stereotactic Funct Neurosurg 63:130–138
11. Shkolnik A, McLone DG (1981) Intraoperative real-time ultrasonic guidance of ventricular shunt placement in infants. Radiology 141:515–517
12. Tsutsumi Y, Andoh Y, Inoue N (1982) Ultrasound-guided biopsy for deep-seated brain tumors. J Neurosurg 57:164–167
13. Rubin JM, Dohrmann GJ (1985) Efficacy of intraoperative US for evaluating intracranial masses. Radiology 157:509–511
14. Knake JE, Chandler WF, Gabrielsen TO, et al (1984) Intraoperative sonographic delineation of low-grade brain neoplasms defined poorly by computed tomography. Radiology 151:735–739
15. Takahashi A, Tamaki N, Kurata H (1996) Experience with intraoperative ultrasonography in neurosurgery. Neurosonology 9:7–11
16. Epstein FJ, Farmer JP, Schneider SJ (1991) Intraoperative ultrasonography: an important surgical adjunct for intramedullary tumors. J Neurosurg 74:729–733
17. Dohrmann GJ, Rubin JM (1982) Intraoperative ultrasound imaging of the spinal cord: syringomyelia, cysts, and tumors—a preliminary report. Surg Neurol 18:395–399
18. Lunardi P, Acqui M, Ferrante L, et al (1994) The role of intraoperative ultrasound imaging in the surgical removal of intramedullary cavernous angiomas. Neurosurgery 34:520–523
19. Katada K, Kato R, Anno H, et al (1996) Guidance with real-time CT fluoroscopy: early clinical experience. Radiology 200:851–856
20. Scholz M, Deli M, Wildforster U, et al (1996) MRI-guided endoscopy in the brain: a feasibility study. Minim Invasive Neurosurg 39:33–37

Application of the ISG Viewing Wand in Skull Base Procedures

Michael W. McDermott and Scott Wachorst

Summary. Tumors arising from or attached to the skull base shift little during surgical removal and are therefore well suited to interactive image-guided surgical techniques. However, most skull base surgical procedures are done without interactive image guidance, as is true at our institution. We have had experience with 16 cases in which the ISG/Elekta Viewing Wand was used during surgery on a skull base tumor; some of these cases were gathered from a prospective trial in which the utility of the system was assessed by the surgeon. Given the number of variables influencing the duration and outcome of each skull base case, "randomized" studies seem inappropriate. We review here some of the technical considerations for use of the Viewing Wand during skull base surgery in general, present some representative cases from our own institution, and discuss selected papers from the literature evaluating image-guided techniques for skull base surgery.

Key words. Viewing Wand—Image-guided surgery (IGS)—Skull base surgery—Tumor removal

Introduction

During the past 10 years, surgical techniques for handling skull base tumors have advanced and the importance of the skull anatomy relevant to these procedures has been reemphasized. Interactive image-guided surgical systems have developed rapidly since the initial pioneering work of Watanabe et al. [1–4]. Tumors arising from the bony skull base, or intimately attached to it, are probably the best suited of any intracranial lesion for interactive image-guided surgery in which the images are derived from preoperative data and therefore the registration set is not subject to the perturbation inherent with the brain shifts that occur during such surgery. On the other hand, many of the exposures necessary for these complex procedures do not require the small, precisely located craniotomies that image-guided systems make

Department of Neurological Surgery, University of California, 533 Parnassus Avenue, Suite U-126, San Francisco, CA 94143-0350, U.S.A.

possible for intraaxial neoplasms or vascular malformations. This delimitation may in part explain why image-guided skull base procedures are less often seen at our institution and others [5–8]. Nonetheless most experienced surgeons find that these systems are complementary to the anatomical knowledge necessary for a safe surgical approach.

This chapter documents our updated experience with use of the ISG/Elekta Viewing Wand (ISG Technologies, Mississauga, Canada) for skull base procedures at the University of California, San Francisco (UCSF) and reviews selected articles from the literature.

Materials and Methods

Viewing Wand System

The ISG/Elekta Viewing Wand is the interactive image-guided system used at our institution since 1993. Only the passive mechanical arm system is used. The arm has electropotentiometers at each of six joints that convert analog angular data into digital probe tip information after physical to imaging space registration. The arm is fixed to the Mayfield headholder attachment, and therefore the relationship of the arm to the patient's head remains constant throughout the procedure. This attachment creates some challenges with patient positioning for complex skull base cases. The arm reach is 60 cm, and the position of the probe tip is updated by the computer every 0.03 s. We still use the original computer platform, which has proven to be extremely reliable. The host computer is a Hewlett-Packard Apollo Series 700 (Palo Alto, CA, USA) and the monitor is a 19-in. display with 1280 × 1024 pixel resolution and 72-Hz refresh rate. Access to the software interface is through a standard mouse–dialogue box or keyboard commands.

Selection of Imaging and Scanning Parameters

Because only one imaging data set can be displayed at a time, the decision to use computed tomography (CT) or magnetic resonance (MR) imaging related to surgeon preference and the primary type of tissue being imaged. Table 1 lists the diagnoses in our 16 cases and the imaging selected for use with the Viewing Wand. Because surgical orientation is referenced to the bony landmarks in most skull base procedures, CT imaging seems most appropriate; tumors such as chordomas, chondrosarcomas arising from the bony base, tumors eroding bone from a primary soft tissue origin, and nonneoplastic conditions in which bony detail is important (cerebrospinal fluid leak, reconstructive procedures) are examples. Reconstructed images from CT-based studies, on the other hand, are inferior in detail compared with those from volume acquisition MR studies. For CT imaging, 3-mm-thick slices without interslice spacing are used with field of view 25 and a 512 × 512 matrix. Commercially available lead shots attached to an adhesive backing are used as fiducials.

In comparison to CT imaging, MR offers better soft tissue detail and resolution and is best suited for soft tissue tumors attached to the skull base such as meningioma,

Table 1. Summary of 16 skull base cases for which Viewing Wand was used

Pathological condition	Number	Imaging Studies
Meningioma		
Tuberculum sellae	1	MR
Cranioorbital	1	MR
Petroclival	2	MR
Chordoma		
Petrous apex	1	CT
Clivus	2	MR
Chondrosarcoma		
Medial sphenoid wing	1	MR
Petroclival	1	CT
Nasal angiofibroma	1	MR
Hemangiopericytoma	1	MR
Adenoid cystic carcinoma, greater sphenoid wing	1	CT
Other nonneoplastic conditions		
Sellar CSF leak	1	CT
Sphenoid sinus mucocele	1	MR
Grave's ophthalmopathy	1	CT
NF1	1	CT

MR, magretic resonance; CT, computed tomography; CSF, cerebrospinal fluid; NF1, neurofibromatosis, type 1.

hemangiopericytoma, and angiofibroma. For very extensive chordomas we have also preferred MR because of the superior detail of sagittal, coronal, and trajectory view images. The MR imaging protocol uses a volume acquisition of 124 slices, 1.5 mm thick, field of view 26, and a spoiled gradient recall (SPGR) sequence. Gelatin vitamin E capsules are used for fiducials.

Two potential problems with skull base procedures in which interactive image-guided surgical devices are used arise from the extremes of positioning and extensive soft and bony tissue opening required for the surgical approach. Because most systems currently rely on "hat-to-head" surface-fitting algorithms using reconstructed skin surfaces from imaging space and fiducial and skin surface points in physical space, the position of the patient, and thus the skin, during scanning may be markedly different from the position in the operating room. Skin surface- or skin-based fiducial sagging may affect the accuracy of the registration process, and some standard skin fiducial placements may not be accessible for registration with extremes of positioning. The extensive soft and bony tissue removal accompanying these procedures may limit the choices for the placement of landmarks necessary for reregistration should movement of the head occur relative to the Wand after the initial registration.

Table 2 lists some common skull base approaches and our choice of fiducial placement and landmark hole placement. An "anterior" fiducial set refers to six fiducials placed over the front of the face and forehead: two at the nasion (superior and inferior), one at each supraorbital margin laterally, and one at each body of the zygoma just below the lateral canthus. A "posterior" fiducial set refers to six fiducials

Table 2. Surgical approach and fiducial system for skull base procedures

Surgical approach	Fiducial system	Landmark site
Transoral/transsphenoidal	Anterior[a]	Gingival sulcus between teeth
Transmaxillary	Anterior	Maxilla
Bifrontal/transbasal	Anterior	Frontal bone
Pterional/orbitozygomatic	Anterior	Frontal and temporal bone
Transcochlear/translabyrinthine	Half and half[b]	Temporal and occipital bone
Retrolabyrinthine		
Retrosigmoid		
Extreme lateral or far lateral	Posterior[c]	Occipital bone

[a] Anterior fiducial set, 2 nasion, 1 each left and right supraorbital margin and left and right zygoma, total 6.
[b] Half and half set, half anterior and half posterior set on side of lesion.
[c] Posterior fiducial set, 2 vertex lambda, 1 each left and right parietal eminence and left and right mastoid, total 6.

placed on the back part of the head: two in the midline vertex in front of the lambda, one on each parietal eminence, and one at each mastoid toward its base, not the tip. The "half and half" designation is a combined anterior and posterior fiducial placement ipsilateral to the site of the lesion.

Intraoperative Registration and Probe Selection

When the patient has been postioned in the operating room with their head fixed in the Mayfield pin headrest, the Viewing Wand is attached to the headrest and the registration of imaging to physical space carried out. The first registration uses the fiducial set only, and if this proves to be accurate then the operation proceeds. If this is not accurate, the registration is repeated using fiducials supplemented by 40 skin surface points. A reserved fiducial and anatomical landmark check is then made to ensure acceptable accuracy. Prior experience from our clinical trial demonstrated that the time required to set up the Viewing Wand for skull base cases was 17.4 min (n = 5), and registration time was 14.3 min (n = 6). The average time from patient positioning to start of operation when the wand was used was 27.7 min (n = 5) [7].

When the registration is complete, the surgeon must determine which probe is best suited for the approach, using the knowledge of distance from the surface of the skull to the deepest side of the skull base being approached (Table 3). Generally, the long probe (152 mm long beyond its attachment point) is used during the crucial parts of the case, and the short probe (76 mm) is used for registration, the earliest part of the procedure, and middle fossa approaches. During the later parts of the procedure, if a shorter focal length microscope lens (200 or 250 mm) has been selected it may be very difficult to place the long probe deep into the wound while maintaining focus. Longer focal length lenses, while inconvenient early in the procedure, provide a greater distance between the skull and microscope, allowing easier access with the long probe.

Table 3. Distance from outer table to specified skull base landmark

Skull base landmark	Distance (mm)
Nasion to tuberculum	50
Pterion to anterior clinoid	55
Floor of middle fossa anterior to tragus to free edge of tentorium	55
Transverse—sigmoid junction to posterior clinoid	70
Midposition transverse sinus to tentorial hiatus midposition between petrosal and straight sinus	65
Inion to tentorial hiatus at straight sinus	60
Superior alveolar crest to floor of sella	70
Superior alveolar crest to clivus	80
Upper central incisor to anterior arch C1	70

Adapted from McDermott and Gutin [7].

Results

Our experience with the Viewing Wand during a prospective clinical trial indicated that surgeons found this new technology generally helpful and easy to use [7]. In spite of this the Wand was used in only 20% of skull base procedures during the time of the trial, with skull base cases accounting for 8.3% of all Viewing Wand applications. As compared to use with convexity lesions, surgeons found that the Viewing Wand was less useful in planning the incision, accurate in its anatomical correlation, helpful with lesion margins, helpful in determining extent of removal, but less easy to use in a skull base location [7]. For the first seven cases, the Wand was brought into the operative field 13 times on average, compared with 7 times for convexity lesions. A comparison of our intital skull base experience using the Viewing Wand ($n = 7$) and that of the Barrow Neurologic Institute ($n = 29$) is presented in Table 4. The author subsequently has had personal experience with nine more skull base cases in which the Viewing Wand was used. The experience is summarized by disease type.

Meningioma

The most obvious application of image-guided systems for surgery of skull base meningiomas is for those that are very large and those in which critical structures on the deep side of the tumor are directly opposed to the surgeon's approach. In our four cases, MR imaging was used. When the tumor is large (>3-cm diameter), interactive image-guided systems can provide updated information as to how much tumor remains deep to the resection cavity as debulking proceeds. This information provides an additional measure of confidence for the surgeon, who can proceed more efficiently with tumor removal knowing how much remains. In addition, the distance to critical structures deep to the tumor that cannot be seen at first can be measured and the trajectory to the structure(s) of concern can be determined. Figure 1 is an example

Table 4. Surgeons' reports from two clinical series on usefulness of Viewing Wand for skull base procedures

Evaluation	UCSF[a] (n = 7)	Barrow[b] (n = 29)
Helpful with incision and planning craniotomy	Yes (0%)	Yes (17.2%)
Accurate anatomical correlation and definition	Yes (100%)	Yes (65.5%)
Helpful with margins	Yes (100%)	Yes (65.5%)

[a] From [7] (UCSF, University of California, San Francisco).
[b] From [5].
Percentages in parentheses are percent of reports.

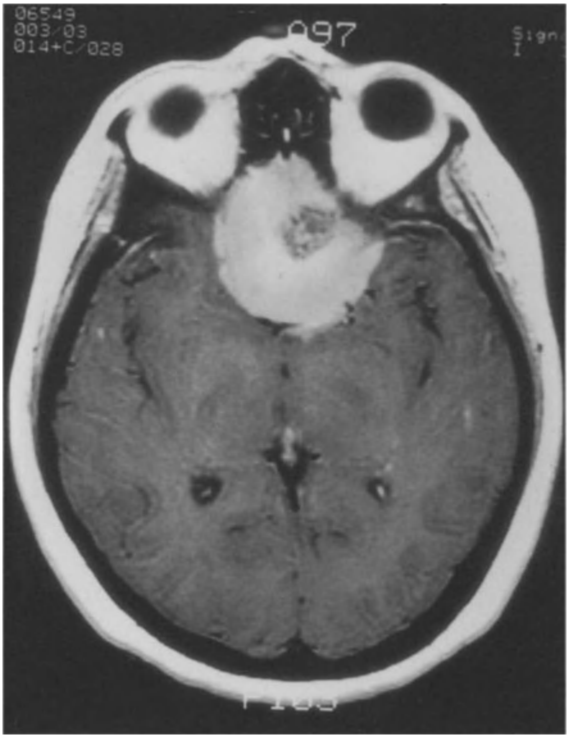

Fig. 1. Axial T_1-weighted magnetic resonance imaging (MRI) with contrast shows large tuberculum sellae meningioma. The ISG Viewing Wand was used with the long probe attachment to determine distance to posterior margin during resection

of a large tuberculum sellae meningioma for which the Wand was helpful in indicating the distance to the back edge of the tumor and optic chiasm as well as information about the position of the optic canals and nerves. For petroclival meningiomas, distance to the pons and basilar artery can be determined repeatedly as resection proceeds, again adding an additional measure of confidence and, we believe, efficiency and safety.

Chordoma and Chondrosarcoma

In one case, a chordoma of the petrous apex had been approached at another institution via a retrosigmoid, intradural route without obtaining a diagnosis. Repeat operation via a subtemporal, extradural approach using CT-based image guidance provided imaging of gross total resection with preservation of the inner ear structures and no injury to the petrous carotid artery, which was encased by the tumor. Two other extensive clival chordomas were operated on using MR imaging primarily because of the superior anatomical detail on sagittal reconstructions, which provided information about the position of the tumor relative to the brainstem (Fig. 2). In one of these cases, in which the patient presented with upper-airway obstruction, image guidance was believed to be accurate from the sella to C2 and eliminated the need for

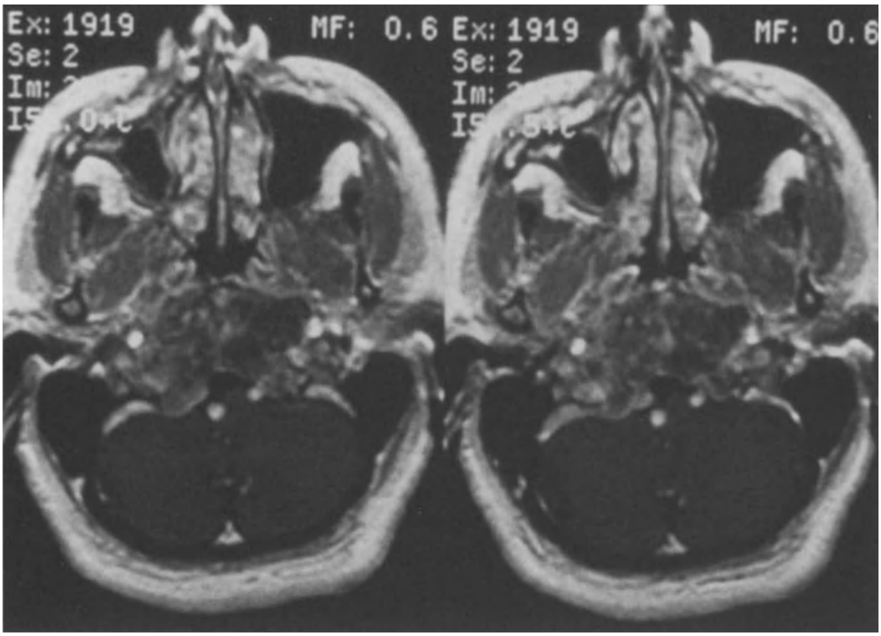

Fig. 2. Axial T_1-weighted MRI with contrast, 1.5-mm slices, of clival chordoma approached via a transoral route. The long probe attachment was used for surgery and the short probe for registration of the anterior fiducial set. Grooves between the teeth at the gingival margin were used for landmarks. Left and right images are configuous axial images separated by 1.5 mm

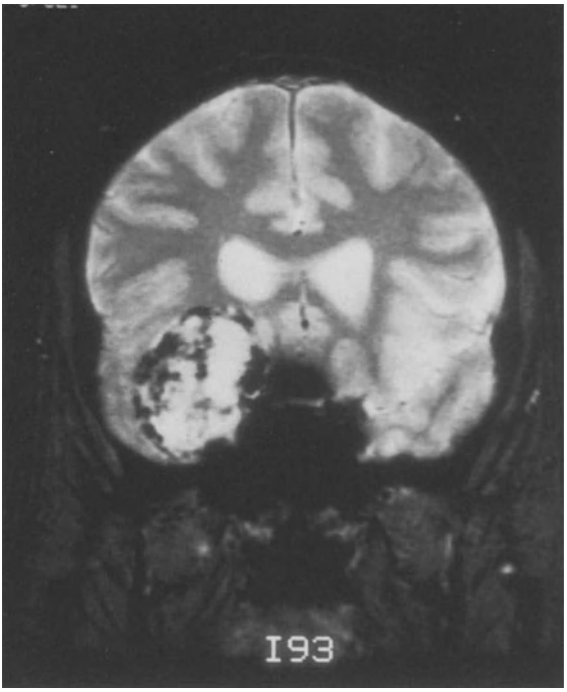

Fig. 3. Coronal T_2, second echo image from diagnostic series shows large medial third sphenoid wing chondrosarcoma. An orbitozygomatic, frontotemporal-sphenoidal craniotomy was used for the approach with an anterior fiducial set. Because the firmness of the tumor prevented its manipulation for identification of the optic nerve and carotid artery by direct vision, the ISG Viewing Wand was very helpful in orienting the surgeon relative to these structures as tumor removal progressed

prolonged intraoperative fluoroscopy. In one case of a medial third sphenoid wing chondrosarcoma (Fig. 3), MR-based image guidance was indispensable in showing the position of the carotid artery attached to and inseparable from the medial side of the tumor.

Other Skull Base Neoplasms

The Wand was used in three other tumor cases. (1) For a juvenile angiofibroma filling the nasal cavity and extending to, but not invading, the anterior inferior and anterior lateral cavernous sinus, the Viewing Wand was very helpful in confirming the posterior resection margin. (2) A huge middle fossa hemangiopericytoma arising from the lateral wall of the cavernous sinus and fed by a lateral capsular artery could not be embolized; the signal flow void of this artery could be seen on the coronal T_1-weighted image, and this was approached early in the procedure via frontotemporal, orbitozygomatic craniotomy. (3) For an adenoid cystic carcinoma invading the floor of the middle cranial fossa up to the petrous carotid artery, the Wand was helpful in determining our position relative to the carotid artery during tumor and bone removal from an extradural approach.

Nonneoplastic Conditions

There were four patients in the nonneoplastic group. The first patient had recurrent meningitis after transphenoidal resection of a pituitary tumor; direct coronal images indicated bony dehiscence at the tuberculum and the dorsum sella, both of which were identified intraoperatively with image guidance. One young patient with diabetes insipidus had a sphenoid bone lesion in which the sinus had not yet fully formed. This lesion, biopsied via a transphenoidal route, was immediately in front of the posterior turn of the petrous carotid artery. In a case of Grave's ophthalmopathy, the Viewing Wand was used to direct a four-wall orbital decompression. In the fourth case, use of the Wand assisted reconstruction of a deficient greater sphenoid wing causing enophthalmos.

Discussion

Skull base neoplasms are well suited to the application of interactive image-guided surgical techniques because, in contrast to intraaxial brain lesions, there is less concern about shift of the target tissue during surgical approach and tumor resection. For intraaxial lesions, drainage of cerebrospinal fluid and distortion of brain tissue with tumor removal or retraction represent sources of error for intraoperative localization. In spite of the apparent benefits of image-guided techniques for skull base surgery, clincial series report a low overall rate of use of this technology in these procedures. Kondziolka and Lunsford reported 6% (5/80) and Golfinos et al. reported 8.9% (29/325) of their image-guided procedures to be skull base surgery [5,6]. Our own experience previously was similar, with a rate of 8.3% (7/84) during a prospective clinical trial [7]. One reason for this low usage may be that the skull base exposure is not significantly changed by image-guided techniques, which is supported by surgeons' reports. However, small tumors frequently are completely hidden in the cranial base and are not identified until the overlying bone is removed. Major vessels intervening between the surgeon and tumor can be readily identified on standard MR images and the appropriate bony foramina on CT images. Also, large skull base neoplasms may envelop major arteries so that only the afferent and efferent portions of the vessel are seen on either end of the tumor. Barnett et al. found that interactive image-guided techniques were helpful in locating the carotid and basilar arterics adjacent to skull base meningiomas, which has been our experience as well [9].

As surgeons develop experience with these devices, further applications for image-guided systems in skull base surgery will be found. Carrau et al. found the Wand more accurate than a Caldwell radiographic template for excising the anterior wall of the frontal sinus during an anterior craniofacial resection and medial maxillectomy [10]. Pollack et al. applied a halo vest for a patient with an odontoid mass compressing the ventral medulla and performed the preoperative CT with the patient in the vest [11]. During a transoral approach to the cervicomedullary junction for decompression, the halo was fixed to the Mayfield apparatus and the orientation of the upper cervical spine to the skull base was maintained. They found that with this technique the Viewing Wand was accurate to within 1–2 mm in the axial, sagittal, and coronal planes when images were compared with intraoperative anatomical landmarks. We have used the Wand for transoral and transphenoidal approaches and found it to be accurate enough that routine fluoroscopy is not necessary. This is particularly helpful with avoiding the fatigue associated with wearing a lead vest for several hours.

Experimental cadaver studies have explored the use of this technology for standard approaches, in particular for middle fossa surgery around the inner ear [12–14]. Bumpous et al. reported a single cadaver dissection of the middle fossa using implanted microscrews as fiducials for the Wand [12]. After registration of CT images, assessments were made of the accuracy of localization of the foramen spinosum, formen ovale, arcuate eminence, internal carotid artery, and internal auditory canal (IAC). Each structure was located within 1 mm with this technique.

Vrionis et al. used a light-emitting diode system for orientation during a middle fossa approach to the IAC in nine cadavers [14]. They fixed a reference emitter to the skull that permitted movement of the head without loss of registration accuracy. Surface anatomical fiducials including the umbo of the tympanic membrane, Henle's spine, the root of the zygoma, and various sutures were used for registration of CT scans of the temporal bone. The mean target localization error varied from 1.20 to 1.38 mm. These systems clearly are accurate and should be helpful in guiding the surgeon to the IAC from the middle fossa approach.

Lawton et al. evaluated four interactive image-guided systems (passive arm, optical tracking system $\times 2$, integrated microscope/stereotactic system) during a clinical series that included 103 skull base procedures. They found that free-hand systems were hampered by tracking interference and that the Wand was accurate, reliable, and the easiest of these systems to use [15].

Conclusions

Interactive image-guided systems are a valuable adjunct to selected skull base procedures and can improve the confidence and safety with which tumors of the cranial base are removed. Extremes of positioning and limited access to preserved bony surfaces for the establishment of intraoperative landmarks require some modifications of approaches used for intraaxial brain lesions. A variety of image-guided systems are currently available, each with its inherent strengths and weaknesses. We have found the Viewing Wand to be helpful with correlating anatomical landmarks, distinguishing tumor margins, and determining the extent of removal in skull base procedures. With increasing familiarity, it is likely that use of interactive image-guided surgical techniques for skull base surgery will increase in the future.

References

1. Kato A, Yoshimine T, Hayakawa T, et al (1991) A frameless, armless navigational system for computer assisted neurosurgery. J Neurosurg 74:845–849
2. Koivukangas J, Louhisalmi Y, Alakuijala J, et al (1993) Ultrasound-controlled neuronavigator-guided brain surgery. J Neurosurg 79:36–42

3. Sipos EP, Tebo SA, Zinreich SJ, et al (1996) In vivo accuracy testing and clinical experience with the ISG Viewing Wand. Neurosurgery (Baltim) 39:194–202
4. Watanabe E, Mayanagi Y, Kosugi Y, et al (1991) Open surgery assisted by the navigator, a stereotactic, articulated, sensitive arm. Neurosurgery (Baltim) 28:792–799
5. Golfinos JG, Fitzpatrick BC, Smith LR, et al (1995) Clinical use of a frameless stereotactic arm: results of 325 cases. J Neurosurg 83:197–205
6. Kondziolka D, Lunsford LD (1995) Guided neurosurgery using the ISG Viewing Wand. Contemp Neurosurg 17:1–6
7. McDermott MW, Gutin PH (1996) Image-guided surgery for skull base neoplasms using the ISG Viewing Wand. Neurosurg Clin North Am 7:285–295
8. Robinson JR, Golfinos JG, Spetzler RF (1996) Skull base tumors. A critical appraisal and clinical series employing image guidance. Neurosurgery Clin North Am 7:297–311
9. Barnett GH, Steiner CP, Weisenberger J (1995) Intracranial meningioma resection using frameless stereotaxy. J Image Guided Surg 1:46–52
10. Carrau RL, Curtin HD, Snyderman CH, et al (1995) Practical applications of image-guided navigation during anterior craniofacial resection. Skull Base Surg 5:51–55
11. Pollack IF, Welch W, Jacobs GB, et al (1995) Frameless stereotactic guidance. An intraoperative adjunct in the transoral approach for ventral cervicomedullary junction decompression. Spine 20:216–220
12. Bumpous JM, Curtin HD, Prokopakis EP, et al (1996) Applications of image-guided navigation in the middle cranial fossa: an anatomic study. Skull Base Surg 6:187–190
13. Fernandez PM, Zamarano L, Nolte L, et al (1997) Interactive image guidance in skull base surgery using an opto-electronic device. Skull Base Surg 7:15–21
14. Vrionis FD, Robertson JH, Foley KT, et al (1997) Image-interactive orientation in the middle cranial fossa approach to the internal auditory canal: an experimental study. Comput Aided Surg 2:34–41
15. Lawton MT, Geldmacher TR, Harrigan M, et al (1997) Clinical evaluation of frameless stereotactic systems. In: Proceedings of the 65th Annual Meeting of the American Association of Neurological Surgeons, April 1997, pp 356–358

Subject Index